CONVERTING AN ONCOGENIC PROTEIN INTO AN APOPTOTIC FACTOR:

TARGETING BCR-ABL TO THE MITOCHONDRIA

by

Jonathan Eric Constance

A dissertation submitted to the faculty of
The University of Utah
in partial fulfillment of the requirements for the degree of

Doctor of Philosophy

Department of Pharmacology and Toxicology

The University of Utah

May 2013

The University of Utah Graduate School

STATEMENT OF DISSERTATION APPROVAL

The dissertation of **Jonathan Eric Constance**
has been approved by the following supervisory committee members:

Michael R. Franklin	, Chair	**7/19/2012** Date Approved
Carol S. Lim	, Co-Chair	**8/16/2012** Date Approved
Donald K. Blumenthal II	, Member	**8/22/2012** Date Approved
Philip Moos	, Member	**8/22/2012** Date Approved
E. Dale Abel	, Member	**8/22/2012** Date Approved

and by **William Crowley**, Chair of
the Department of **Pharmacology and Toxicology**

and by Charles A. Wight, Dean of The Graduate School.

ABSTRACT

The advent of rational drug design to target a single molecular event, as so aptly demonstrated with tyrosine kinase inhibitor (TKI) therapy and Bcr-Abl, has set a precedent for the ability to attack malignancy directly at the level of the oncogenic event. However, in the last decade it has become clear that new therapeutic strategies for chronic myelogenous leukemia (CML) must move beyond the mere inhibition of Bcr-Abl's tyrosine kinase activity if a cure is to be found. TKI resistance, persistent leukemic stem cells, and the acute blast phase crisis remain major problems to be solved. This work describes the efforts to use the central leukemogenic protein of CML, Bcr-Abl (oncogenic event itself), to selectively destroy the diseased cells that harbor it.

The subcellular localization of Bcr-Abl determines its function. This is also true for Bcr-Abl's normal counterpart, c-Abl. When localized to the mitochondria, c-Abl is a potent inducer of cell death. However, c-Abl pro-death activity is disrupted in CML. The mitochondriolytic mechanism of 'death-directed' c-Abl is unknown. Yet, under conditions of cell stress from a variety of sources (e.g., endoplasmic reticulum stress, genotoxic agents, and oxidative stress) active c-Abl migrates to the mitochondria causing dysfunction and cell death. Our direct targeting of c-Abl and Bcr-Abl to the mitochondria demonstrated the sufficiency of c-Abl alone to kill leukemia cells and of Bcr-Abl's ability to recapitulate this function.

The central hypothesis of this study is that *forcing Bcr-Abl to the mitochondria will selectively induce the death of leukemic cells by converting Bcr-Abl into an apoptotic factor*. This approach restores a defunct apoptotic pathway (i.e., the mitochondrial 'death-directed' c-Abl pathway) and does not rely on the indirect engagement of (often dysregulated) cell death mechanisms like many chemotherapeutics. c-Abl requires a mitochondrial chaperone (protein kinase Cδ). Therefore, we designed a protein chaperone, the intracellular cryptic escort (iCE), for Bcr-Abl that selectively functions in the pro-oxidative environment of CML cells. Though, the iCE did not move Bcr-Abl to the mitochondria, it did synergistically and selectively kill CML cells as a combination with imatinib or alone was as toxic as high dose imatinib.

TABLE OF CONTENTS

LIST OF FIGURES

LIST OF TABLES

LIST OF ABBREVIATIONS

ABD	Actin binding domain
ADA	Anti-drug antibodies
AIF	Apoptosis-inducing factor
ANT	Adenine nucleotide translocase
apaf-1	Apoptotic protease activating factor 1
Arg	Abl related gene
ATAP	Amphipathic tail-anchoring peptide
B-ALL	B-cell acute lymphoblastic leukemia
Bcl-2	B-cell lymphoma-2
Bcl-X_L	B-cell lymphoma-extra large
BCR	Break point cluster region
BH	Bcl-2 homology domain
BHAP	Bi-functional, HER2-blocking and apoptosis-inducing peptide
B-Raf	Serine/threonine kinase B-Raf
c-Abl	Abelson proto-oncoprotein
CAS	Crk-associated substrate
CC	Coiled-coil
ccmut3	Coiled-coil mutation set 3
CCyR	Complete cytogenetic response
CLL	Chronic lymphocytic leukemia
CML	Chronic myelogenous leukemia
CMolR	Complete molecular response
cMTS	Cryptic mitochondrial translocation sequence
COX	Cytochrome c oxidase
CPP	Cell penetrating peptide
Crk	Cytoskeleton-associated adaptor protein
CYPD	Cyclophilin D
cyt c	Cytochrome c
DCA	Dichloroacetate
DHPH	Dbl homology/Pleckstrin homology
Drp1	Dynamin related protein 1

EGFP	Enhanced green fluorescent protein
EGFR	Epidermal growth factor receptor
Endo G	Endonuclease G
ER	Endoplasmic reticulum
ETC	Electron transport chain
FGF1	Fibroblast growth factor 1
FHIT	Fragile histidine triad protein
GAP	GTPase activating protein
G-CSF	Granulocyte-colony stimulating factor
GDP	Guanosine diphosphate
GEF	Guanine nucleotide exchange factor
GSAO	4-(N-(S-glutathionylacetyl)amino) phenylarsonous acid
GSTA4-4	Glutathione S-transferase A4-4
GTP	Guanosine triphosphate
H_2O_2	Hydrogen peroxide
HDM2	Human double minute 2
HER2	Human epidermal growth factor receptor 2
HIF-1	Hypoxia inducible factor-1
HIV-TAT	Human immunodeficiency virus – Trans-activator of transcription
HK	Hexokinase
HR	Complete hematologic response
HSP	Heat shock protein
HtrA2	High temperature requirement protein A2
IAP	Inhibitor of apoptosis
iCE	Intracellular cryptic escort
IFN-α	Interferon-α
IM	Imatinib mesylate
IMM	Inner mitochondrial membrane
IMS	Intermitochondrial membrane space
IP3R	Inositol 1,4,5-triphosphate receptor
JACoP	Just another colocalization plugin
JNK	c-jun NH_2 kinase
Kv	Voltage-gated potassium (channel)
LDH	Lactate dehydrogenase
LMB	Leptomycin B
LSC	Leukemic stem cell
MAPK	Mitogen-activated protein kinase
MCP	Mitochondrial carrier protein
MCU	Mitochondrial calcium uniporter

Mfn1	Mitofusin 1
Mfn2	Mitofusin 2
$MitoK^+$	Mitochondrial potassium (channel)
MnSOD	Manganese superoxide dismutase
MOM	Mitochondrial outer membrane
MOMP	Mitochondrial outer membrane permeabilization
MTCH2/MIMP	Mitochondrial carrier homologue 2/Met-induced mitochondrial protein
mtDNA	Mitochondrial DNA
mTOR	Mammalian target of rapamycin
MUC-1	Mucin-1
mUPR	Mitochondrial unfolded protein response
Nab	Neutralizing antibodies
nAChR	Nicotinic acetylcholine receptor
NES	Nuclear export signal
NF-κB	Nuclear factor-kappaB
NLS	Nuclear localization signal
NOS	Nitric-oxide synthase
OMM	Outer mitochondrial membrane
Opa1	Optic atrophy 1
OXPHOS	Oxidative phosphorylation
p38	Protein 38 mitogen-activated protein kinase
p53	Tumor suppressor protein 53
p63	Tumor suppressor protein 63
p73	Tumor suppressor protein 73
PBSC	Peripheral blood stem cells
PCC	Pearson's correlation coefficient
PCD	Programmed cell death
PDGFR	Platelet-derived growth factor receptor
PDH	Pyruvate dehydrogenase
PDK1	Pyruvate dehydrogenase kinase
PENAO	4-(N-(S-penicillaminylacetyl)amino) phenylarsonous acid
Ph	Philadelphia chromosome
PI3K	Phosphoinositide-3 kinase
PKA	Protein kinase A
PKC	Protein kinase C
PLSCR1	Phospholipid scramblase 1
PMA	Phorbol myristate acetate
PS	Phosphatidylserine
PTP	Permeability transition pore

PUMA	p53-upregulated modulator of apoptosis
q-PCR	Real-time quantative polymerase chain reaction
RAS	Rat sarcoma
RB	retinoblastoma protein
RhoA	Ras homolog gene family member A
ROI	Region of interest
ROS	Reactive oxygen species
S	Serine
S/T kinase	Serine/threonine kinase
SAHB	Stabilized alpha-helices of Bcl-2 family protein
SH2	Src homology domain 2
SH3	Src homology domain 3
Smac	Second mitochondria-derived activator of caspase
STAT5	Signal transducer and activator of transcription
T	Threonine
tBid	Truncated Bid
TCA	Tricarboxylic acid (cycle)
TEAM-VP	Targeted endothelial apoptogenic mitochondrio-active VpR-derived peptide
TIM	Translocase of the inner membrane
TKI	Tyrosine kinase inhibitor
TNF-α	Tumor necrosis factor α
TOM	Translocase of the outer membrane
TRAIL	TNF-related apoptosis-inducing ligand
TRAP-1	Tumor necrosis factor receptor-associated protein-1
TSPO	Translocator protein
UPR	Unfolded protein response
VDAC	Voltage-dependent anion channel
VpR	Viral protein R
Y	Tyrosine

ACKNOWLEDGEMENTS

The work described herein was completed in the C.S. Lim Laboratory, Department of Pharmaceutics and Pharmaceutical Chemistry at the University of Utah, during the years 2008-2012.

There are many people to whom I owe a debt of gratitude, but none more than my wife, Cherie, who has made this possible. My two boys, Isaac and Henry, have brought me a deep joy that grows, as they do, and the support of my parents has also been ever present. Of course, I would not have started graduate school if it had not been for L. Wojcik (who put the idea in my head), two very good friends, Roy Smeal and Bryon Wright, and Michael Franklin, who took a chance on me and has been my mentor from long before the beginning. I was amazingly fortunate to have been able to 'incubate' in the MRF lab and get to know and learn much from Rosie, Greg Lamb, Wael El-Sayed, Tarek Aboul-Fadl, Dori Arch and the ADD group. Somehow the MRF and Yost lab (Yin and Yang of P450 pharmacology) coexist in suite 318, BPRB and I am grateful to Gary Yost and his lab bunch (Diane Lanza, Chris Reilly (who owes me two beers), Shane Cutler, Kiu Shahrokh, Chad Moore, Karen Thomas, Fred Henion) for the camaraderie and support through the years.

My early graduate days were spent training in the laboratories of Philip Moos (big thanks to Matt Honeggar, Robin Poerschke, and Colleen Rock) and Kristen Keefe, I have been able to put to use what they taught me practically every day since. If I wasn't in the lab, I was probably in class, likely taught by Don Blumenthal, who has wisdom and

patience in rare quantities, or William Crowley who demanded the best and then made you better still. I was also taught, and given the chance to teach, by Doug Rollins and Steven Bealer and I will always be grateful to them for their advice and encouragement.

Ultimately, I wound up in the Lim lab, a world unto itself. I have been able to work and become friends with the very best: Mudit Kakar, Amy Cadwallader, Rian Davis, Andy Dixon, Mohanad Mossalam, Karina Matissek, David Woessner (fellow PHTX secret society member), and the newbies like Abdul 'full pass' Okal, Ben Bruno, Geoff 'the scientist' Miller, and Shams Reaz. To my gifted mentees, Emmeline Tran, Akemi Nishida, and Sam 'potash' Despres, thank you for letting me participate in your scholarly endeavors.

Carol Lim's mentorship has been the cornerstone of my professional development. Joining the Lim lab was the right decision, but Carol Lim has made it an invaluable one. The gifts of her wisdom and guidance have seen me through my graduate work and will continue to resonate throughout my professional life. I can never thank her enough.

Finally, I would like to thank my dissertation committee members, Carol Lim, Michael Franklin, Don Blumenthal, Philip Moos and Dale Abel, each of whom has freely given me their time and scientific advice. It is my hope that they can see their influence in this and my future work.

CHAPTER 1

BACKGROUND AND SIGNIFICANCE

Summary

Tyrosine kinase inhibitors (i.e., imatinib and, more recently, nilotinib and dasatinib) represent the current gold standard for CML therapy but are not curative (1). The ever present threat of relapse and/or disease progression from the retention of a "Bcr-Abl enriched" $CD34^+$ refractory leukemic stem cell (LSC) population has been described as the sword of Damocles hanging over every CML patient (2-8). A commonality across therapy-indifferent CML is high Bcr-Abl expression (8). Nonetheless, it is now clear that new therapies with a curative aim must operate beyond the mere inhibition of Bcr-Abl's kinase activity (9).

The oncogenic fusion protein Bcr-Abl and the normal c-Abl are essentially two forms of the same protein but in different "moods" (10). The functional specificity (often antagonistic) of both Bcr-Abl and c-Abl is dictated by subcellular location (11-17). For instance, c-Abl can promote mitogenesis when located in the cytoplasm, cell cycle arrest when activated in the nucleus, and upon translocation to the mitochondria it can induce the loss of mitochondrial membrane potential (ψ_{MIT}), depletion of ATP, and apoptotic/necrotic cell death (13). Likewise, in CML cells, Bcr-Abl is oncogenic in the cytoplasmic space but causes cell death if moved to the nucleus (12, 18, 19). While the

nuclear entrapment or targeting of Bcr-Abl to the nucleus of CML cells has proved effective in killing some CML cells, the effect is relatively mild and does not kill $CD34^+$ leukemic stem cells (LSC) (12, 19-21).

Targeting the mitochondria to induce irreversible cell death, selectively for malignant cells, is considered a prime strategy for success in hematological malignancies (22) and is reviewed in Chapter 2. Broadly, the mitochondrion in a cancer context is an attractive target because the mitochondrion is central to cell death induction (23), is often in a state of precarious apoptotic balance described as, 'primed for death'(24), and exhibits structural and functional differences that can be exploited for therapy (25).

The mitochondrial translocation of c-Abl from the nucleus (e.g., genotoxic agents (26), ionizing radiation, TNFα, and Fas signaling), the endoplasmic reticulum (e.g. unfolded protein response (26, 27)), and the cytoplasm (e.g., proteasome inhibition (28) and ROS (29, 30)) has been determined, in many cases, to be essential for the induction of apoptosis (31, 32). Moreover, two highly effective $CD34^+$ LSC killing agents, arsenic trioxide and bortezomib (proteasome inhibitor), both induce cell death through the intrinsic apoptotic pathway by a c-Abl dependent mechanism (28, 33-35). However, the c-Abl death-directed pathway is suppressed in CML (36). Chapter 3 demonstrates, for the first time, without an external cellular insult (e.g., genotoxic agent), that restoring c-Abl translocation to the mitochondria is a viable mechanism for killing CML cells.

Since Bcr-Abl shares many of the same substrates as c-Abl (37-40) routing Bcr-Abl to the mitochondria may reiterate 'death-directed' c-Abl function (*Fig. 1.1*). Chapter 4 demonstrates the toxic consequences of targeting Bcr-Abl to the mitochondria and that the cell death effect, unlike c-Abl, is independent of Bcr-Abl's tyrosine kinase activity.

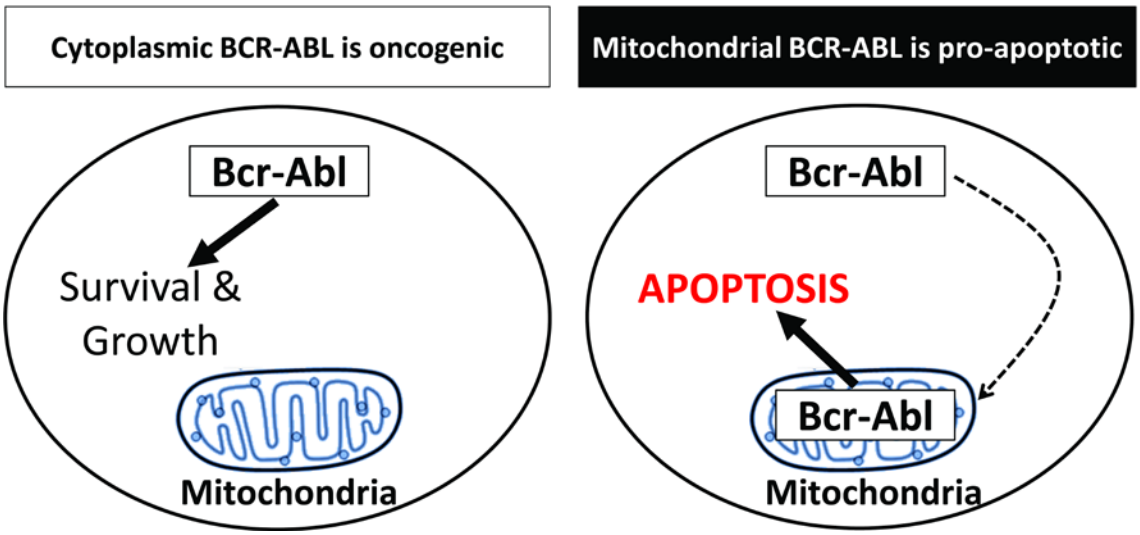

Figure 1.1. Conversion of Bcr-Abl to a pro-apoptotic factor. Within its cytoplasmic niche Bcr-Abl suppresses apoptosis and stimulates proliferation (left). If relocated to the mitochondria Bcr-Abl may re-engage the conventional c-Abl apoptotic mechanism (right).

This feature makes the Bcr-Abl-to-mitochondria strategy compatible with current tyrosine kinase inhibitor therapy. The proficiency of mitochondrial Bcr-Abl killing of CML cells led to the development of a small protein (the intracellular cryptic escort (iCE)) intended to force Bcr-Abl to the mitochondria (also described in Chapter 4). While the iCE bound to Bcr-Abl it did not translocate to the mitochondria. Yet, the iCE was uniquely toxic to CML cells with an equivalency to high dose imatinib and, as a combination with imatinib, strongly potentiated cell death. Therefore, the iCE is selectively active against CML cells by a mechanism that is separate from the inhibition of Bcr-Abl tyrosine kinase activity.

This endeavor has been based on developing a 'biologic' pharmacological approach to restore a suppressed apoptotic mechanism by converting Bcr-Abl and causative agent of CML, into an apoptotic instrument for eliminating leukemic cells (*Fig. 1.2*). The intent of this project has been to develop potential avenues that could be used to address the three major obstacles in current CML therapy all typified by high Bcr-Abl expression: resistance to tyrosine kinase inhibitors, persistent LSCs, and therapy-resistant blast phase crisis.

Background

Philadelphia chromosome positive leukemia

Chronic myelogenous leukemia (CML) is the most common form (>90%) of the Philadelphia (Ph) chromosome positive leukemias, which result from the t(9;22)(q34;q11) reciprocal translocation (41). From this translocation the oncoprotein Bcr-Abl, with its exclusively cytoplasmic distribution and aberrantly active tyrosine kinase, creates the pathogenesis of CML (41). The fusion of ABL1 (Abelson proto-

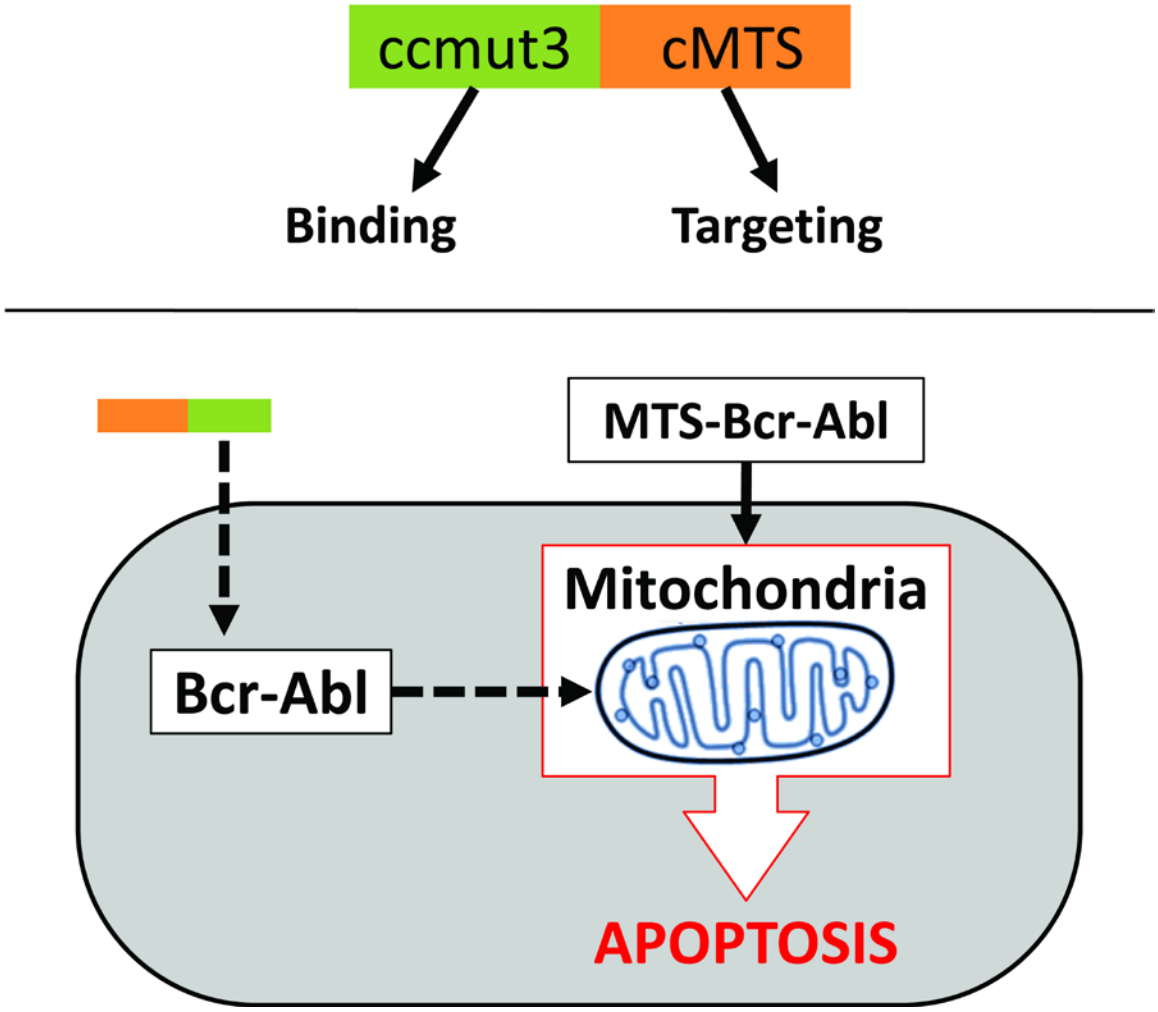

Figure 1.2. Schematic of major hypothesis. Exogenous Bcr-Abl targeted to the mitochondria (MTS-Bcr-Abl) will establish the proof of concept that mitochondrial Bcr-Abl induces CML cell death. The ccmut3 and cryptic mitochondrial targeting signal (cMTS) together create the intracellular cryptic escort (iCE) that is designed to bind to endogenous Bcr-Abl and then upon activation of the cMTS, translocate the iCE/Bcr-Abl complex to the mitochondria.

oncogene) and BCR (breakpoint cluster region) can occur at different breakpoints giving rise to three main variants of Bcr-Abl each with a distinct molecular weight (38). The $p190^{BCR-ABL1}$ (i.e., 190 kDa Bcr-Abl) gives rise to rare cases of CML and to almost 70% of cases of Ph^+ B-cell acute lymphoblastic leukemia (Ph^+ B-ALL). The $p210^{BCR-ABL1}$ variant is present in 90-95% of CML and around 30% of Ph^+ B-ALL patients, and finally, $p230^{BCR-ABL1}$ is present in patients with chronic neutrophilic leukemia (40, 41). All of these BCR to ABL1 fusions (but not the ABL to BCR) disrupt structural c-Abl autoinhibition and result in the constitutive activation of the tyrosine kinase (41). The precise manifestation of the leukemia is dependent on cellular context and intrinsic kinase activity of the Bcr-Abl fusion (1).

The Ph in CML presents across all hematopoietic lineages and the interchromosomal recombination phenomenon is more probable in primitive hematopoietic cells because of the closer spatial association of the BCR and ABL genes in early stages of the cell cycle compared to mature phenotypes (42). Accordingly, there is a general consensus that the origination of a Ph^+ translocation in a primitive pluripotent stem cell enables escape from the regulation of self-renewal mechanisms to establish a small population of leukemic stem cells (LSCs) (43). The rare LSCs are thought to be responsible for the maintenance of CML, by cycling between quiescent and active states (44). Progenitors of the LSCs preferentially expand in the myeloid lineage but the Ph^+ translocation is also found in erythroid and lymphoid lineages (45).

Both Bcr and c-Abl have intricate domain arrangements (*Fig. 1.3*) and when fused together, as Bcr-Abl, activate a variety of signaling pathways (41). c-Abl (within Bcr-Abl) contains the highly conserved Src-homology domains SH2 and SH3, a tyrosine

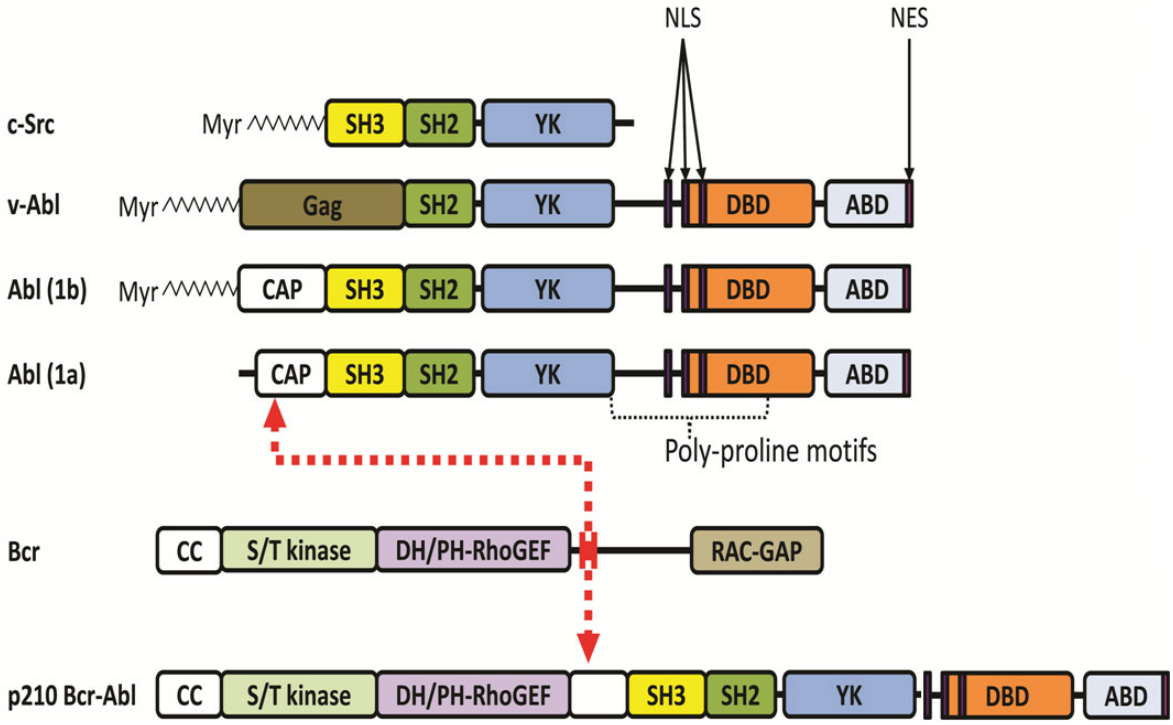

Figure 1.3. Domain arrangements. There are two isoforms of c-Abl that are identical except for the extreme N-termini of the so-called 'cap' region where the residue sequences vary. c-Abl 1b contains a 14-carbon myristoyl moiety (Myr) as does c-Src and the viral Gag fused v-Abl. Upon fusion to Bcr (dashed red line indicates approximate fusion points), the cap region of c-Abl is variously truncated to produce the p210 version of Bcr-Abl. Abbreviations used: Src homology 2 and 3 (SH2/SH3), catalytic tyrosine kinase (YK), DNA binding domain (DBD), actin binding domain (ABD), nuclear localization signal (NLS), nuclear export signal (NES), coiled-coil oligomerization domain (CC), serine/threonine kinase domain (S/T kinase), Dbl homology/pleckstrin homology-Rho guanine nucleotide exchange factor (DH/PH-RhoGEF).

kinase domain, four proline-rich SH3 binding motifs, a DNA binding domain, an actin binding domain (ABD), three nuclear localization sequences (NLS), and a nuclear export sequence (NES) (41). Essentially, the wild-type NH_2 "cap" region of c-Abl is, to varying degrees, replaced by Bcr depending upon the breakpoint in ABL1 (41). Bcr itself (within p210 Bcr-Abl) contains a coiled-coil oligomerization domain (CC), a serine/threonine kinase domain, and Dbl homology and pleckstrin homology domains (DHPH) (41). Not only does Bcr disrupt the autoinhibitory mechanisms of c-Abl upon fusion but it also facilitates via the CC domain the association of antiparallel Bcr-Abl homodimers that can stack to form a tetramer (41, 45). The dimerization of Bcr-Abl instigates transautophosphorylation of tyrosine residues in the activation loop of the catalytic domain and thereby reinforces its own aberrant tyrosine kinase activity (41).

The abnormal tyrosine kinase activity of Bcr-Abl successfully cancels out, in several ways, one of the most crucial cellular homeostatic regulators that can engage cell suicide mechanisms, that is, c-Abl (46-48). While c-Abl primarily promotes survival and suppresses apoptosis from the cytoplasm it can also induce apoptosis through a cytoskeletal cytoplasmic cell fate pathway (CAS/Crk cell suicide program) (49). Bcr-Abl's annexation of c-Abl's physiological tyrosine kinase function thwarts the cytoplasmic regulatory actions of c-Abl (e.g., by phosphorylating CrkL (which activates the RAS signaling pathway) instead of Crk) (28, 50), blocks c-Abl translocation (49), and as Bcr-Abl expression levels increase, c-Abl expression levels decrease (36). Perhaps most importantly, with diminished c-Abl function genetic damage accrues, the fidelity of DNA repair decreases, and the cell death threshold is drastically increased (13). Beyond the effects on c-Abl, Bcr-Abl blocks the intrinsic apoptotic pathway at multiple points.

Bcr-Abl expression decreases the free releasable calcium in the ER and attenuates ER/mitochondrial apoptotic coupling (51). Cytochrome c release is blocked by Bcr-Abl stimulated pathways inhibiting the proapoptotic protein Bad (via PI3K) (52) and antiapoptotic Bcl-2 family proteins are upregulated (via STAT5) (53). Downstream of cytochrome c release, Bcr-Abl interrupts the association of caspase-9 and apaf-1 preventing apoptosome formation (54).

It is difficult to appreciate Bcr-Abl's transformative power by dissecting individual pathways because there is a cumulative effect from the numerous downstream pathways often converging at common nodes which lead to cross-talk and reinforcement, thereby becoming something more than the sum of its parts (41). This has been demonstrated by introducing dominant-negative versions of STAT5, PI3K, and RAS where functional cooperation was required between any two of the three (in any combination) for the complete fruition of Bcr-Abl's oncogenicity when expressed in K562 cells (55). The originating cytosolic Bcr-Abl stimulation of these ramifying and converging pathways culminates in the intense promotion of cell survival and proliferation while suppressing apoptosis (41).

The expression of Bcr-Abl consequently manifests with the overproduction of immature white blood cells (56). The vast majority (90-95%) of patients are diagnosed with CML in the chronic phase where there is an excess of myeloid cell production (54). Without intervention, CML typically will progress, through an indolent (chronic) phase lasting 3-5 years on average, through a brief "accelerated phase" before transitioning into a therapy-resistant acute leukemia (blast phase crisis), which is fatal (1). Progression from chronic to blast phase, mechanistically, is not well understood, but is considered to

be dependent upon achieving a threshold of genetic damage that limits the capacity for differentiation beyond a primitive blast cell (55).

Therapy for chronic myelogenous leukemia

In 1998 clinical use of imatinib (Novartis, Basel, Switzerland) began and was approved by the FDA in 2001 ushering in the tyrosine kinase inhibitor (TKI) era of CML treatment (1, 57). Therapeutic success is defined specifically in CML by different levels of patient response. The scale ranges across 'complete hematologic response' (HR: normal blood cell counts and the patient is asymptomatic), to a 'complete cytogenetic response' (CCyR: no detectable Ph^+ metaphases), and finally, optimal response is a 'complete molecular response' (CMolR: absence of Bcr-Abl transcript as determined by q-PCR) (58). Prior to TKIs, CML was treated orally with hydroxyurea or busulfan which allowed patients to achieve normalization of blood cell counts (HR) but disease progression was not changed (59). With the introduction of interferon-alpha (IFN-α), CML patients could attain an improved hematological response and an increase in overall survival compared with hydroxyurea (60). IFN-α was generally paired with the antimetabolite agent cytosine arabinoside (cytarabine) as a standard therapeutic regimen until the advent of TKI therapy (61). There is a continued interest in the 'old', and arguably the original (62), anti-leukemic agent, arsenic trioxide (As_2O_3), as a potential candidate in resistant and/or residual stem cell forms of CML as well as in other leukemias (63, 64). It exhibits selective toxicity to Ph^+ versus Ph^- cells (the array of mechanisms of action attributable to As_2O_3 seem to be contingent upon cell type and context (65)) that is independent of Bcr-Abl kinase activity (35, 45). The proposed use of IFN-α in CML is also being revisited as an adjunct to TKI therapy for potential activity

against LSCs (66). However, the use of both As_2O_3 and IFN-α for the elimination of persistent LSCs remains tentative (67) and their use as adjunctive therapy still needs to be borne out in clinical trials, thus, for now, TKIs alone dominate the current therapeutic landscape for CML (68).

Imatinib mesylate (Gleevec®; originally STI571 for Signal Transduction Inhibitor 571) therapy is the current gold standard for CML and has revolutionized the treatment and outcomes for patients with CML (69). Administration of imatinib in the chronic phase very effectively delays, and in rare cases eliminates, the progression from chronic phase to blast phase crisis for most patients with CML (1). It takes on average 5-6 months for patients newly diagnosed with CML to achieve CCyR (70). With non-resistant forms of CML, TKIs suppress the pro-survival/anti-apoptotic signaling of Bcr-Abl and restore cellular apoptotic control (3). Most patients initially respond to imatinib therapy but, over time many ultimately become resistant (i.e., 'acquired' versus 'primary' resistance) and progress to blast phase crisis (69, 71, 72). With acquired resistance being determined as the loss of CCyR or HR during therapy (72).

Since the introduction of TKI therapy, resistant forms of CML have emerged as a major problem (69). Resistance to TKIs can manifest in a variety of forms (72). For example, in cases where the Src kinase, Lyn, is overexpressed, Lyn effectively keeps Bcr-Abl perpetually in an active state conformation (5) where imatinib cannot bind (4). Additionally, mechanisms such as increased drug efflux (73), clonal cytogenetic evolution, high expression levels of Bcr-Abl or STAT5 (74), and point mutations in Bcr-Abl are contributing factors to TKI resistance (6). At present, there are over 50 reported residue mutations in the tyrosine kinase domain from CML-resistant patients. These

residue substitutions can either influence Bcr-Abl conformation (e.g., conformations that less readily bind imatinib) or disrupt a contact/binding site for imatinib (72).

There are now two second generation TKIs, which are more potent inhibitors of Bcr-Abl (and inhibit a wider spectrum of kinases), nilotinib (Novartis) and dasatinib (Bristol-Myers Squibb, Princeton, NJ), which have been approved for imatinib-resistant forms of Bcr-Abl (75, 76). The notable exception is resistance due to the T315I Bcr-Abl kinase domain mutation that is currently untreatable and in these cases an allogenic stem cell transplant is recommended (72). However, in the last few years there has been an intensive effort to develop agents that are active against T315I mutants. Ponatinib, the most advanced third generation TKI, is active against T315I and other Bcr-Abl mutants, and is in the planning stages for phase III clinical trials (77). It may eventually supplant the use of nilotinib and dasatinib in imatinib-resistant CML (78). Additionally, several 'multi-targeted' kinase inhibitors developed initially against the S/T aurora kinases (and currently progressing through early clinical trials) have also shown efficacy in blocking the Bcr-Abl T315I activity (79). Pre-clinically, several small molecule agents are in development that allosterically inhibit Bcr-Abl (e.g., Genomics Novartis Foundation-2 (GNF-2)) or induce the degradation of Bcr-Abl (e.g., WP1130 and phenethyl isothiocyanate (PEITC; found in cruciferous vegetables)) with high specificity for and activity against Bcr-Abl (including T315I) (80, 81). Bcr-Abl activity can also be blocked by disrupting its coiled-coil domain mediated homo-oligomerization with an optimized coiled-coil (e.g., ccmut3) (82). Peptide inhibitors such as the ccmut3 are also less likely to succumb to Bcr-Abl point mutation acquired resistance or be subject to increased drug efflux mechanisms compared to small molecules (83).

Accompanying the emerging problems with resistance is the increasing literature on the longer term consequences of TKI therapy (84). Most adverse events are hematologic in nature; however, these toxicities seem particular to each TKI and the alternate use of another approved TKI has been effective in circumventing intolerance (85). Still the potential for compromised genetic stability/DNA repair and cell homeostasis in non-CML cells due to c-Abl inhibition (4, 73) as well as possible cardiovascular risks (74) are problematic. For instance, nilotinib has a black box warning for QT prolongation (78) and ponatinib is associated with platelet dysfunction (86). Moreover, some situations are considered ill-suited to TKI use such as those requiring combination chemotherapies, which depend on c-Abl-induced functional DNA mismatch repair activation responses for efficacy (6).

With TKI therapy the durability of response, response rate, and rate of progression from chronic to blast phase CML are all critically dependent upon both early treatment and the level of Bcr-Abl expression (1, 41). Postponement of treatment increases the risk of resistance and narrows the time to blast phase crisis (41). The only known cure for CML remains allogenic stem cell transplantation but is rarely used due to the high associated morbidity and mortality (87). The vast majority of patients on TKI therapy have persistent CML and relapse if therapy is stopped, even in patients that have undetectable levels of Bcr-Abl (i.e., cMolR) (69, 88). Therefore, TKI therapy is currently recommended to be continued daily for one's lifetime (89).

Linked to the problem of molecular resistance in CML is the issue of persistent LSCs. LSCs may be responsible for the emergence of TKI-resistant strains of Bcr-Abl (2) (perhaps through clonal evolution and/or selective pressure from treatment (90)) with

drug target mutations (1, 3, 91). LSCs are generally considered to be the true crux of the problem in finding a cure to CML (63, 88).

A model developed to fit with the kinetics of the molecular response to imatinib by Michor and colleagues (43), fits with the general consensus regarding LSCs (44, 92, 93) and describes four 'compartments' aligning with the development of hematopoietic cells. After the chromosomal translocation occurs in a leukemia-initiating cell (presumably phenotypically indistinguishable from a normal $Lin^{-}CK34^{+}CD38^{-}$ hematopoietic stem cell (2)) a subpopulation of LSCs is established that can continuously renew. Derived from the LSCs are the progenitor cell (non-self-renewing), differentiated cell, and mature terminally differentiated cell populations (43). Each of the four compartments of leukemia cells are killed by TKIs except the LSCs. Failure by TKI therapy to eradicate LSCs is thought to be due to the LSCs adopting a quiescent state or another molecular mechanism circumventing the necessity of Bcr-Abl activity for continued survival (2, 93).

The TKI refractory LSCs are, to a point, dependent upon Bcr-Abl-mediated tyrosine phosphorylation and stabilization of β-catenin (44). The cooperativity between Bcr-Abl and β-catenin provides an alternate route by which CML cells can survive TKI therapy (2). However, TKIs do eliminate a portion of the LSC pool initially (providing a basis for some of the debate over whether or not LSCs are sensitive to Bcr-Abl inhibition (94)), but the residual LSC levels return despite continued TKI treatment (2). It is thought that cells with less Bcr-Abl are more readily killed thereby selecting for LSCs containing higher levels of Bcr-Abl (95). Other studies have determined that the refractory LSC population is "enriched" for Bcr-Abl (7, 94, 95). It seems likely that both increased

expression of Bcr-Abl and states of dormancy serve as mechanisms for LSCs to escape TKI therapy.

It has been proposed that stimulating quiescent cells to enter active cycling could make them vulnerable to current therapeutics (43). The use of granulocyte-colony-stimulating factor (G-CSF) has been evaluated for the induction of stem cell mobilization in patients who achieved complete cytogenetic conversion in order to obtain enough peripheral blood stem cells for autografting (even suggesting that PBSC collection yields were enhance by withholding imatinib (96)) (96-98). The strategy of stimulating quiescent leukemic stem cells as a means to sensitize them to TKI therapy has been pursued, based on promising *in vitro* studies (99). Several pilot safety and clinical trials have investigated the combined use of imatinib and G-CSF (100-102). However, the stimulation of quiescent stem cells is thought to carry a significant risk for the acquisition of resistance mutations in addition to increasing disease burden (or progression to blast phase) if leukemic stem cells are not responsive to imatinib. Treating with G-CSF even raises the possibility that the stimulating factors themselves could lead to the protection of LSCs (43). The premise of using G-CSF is particularly brought into question when recent work by Corbin et al. demonstrated that inhibiting Bcr-Abl kinase activity does not decrease CML stem cell survival (103). This has revealed a different dynamic between Bcr-Abl and Ph^+ primitive cells. Instead of being 'oncogene addicted' the LSCs can merely revert to a normal dependence on cytokines for survival (89, 103). For that reason, therapies that biochemically ablate Bcr-Abl will not be sufficient to address the problem of LSCs (78).

Other approaches to target the LSC population have been to engage the immune response (e.g., 'immune engineering' (58) or IFN-α treatment (66)) or stimulate the activity of tumor suppressor proteins (72). Clinical trials using Bcr-Abl junction-specific peptides as immunogenic tumor-associated antigens to vaccinate patients in CCyR on imatinib showed overall improvement in disease stabilization (104). While there is promise in this strategy the optimization of antigenic peptides is proving to be non-trivial (e.g., uneven response profiles across CML cell subpopulations) (105). LSCs have also been shown to be susceptible to the induced activation of the tumor suppressor p53 (88). However, the p53 loci is the most frequently (~25% in blast phase (106)) mutated as CML progresses (72, 107) and several genes responsible for the up-regulation of p53 are also mutated at a high frequency in CML (72) making this strategy difficult to widely implement.

Intrinsic to the LSC debate is the interpretation of the recently completed STIM (STop IMatinib) trial (108). The STIM trial assessed whether CML patients who had achieved cMolR (>2 years) could safely discontinue imatinib therapy. The findings indicated that, at least in some patients, the discontinuation of imatinib was possible, but overall disease relapse was more common (108). However, whether or not a patient is 'cured' of CML remains both to be determined and a tremendous technological challenge (109, 110).

Subcellular location dictates function

Bcr

Bcr is expressed in 130, 160 (major variant) and 190 kDa versions and is associated with endosomal membranes as a part of the endosomal sorting complex (111).

The functions of Bcr are generally not well understood but Bcr is known to play a key signaling role as it relates to the negative regulation of Rac (a small GTPase of the Rho family) in macrophage phagocytosis (112). Bcr contains a coiled-coil oligomerization domain, serine/threonine kinase domain, a Dbl/Pleckstrin homology Rho-specific guanine nucleotide exchange factor (RhoGEF) domain, and a C-terminal Rac-GTPase activating (Rac-GAP) domain (*Fig. 1.3*) (113). The Rac-GAP domain is not included in Bcr-Abl, but is included in the complementary non-transformative Abl-Bcr which is also expressed in most CML patients (113, 114). Interestingly, Bcr can act as a negative regulator of Bcr-Abl (115), but the S/T kinase function is required (116). This implies that Bcr does not act as a dominant-negative via the coiled-coil domain as Bcr and Bcr-Abl are, for the most part, spatially separated (111).

The CC is of central importance with respect to the transformative potential in the Bcr portion of Bcr-Abl (117). However, key phospho-tyrosine sites and RhoGEF activity also contribute to the oncogenic capacity of Bcr-Abl (118). The Bcr RhoGEF is constitutively active in Bcr-Abl and functions, independently of tyrosine kinase activity, to catalyze the exchange of GDP for GTP for the activation of the only known substrate, RhoA (119, 120). The pharmacologic inhibition of RhoA signaling synergized with imatinib to block the proliferation of $CD34^{+}$ patient-derived CML cells (121). This demonstrated the therapeutic relevance of inhibiting the activity of the Bcr portion of Bcr-Abl in addition to the tyrosine kinase.

Additionally, the Bcr phospho-Y177 residue is a particularly important binding site for Grb2 which activates the RAS pathway (122). Although the kinase activity of Bcr-Abl is usually responsible for the auto-phosphorylation of Y177, a Src tyrosine

kinase (Hematopoietic cell kinase (Hck)) can also phosphorylate Y177. This allows for Bcr-Abl kinase-independent RAS activation, with Bcr-Abl acting as a scaffold for oncogenic signaling complex formation.

c-Abl

The 140 kDa nonreceptor tyrosine kinase c-Abl is one of two tyrosine kinases (i.e., c-Abl and Arg) in a subclass of the Src family of kinases (11). Normally, c-Abl is found widely distributed intracellularly within the nucleus, endoplasmic reticulum, cytosol, with the cytoskeleton, and at the cell membrane with only a small fraction associated with the mitochondria (< 4%) (11, 26). The activity of c-Abl is tightly regulated through autoinhibitory intramolecular interactions (10), posttranslational modifications (11), and protein interactions (e.g., 14-3-3 proteins (123) and retinoblastoma protein (124)).

As the 'central apoptotic tyrosine kinase' the pro-death activity of c-Abl has been extensively studied (125). c-Abl can trigger apoptosis at the level of the nucleus, cytoskeleton, and/or mitochondria via a host of interactions (10, 11). For instance, c-Abl stimulates and typically amplifies cell death induction cascades via direct interactions with p53 (11, 123, 124), p63 (126), p73 (37, 127), phospholipid scramblase 1 (PLSCR1; a major regulator of PS exposure in apoptotic cells that is also present in the mitochondria (128)) (37, 129, 130), p38 MAPK (131) and initiator and effector caspases (37, 126, 132, 133). c-Abl has an interdependent, but indirect, relationship with the pro-death signaling of c-jun NH_2-terminal kinase (JNK) (134). c-Abl is an early amplification factor in apoptosis through positive feedback mechanisms relating to direct interactions

(cleavage into constitutively active forms) with caspases 3, 7, 8 and 9 (126, 135-137) before cell death is morphologically apparent (138).

c-Abl translocation to the mitochondria induces cell death

c-Abl has been termed a "mitochondrial wracking factor" (32) and was the first tyrosine kinase found to associate with the mitochondria (139). In leukemic cells, treatment with H_2O_2 stimulates c-Abl translocation (mediated by the novel protein kinase C δ (PKCδ) (140)) to the mitochondria resulting in an increase from ~4% to ~20% of total cellular c-Abl followed by mitochondrial dysfunction and cell death (30). Moreover, the H_2O_2 induced cell death effect can be blocked with imatinib (29). Likewise, under conditions of ER stress (e.g., unfolded protein response (UPR)), c-Abl is activated and translocates (again mediated by PKCδ) from the ER to the mitochondria and is essential for ER-stress-induced mitochondrial-dependent apoptosis (26, 27).

At present the submitochondrial location and substrates for c-Abl are unidentified (29). The JNK and p38 MAPK pathways have been proposed to be involved in mitochondrial c-Abl mediated cell death (26, 27, 141). In a reciprocal manner, c-Abl is essential to the activation of the p38 and JNK stress pathways (131, 141) in response to genotoxic agent (e.g., cisplatin, etoposide, and doxorubicin)-induced cell death (126). Interestingly, both c-Abl and Bcr-Abl directly activate p38 in response to cisplatin and can do so independently of their tyrosine kinase activity (38). The kinase activity of c-Abl and Bcr-Abl is, in certain cases, dispensable for the induction of apoptosis (31, 38, 142). Furthermore, under conditions of genotoxic stress, ionizing radiation, TNFα and Fas signaling, active c-Abl relocates from the nucleus to the cytoplasm in hematopoietic

cells and activates the JNK stress pathway (26). Both JNK (JNK translocates to the mitochondria in response to DNA damage (143)) and c-Abl have been found to coimmunoprecipitate with mitochondrial Bcl-X_L (27, 38). Since JNK mitochondrial translocation is also stimulated by the phorbol ester response (i.e., agents that activate protein kinase C) (144) this raises the possibility of a JNK-cAbl-PKCδ complex that targets the mitochondria.

Mitochondrial dysfunction and cell death from active c-Abl translocation does not require any new gene expression and has been shown to be independent of p53, p73, Bax, retinoblastoma protein (Rb) and Fas receptor presence (145, 146). The residues that c-Abl interacts with in p53, p63, and p73 are highly conserved, and since Bcr-Abl interacts with p73 at these same residues, it is possible, but unconfirmed, that Bcr-Abl could also interact with p53 and p63 (37, 126).

Bcr-Abl

The oncogenic capacity of Bcr-Abl is uniquely suited but limited a specific cytoplasmic environment (13-15). As with c-Abl, Bcr-Abl has demonstrated opposing functions that are dependent upon its subcellular location (12), and c-Abl and Bcr-Abl broadly share many of the same substrates (e.g., p38 (38) and p73 (37)) (39, 40).

Although Bcr-Abl is mostly bound to actin (~70%) (16) this binding interaction can be overcome with imatinib (19, 147). Aggregates of Bcr-Abl in discrete cytoplasmic foci relocalize in the nucleus upon treatment with imatinib (18, 148). However, these foci are very rapidly exported back into the cytoplasm (12). Vigneri and Wang demonstrated Bcr-Abl's dual nature by trapping Bcr-Abl in the nuclear compartment which caused CML cell death (12). Entrapping Bcr-Abl in the nucleus using imatinib and leptomycin B

(nuclear export inhibitor) was partially selective for Ph^+ cells (12, 20). Yet nuclear entrapment by this method is not clinically viable as the imatinib dose was 10-fold higher than used therapeutically and leptomycin B is extremely neurotoxic (20). The Lim Laboratory used a different approach to 'trap' Bcr-Abl in the nucleus, either through expression of an exogenous Bcr-Abl fused to NLSs (i.e., 4NLS-Bcr-Abl) or by moving endogenous Bcr-Abl to the nucleus with an optimized Bcr-Abl-binding coiled-coil fused to NLSs (i.e., 4NLS-ccmut3) (19, 147). Corroborating earlier results by Vigneri and Wang, the exogenously expressed Bcr-Abl targeted to the nucleus caused CML cell death (19). This also provided evidence that Bcr-Abl was actively toxic in the nuclear compartment and that cytoplasmic depletion was not the cause (or sole cause) of cell death.

The original study by Wang suggested that after nuclear entrapment of Bcr-Abl, washout of imatinib was required for cell death and therefore, kinase activity was essential (12). Later however, Wang discovered that nuclear c-Abl could efficiently cause cell death by a kinase-independent mechanism (149). Work in the Lim Laboratory (by Emmeline Tran) demonstrated that the direct nuclear targeting of a kinase-dead Bcr-Abl mutant (i.e., 4NLS-Bcr-Abl-KD) in K562 cells caused cell death equivalent to the kinase active 4NLS-Bcr-Abl (150). At a later time, it was shown that the forced nuclear translocation of Bcr-Abl by the 4NLS-ccmut3 (Andy Dixon, Lim Laboratory) did not induce cell death beyond control in K562 cells (personal communication, Andy Dixon, PhD). Taken together, the implication is that the homodimerization of Bcr-Abl but not the tyrosine kinase activity is the mechanistically important feature underpinning the toxicity of nuclear Bcr-Abl. Bcr-Abl may be acting only as a partial proxy to c-Abl

whether in the cytoplasm (prosurvival) or nucleus (prodeath) (12). However, if nuclear Bcr-Abl is operating in an analogous manner to nuclear c-Abl, the relatively modest amount of cell death may be explained by the interrupted nuclear DNA damage response in CML cells and/or through layers of negative regulation present for nuclear localized c-Abl (138, 151, 152).

Mitochondrial translocation signals

Protein localization to different subcellular compartments is directed by signal sequences encoded in the protein itself (19). Mitochondria are unique cellular organelles in that, like the nucleus, they contain DNA (mtDNA). Nonetheless, the vast majority (~99%) of mitochondrial proteins are coded for in nuclear DNA requiring the import of ~1000 different cytosolic proteins (12, 153, 154). The mechanics of protein import at the level of the mitochondrial membranes are intimately linked to mitochondrial function (e.g., membrane organization, respiration, and endoplasmic reticulum-to-mitochondria contact) (155) and the import of proteins (i.e., cytosolic versus mitochondrial balance of proteins containing an import sequence) can be influenced by the physiologic status of the cell creating an adaptive system for regulating homeostasis at the cellular level (156, 157).

Mitochondrial protein import can occur by at least five different pathways. Conventional protein import into the mitochondria is conducted by the pre-sequence pathway or the carrier pathway for proteins with internal noncleavable MTSs (158). For example, most matrix-targeted proteins (e.g., ornithine transcarbamlyase (OTC)) are recognized and imported via the pre-sequence pathway through positively charged N-

terminal sequences of about 20-60 residues with an amphipathic (one face is positively charged and the other is hydrophobic) α-helical structure (159, 160). Import signal structure becomes more complex to accommodate variations in sorting to submitochondrial locations (including specific regions of the matrix) and are encoded by internal and/or pre-sequences (158). Recently, the β-barrel import pathway, mitochondrial intermembrane space assembly, and α-helical insertion pathways have been elucidated (155).

Each pathway, to varying degrees can facilitate protein targeting to four general mitochondrial regions, the OMM, IMS, IMM and the matrix (161) (*Table 1.1*) . Central to all of the import pathways are the protein translocases located at and within the mitochondrial membranes (152). These translocases recognize signal sequences or motifs on proteins and direct the import and submitochondrial localization of the sequence bearing proteins (138). The outer membrane (OMM) of the mitochondria hosts the translocase complex of the outer membrane (TOM) while the inner membrane (IMM) contains translocase of the inner membrane complexes (TIM) (162). The precise system of mitochondrial protein routing and distribution is achieved by the decoding of signal sequences, regulation (e.g., posttranslational modifications such as phosphorylation at the level of the imported protein or the import machinery), and the dynamic coordination of the import/sorting machinery.

A cryptic MTS is a sequence that is not imported into the mitochondria unless it is activated or revealed by a molecular event such as, proteolytic cleavage (153), phosphorylation (163), or a point mutation (164). For instance, phosphorylation can induce a conformational change in a protein allowing chaperone proteins to recognize

Table 1.1. Sequences for targeting proteins to specific submitochondrial compartments. Well characterized residue sequences that specifically target proteins (hetero-proteins) to the various submitochondrial compartments listed. These MTSs are used in Chapters 3 and 4 to target c-Abl and Bcr-Abl, respectively, to the mitochondria.

Target compartment	**MTS**	**Sequence**	**Derived from**	**Refs**
mitochondrial matrix	Matrix	MLFNLRILLNNAAFRN GHNFMVRNFRCGQPL QNKVQ	Ornithine transcarbamylase (OTC) Glutathione S-transferase A4-4 (cMTS)	(165) (163)
mitochondrial intermembrane space	IMS	RSVCSLFRYRQRFPVL ANSKKRCFSELIKPWH KTVLTGFGMTLCAVPI	Second mitochondria-derived activator of caspases (SMAC)	(166)
mitochondrial inner membrane	IMM	MSVLTPLLLRGLTGSA RRLPVPRAKIHSL	Subunit VIII of cytochrome c oxidase	(167)
mitochondrial outer membrane	OMM	RKGQERFNRWFLTGM TVAGVVLLGSLFSRK	Bcl-X_L	(168)

and bind a formerly cryptic signal (169). The glutathione S-transferase A4-4 (GSTA4-4) cryptic MTS (cMTS) translocates from the cytoplasm to the mitochondria upon serine and/or threonine phosphorylation (163). The activating cMTS phosphorylation is mediated by the PKA and/or PKC families of protein kinases based on the intracellular level of reactive oxygen species (ROS) (163). Under conditions of increased oxidative stress, as found in CML cells (40, 170-172), the cMTS is robustly targeted from the cytoplasm to the mitochondria (163). Bcr-Abl strongly stimulates the production of ROS causing CML cells to have a high cellular oxidative stress background (40, 172). cMTS targeting can be further enhanced with the addition of PKA/PKC activators, several of which have demonstrated antileukemic properties (144). Chapter 3 confirms and extends the oxidative stress activated translocation of the cMTS which is robustly targeted to the mitochondria by the inherent level of ROS in K562 cells.

K562 cells and ROS

The multipotential undifferentiated blastic Ph^+ K562 cell line was derived from a CML patient in terminal blast phase crisis and is considered a highly relevant model of CML (173, 174). K562 cells have high basal levels of ROS due to Bcr-Abl's stimulation of the PI3K/mTOR pathway leading to overactivation of the mitochondrial electron transport chain (175). Elevated intracellular ROS can lead to the activation of transcription factors (e.g., HIF-1 and NF-κB) leading to a host of protein expression profiles that contribute to malignancy such as, proliferation, survival, and metastasis (25). The K562 cell line serves as a prototypical example of elevated ROS in oncogenically transformed cells (176). Bcr-Abl signaling also induces the expression of NF-κB which

acts to temper ROS production. Thereby, Bcr-Abl elevates ROS levels while keeping the total ROS below a cytotoxic threshold (177). Overall, the elevated ROS in a leukemic context are not solely dependent upon Bcr-Abl. Elevated ROS is common in many cancers, and as mutations in mtDNA or nuclear DNA accrue this affects components of the mitochondrial respiratory chain and results in ROS overproduction and oxidative damage to mitochondria and other macromolecules (DNA) in a vicious spiral (178).

Imatinib, while inhibiting Bcr-Abl, also induces cytotoxic levels of ROS production by a mechanism separate from that of Bcr-Abl. In cells with and without Bcr-Abl (K562 and melanoma B16F, respectively), imatinib treatment induced cytotoxic levels of ROS via a JNK-mediated mechanism (177, 179). However, in Bcr-Abl-positive cells imatinib leads to an initial decrease in ROS by Bcr-Abl inhibition (via block of PI3K signaling). Yet, imatinib treatment induces apoptosis by both classical and atypical routes (e.g., via Omi/HtrA2 serine protease activity) (180). The classical route is typified by ROS overproduction while the atypical apoptotic pathway can occur in a ROS-independent manner (181). Bcr-Abl's activation of NF-κB prevents cytotoxic levels of ROS from developing but this is blocked by imatinib (177). Therefore, ROS levels are elevated due to the presence of Bcr-Abl, and when Bcr-Abl is inhibited by imatinib ROS production initially dips but then rise to cytotoxic levels via classical apoptotic mechanisms. This situation leads to a seeming 'ROS paradox'. However, an increase in magnitude of the already elevated ROS in cancer cells is likely to exceed the antioxidant capacity of the cancer and cause cell death (25). Furthermore, the Bcr-Abl/ROS scenario of K562 cells mimics the situation with other oncogenic kinases (e.g., epidermal growth factor receptor (EGFR), platelet-derived growth factor receptor (PDGFR), and B-Raf)

where the current spectrum of kinase inhibitors similarly kills in a ROS-dependent mechanism (182, 183).

Additionally, many antineoplastic agents like imatinib exert their cytotoxic effects through the generation of ROS (179). However, the underlying mechanisms for the essential ROS-mediated killing by chemotherapeutics and radiation therapy is not well understood (184). Imatinib presumably blocks any contribution to chronic ROS-mediated by Bcr-Abl, but as with other antineoplastic agents its killing mechanism can rely on an apoptotic process that induces ROS levels.

Bcr-Abl is considered a highly toxic protein when put into the right cellular context (Chapter 4). Forcing Bcr-Abl to the mitochondria may seem more akin to "throwing a wrench into the system" but this gets to the point that under contingencies such as genotoxic damage, c-Abl acts as the wrench to prevent the system from becoming malignant in the first place (16, 147). The intracellular cryptic escort (iCE) is uniquely suited to confer selective toxicity to CML cells over nonmalignant cells by virtue of two conditions, oxidative stress is required for activation of the iCE and Bcr-Abl is exclusive to CML cells.

Statement of objectives

Overall the aim of this study was to investigate the feasibility of converting the oncogenic Bcr-Abl tyrosine kinase into a mitochondrially targeted pro-apoptotic factor. This would restore a suppressed apoptotic pathway in CML using the cause to become the cure.

In this project, the major hypothesis was proposed with corresponding aims, as follows:

Major hypothesis: Forcing cytoplasmic Bcr-Abl to the mitochondria, via an intracellular cryptic escort, will selectively induce cell death in chronic myelogenous leukemia cells**.**

1) **Specific Aim 1**: Bcr-Abl containing a mitochondrial targeting sequence (MTS-Bcr-Abl) will induce cell death in leukemia cells upon localization to the mitochondria. Four previously characterized MTSs (i.e., matrix, intermembrane space, and inner and outer membranes) will be subcloned into pEGFP-Bcr-Abl (wild-type p210 Bcr-Abl). The MTS-Bcr-Abl constructs will be transiently transfected into leukemia cells and assessed for mitochondrial localization and apoptotic activity.

    a. Hypothesis: MTS-Bcr-Abl will localize to the mitochondria of leukemia cells.

    b. Hypothesis: MTS-Bcr-Abl will induce cell death in leukemia cells.

2) **Specific Aim 2**: The intracellular cryptic escort (iCE) will bind and facilitate endogenous Bcr-Abl translocation from the cytoplasm to the mitochondria.
3) **Specific Aim 3**: The intracellular cryptic escort will selectively induce cell death in Ph positive cells.

The hypotheses and aims are discussed in Chapters 3 and 4; these chapters have been published in (185) or submitted to (*Molecular Pharmaceutics*) peer-reviewed journals, respectively. Chapter 2 reviews the targeting of peptide/protein agents to the mitochondria in the context of malignancy and has been accepted to the peer-reviewed journal *Therapeutic Delivery*. Chapter 3 builds a foundation for the use of a cryptic peptide to selectively target the mitochondria of cells with a high ROS phenotype and sets a precedent for the restoration of the c-Abl death-directed pathway in CML. The results of Chapter 4 focus on addressing the major hypothesis.

References

1. B.J. Druker. Translation of the Philadelphia chromosome into therapy for CML. Blood. 112:4808-4817 (2008).

2. E. Nicholson and T. Holyoake. The chronic myeloid leukemia stem cell. Clin Lymphoma Myeloma. 9 Suppl 4:S376-381 (2009).

3. F.P. Santos and F. Ravandi. Advances in treatment of chronic myelogenous leukemia--new treatment options with tyrosine kinase inhibitors. Leuk Lymphoma. 50 Suppl 2:16-26 (2009).

4. T. O'Hare, C.A. Eide, and M.W. Deininger. Persistent LYN signaling in imatinib-resistant, BCR-ABL-independent chronic myelogenous leukemia. J Natl Cancer Inst. 100:908-909 (2008).

5. J. Wu, F. Meng, H. Lu, L. Kong, W. Bornmann, Z. Peng, M. Talpaz, and N.J. Donato. Lyn regulates BCR-ABL and Gab2 tyrosine phosphorylation and c-Cbl protein stability in imatinib-resistant chronic myelogenous leukemia cells. Blood. 111:3821-3829 (2008).

6. A. Quintas-Cardama and J.E. Cortes. The next generation of therapies for chronic myeloid leukemia. Clin Lymphoma Myeloma. 9 Suppl 4:S395-403 (2009).

7. R. Bhatia, M. Holtz, N. Niu, R. Gray, D.S. Snyder, C.L. Sawyers, D.A. Arber, M.L. Slovak, and S.J. Forman. Persistence of malignant hematopoietic progenitors in chronic myelogenous leukemia patients in complete cytogenetic remission following imatinib mesylate treatment. Blood. 101:4701-4707 (2003).

8. R. Hehlmann and S. Saussele. Treatment of chronic myeloid leukemia in blast crisis. Haematologica. 93:1765-1769 (2008).

9. A. Hamilton, G.V. Helgason, M. Schemionek, B. Zhang, S. Myssina, E.K. Allan, F.E. Nicolini, C. Muller-Tidow, R. Bhatia, V.G. Brunton, S. Koschmieder, and T.L. Holyoake. Chronic myeloid leukemia stem cells are not dependent on Bcr-Abl kinase activity for their survival. Blood. 119:1501-1510 (2012).

10. O. Hantschel and G. Superti-Furga. Regulation of the c-Abl and Bcr-Abl tyrosine kinases. Nat Rev Mol Cell Biol. 5:33-44 (2004).

11. A. Sirvent, C. Benistant, and S. Roche. Cytoplasmic signalling by the c-Abl tyrosine kinase in normal and cancer cells. Biol Cell. 100:617-631 (2008).

12. P. Vigneri and J.Y. Wang. Induction of apoptosis in chronic myelogenous leukemia cells through nuclear entrapment of BCR-ABL tyrosine kinase. Nat Med. 7:228-234 (2001).

13. J. Dierov, P.V. Sanchez, B.A. Burke, H. Padilla-Nash, M.E. Putt, T. Ried, and M. Carroll. BCR/ABL induces chromosomal instability after genotoxic stress and alters the cell death threshold. Leukemia. 23:279-286 (2009).

14. A.Y. Ting, K.H. Kain, R.L. Klemke, and R.Y. Tsien. Genetically encoded fluorescent reporters of protein tyrosine kinase activities in living cells. Proc Natl Acad Sci U S A. 98:15003-15008 (2001).

15. L. Veracini, M. Franco, A. Boureux, V. Simon, S. Roche, and C. Benistant. Two distinct pools of Src family tyrosine kinases regulate PDGF-induced DNA synthesis and actin dorsal ruffles. J Cell Sci. 119:2921-2934 (2006).

16. J.R. McWhirter and J.Y. Wang. An actin-binding function contributes to transformation by the Bcr-Abl oncoprotein of Philadelphia chromosome-positive human leukemias. EMBO J. 12:1533-1546 (1993).

17. P.J. Woodring, T. Hunter, and J.Y. Wang. Regulation of F-actin-dependent processes by the Abl family of tyrosine kinases. J Cell Sci. 116:2613-2626 (2003).

18. H. Patel, S.B. Marley, L. Greener, and M.Y. Gordon. Subcellular distribution of p210(BCR-ABL) in CML cell lines and primary CD34+ CML cells. Leukemia. 22:559-571 (2008).

19. A.S. Dixon, M. Kakar, K.M. Schneider, J.E. Constance, B.C. Paullin, and C.S. Lim. Controlling subcellular localization to alter function: Sending oncogenic Bcr-Abl to the nucleus causes apoptosis. J Control Release. 140:245-249 (2009).

20. J. Melo. Inviting leukemic cells to waltz with the devil. Nat Med. 7:156-157 (2001).

21. E.K. Allan, A. Hamilton, S. Hatziieremia, P. Zhou, H.G. Jorgensen, P. Vigneri, and T.L. Holyoake. Nuclear entrapment of BCR-ABL by combining imatinib mesylate with leptomycin B does not eliminate CD34+ chronic myeloid leukaemia cells. Leukemia. 23:1006-1008 (2009).

22. E. Solary, A. Bettaieb, L. Dubrez-Daloz, and L. Corcos. Mitochondria as a target for inducing death of malignant hematopoietic cells. Leuk Lymphoma. 44:563-574 (2003).

23. S.W. Tait and D.R. Green. Mitochondria and cell death: outer membrane permeabilization and beyond. Nature Reviews Molecular Cell Biology. 11:621-632 (2010).

24. M. Certo, V. Del Gaizo Moore, M. Nishino, G. Wei, S. Korsmeyer, S.A. Armstrong, and A. Letai. Mitochondria primed by death signals determine cellular addiction to antiapoptotic BCL-2 family members. Cancer Cell. 9:351-365 (2006).

25. S.J. Ralph, S. Rodriguez-Enriquez, J. Neuzil, E. Saavedra, and R. Moreno-Sanchez. The causes of cancer revisited: "mitochondrial malignancy" and ROS-induced oncogenic transformation - why mitochondria are targets for cancer therapy. Mol Aspects Med. 31:145-170 (2010).

26. Y. Ito, P. Pandey, N. Mishra, S. Kumar, N. Narula, S. Kharbanda, S. Saxena, and D. Kufe. Targeting of the c-Abl tyrosine kinase to mitochondria in endoplasmic reticulum stress-induced apoptosis. Mol Cell Biol. 21:6233-6242 (2001).

27. X. Qi and D. Mochly-Rosen. The PKCdelta -Abl complex communicates ER stress to the mitochondria - an essential step in subsequent apoptosis. J Cell Sci. 121:804-813 (2008).

28. M. Holcomb, A. Rufini, D. Barila, and R.L. Klemke. Deregulation of proteasome function induces Abl-mediated cell death by uncoupling p130CAS and c-CrkII. J Biol Chem. 281:2430-2440 (2006).

29. S. Kumar, N. Mishra, D. Raina, S. Saxena, and D. Kufe. Abrogation of the cell death response to oxidative stress by the c-Abl tyrosine kinase inhibitor STI571. Mol Pharmacol. 63:276-282 (2003).

30. S. Kumar, A. Bharti, N.C. Mishra, D. Raina, S. Kharbanda, S. Saxena, and D. Kufe. Targeting of the c-Abl tyrosine kinase to mitochondria in the necrotic cell death response to oxidative stress. J Biol Chem. 276:17281-17285 (2001).

31. M. Le Bras, I. Rouy, and C. Brenner. The modulation of inter-organelle cross-talk to control apoptosis. Med Chem. 2:1-12 (2006).

32. J.Y. Wang. Nucleo-cytoplasmic communication in apoptotic response to genotoxic and inflammatory stress. Cell Res. 15:43-48 (2005).

33. H. Yan, Y.C. Wang, D. Li, Y. Wang, W. Liu, Y.L. Wu, and G.Q. Chen. Arsenic trioxide and proteasome inhibitor bortezomib synergistically induce apoptosis in leukemic cells: the role of protein kinase Cdelta. Leukemia. 21:1488-1495 (2007).

34. N.B. Heaney, F. Pellicano, B. Zhang, L. Crawford, S. Chu, S.M. Kazmi, E.K. Allan, H.G. Jorgensen, A.E. Irvine, R. Bhatia, and T.L. Holyoake. Bortezomib induces apoptosis in primitive chronic myeloid leukemia cells including LTC-IC and NOD/SCID repopulating cells. Blood. 115:2241-2250 (2010).

35. E. Puccetti, S. Guller, A. Orleth, N. Bruggenolte, D. Hoelzer, O.G. Ottmann, and M. Ruthardt. BCR-ABL mediates arsenic trioxide-induced apoptosis independently of its aberrant kinase activity. Cancer Res. 60:3409-3413 (2000).

36. M. Gupta, L. Milani, M. Hermansson, B. Simonsson, B. Markevarn, A.C. Syvanen, and G. Barbany. Expression of BCR-ABL1 oncogene relative to ABL1 gene changes overtime in chronic myeloid leukemia. Biochem Biophys Res Commun. 366:848-851 (2008).

37. A. Vilgelm, W. El-Rifai, and A. Zaika. Therapeutic prospects for p73 and p63: rising from the shadow of p53. Drug Resist Updat. 11:152-163 (2008).

38. E.M. Galan-Moya, J. Hernandez-Losa, C.I. Aceves Luquero, M.A. de la Cruz-Morcillo, C. Ramirez-Castillejo, J.L. Callejas-Valera, A. Arriaga, A.F. Aranburo, S. Ramon y Cajal, J. Silvio Gutkind, and R. Sanchez-Prieto. c-Abl activates p38 MAPK independently of its tyrosine kinase activity: Implications in cisplatin-based therapy. Int J Cancer. 122:289-297 (2008).

39. J. Zhu and S.K. Shore. c-ABL tyrosine kinase activity is regulated by association with a novel SH3-domain-binding protein. Mol Cell Biol. 16:7054-7062 (1996).

40. M. Sattler, S. Verma, G. Shrikhande, C.H. Byrne, Y.B. Pride, T. Winkler, E.A. Greenfield, R. Salgia, and J.D. Griffin. The BCR/ABL tyrosine kinase induces production of reactive oxygen species in hematopoietic cells. J Biol Chem. 275:24273-24278 (2000).

41. A. Quintas-Cardama and J. Cortes. Molecular biology of bcr-abl1-positive chronic myeloid leukemia. Blood. 113:1619-1630 (2009).

42. H. Neves, C. Ramos, M.G. da Silva, A. Parreira, and L. Parreira. The nuclear topography of ABL, BCR, PML, and RARalpha genes: evidence for gene proximity in specific phases of the cell cycle and stages of hematopoietic differentiation. Blood. 93:1197-1207 (1999).

43. J. Foo, M.W. Drummond, B. Clarkson, T. Holyoake, and F. Michor. Eradication of chronic myeloid leukemia stem cells: a novel mathematical model predicts no therapeutic benefit of adding G-CSF to imatinib. PLoS Comput Biol. 5:e1000503 (2009).

44. M. Savona and M. Talpaz. Getting to the stem of chronic myeloid leukaemia. Nat Rev Cancer. 8:341-350 (2008).

45. J.C. Chomel, C. Villalva, N. Sorel, F. Chazelas, F. Guilhot, and A.G. Turhan. Evaluation of beta-catenin activating mutations in chronic myeloid leukemia. Leuk Res. 32:838-839 (2008).

46. N. Takao, R. Mori, H. Kato, A. Shinohara, and K. Yamamoto. c-Abl tyrosine kinase is not essential for ataxia telangiectasia mutated functions in chromosomal maintenance. J Biol Chem. 275:725-728 (2000).

47. Y. Shaul and M. Ben-Yehoyada. Role of c-Abl in the DNA damage stress response. Cell Res. 15:33-35 (2005).

48. S. Kharbanda, Z.M. Yuan, R. Weichselbaum, and D. Kufe. Determination of cell fate by c-Abl activation in the response to DNA damage. Oncogene. 17:3309-3318 (1998).

49. M. Mancini, N. Veljkovic, V. Corradi, E. Zuffa, P. Corrado, E. Pagnotta, G. Martinelli, E. Barbieri, and M.A. Santucci. 14-3-3 ligand prevents nuclear import of c-ABL protein in chronic myeloid leukemia. Traffic. 10:637-647 (2009).

50. K.H. Kain, S. Gooch, and R.L. Klemke. Cytoplasmic c-Abl provides a molecular 'Rheostat' controlling carcinoma cell survival and invasion. Oncogene. 22:6071-6080 (2003).

51. K. Piwocka, S. Vejda, T.G. Cotter, G.C. O'Sullivan, and S.L. McKenna. Bcr-Abl reduces endoplasmic reticulum releasable calcium levels by a Bcl-2-independent mechanism and inhibits calcium-dependent apoptotic signaling. Blood. 107:4003-4010 (2006).

52. M.S. Neshat, A.B. Raitano, H.G. Wang, J.C. Reed, and C.L. Sawyers. The survival function of the Bcr-Abl oncogene is mediated by Bad-dependent and -independent pathways: roles for phosphatidylinositol 3-kinase and Raf. Mol Cell Biol. 20:1179-1186 (2000).

53. M. Horita, E.J. Andreu, A. Benito, C. Arbona, C. Sanz, I. Benet, F. Prosper, and J.L. Fernandez-Luna. Blockade of the Bcr-Abl kinase activity induces apoptosis of chronic myelogenous leukemia cells by suppressing signal transducer and activator of transcription 5-dependent expression of Bcl-xL. J Exp Med. 191:977-984 (2000).

54. M. Kurokawa, C. Zhao, T. Reya, and S. Kornbluth. Inhibition of apoptosome formation by suppression of Hsp90beta phosphorylation in tyrosine kinase-induced leukemias. Mol Cell Biol. 28:5494-5506 (2008).

55. J. Sonoyama, I. Matsumura, S. Ezoe, Y. Satoh, X. Zhang, Y. Kataoka, E. Takai, M. Mizuki, T. Machii, H. Wakao, and Y. Kanakura. Functional cooperation among Ras, STAT5, and phosphatidylinositol 3-kinase is required for full oncogenic activities of BCR/ABL in K562 cells. J Biol Chem. 277:8076-8082 (2002).

56. Y. Maru. Molecular biology of chronic myeloid leukemia. Int J Hematol. 73:308-322 (2001).

57. B.J. Druker, C.L. Sawyers, H. Kantarjian, D.J. Resta, S.F. Reese, J.M. Ford, R. Capdeville, and M. Talpaz. Activity of a specific inhibitor of the BCR-ABL tyrosine kinase in the blast crisis of chronic myeloid leukemia and acute lymphoblastic leukemia with the Philadelphia chromosome. N Engl J Med. 344:1038-1042 (2001).

58. M. Bocchia. Is there any role left for p210-derived peptide vaccines in chronic myeloid leukemia? Haematologica. 87:675-677 (2002).

59. R. Hehlmann, H. Heimpel, J. Hasford, H.J. Kolb, H. Pralle, D.K. Hossfeld, W. Queisser, H. Loffler, B. Heinze, A. Georgii, and et al. Randomized comparison of busulfan and hydroxyurea in chronic myelogenous leukemia: prolongation of survival by hydroxyurea. The German CML Study Group. Blood. 82:398-407 (1993).

60. F. Guilhot, L. Roy, J. Guilhot, and F. Millot. Interferon therapy in chronic myelogenous leukemia. Hematol Oncol Clin North Am. 18:585-603 (2004).

61. A. Ferrajoli, A.M. Liberati, P. Caricchi, E. Donti, E. Morra, M. Lazzarino, A.R. Betti, P. Bernasconi, and G. Saglio. Interferon-alpha plus low-dose cytosine arabinoside in advanced phase chronic myelogenous leukaemia patients. Eur J Haematol. 55:184-188 (1995).

62. K.H. Antman. Introduction: the history of arsenic trioxide in cancer therapy. Oncologist. 6 Suppl 2:1-2 (2001).

63. M.A. Essers and A. Trumpp. Targeting leukemic stem cells by breaking their dormancy. Mol Oncol. 4:443-450 (2010).

64. E.M. Beauchamp, L. Ringer, G. Bulut, K.P. Sajwan, M.D. Hall, Y.C. Lee, D. Peaceman, M. Ozdemirli, O. Rodriguez, T.J. Macdonald, C. Albanese, J.A. Toretsky, and A. Uren. Arsenic trioxide inhibits human cancer cell growth and tumor development in mice by blocking Hedgehog/GLI pathway. J Clin Invest. 121:148-160 (2011).

65. D. Douer and M.S. Tallman. Arsenic trioxide: new clinical experience with an old medication in hematologic malignancies. J Clin Oncol. 23:2396-2410 (2005).

66. A. Burchert, M.C. Muller, P. Kostrewa, P. Erben, T. Bostel, S. Liebler, R. Hehlmann, A. Neubauer, and A. Hochhaus. Sustained molecular response with interferon alfa maintenance after induction therapy with imatinib plus interferon alfa in patients with chronic myeloid leukemia. Journal of Clinical Oncology :

Official Journal of the American Society of Clinical Oncology. 28:1429-1435 (2010).

67. V. Pitini, C. Arrigo, and G. Altavilla. How cells respond to interferons. Journal of clinical oncology : official journal of the American Society of Clinical Oncology. 28:e439; author reply e440 (2010).

68. S. Roychowdhury and M. Talpaz. Managing resistance in chronic myeloid leukemia. Blood Rev. 25:279-290 (2011).

69. J. Sessions. Chronic myeloid leukemia in 2007. J Manag Care Pharm. 13:4-7 (2007).

70. J. Hasford, M. Pfirrmann, P. Shepherd, J. Guilhot, R. Hehlmann, F.X. Mahon, H.C. Kluin-Nelemans, K. Ohnishi, J.L. Steegmann, and J. Thaler. The impact of the combination of baseline risk group and cytogenetic response on the survival of patients with chronic myeloid leukemia treated with interferon alpha. Haematologica. 90:335-340 (2005).

71. A. Lakshmikuttyamma, E. Pastural, N. Takahashi, K. Sawada, D.P. Sheridan, J.F. DeCoteau, and C.R. Geyer. Bcr-Abl induces autocrine IGF-1 signaling. Oncogene. 27:3831-3844 (2008).

72. T. Ernst and A. Hochhaus. Chronic myeloid leukemia: clinical impact of BCR-ABL1 mutations and other lesions associated with disease progression. Semin Oncol. 39:58-66 (2012).

73. A.M. Kalle, S. Sachchidanand, and R. Pallu. Bcr-Abl-independent mechanism of resistance to imatinib in K562 cells: Induction of cyclooxygenase-2 (COX-2) by histone deacetylases (HDACs). Leuk Res. 34:1132-1138 (2010).

74. W. Warsch, K. Kollmann, E. Eckelhart, S. Fajmann, S. Cerny-Reiterer, A. Holbl, K.V. Gleixner, M. Dworzak, M. Mayerhofer, G. Hoermann, H. Herrmann, C. Sillaber, G. Egger, P. Valent, R. Moriggl, and V. Sexl. High STAT5 levels mediate imatinib resistance and indicate disease progression in chronic myeloid leukemia. Blood. 117:3409-3420 (2011).

75. M. Talpaz, N.P. Shah, H. Kantarjian, N. Donato, J. Nicoll, R. Paquette, J. Cortes, S. O'Brien, C. Nicaise, E. Bleickardt, M.A. Blackwood-Chirchir, V. Iyer, T.T. Chen, F. Huang, A.P. Decillis, and C.L. Sawyers. Dasatinib in imatinib-resistant Philadelphia chromosome-positive leukemias. N Engl J Med. 354:2531-2541 (2006).

76. H. Kantarjian, F. Giles, L. Wunderle, K. Bhalla, S. O'Brien, B. Wassmann, C. Tanaka, P. Manley, P. Rae, W. Mietlowski, K. Bochinski, A. Hochhaus, J.D. Griffin, D. Hoelzer, M. Albitar, M. Dugan, J. Cortes, L. Alland, and O.G.

Ottmann. Nilotinib in imatinib-resistant CML and Philadelphia chromosome-positive ALL. N Engl J Med. 354:2542-2551 (2006).

77. J.M. Gozgit, M.J. Wong, S. Wardwell, J.W. Tyner, M.M. Loriaux, Q.K. Mohemmad, N.I. Narasimhan, W.C. Shakespeare, F. Wang, B.J. Druker, T. Clackson, and V.M. Rivera. Potent activity of ponatinib (AP24534) in models of FLT3-driven acute myeloid leukemia and other hematologic malignancies. Mol Cancer Ther. 10:1028-1035 (2011).

78. D.W. Woessner, C.S. Lim, and M.W. Deininger. Development of an effective therapy for chronic myelogenous leukemia. Cancer J. 17:477-486 (2011).

79. R. Tanaka, M.S. Squires, S. Kimura, A. Yokota, R. Nagao, T. Yamauchi, M. Takeuchi, H. Yao, M. Reule, T. Smyth, J.F. Lyons, N.T. Thompson, E. Ashihara, O.G. Ottmann, and T. Maekawa. Activity of the multitargeted kinase inhibitor, AT9283, in imatinib-resistant BCR-ABL-positive leukemic cells. Blood. 116:2089-2095 (2010).

80. H. Sun, V. Kapuria, L.F. Peterson, D. Fang, W.G. Bornmann, G. Bartholomeusz, M. Talpaz, and N.J. Donato. Bcr-Abl ubiquitination and Usp9x inhibition block kinase signaling and promote CML cell apoptosis. Blood. 117:3151-3162 (2011).

81. J. Zhang, F.J. Adrian, W. Jahnke, S.W. Cowan-Jacob, A.G. Li, R.E. Iacob, T. Sim, J. Powers, C. Dierks, F. Sun, G.R. Guo, Q. Ding, B. Okram, Y. Choi, A. Wojciechowski, X. Deng, G. Liu, G. Fendrich, A. Strauss, N. Vajpai, S. Grzesiek, T. Tuntland, Y. Liu, B. Bursulaya, M. Azam, P.W. Manley, J.R. Engen, G.Q. Daley, M. Warmuth, and N.S. Gray. Targeting Bcr-Abl by combining allosteric with ATP-binding-site inhibitors. Nature. 463:501-506 (2010).

82. A.S. Dixon, G.D. Miller, B.J. Bruno, J.E. Constance, D.W. Woessner, T.P. Fidler, J.C. Robertson, T.E. Cheatham, 3rd, and C.S. Lim. Improved coiled-coil design enhances interaction with Bcr-Abl and induces apoptosis. Mol Pharm. 9:187-195 (2011).

83. E.A. Dubikovskaya, S.H. Thorne, T.H. Pillow, C.H. Contag, and P.A. Wender. Overcoming multidrug resistance of small-molecule therapeutics through conjugation with releasable octaarginine transporters. Proceedings of the National Academy of Sciences of the United States of America. 105:12128-12133 (2008).

84. S.M. Tinsley. Safety profiles of second-line tyrosine kinase inhibitors in patients with chronic myeloid leukaemia. J Clin Nurs. 19:1207-1218 (2010).

85. M.J. Mauro and M.W. Deininger. Management of drug toxicities in chronic myeloid leukaemia. Best Pract Res Clin Haematol. 22:409-429 (2009).

86. P. Neelakantan, D. Marin, M. Laffan, J. Goldman, J. Apperley, and D. Milojkovic. Platelet dysfunction associated with ponatinib, a new pan BCR-ABL inhibitor with efficacy for chronic myeloid leukemia resistant to multiple tyrosine kinase inhibitor therapy. Haematologica. Epub ahead of print (2012).

87. M. Baccarani, G. Saglio, J. Goldman, A. Hochhaus, B. Simonsson, F. Appelbaum, J. Apperley, F. Cervantes, J. Cortes, M. Deininger, A. Gratwohl, F. Guilhot, M. Horowitz, T. Hughes, H. Kantarjian, R. Larson, D. Niederwieser, R. Silver, and R. Hehlmann. Evolving concepts in the management of chronic myeloid leukemia: recommendations from an expert panel on behalf of the European LeukemiaNet. Blood. 108:1809-1820 (2006).

88. L. Li, L. Wang, Z. Wang, Y. Ho, T. McDonald, T.L. Holyoake, W. Chen, and R. Bhatia. Activation of p53 by SIRT1 inhibition enhances elimination of CML leukemia stem cells in combination with imatinib. Cancer Cell. 21:266-281 (2012).

89. A. Perl and M. Carroll. BCR-ABL kinase is dead; long live the CML stem cell. J Clin Invest. 121:22-25 (2011).

90. M. Greaves. Cancer stem cells: back to Darwin? Semin Cancer Biol. 20:65-70 (2010).

91. T. Lenaerts, J.M. Pacheco, A. Traulsen, and D. Dingli. Tyrosine kinase inhibitor therapy can cure chronic myeloid leukemia without hitting leukemic stem cells. Haematologica. 95:900-907 (2009).

92. S.A. Stuart, Y. Minami, and J.Y. Wang. The CML stem cell: evolution of the progenitor. Cell Cycle. 8:1338-1343 (2009).

93. Y. Tabe, L. Jin, K. Iwabuchi, R.Y. Wang, N. Ichikawa, T. Miida, J. Cortes, M. Andreeff, and M. Konopleva. Role of stromal microenvironment in nonpharmacological resistance of CML to imatinib through Lyn/CXCR4 interactions in lipid rafts. Leukemia. 26:883-892 (2011).

94. M. Copland, A. Hamilton, L.J. Elrick, J.W. Baird, E.K. Allan, N. Jordanides, M. Barow, J.C. Mountford, and T.L. Holyoake. Dasatinib (BMS-354825) targets an earlier progenitor population than imatinib in primary CML but does not eliminate the quiescent fraction. Blood. 107:4532-4539 (2006).

95. Y. Hu, Y. Chen, L. Douglas, and S. Li. beta-Catenin is essential for survival of leukemic stem cells insensitive to kinase inhibition in mice with BCR-ABL-induced chronic myeloid leukemia. Leukemia. 23:109-116 (2009).

96. C.H. Hui, K.Y. Goh, D. White, S. Branford, A. Grigg, J.F. Seymour, Y.L. Kwan, S. Walsh, R. Hoyt, A. Trickett, B. Rudzki, D.D. Ma, L.B. To, and T.P. Hughes.

Successful peripheral blood stem cell mobilisation with filgrastim in patients with chronic myeloid leukaemia achieving complete cytogenetic response with imatinib, without increasing disease burden as measured by quantitative real-time PCR. Leukemia. 17:821-828 (2003).

97. G. Martinelli, N. Testoni, M. Amabile, F. Bonifazi, A. De Vivo, P. Farabegoli, C. Terragna, V. Montefusco, E. Ottaviani, G. Saglio, D. Russo, M. Baccarani, G. Rosti, and S. Tura. Quantification of BCR-ABL transcripts in CML patients in cytogenetic remission after interferon-alpha-based therapy. Bone Marrow Transplant. 25:729-736 (2000).

98. J.C. Hernandez-Boluda, E. Carreras, F. Cervantes, P. Marin, E. Arellano-Rodrigo, M. Rovira, F. Sole, E. Lloveras, B. Espinet, A. Ocejo, and E. Montserrat. Collection of Philadelphia-negative stem cells using recombinant human granulocyte colony-stimulating factor in chronic myeloid leukemia patients treated with alpha-interferon. Haematologica. 87:17-22 (2002).

99. H.G. Jorgensen, M. Copland, E.K. Allan, X. Jiang, A. Eaves, C. Eaves, and T.L. Holyoake. Intermittent exposure of primitive quiescent chronic myeloid leukemia cells to granulocyte-colony stimulating factor in vitro promotes their elimination by imatinib mesylate. Clin Cancer Res. 12:626-633 (2006).

100. B. Fang, L. Mai, N. Li, Y. Song, and R. Chunhua Zhao. Imatinib plus Granulocyte Colony-Stimulating Factor in Chronic Myeloid Leukemia Patients Who Have Achieved Partial or Complete Cytogenetic Response while on Imatinib. Case Rep Oncol. 4:192-197 (2011).

101. A.R. Walker, R.S. Komrokji, J. Ifthikharuddin, P. Messina, D. Mulford, M. Becker, J. Friedberg, J. Oliva, G. Phillips, J.L. Liesveld, and C. Abboud. Phase I study of cladribine, cytarabine (Ara-C), granulocyte colony stimulating factor (G-CSF) (CLAG Regimen) and simultaneous escalating doses of imatinib mesylate (Gleevec) in relapsed/refractory AML. Leuk Res. 32:1830-1836 (2008).

102. M.W. Drummond, N. Heaney, J. Kaeda, F.E. Nicolini, R.E. Clark, G. Wilson, P. Shepherd, J. Tighe, L. McLintock, T. Hughes, and T.L. Holyoake. A pilot study of continuous imatinib vs pulsed imatinib with or without G-CSF in CML patients who have achieved a complete cytogenetic response. Leukemia. 23:1199-1201 (2009).

103. A.S. Corbin, A. Agarwal, M. Loriaux, J. Cortes, M.W. Deininger, and B.J. Druker. Human chronic myeloid leukemia stem cells are insensitive to imatinib despite inhibition of BCR-ABL activity. J Clin Invest. 121:396-409 (2011).

104. M. Bocchia, S. Gentili, E. Abruzzese, A. Fanelli, F. Iuliano, A. Tabilio, M. Amabile, F. Forconi, A. Gozzetti, D. Raspadori, S. Amadori, and F. Lauria. Effect of a p210 multipeptide vaccine associated with imatinib or interferon in patients

with chronic myeloid leukaemia and persistent residual disease: a multicentre observational trial. Lancet. 365:657-662 (2005).

105. M. Smahel. Antigens in chronic myeloid leukemia: implications for vaccine development. Cancer Immunol Immunother. 60:1655-1668 (2011).

106. E. Feinstein, G. Cimino, R.P. Gale, G. Alimena, R. Berthier, K. Kishi, J. Goldman, A. Zaccaria, A. Berrebi, and E. Canaani. p53 in chronic myelogenous leukemia in acute phase. Proc Natl Acad Sci U S A. 88:6293-6297 (1991).

107. H.G. Wendel, E. de Stanchina, E. Cepero, S. Ray, M. Emig, J.S. Fridman, D.R. Veach, W.G. Bornmann, B. Clarkson, W.R. McCombie, S.C. Kogan, A. Hochhaus, and S.W. Lowe. Loss of p53 impedes the antileukemic response to BCR-ABL inhibition. Proc Natl Acad Sci U S A. 103:7444-7449 (2006).

108. F.X. Mahon, D. Rea, J. Guilhot, F. Guilhot, F. Huguet, F. Nicolini, L. Legros, A. Charbonnier, A. Guerci, B. Varet, G. Etienne, J. Reiffers, and P. Rousselot. Discontinuation of imatinib in patients with chronic myeloid leukaemia who have maintained complete molecular remission for at least 2 years: the prospective, multicentre Stop Imatinib (STIM) trial. Lancet Oncol. 11:1029-1035 (2010).

109. M. Tang, J. Foo, M. Gonen, J. Guilhot, F.X. Mahon, and F. Michor. Selection pressure exerted by imatinib therapy leads to disparate outcomes of imatinib discontinuation trials. Haematologica Epub ahead of print (2012).

110. M. Deininger. Hematology: curing CML with imatinib--a dream come true? Nat Rev Clin Oncol. 8:127-128 (2011).

111. O.O. Olabisi, G.M. Mahon, E.V. Kostenko, Z. Liu, H.L. Ozer, and I.P. Whitehead. Bcr interacts with components of the endosomal sorting complex required for transport-I and is required for epidermal growth factor receptor turnover. Cancer Research. 66:6250-6257 (2006).

112. Y.J. Cho, J.M. Cunnick, S.J. Yi, V. Kaartinen, J. Groffen, and N. Heisterkamp. Abr and Bcr, two homologous Rac GTPase-activating proteins, control multiple cellular functions of murine macrophages. Mol Cell Biol. 27:899-911 (2007).

113. X. Zheng, S. Guller, T. Beissert, E. Puccetti, and M. Ruthardt. BCR and its mutants, the reciprocal t(9;22)-associated ABL/BCR fusion proteins, differentially regulate the cytoskeleton and cell motility. BMC Cancer. 6:262 (2006).

114. E. Laurent, M. Talpaz, H. Kantarjian, and R. Kurzrock. The BCR gene and philadelphia chromosome-positive leukemogenesis. Cancer Research. 61:2343-2355 (2001).

115. R.B. Arlinghaus. Bcr: a negative regulator of the Bcr-Abl oncoprotein in leukemia. Oncogene. 21:8560-8567 (2002).

116. B. Perazzona, H. Lin, T. Sun, Y. Wang, and R. Arlinghaus. Kinase domain mutants of Bcr enhance Bcr-Abl oncogenic effects. Oncogene. 27:2208-2214 (2008).

117. J.R. McWhirter, D.L. Galasso, and J.Y. Wang. A coiled-coil oligomerization domain of Bcr is essential for the transforming function of Bcr-Abl oncoproteins. Molecular and Cellular Biology. 13:7587-7595 (1993).

118. D. Vigil, J. Cherfils, K.L. Rossman, and C.J. Der. Ras superfamily GEFs and GAPs: validated and tractable targets for cancer therapy? Nat Rev Cancer. 10:842-857 (2010).

119. S. Sahay, N.L. Pannucci, G.M. Mahon, P.L. Rodriguez, N.J. Megjugorac, E.V. Kostenko, H.L. Ozer, and I.P. Whitehead. The RhoGEF domain of p210 Bcr-Abl activates RhoA and is required for transformation. Oncogene. 27:2064-2071 (2008).

120. T. Daubon, J. Chasseriau, A. El Ali, J. Rivet, A. Kitzis, B. Constantin, and N. Bourmeyster. Differential motility of p190bcr-abl- and p210bcr-abl-expressing cells: respective roles of Vav and Bcr-Abl GEFs. Oncogene. 27:2673-2685 (2008).

121. J. Burthem, K. Rees-Unwin, R. Mottram, J. Adams, G.S. Lucas, E. Spooncer, and A.D. Whetton. The rho-kinase inhibitors Y-27632 and fasudil act synergistically with imatinib to inhibit the expansion of ex vivo CD34(+) CML progenitor cells. Leukemia : official journal of the Leukemia Society of America, Leukemia Research Fund, UK. 21:1708-1714 (2007).

122. Y. He, J.A. Wertheim, L. Xu, J.P. Miller, F.G. Karnell, J.K. Choi, R. Ren, and W.S. Pear. The coiled-coil domain and Tyr177 of bcr are required to induce a murine chronic myelogenous leukemia-like disease by bcr/abl. Blood. 99:2957-2968 (2002).

123. A.M. Pendergast. Stress and death: breaking up the c-Abl/14-3-3 complex in apoptosis. Nat Cell Biol. 7:213-214 (2005).

124. P.J. Welch and J.Y. Wang. Abrogation of retinoblastoma protein function by c-Abl through tyrosine kinase-dependent and -independent mechanisms. Molecular and Cellular Biology. 15:5542-5551 (1995).

125. J.Y. Wang. Regulation of cell death by the Abl tyrosine kinase. Oncogene. 19:5643-5650 (2000).

126. S. Gonfloni, L. Di Tella, S. Caldarola, S.M. Cannata, F.G. Klinger, C. Di Bartolomeo, M. Mattei, E. Candi, M. De Felici, G. Melino, and G. Cesareni. Inhibition of the c-Abl-TAp63 pathway protects mouse oocytes from chemotherapy-induced death. Nat Med. 15:1179-1185 (2009).

127. R.V. Sionov, E. Moallem, M. Berger, A. Kazaz, O. Gerlitz, Y. Ben-Neriah, M. Oren, and Y. Haupt. c-Abl neutralizes the inhibitory effect of Mdm2 on p53. J Biol Chem. 274:8371-8374 (1999).

128. G. Palacios, H.C. Crawford, A. Vaseva, and U.M. Moll. Mitochondrially targeted wild-type p53 induces apoptosis in a solid human tumor xenograft model. Cell Cycle. 7:2584-2590 (2008).

129. A.E. Sayan, B.S. Sayan, V. Gogvadze, D. Dinsdale, U. Nyman, T.M. Hansen, B. Zhivotovsky, G.M. Cohen, R.A. Knight, and G. Melino. P73 and caspase-cleaved p73 fragments localize to mitochondria and augment TRAIL-induced apoptosis. Oncogene. 27:4363-4372 (2008).

130. M. Mihara, S. Erster, A. Zaika, O. Petrenko, T. Chittenden, P. Pancoska, and U.M. Moll. p53 has a direct apoptogenic role at the mitochondria. Mol Cell. 11:577-590 (2003).

131. S.Y. Choi, M.J. Kim, C.M. Kang, S. Bae, C.K. Cho, J.W. Soh, J.H. Kim, S. Kang, H.Y. Chung, Y.S. Lee, and S.J. Lee. Activation of Bak and Bax through c-abl-protein kinase Cdelta-p38 MAPK signaling in response to ionizing radiation in human non-small cell lung cancer cells. J Biol Chem. 281:7049-7059 (2006).

132. R.V. Sionov, S. Coen, Z. Goldberg, M. Berger, B. Bercovich, Y. Ben-Neriah, A. Ciechanover, and Y. Haupt. c-Abl regulates p53 levels under normal and stress conditions by preventing its nuclear export and ubiquitination. Mol Cell Biol. 21:5869-5878 (2001).

133. G. Wei, A.G. Li, and X. Liu. Insights into selective activation of p53 DNA binding by c-Abl. J Biol Chem. 280:12271-12278 (2005).

134. L. Xiao, D. Chen, P. Hu, J. Wu, W. Liu, Y. Zhao, M. Cao, Y. Fang, W. Bi, Z. Zheng, J. Ren, G. Ji, Y. Wang, and Z. Yuan. The c-Abl-MST1 signaling pathway mediates oxidative stress-induced neuronal cell death. J Neurosci. 31:9611-9619 (2011).

135. T. Nakamaki, J. Okabe-Kado, Y. Yamamoto-Yamaguchi, K. Hino, S. Tomoyasu, Y. Honma, and T. Kasukabe. Role of MmTRA1b/phospholipid scramblase1 gene expression in the induction of differentiation of human myeloid leukemia cells into granulocytes. Exp Hematol. 30:421-429 (2002).

136. S.C. Frasch, P.M. Henson, J.M. Kailey, D.A. Richter, M.S. Janes, V.A. Fadok, and D.L. Bratton. Regulation of phospholipid scramblase activity during apoptosis and cell activation by protein kinase Cdelta. J Biol Chem. 275:23065-23073 (2000).

137. K. Bailey, H.W. Cook, and C.R. McMaster. The phospholipid scramblase PLSCR1 increases UV induced apoptosis primarily through the augmentation of the intrinsic apoptotic pathway and independent of direct phosphorylation by protein kinase C delta. Biochim Biophys Acta. 1733:199-209 (2005).

138. M. Kurokawa and S. Kornbluth. Caspases and kinases in a death grip. Cell. 138:838-854 (2009).

139. D. Raina, P. Pandey, R. Ahmad, A. Bharti, J. Ren, S. Kharbanda, R. Weichselbaum, and D. Kufe. c-Abl tyrosine kinase regulates caspase-9 autocleavage in the apoptotic response to DNA damage. J Biol Chem. 280:11147-11151 (2005).

140. B.C. Oxhorn, A.R. Sanguinetti, C.C. Mastick, and I.L. Buxton. c-Abl is required for staurosporine-induced caspase activity. Proc West Pharmacol Soc. 48:110-117 (2005).

141. B.S. Westlund, B. Cai, J. Zhou, and J.R. Sparrow. Involvement of c-Abl, p53 and the MAP kinase JNK in the cell death program initiated in A2E-laden ARPE-19 cells by exposure to blue light. Apoptosis. 14:31-41 (2009).

142. F. Cong and S.P. Goff. c-Abl-induced apoptosis, but not cell cycle arrest, requires mitogen-activated protein kinase kinase 6 activation. Proceedings of the National Academy of Sciences of the United States of America. 96:13819-13824 (1999).

143. R. Kamath, Z. Jiang, G. Sun, J.C. Yalowich, and R. Baskaran. c-Abl kinase regulates curcumin-induced cell death through activation of c-Jun N-terminal kinase. Mol Pharmacol. 71:61-72 (2007).

144. Y. Ito, N.C. Mishra, K. Yoshida, S. Kharbanda, S. Saxena, and D. Kufe. Mitochondrial targeting of JNK/SAPK in the phorbol ester response of myeloid leukemia cells. Cell Death Differ. 8:794-800 (2001).

145. M. Lasfer, L. Davenne, N. Vadrot, C. Alexia, Z. Sadji-Ouatas, A.F. Bringuier, G. Feldmann, D. Pessayre, and F. Reyl-Desmars. Protein kinase PKC delta and c-Abl are required for mitochondrial apoptosis induction by genotoxic stress in the absence of p53, p73 and Fas receptor. FEBS Lett. 580:2547-2552 (2006).

146. S. Kharbanda, S. Saxena, K. Yoshida, P. Pandey, M. Kaneki, Q. Wang, K. Cheng, Y.N. Chen, A. Campbell, T. Sudha, Z.M. Yuan, J. Narula, R. Weichselbaum, C.

Nalin, and D. Kufe. Translocation of SAPK/JNK to mitochondria and interaction with Bcl-x(L) in response to DNA damage. J Biol Chem. 275:322-327 (2000).

147. A.S. Dixon, J.E. Constance, T. Tanaka, T.H. Rabbitts, and C.S. Lim. Changing the subcellular location of the oncoprotein Bcr-Abl using rationally designed capture motifs. Pharm Res. 29:1098-1109 (2011).

148. M. Preyer, P. Vigneri, and J.Y. Wang. Interplay between kinase domain autophosphorylation and F-actin binding domain in regulating imatinib sensitivity and nuclear import of BCR-ABL. PLoS One. 6:e17020 (2011).

149. M. Preyer, C.W. Shu, and J.Y. Wang. Delayed activation of Bax by DNA damage in embryonic stem cells with knock-in mutations of the Abl nuclear localization signals. Cell Death Differ. 14:1139-1148 (2007).

150. E. Tran. Nuclear Bcr-Abl Induces Apoptosis Independently of its Tyrosine Kinase Activity in K562 Leukemia Cells. Senior Honors Thesis in Chemistry. University of Utah: (2010).

151. M.O. Nowicki, R. Falinski, M. Koptyra, A. Slupianek, T. Stoklosa, E. Gloc, M. Nieborowska-Skorska, J. Blasiak, and T. Skorski. BCR/ABL oncogenic kinase promotes unfaithful repair of the reactive oxygen species-dependent DNA double-strand breaks. Blood. 104:3746-3753 (2004).

152. R.A. Van Etten. c-Abl regulation: a tail of two lipids. Curr Biol. 13:R608-610 (2003).

153. O. Schmidt, N. Pfanner, and C. Meisinger. Mitochondrial protein import: from proteomics to functional mechanisms. Nature Reviews Molecular Cell Biology. 11:655-667 (2010).

154. R.I. Morimoto, A.J. Driessen, R.S. Hegde, and T. Langer. The life of proteins: the good, the mostly good and the ugly. Nat Struct Mol Biol. 18:1-4 (2011).

155. T. Becker, L. Bottinger, and N. Pfanner. Mitochondrial protein import: from transport pathways to an integrated network. Trends Biochem Sci. 37:85-91 (2012).

156. S. Rao, O. Schmidt, A.B. Harbauer, B. Schonfisch, B. Guiard, N. Pfanner, and C. Meisinger. Biogenesis of the preprotein translocase of the outer mitochondrial membrane: protein kinase A phosphorylates the precursor of Tom40 and impairs its import. Mol Biol Cell. 23:1618-1627 (2012).

157. N. Regev-Rudzki, E. Battat, I. Goldberg, and O. Pines. Dual localization of fumarase is dependent on the integrity of the glyoxylate shunt. Mol Microbiol. 72:297-306 (2009).

158. N. Pfanner and A. Geissler. Versatility of the mitochondrial protein import machinery. Nature Reviews Molecular Cell Biology. 2:339-349 (2001).

159. A.L. Horwich, W.A. Fenton, K.R. Williams, F. Kalousek, J.P. Kraus, R.F. Doolittle, W. Konigsberg, and L.E. Rosenberg. Structure and expression of a complementary DNA for the nuclear coded precursor of human mitochondrial ornithine transcarbamylase. Science. 224:1068-1074 (1984).

160. J.M. Herrmann. Putting a break on protein translocation: metabolic regulation of mitochondrial protein import. Mol Microbiol. 72:275-278 (2009).

161. P. Dolezal, V. Likic, J. Tachezy, and T. Lithgow. Evolution of the molecular machines for protein import into mitochondria. Science. 313:314-318 (2006).

162. K. Okamoto, A. Brinker, S.A. Paschen, I. Moarefi, M. Hayer-Hartl, W. Neupert, and M. Brunner. The protein import motor of mitochondria: a targeted molecular ratchet driving unfolding and translocation. EMBO J. 21:3659-3671 (2002).

163. M.A. Robin, S.K. Prabu, H. Raza, H.K. Anandatheerthavarada, and N.G. Avadhani. Phosphorylation enhances mitochondrial targeting of GSTA4-4 through increased affinity for binding to cytoplasmic Hsp70. J Biol Chem. 278:18960-18970 (2003).

164. W. Neupert and J.M. Herrmann. Translocation of proteins into mitochondria. Annu Rev Biochem. 76:723-749 (2007).

165. G. Isaya, W.A. Fenton, J.P. Hendrick, K. Furtak, F. Kalousek, and L.E. Rosenberg. Mitochondrial import and processing of mutant human ornithine transcarbamylase precursors in cultured cells. Molecular and Cellular Biology. 8:5150-5158 (1988).

166. T. Ozawa, Y. Natori, Y. Sako, H. Kuroiwa, T. Kuroiwa, and Y. Umezawa. A minimal peptide sequence that targets fluorescent and functional proteins into the mitochondrial intermembrane space. ACS Chem Biol. 2:176-186 (2007).

167. R. Rizzuto, A.W. Simpson, M. Brini, and T. Pozzan. Rapid changes of mitochondrial Ca2+ revealed by specifically targeted recombinant aequorin. Nature. 358:325-327 (1992).

168. T. Kaufmann, S. Schlipf, J. Sanz, K. Neubert, R. Stein, and C. Borner. Characterization of the signal that directs Bcl-x(L), but not Bcl-2, to the mitochondrial outer membrane. The Journal of Cell Biology. 160:53-64 (2003).

169. S. Karniely and O. Pines. Single translation--dual destination: mechanisms of dual protein targeting in eukaryotes. EMBO Rep. 6:420-425 (2005).

170. B. Li. c-Abl in oxidative stress, aging and cancer. Cell Cycle. 4:246-248 (2005).

171. B.N. Lyu, S.B. Ismailov, B. Ismailov, and M.B. Lyu. Mitochondrial concept of leukemogenesis: key role of oxygen-peroxide effects. Theor Biol Med Model. 5:23 (2008).

172. P. Storz. Reactive oxygen species in tumor progression. Front Biosci. 10:1881-1896 (2005).

173. G. Grosveld, T. Verwoerd, T. van Agthoven, A. de Klein, K.L. Ramachandran, N. Heisterkamp, K. Stam, and J. Groffen. The chronic myelocytic cell line K562 contains a breakpoint in bcr and produces a chimeric bcr/c-abl transcript. Molecular and Cellular Biology. 6:607-616 (1986).

174. C.M. Croce, K. Huebner, M. Isobe, E. Fainstain, B. Lifshitz, E. Shtivelman, and E. Canaani. Mapping of four distinct BCR-related loci to chromosome region 22q11: order of BCR loci relative to chronic myelogenous leukemia and acute lymphoblastic leukemia breakpoints. Proceedings of the National Academy of Sciences of the United States of America. 84:7174-7178 (1987).

175. J.H. Kim, S.C. Chu, J.L. Gramlich, Y.B. Pride, E. Babendreier, D. Chauhan, R. Salgia, K. Podar, J.D. Griffin, and M. Sattler. Activation of the PI3K/mTOR pathway by BCR-ABL contributes to increased production of reactive oxygen species. Blood. 105:1717-1723 (2005).

176. M. Koptyra, R. Falinski, M.O. Nowicki, T. Stoklosa, I. Majsterek, M. Nieborowska-Skorska, J. Blasiak, and T. Skorski. BCR/ABL kinase induces self-mutagenesis via reactive oxygen species to encode imatinib resistance. Blood. 108:319-327 (2006).

177. S.J. Stein and A.S. Baldwin. NF-kappaB suppresses ROS levels in BCR-ABL(+) cells to prevent activation of JNK and cell death. Oncogene. 30:4557-4566 (2011).

178. S. Fulda, L. Galluzzi, and G. Kroemer. Targeting mitochondria for cancer therapy. Nat Rev Drug Discov. 9:447-464 (2010).

179. S.P. Chang, S.C. Shen, W.R. Lee, L.L. Yang, and Y.C. Chen. Imatinib mesylate induction of ROS-dependent apoptosis in melanoma B16F0 cells. J Dermatol Sci. 62:183-191 (2011).

180. M. Okada, S. Adachi, T. Imai, K. Watanabe, S.Y. Toyokuni, M. Ueno, A.S. Zervos, G. Kroemer, and T. Nakahata. A novel mechanism for imatinib mesylate-induced cell death of BCR-ABL-positive human leukemic cells: caspase-

independent, necrosis-like programmed cell death mediated by serine protease activity. Blood. 103:2299-2307 (2004).

181. G. Kroemer, L. Galluzzi, P. Vandenabeele, J. Abrams, E.S. Alnemri, E.H. Baehrecke, M.V. Blagosklonny, W.S. El-Deiry, P. Golstein, D.R. Green, M. Hengartner, R.A. Knight, S. Kumar, S.A. Lipton, W. Malorni, G. Nunez, M.E. Peter, J. Tschopp, J. Yuan, M. Piacentini, B. Zhivotovsky, and G. Melino. Classification of cell death: recommendations of the Nomenclature Committee on Cell Death 2009. Cell Death and Differentiation. 16:3-11 (2009).

182. K.M. Aird, J.L. Allensworth, I. Batinic-Haberle, H.K. Lyerly, M.W. Dewhirst, and G.R. Devi. ErbB1/2 tyrosine kinase inhibitor mediates oxidative stress-induced apoptosis in inflammatory breast cancer cells. Breast Cancer Res Treat. 132:109-119 (2012).

183. X. Qian, J. Li, J. Ding, Z. Wang, W. Zhang, and G. Hu. Erlotinib activates mitochondrial death pathways related to the production of reactive oxygen species in the human non-small cell lung cancer cell line A549. Clin Exp Pharmacol Physiol. 36:487-494 (2009).

184. S.C. Gupta, D. Hevia, S. Patchva, B. Park, W. Koh, and B.B. Aggarwal. Upsides and downsides of reactive oxygen species for cancer: the roles of reactive oxygen species in tumorigenesis, prevention, and therapy. Antioxid Redox Signal. 16:1295-1322 (2012).

185. J.E. Constance, S.D. Despres, A. Nishida, and C.S. Lim. Selective Targeting of c-Abl via a Cryptic Mitochondrial Targeting Signal Activated by Cellular Redox Status in Leukemic and Breast Cancer Cells. Pharmaceutical Research (2012).

CHAPTER 2

TARGETING MALIGNANT MITOCHONDRIA WITH THERAPEUTIC PEPTIDES

Abstract

The current status of peptides that target the mitochondria in the context of cancer is the focus of this review. Chemotherapy and radiotherapy used to kill tumor cells are principally mediated by the process of apoptosis which is governed by the mitochondria. The failure of anti-cancer therapy often resides at the level of the mitochondria. Therefore, the mitochondrion is a key pharmacological target in cancer due to many of the differences that arise between malignant and healthy cells at the level of this ubiquitous organelle. Additionally, targeting the characteristics of malignant mitochondria often rely on disruption of protein-protein interactions that are not generally amenable to small molecules. We discuss anti-cancer peptides that intersect with pathological changes in the mitochondrion.

Introduction

The mitochondrion holds importance among cellular organelles in consideration of selective anti-cancer therapy because it is the nexus for propagating malignant

Reprinted by permission from Ther Deliv. 3:961-979 (2012). Copyright 2012 Future Science LTD.

transformation and controls cell death. The mitochondrion is a universal target in all cancer cells, and new information about functional and structural differences between healthy and malignant cells continues to emerge (1). Peptides that specifically target malignant mitochondria offer advantages of low toxicity, high specificity and generally increase the range of interactions that are difficult to target with small molecules (e.g., protein-protein, protein-lipid and, protein-DNA) (2). However, the benefits of peptides are offset by difficulties in delivery such as degradation by proteases and rapid clearance. As such, the delivery of peptide/protein therapeutics is almost exclusively by the parenteral route, but the status quo is actively being challenged by broad efforts (e.g., liposomes, microparticles, nanoparticles, 'smart' polymers, hydrogels, chemical modifications to the peptide/protein) to achieve more convenient routes of administration (i.e., oral, nasal, transdermal) and improved pharmacokinetics (3-5). Yet, peptides, in many cases, are far from passive in the delivery process and through the maze that is drug delivery (from route of administration to perhaps a target residing within a specific organelle) peptides are employed as the vehicle, homing motif, and trans/intra-cellular passport (6).

There is an emerging view in cancer therapy that the way in which a cancer cell dies (i.e., immunogenic cell death) is important for a durable response (7). However, traditional chemotherapy and immune response are in conflict because chemotherapy (e.g., DNA-damaging agents) often induces the substantial destruction of immune effectors (8). However, targeting the mitochondria may be the key to initiate or manipulate the type of death a cell dies and commit a cancer cell to 'immunogenic apoptosis' (9). Pairing therapeutic peptides targeting malignant mitochondria with

existing small molecule chemotherapy could lower dose requirements and curb traditional treatment-associated toxicity (10). Thereby combined therapy could spare the immune system, reduce patient side effects, sensitize cancer cells to death, and establish a durable response (11).

The mitochondrion is now dually famous as both the cellular ‘powerhouse’ and as central regulator of the cell death pathway that bears its name. The outer membrane of the mitochondrion (OMM) is generally permeable to metabolites and ions, while the inner membrane (IMM) maintains a tightly regulated ion flux. Respiration-driven efflux of protons across the IMM during oxidative phosphorylation sets up a large electrochemical gradient comprised of a difference in both the voltage ($\Delta\Psi_m$) and the concentration of ions across the membrane (Δ_pIon). This electrochemical gradient is the driving force for the production of ATP. Importantly, the negative interior, called the mitochondrial matrix (where the citric acid cycle and fatty acid beta-oxidation transpire), allows the accumulation of molecules with cationic character. The intermembrane space (IMS) hosts an array of cytotoxic proteins that are released upon OMM permeabilization (12).

Newer cancer therapies are expected to kill malignant cells while producing minimal or no toxicity to normal cells. This expectation is borne out of the tremendous pace at which our understanding of tumor-specific molecular profiles has occurred in the last decade. The identification of tumor markers has lead to the development of new selective cancer therapies such as trastuzumab which targets the overexpression of HER2/neu in 30% of patients with breast cancer (13). However, the search is on for more global cancer markers with the hope of generating a more generic cancer therapy. Peptides could properly be referred to as ‘smart’ nanoparticles because they are capable

of encoding targeting, entry, and therapeutic modality into one customizable unit (14). To this end, one of the emerging strategies is the therapeutic targeting of proteins that affect multiple downstream pathways (i.e., so-called nodal proteins) in cancer signaling (15). In this respect, the mitochondrion has become the focus of much interest for cancer therapy as it is the central 'node' of cell death induction (*Fig. 2.1*) (11).

The mitochondria of tumor cells are structurally and functionally different from those of untransformed cells (1). The alterations in malignant mitochondria or the metabolic pathways governing mitochondrial function vary by cancer type and level of disease progression (16). Mitochondrial adaptations that take place in cancer range from subtle (e.g., isoform switching) to profound dysfunction (17). Yet, any deviation between healthy and malignant cells is an opportunity to be therapeutically leveraged. Many of the current and emerging therapeutic mitochondrial targets are protein-protein/lipid/DNA interactions which are less amenable to small molecule intervention. Peptide (and protein) therapeutics, as a class of drugs, are well suited to exploit the often subtle differences between healthy and diseased mitochondria. This review focuses on current and potential mitochondrial anti-cancer targets in connection with therapeutic peptides.

Mitochondrial cell death pathway

Cell death is generally categorized into either subtypes of step-wise regulated programmed cell death (PCD) or a passive disintegration termed necrosis (18). PCD that is intracellular in origin is known as the intrinsic apoptotic or mitochondrial cell death

Figure 2.1. Targeting the mitochondria with peptides. Selective targeting of the mitochondria of malignant cells can be achieved by engineering motifs that drive mitochondrial accumulation of the toxic peptide based on differences that commonly exist between cancerous and healthy cells. Internalization of the peptides can be mediated based on the nature of the peptide (e.g., CPPs) and its interaction with the plasma membrane or via receptor complex endocytosis (e.g., tumor homing motif). The internal milieu of malignant cells (e.g., pro-oxidative environment or upregulated enzymes, such as kinases) can provide the opportunity to customize the mitochondrial targeting of a peptide. For instance, a cryptic MTS can be employed that requires phosphorylation (highlighted "P") prior to mitochondrial trafficking. Depending on the sequence, mitochondriotoxic peptides can be 'addressed' to individual or multiple submitochondrial locations. CPP, cell-penetrating peptide; MTS, mitochondrial targetingsequence; OMM, outer mitochondrial membrane; IMS, intermitochondrial membrane space; IMM, inner mitochondrial membrane.

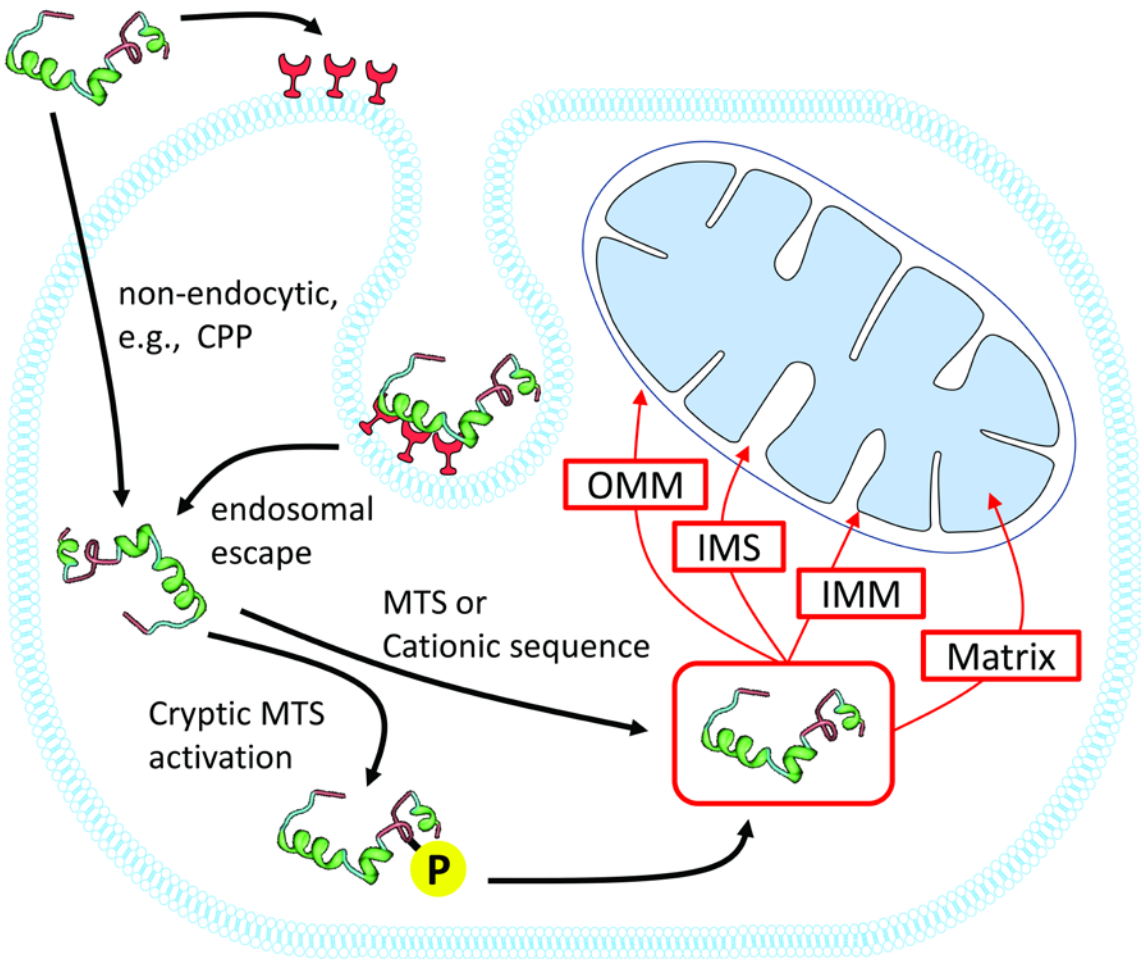
non-endocytic,
e.g., CPP
endosomal
escape
MTS or
Cationic sequence
Cryptic MTS
activation
P
OMM
IMS
IMM
Matrix

pathway. However, the mitochondrion ultimately plays a key role in all active PCD cell death pathways (18). Most cytotoxic anti-cancer agents, in spite of having diverse mechanisms of action, cause death through the mitochondrial pathway (19). More precisely, death induction signaling from chemotherapy funnels down to the activation of mitochondrial outer membrane permeabilization (MOMP) which, in turn, is controlled by the balance between positive or negative regulators of OMM integrity (*Figure 2.2*) (19). In many cancers (e.g., leukemia, melanoma, and hepatocellular carcinoma), resistance to chemotherapy has been directly attributed to the overexpression of the anti-apoptotic Bcl-2 (B-cell lymphoma-2) family members (20).

The Bcl-2 family of proteins are categorized as members with four Bcl-2 homology domains (BH1-BH4) or with only one BH domain, the BH3-only proteins. All of the BH3-only proteins (e.g., PUMA, NOXA, Bad, Bim, and Bid) are classified as pro-apoptotic while Bcl-2 proteins with four BH3 domains are anti-apoptotic (e.g., Bcl-2, Bcl-x_L, Bcl-w, Mcl-1, and Bfl1) with the exceptions of Bak and Bax. MOMP proceeds by activation and oligomerization of Bax and/or Bak 'effectors' to form pores in the mitochondrial outer membrane allowing the release of pro-apoptotic factors such as cytochrome c, apoptosis-inducing factor (AIF), second mitochondria-derived activator of caspase (Smac), endonucleases and HtrA2. Upon release of the apoptotic factors from the IMS, cytosolic caspases are activated, and the cell is committed to destruction (21).

Bak is constitutively found at the OMM while Bax is cytosolic, until activated, whereupon it translocates via an N-terminal MTS to the OMM. The anti-apoptotic members of the Bcl-2 family, such as Bcl-2 and Bcl-x_L, have been found to localize at the OMM, the endoplasmic reticulum, and nuclear membranes (21). Bax or Bak monomers

Figure 2.2. Mitochondriotoxic peptides. Mitochondriotoxic peptides facilitate mitochondrial dysfunction by either direct or indirect induction of MOMP through Bcl-2 family interactions, PTP opening, or membrane disruption. MOMP initiated by manipulation of Bcl-2 family members converges on Bax and Bak homo- or hetero-oligomerization in the OMM to form pores that allows the cytosolic release of IMS proteins such as cytochrome c, Smac, and AIF. Bax activation also inhibits the mitoKv1.3 IMM channel leading to IMM hyperpolarization and increased ROS production. Upon PTP opening is there is an unregulated influx of cytosolic solute, loss of $\Delta\psi_m$, and mitochondrial swelling. Mitochondrial swelling bursts the OMM and releases the pro-death IMS proteins. The PTP is minimally comprised of the voltage-dependent anion channel (VDAC), adenine nucleotide translocase (ANT), and cyclophilin D (CYPD). PTP opening can be suppressed by interaction with anti-apoptotic Bcl-2 family members, hexokinase (HK), translocator protein (TSPO), and the heat shock proteins Hsp90 and TNF receptor-associated protein (TRAP-1). MOMP and release of IMS apoptogenic factors can also occur through the direct disruption of membrane integrity. Therapeutic peptides are represented in red boxes. Solid red lines show peptide target. Dashed lines indicate peptides that have multiple targets.

MOMP, mitochondrial outer membrane permeabilization; PTP, permeability transition pore complex; OMM, outer mitochondrial membrane; IMS, intermitochondrial membrane space; IMM, inner mitochondrial membrane; Cyt c, cytochrome c; Smac, second mitochondria-derived activator of caspases; AIF, apoptosis-inducing factor; Endo G, endonuclease G; HtrA2, high temperature requirement protein A2; OXPHOS,

oxidative phosphorylation; EGFR, epidermal growth factor receptor; HER2, human epidermal growth factor receptor 2; MUC1, mucin 1.

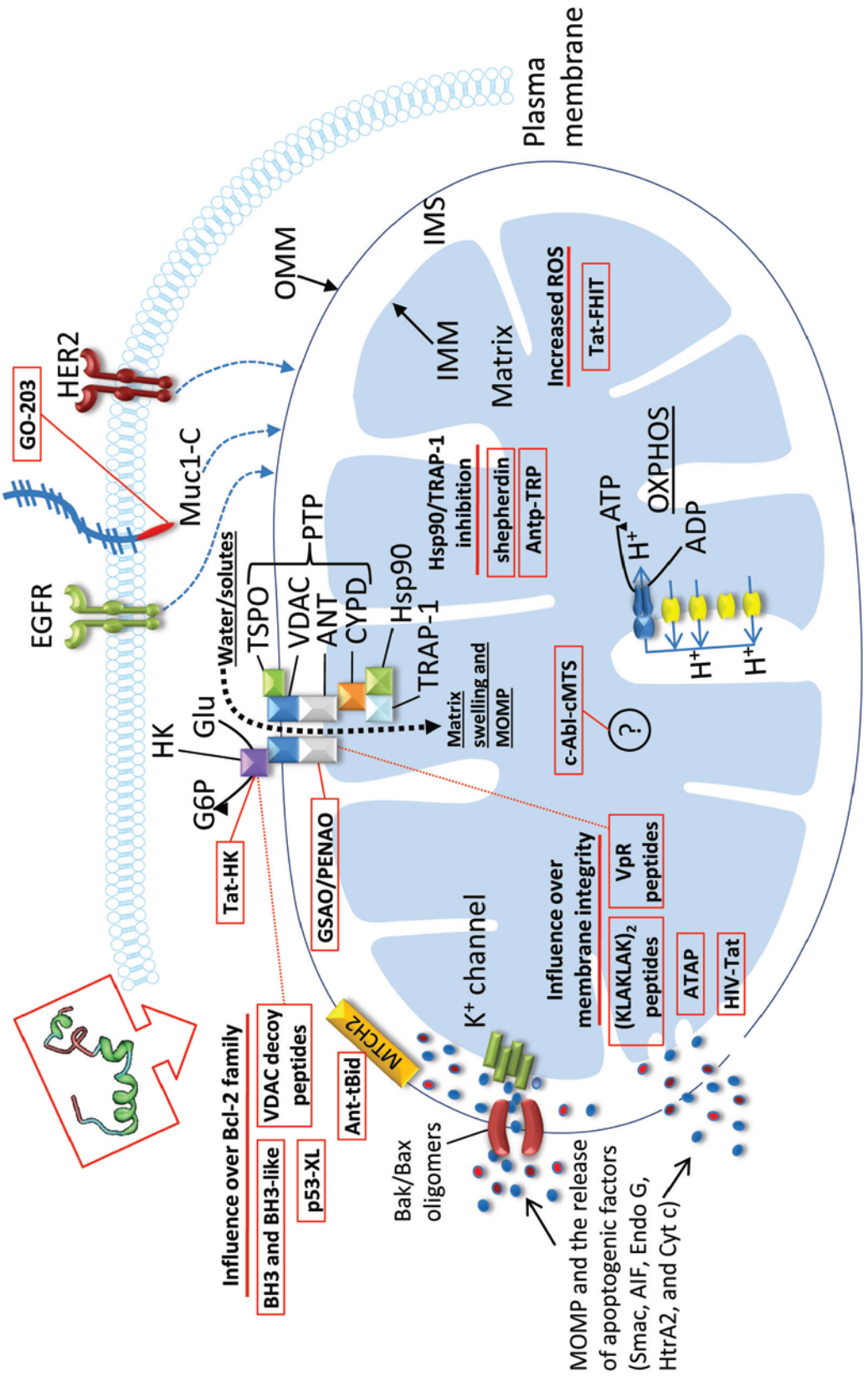
Plasma membrane
OMM
IMS
IMM
Matrix
HER2
GO-203
Muc1-C
EGFR
Water/solutes
TSPO
VDAC
ANT
CYPD
PTP
Hsp90
TRAP-1
Hsp90/TRAP-1 inhibition
shepherdin
Antp-TRP
Increased ROS
Tat-FHIT
OXPHOS
ATP
ADP
H+
HK
Glu
G6P
Tat-HK
GSAO/PENAO
Matrix swelling and MOMP
c-Abl-cMTS
?
Influence over membrane integrity
VpR peptides
(KLAKLAK)2 peptides
ATAP
HIV-Tat
K+ channel
MTCH2
Ant-tBid
Influence over Bcl-2 family
BH3 and BH3-like
VDAC decoy peptides
p53-XL
Bak/Bax oligomers
MOMP and the release of apoptogenic factors (Smac, AIF, Endo G, HtrA2, and Cyt c)

or hetero-oligomers of both proteins form aqueous channels in the OMM. The activation of Bak and Bax may be initiated by many different stimuli including direct interaction with p53 (22), BH3-only proteins such as Bid or Bim, and post-translational modifications (23). Bax inhibition of a IMM potassium channel (mitoKv1.3) also seems to be crucial to cytochrome c, AIF, and Endo G release from the IMS, unlike Smac and HtrA2 which are released independently of mitoKv1.3 function. It has been suggested that the release of cytochrome c, AIF, and Endo G are all dependent on a mechanism based on increased ROS and that this coincides with the inhibition of the mitoKv1.3 channel (24). ROS increase is a central event in the release of cytochrome c release from the IMS where it is bound to the IMM in association with the unique mitochondrial phospholipid cardiolipin (21). However, it remains unclear whether the efflux of cytochrome c occurs solely by oligomeric Bax and other protein channels and/or by the activation of a matrix to cytosol spanning permeability transition pore (PTP) and cristae remodeling (25, 26).

The mitochondrial PTP may generally function as a mitochondrial Ca^{2+} release channel to regulate physiological Ca^{2+} dynamics; however, it also plays an important role in apoptosis. The PTP is comprised of the Translocator Protein (TSPO; formerly named peripheral-type benzodiazepine receptor (PBR)) located at the outer/inner mitochondrial membrane contact sites, the voltage-dependent anion channel (VDAC), and the adenine nucleotide translocase (ANT). The anti-apoptotic Bcl-x_L interacts with the ANT, and it has been proposed that this interaction can prevent cell death. In addition, Bcl-2 and Bax may modulate VDAC activity (24).

In some cases, nonselective toxins kill malignant cells more readily than healthy cells (27). This phenomenon is analogous to non-specific cytotoxic drugs that attack common targets such as DNA or microtubule formation, but which nonetheless kill rapidly proliferating tumor cells preferentially. A recent study correlates cytotoxic chemotherapy efficacy with a 'primed' status of malignant cell mitochondria (28). However, like classical chemotherapy, any agent that is nonselective runs the risk of toxic side effects. The same reasons that make mitochondria an excellent anti-cancer target (i.e., cell death and oncogenic transformation functions) also suggests indiscriminate mitochondrial toxins will be unacceptable as chemotherapeutics. The strategy of mitochondrial targeting with intent to cause dysfunction ought to include a 'cancerotropic' modality. Depending upon the mitochondrial toxin and type of malignancy, the mitochondria of cancer cells may be self-selecting by way of being in a so-called 'primed' state such that the therapeutic index between healthy and cancerous cells for a nonspecific mitochondrial toxin may be very broad. This is unlikely to be true across the typical heterogeneity of cancer, however, and developing selective agents is a prudent course.

Peptide therapeutics can be readily designed to minimize off-target effects in three ways: first, by including a targeting moiety selective to cancer cells coupled to nondiscriminating mitochondriolytic entities; secondly, by using an agent that has a mechanism of action based on structural and/or functional differences inherent between healthy and malignant mitochondria; or third, using a therapeutic entity toxic to mitochondrial but which remains spatially segregated from the mitochondria unless intracellular pathologic conditions common to cancer cells initiate mitochondrial

translocation. Ideally, a combination of these approaches could be used to minimize off-target effects (*Fig. 2.1*).

Malignant mitochondria (the tumor signature)

Recognition of a difference between the mitochondrial function of healthy cells and those of malignant cells was made by Otto Warburg in the late 1920's. Warburg discovered malignant cells produce ATP via glycolysis even under aerobic conditions (i.e., the so-called Warburg effect) (12). Warburg's attempt to attack malignant mitochondria on a bioenergetic basis was unsuccessful because the glycolytic shift in malignant cells is not (as presumed by Warburg) due to a fundamental dysfunction of mitochondrial oxidative phosphorylation but instead related to changes in metabolic signaling pathways (1). However, recent discoveries (including the mitochondrion as a central regulator of cell death) concerning bioenergetic alterations and malignant transformation have brought Warburg's general strategy back into favor (12). In addition to corrupted bioenergetic pathways, mitochondrial proteins responsible for controlling the processes of apoptosis/necrosis, respiration, and mitochondrial membrane integrity are being exploited for the selective destruction of malignant cells over healthy cells (11).

Even if mitochondrial function is not fundamentally impaired in cancer cells, mitochondrial activity is altered by environmental changes (e.g., low oxygen) and genetic reprogramming (1). Rapidly expanding tumor cells, in addition to adapting for continued survival, also exploit adaptive mechanisms to meet the vast energetic requirements for proliferation. Metabolic reprogramming is a way to increase ATP production in an oxygen-independent manner while supplying the necessary constituents for anabolism.

The shift between glycolysis and oxidative phosphorylation is controlled by two enzymes, mitochondrial pyruvate dehydrogenase (PDH) and lactate dehydrogenase (LDH), that control the catabolic fate of pyruvate (1). Hypoxia inducible factor-1 (HIF-1) plays a key role in metabolic adaption either to hypoxia itself or through loss-of-function mutations in oxygen-sensing genes. In connection to pyruvate catabolism, HIF-1 upregulates pyruvate dehydrogenase kinase (PDK1) which inactivates PDH and suppresses oxidative metabolism of pyruvate in the TCA cycle. This glycolytic shift may also serve to protect cancer cells from producing cytotoxic levels of ROS (12). The success of a small molecule inhibitor of PDK1 (dicholoroacetate) has validated targeting cancer energy metabolism. This drug specifically acts on the mitochondria of cancer cells without disturbing the physiology of nonmalignant cells (29).

Other mitochondrial changes can also attend the metabolic adaptations in malignancy that impact mitochondrial function and can reinforce metastatic potential. For instance, increased superoxide formation (ROS), increased mitochondrial membrane potential, isoform switching, and alterations in ion channel expression levels have been linked to perpetuating malignancy or chemotherapeutic resistance (30).

Mitochondrial reactive oxygen species

Circumstances dealing with ROS and malignancy often seem contradictory (31). Increased ROS levels caused by oncogenic processes and perpetuating tumorigenicity seem inconsistent with therapeutic ROS generation leading to cell death induction (32). Elevated intracellular ROS can lead to the activation of transcription factors (e.g., HIF-1 and NF-κB) leading to a host of protein expression profiles that contribute to malignancy

such as proliferation, survival, and metastasis (31). This situation leads to a seeming 'ROS paradox' where many antineoplastic agents exert their cytotoxic effects through the generation of ROS (33). The underlying mechanisms for the essential ROS-mediated killing by chemotherapeutics and radiation therapy is not well understood (31). However, increased ROS magnitude from therapeutic treatment adds to the already high oxidative burden of the cancer cell overwhelming the antioxidant capacity and thereby causing cell death (34). Moreover, the elevated ROS condition is likely to contribute to cytochrome c mobilization in malignant cells (35). Unfortunately, the heterogeneity of cancer cell survival mechanisms can also operate by strongly suppressing ROS production as occurs in resistant breast cancer tumor stem cells (32). This often occurs through the overexpression of mitochondrial ROS scavenging enzymes such as peroxiredoxin 3, thioredoxin reductase and/or manganese superoxide dismutase (MnSOD) (36).

The targeted delivery of a therapeutic fusion protein to the mitochondria has been used to exploit the production of cytotoxic levels of ROS in cancer models (37). One such protein that can generate ROS is fragile histidine triad protein (FHIT). Across a variety of cancer types apoptosis is induced by transfection or transduction of the fragile histidine triad protein (FHIT) gene. The (FHIT) is a tumor suppressor that exerts its pro-apoptotic action (in a complex with ferrodoxin reductase) at the mitochondria by generating ROS and stimulating calcium uptake (38). Recently, a HIV-Tat derived protein transduction domain fusion with FHIT (TAT-FHIT) was used to induce apoptosis in hepatocellular carcinoma cells (*Table 2.1*) (37).

Table 2.1. Anti-cancer proteins/peptides targeting the mitochondria

Peptide/protein	Mitochondrial target	Mode of action	Refs
HIV-1 Tat	*Mitochondrial membranes*	*MOMP*	*(39)*
TAT-HK	*Hexokinase isoform 2 associated with OMM*	*Disruption of HK association with OMM and disinhibition of PTP opening*	*(40)*
TAT-FHIT	*Ferrodoxin reductase*	*Increased ROS and calcium flux*	*(37)*
HIV-VpR	*VDAC/ANT/Bax mediated IMM and OMM permeabilization; reduced expression of mitofusin 2*	*MOMP via disinhibition of PTP complex and/or Bax activation; interruption of mitochondrial-endoplasmic reticulum interaction*	*(41, 42)*
TEAM-VP (RGD-VpR)	*VDAC/ANT mediated IMM and OMM permeabilization*	*MOMP*	*(43)*
BHAP (bifunctional: contains ar AHNP is anti-HER2 moti and $(KLAKLAK)_2$)	*Mitochondrial membranes*	*MOMP*	(44)
RGD-4C-GG-D-$(KLAKLAK)_2$	*Mitochondrial membranes*	*MOMP*	*(45,46)*
ATAP	*OMM*	*MOMP*	*(47)*
Ant-BH3	*Bcl-x_L*	*MOMP*	*(48)*
LHRH-BH3	*Bcl-x_L and Bcl-2*	*MOMP*	*(49)*
SAHBs (e.g., BIM-SAHB)	*Anti-apoptotic and effector (Bak/Bax) Bcl-2 family proteins at the OMM*	*MOMP*	*(50)*
072RB (Bim derived peptide fused to Ant internalization sequence)	*(Bcl-x_L) but likely other anti-apoptotic and effector (Bak/Bax) Bcl-2 family proteins at the OMM*	*Bax activation and MOMP*	*(51)*
IP3R decoy peptides	*Bcl-2 (on endoplasmic reticulum)*	*Pro-apoptotic calcium release*	*(52)*
shepherdin	*Mitochondrial Hsp90 and TRAP-1*	*Disinhibition of PTP opening, mitochondrial depolarization*	*(53)*
Antp-TRP	*Hsp90*	*Apoptosis*	*(54)*
Ant-tBid (111-125) and Ant-tBid (59-73)	*MTCH2 interaction at OMM*	*Apoptosis*	*(55)*
GSAO and PENAO	*ANT*	*PTP opening, mitochondrial depolarization*	*(56)*
VDAC decoy peptides	*Multiple targets: hexokinase, Bcl-2, and Bcl-x_L*	*Mitochondrial sensitization to apoptotic stimuli*	*(57)*
p53-XL (p53 targeted to the OMM)	*Interaction with Bcl-2 family members: Bcl-x_L, Bak, and Bax*	*MOMP*	*(58)*
c-Abl-cMTS (matrix targeted c-Abl)	*Unknown*	*Apoptosis*	*(59)*
GO-203	*C-terminal portion of MUC1*	*Disrupts MUC1-C ROS suppression*	*(60)*

Table 2.1 Continued

ANT, adenine nucleotide translocase; VDAC, voltage-dependent anion channel; Mfn2, mitofusin 2; DRP1, dynamin-related protein 1; Bcl-2, B-cell lymphoma protein 2; GSAO, 4-(N-(S-glutathionylacetyl)amino)phenylarsenoxide; PENAO, (4-(N-(S-penicillaminylacetyl)amino) phenylarsonous acid); ant or antp, Antennapedia helix III, also called Penetratin; Hsp90, heat-shock protein, 90 kDa; ROS, reactive oxygen species; MOMP, mitochondrial outer membrane permeabilization; OMM, outer mitochondrial membrane; IMM, inner mitochondrial membrane; p53-XL, tumor suppressor protein p53 fused to the canonical MTS of Bcl-x_L; cMTS, cryptic mitochondrial translocation sequence; mitoKv1.3, mitochondrial voltage-gated potassium channel 1.3; $\Delta\psi_m$, potential difference across inner mitochondrial membrane; HIV-1, human immunodeficiency virus 1; TAT or Tat, transactivator of transcription; VpR, viral protein R; PTP, permeability transition pore; EGFR, epidermal growth factor receptor; MUC1, mucin 1; HK, hexokinase; BHAP, bifunctional, HER-2-blocking and apoptosis-inducing peptide; TEAM-VP, Targeted to Endothelial Apoptogenic Mitochondrio-active VpR-derived Peptide; BH3, Bcl-2 homology domain 3; LHRH, luteinizing hormone-releasing hormone; SAHB, stabilized alpha-helices of Bcl-2 family protein; IP3R, inositol 1,4,5-trisphosphate receptor; FHIT, fragile histidine triad; tBid, truncated Bid.

Mitochondrial DNA

The mitochondrion, like the nucleus, but unlike any other organelle contains DNA. The mitochondrial DNA (mtDNA) is thought to be particularly vulnerable to ROS-mediated damage due to its proximity to ROS production via the ETC and less robust DNA repair mechanisms, as compared to the nuclear system of DNA repair (61). The susceptibility of mtDNA oxidative damage may be a key contributor to tumor cell formation where the overproduction of mitochondrial ROS can lead to a vicious cycle that increases metastatic potential. To this point, tumor cell development is associated with impaired production of ETC proteins which, in turn, are less efficient and generate increased ROS (30, 33).

Mitochondrial membrane potential

Tumor progression and expansion has been correlated to increased mitochondrial membrane potential ($\Delta\Psi_m$). Within tumor cell subpopulations, the higher the $\Delta\Psi_m$, the more likely the contribution to tumor progression and expansion (62). In human epidermoid adenocarcinoma and hepatoma cancer cells, a higher $\Delta\Psi_m$ defines resistance to cisplatin (63). As the $\Delta\Psi_m$ increases, intracellular cationic entities will increasingly permeate the mitochondria. Therefore, even slight gains in $\Delta\Psi_m$ may confer a greater killing capacity for cationic agents (including peptides; e.g., shepherdin, *see below*) in cancer cells (62).

Isoform switching

Malignant cells adapt in many ways including isoform switching at the mitochondria to compensate for bioenergetic demands (e.g., M2 isoform of pyruvate kinase (17)) and to survive harsh environmental conditions (64). For instance, as a potential way of reducing the ROS burden, cellular adaptation to low oxygen conditions is often accompanied by isoform switching of the mitochondrial respiratory chain via activity of the hypoxia transcription factor, HIF-1 (64). In some forms of cancer, HIF-1 induces a more efficient COX4-2 (cytochrome c oxidase subunit IV isoform 2) expression and the degradation of COX4-1 isoform thereby allowing respiration to proceed with less ROS produced as a byproduct (64).

Interestingly, Lacoeur et al. showed that a synthetic human immunodeficiency virus trans-activator of transcription (HIV-Tat) protein (86 residues) inhibits cytochrome c oxidase (COX) activity in disrupted mitochondria. The HIV-Tat protein also caused loss of $\Delta\Psi m$ and cytochrome c release independent of PTP and Bcl-2 family status (39). Also, an acetylated HIV-Tat (residue 28) was shown to stimulate the mitochondrial translocation of the pro-apoptotic Bim (39). HIV-Tat may be a useful platform for future investigations into MOMP/PTP-independent targeting of malignant mitochondria. The toxic consequences of HIV-Tat are related to another mitochondriotoxic HIV proteins (HIV-1 viral protein R or VpR, (*Table 2.1*)) that have been used to target the mitochondria of cancer cells (65).

Mitochondrial ion channels

Potassium channels, components of the permeability transition pore, and mitochondrial calcium uniporter are mitochondrial ion channels that have been recognized as therapeutically important targets in cancer (66). Peptide toxins have long been used for pharmacologic targeting of ion channels. Some of these may have utility in targeting aberrantly expressed mitochondrial potassium channels such as the mitoKv1.3 (66).

The expression profiles of voltage-gated potassium (Kv) channels, which have a role in controlling membrane potential, are remodeled in the majority of cancers with a correlation between Kv overexpression and grade of tumor malignancy in certain tumor types (66). Mitochondrial potassium ($MitoK^+$) channels are also found to play important roles in both cytoprotection and apoptosis (recently reviewed in (67)). Because of this, $mitoK^+$ channels are considered promising therapeutic targets in cancer (68). The IMM localized Kv1.3 is the best characterized mitochondrial Kv, and the Kv1.3 channel (mitochondrial and plasma membrane) is characterized by a very selective and potent peptide toxin pharmacology (25).

Interestingly, mitoKv1.3 is inhibited by an interaction within the IMS with the OMM spanning pro-apoptotic Bax, leading to hyperpolarization of the IMM, resulting in increased ROS production, loss of cytochrome c, propagation of mitochondrial dysfunction and apoptosis (25). Bax inhibition of mitoKv1.3 was dependent on a specific highly conserved Bax residue, Lys 128. In spite of Bax inhibition of mitoKv1.3 being required for efficient induction of apoptosis, the absence of the mitoKv1.3 can cause resistance to apoptosis (25). Szabo et al. recently reported that the action of Bax at the

OMM can be substituted by peptide toxins of the mitoKv1.3 channel (67). The steadily increasing recognition of the role of MitoK^+ channels in cancer and mitochondrial function puts a new emphasis on the importance of these channels in the development of targeted anti-cancer therapy (e.g., MitoK^+ channel, TASK-3, is indispensable for survival of melanoma cells) (69, 70).

After decades of searching, the mitochondrial calcium channel (mitochondrial calcium uniporter or MCU) has been newly discovered (71). Increased expression of the MCU increases mitochondrial calcium accumulation, and sensitizes cells to apoptotic stimuli (71). Since calcium is one of the triggers (ROS is another) for PTP opening, this channel is highly relevant in pathological conditions, such as cancer (72). The MCU will undoubtedly be intensely focused on as a target for modulating cell death (72).

Plasma membrane to mitochondria protein translocation

Tumor cells re-program intracellular mitochondrial trafficking as a mechanism to escape apoptosis (73). Several cell surface proteins translocate to the mitochondria and elicit distinct biological functions in malignant cells (73). For instance, EGFR (epidermal growth factor receptor), MUC1-C (C-terminal portion of the oncogenic transmembrane glycoprotein mucin 1) (74), and HER2 (human epidermal growth factor receptor 2) aberrantly localize to the mitochondria and antagonize apoptosis (*Figure 2.2*). The EGFR family (e.g., EGFR/ERBB1, HER2/ERBB2, and HER3/ERBB3) are often overexpressed and associated with progression, proliferation, and drug resistance in many forms of cancer (75). However, EGFR tyrosine kinase inhibitor (TKI; e.g., gefitinib, lapatinib, erlotinib) and monoclonal antibody anti-EGFR therapeutic agents have met with only

modest efficacy in clinical trials (73). Unfortunately, the process of mitochondrial translocation and antagonism of apoptosis by EGFR is actually enhanced by TKI treatment (76). At the mitochondria, EGFR interacts with and inhibits the pro-apoptotic PUMA (p53-upregulated modulator of apoptosis) (76). The consequences are reduced efficacy of EGFR inhibitors and increased apoptotic threshold of cancer cells (73). Interestingly, in clinical trials, pre-treatment (more so than concomitant treatment) of medulloblastoma and glioblastoma cells with obatoclax (GX15-070), a small molecule inhibitor of Bcl-x_L and Mcl-1, led to a greater than additive enhancement of TKI lapatinib-induced cell death (77), indicating that the disruption of the protein-protein interaction between EGFR and PUMA could be an important therapeutic modality in glioblastoma multiforme and possibly other cancers (76).

Abnormal expression of MUC1 in multiple types of cancer can be targeted with a peptide inhibitor, GO-203, which is in phase 1 clinical trials. GO-203 blocks the pleiotropic MUC1-C oncogene causing a derepression of ROS production (60, 78).

Mitochondrial membranes

One of the key differences between malignant and healthy mitochondria may be the lipid composition of the OMM (26). Mitochondrial membrane composition and the spatial organization of its components may fundamentally affect the processes of apoptosis (21). For instance, in healthy cells the cholesterol content in OMM (and possibly the shape) of the mitochondria may prevent Bax activation (21). Cardiolipin, a phospholipid found exclusively in mitochondrial membranes (primarily the IMM), interacts with the α-helices of tBid (79). A protein/lipid complex containing

cardiolipin/tBid (also, the protein MTCH2/MIMP, see section '*MTCH2*') at the OMM are thought to facilitate pore formation by Bax oligomers (21). However, the exact protein structure/function relationship is not well understood in the context of proteins becoming embedded in the dynamic mitochondrial membrane environment, making the precise mechanistic elucidation of MOMP a challenge (21). As mentioned previously, Bax and Bak OMM localization in 'primed' malignant mitochondria is not random but likely coincides with mitochondrial fission sites for optimal MOMP formation (21).

Membrane disrupting mitochondriotoxic peptides

The 96-amino acid HIV-VpR protein, comprised of 3 α-helical domains, can integrate into and permeabilize mitochondrial membranes reducing the $\Delta\psi_m$, causing fragmentation and cristae swelling (41). In addition, HIV-VpR can influence apoptosis by interactions with ANT, VDAC and/or Bax (42). In contrast to other viral proteins that target the mitochondria, the HIV-VpR lacks a canonical MTS, and its association with mitochondria is also independent of the translocase of the outer membrane (TOM) complex (80).

An amphipathic tail-anchoring peptide (ATAP) derived from Bcl-2 family member Bfl-1 was effective in inducing MOMP, possibly by homo-oligomerization and pore formation. A green fluorescent protein fused ATAP was shown to target the mitochondria (via an intrinsic MTS) (47). However, as with other pore-forming peptides, ensuring selective targeting to tumor cells will be a priority consideration for future therapeutic development.

Various cationic peptides exhibit an immediate cytotoxic effect against cancer cells, in many cases by binding and disrupting the plasma membrane (81, 82). However, due to the difference in potential at the mitochondria versus the plasma membrane, cationic peptides selectively disrupt mitochondrial membranes at concentrations hundreds of times lower that what is required to interfere with plasma membrane integrity (83). As one of the pathological hallmarks of cancer is a stably increased $\Delta\Psi_m$, even modest gains in attraction of cationic mitochondriolytic peptides, although nonselective, may confer a greater killing capacity for cancer cells (62). A common mitochondriotoxic peptide motif is the $(KLAKLAK)_2$ (synthetic derivative of a natural antimicrobial peptide) which causes mitochondrial membrane damage and subsequent triggering of apoptosis. The $(KLAKLAK)_2$ peptide does not efficiently cross the plasma membranes of eukaryotic cells and has low toxicity unless it is coupled to selective targeting domains allowing internalization by cells (45). For instance, the RGD-4C-GG_D-$(KLAKLAK)_2$ or 'BHAP' (HER-2-blocking and apoptosis-inducing peptide; exocyclic AHNP motif fused to $(KLAKLAK)_2$) hybrid peptides allow targeting to endothelial cells of the angiogenic vasculature (45) or HER2-positive cells, respectively (44, 46).

Screening is also ongoing for oncolytic peptides to be found among antimicrobial or host-defense peptides. Evolutionarily conserved mitochondriotoxic pore-forming peptides (e.g., colicins, and translocation domain of diphtheria toxin) exhibit a structural similarity to Bax and Bak (21).

Bcl-2 family

The anti-apoptotic members of the Bcl-2 family (e.g., Mcl-1, Bcl-2 and Bcl-x_L) are often relegated to merely having a redundant role in apoptosis. In recent years, however, each Bcl-2 family member (anti- and pro-apoptotic) have been found to have their own specialized niches within the apoptotic program (and in non-apoptotic cellular functions) (84). For instance, each anti-apoptotic Bcl-2 family member binds a distinct subset of the pro-apoptotic Bcl-2 members (85). This class of mitochondrial proteins is considered to have tremendous potential for both small molecule and peptide targeted therapies (11). BH3 domains of pro-apoptotic Bcl-2 family members or small molecule BH3 mimetics are currently used to neutralize the anti-apoptotic action of Bcl-x_L, Bcl-w, and/or Bcl-2, thereby shifting the balance of power on the OMM from anti-apoptotic to pro-apoptotic to provoke MOMP (86). BH3 mimetics (e.g., ABT-263 (navitoclax), ABT-737, and GX15-070 (obatoclax)) are currently being evaluated in phase 1/2 clinical trials for patients with hematologic malignancies. However, thrombocytopenia is a major side effect of this class of drugs due to their ability to antagonize the pro-survival function of Bcl-x_L in platelets (86).

Early work targeting the Bcl-2 family employed a BH3-only domain (Bak) fused to either a cell penetrating peptide (CPP; derived from the Antennapedia protein (48)) or receptor-specific sequence from luteinizing hormone-releasing hormone, creating Ant-BH3 or LHRH-BH3, respectively (49). There are several variations on conformationally constrained BH3-only domains. For example ‘hydrocarbon-stapled’ peptides containing BH3 domains (stabilized alpha-helices of Bcl-2 family proteins or SAHBs; Bim-SAHB) are currently being developed as anti-cancer agents (50, 87). Also, modifications of the

BH3 domain using natural and non-natural amino acids to improve stability and enhance target specificity have been used as with the Bim-BH3 mimic, 072RB (51). As certain neoplasias are likely the consequence of mutations or aberrant regulation exclusively of Bim (88), the restoration of a 'therapeutic' Bim is an attractive possibility.

Bcl-2 itself is not a strictly mitochondrial protein and has several pro-survival functions including acting as a pro-angiogenic signaling molecule. Bcl-2 also controls cytoplasmic calcium levels via its BH4 domain in an interaction with inositol 1,4,5-trisphosphate receptors (IP3Rs) on the endoplasmic reticulum (ER). This interaction suppresses pro-apoptotic calcium signaling and buffers cells against pro-apoptotic stimuli (89). The apoptotic suppression by the BH4 domain of Bcl-2 is more potent than that of the well recognized pro-survival BH4 domain from Bcl-x_L against staurosporine treatment (90). The BH4 domain of Bcl-2 has been targeted with IP3R-mimetic peptides to trigger pro-apoptotic calcium signaling in malignant lymphocytes (in chronic lymphocytic leukemia) with suppressed IP3R Ca^{2+} signaling (52). Importantly, different iterations of the IP3R decoy peptide could alter the magnitude of the released calcium, and the calcium release was sufficient to kill these apoptosis-resistant lymphocytes (52).

Noxa's role in establishing the rate by which apoptosis occurs, in addition to its key role in changing the balance of autophagic processes toward cell death rather than survival, could provide a unique activity for a BH3-only protein if developed as a therapeutic entity (91). For instance, Noxa influences the kinetics in ABT-737- and TRAIL-induced apoptosis, since knockdown of Noxa delays the velocity of cell death induction in primary glioblastoma cultures derived from patient samples and in an *in vivo* tumor model (92). In light of Noxa's ability to alter the rapidity of cell death, specifically

targeting Noxa may be a means to manage the type of cell death a cell undergoes (i.e., immunogenic apoptosis) (93).

Mcl-1 is commonly associated with tumor cell resistance in several cancers, and certain therapies (radiation) can inadvertently cause resistance by increasing Mcl-1 expression (90, 94). The corollary is that suppression of Mcl-1 restores sensitivity to apoptotic inducers. Introducing the Mcl-1 BH3 helix was sufficient to inhibit Mcl-1 and permit apoptosis (95) whereas several attempts to inactivate positive regulators (e.g., GSK-3β) upstream of Mcl-1 have been largely unsuccessful. Mcl-1, however, is not blocked by the BH3 mimetic ABT-737 (86).

Permeability transition pore

Along with the Bcl-2 family, the members of the permeability transition pore (PTP) complex control mitochondrial membrane integrity. Therefore, the PTP is a key node for MOMP (96). Not surprisingly, dysregulation of the PTP is another mechanism allowing cancer cells to escape death (97). The PTP complex spans from the OMM to the matrix and primarily is thought to include: 1) Cyclophilin D (CYPD), a mitochondrial matrix constituent that is a peptidyl-prolyl cis-trans isomerase (and target for inhibition of cyclosporine A); 2) the adenine nucleotide translocase (ANT), an IMM protein, which is an example of isoform switching in cancer, through the overexpression of a MOMP resistant isoform ANT2 (96); and 3) the multifunctional voltage-dependent anion channel (VDAC), also called mitochondrial porin, which is localized to the OMM and serves as a key regulator of mitochondrial metabolite flux and apoptosis (98) (*Figure 2.2*). The PTP can also include the channel-like translocator protein (TSPO; formerly called the

peripheral benzodiazepine receptor) which contacts the VDAC and ANT from the OMM where it is localized and serves to transport cholesterol and other lipophilic molecules across the IMS in addition to possibly facilitating cytosolic to mitochondrial communication (99). Since TSPO basal expression is altered in a number of human pathologies including cancer, it is a promising drug target for a number of therapeutic applications (100). Another mitochondrial peculiarity that arises in cancer is the association of hexokinase (isoforms I or II) with the PTP at the surface of the OMM with VDAC. Upon displacement of hexokinase from PTP interaction (i.e., VDAC) on the mitochondrial surface by treatment with either small molecules or peptides (e.g., TAT-HK peptide (40)), MOMP and apoptosis ensues (96, 101). One of the functions of ANT particularly relevant in cancer is the provision of ATP to hexokinase. This promulgates the pathologic metabolic shift to glucose and stabilizes the closed conformation of the PTP complex (96).

A peptide derived from the mitochondriotoxic HIV Vpr (Vpr67-82) was fused to a homing/internalization peptide sequence RGD (cysteine-cyclized peptide frame holds the RGD motif in a restricted conformation; also used with $(KLAKLAK)_2$, *see above*, *'Membrane disrupting mitochondriotoxic peptides' section*) that recognizes the integrin $\alpha_v\beta_3$ receptor which is often upregulated in invasive tumor types. This fusion peptide (named TEAM-VP for Targeted to Endothelial Apoptogenic Mitochondrio-active Vpr-derived Peptide) selectively induced IMM and OMM permeabilization in a mechanism associated with VDAC and ANT interaction (43). Interestingly, this group also noted that mitochondrial fission occurred with administration of TEAM-VP (43).

Two peptide trivalent arsenical agents that target ANT are GSAO (4-(N-(S-glutathionylacetyl)amino) phenylarsonous acid) and PENAO (4-(N-(S-penicillaminylacetyl)amino) phenylarsonous acid, a cysteine mimetic analog of GSAO that is less prone to cellular efflux). ANT becomes inactivated upon the interaction between its matrix side cysteine residues and the arsenical component of GSAO or PENAO. The inactivation of ANT permits opening of the PTP and mitochondrial depolarization. Both GSAO and PENAO are currently in phase 1 clinical trials for patients with advanced solid tumors (56, 102).

VDAC activity can be modulated by a variety of proteins, notably members of the Bcl-2 family. The pro-apoptotic Bax and tBid, upon interaction with VDAC, increase the channel pore size (103). Contrastingly, in cancer VDAC is usually inhibited by the anti-apoptotic Bcl-2 proteins (e.g., Bcl-2 and Bcl-x_L) and hexokinase I and II. Shoshan-Barmatz et al. have developed a set of VDAC-mimetic peptides to relieve the anti-apoptotic pressure on VDAC (57). This resensitizes the malignant cell to death signaling. VDAC-derived peptides have been optimized to act as VDAC decoys for hexokinase, Bcl-2 and Bcl-x_L to restore apoptotic sensitivity to cancer cells. The addition of a cell penetrating peptide (CPP) motif to VDAC-mimetic peptides was effective in several cancer cell lines, including B-cell chronic lymphocytic leukemia (CLL) patient samples and chemo-resistant cell lines (57). Pharmacologic manipulation of the PTP/VDAC interactions may be an avenue to potentiate the efficacy of conventional chemotherapy (57).

Recently, nicotinic acetylcholine receptors (nAChRs) have been found in the OMM and interact with VDAC to regulate PTP function in response to apoptogenic

stimuli (e.g., calcium overload or H_2O_2) (104). Typically, nAChRs are associated with the cell plasma membrane in synaptic transmission in the muscle and nervous system (104). However, with the discovery of nAChRs at the OMM paired with the wealth of pharmacological agents known to modulate this class of channel, it is likely that mitochondrial nAChRs will become a prime therapeutic target (104).

Mitochondrial fission and fusion dynamics

There is a link between Bak and Bax, pro-apoptotic members of the Bcl-2 family and the processes of mitochondrial fission in apoptosis (21). To this point, Bax, Bak, and possibly Bcl-x_L are required for normal mitochondrial dynamics (105). However, a direct mechanistic tie remains controversial between MOMP and the processes of mitochondrial fission. Upon apoptotic induction the mitochondrial fission protein dynamin-related protein (Drp1) is recruited, along with Bax, to the OMM. Both active Bax and Bak form foci at mitochondrial fission sites (21).

One of the mechanisms whereby cancer cells evade death is by exploiting the pathway known as autophagy which is used by both normal and cancer cells to sustain metabolism and adapt to stressful conditions (106, 107). Typically under conditions of starvation, a cell can engage this lysosomal catabolic route to sustain metabolic demands (108). Autophagy is, paradoxically, considered both a cell death and cell survival mechanism, however, in the context of malignancy the true function of autophagy is thwarted and is therefore considered an escape route allowing survival (108). The engagement of this catabolic pathway is dependent on the mitochondria. Mitochondrial morphology determines the cellular response to autophagy (109) such that mitochondrial fusion spares the cell from death. Elongated mitochondria escape autophagic degradation

and exhibit optimized ATP production. Conversely, when elongation is blocked either genetically or pharmacologically the mitochondria consume ATP and trigger starvation-induced death (109). This autophagic mitochondrial fusion is driven by phosphorylation events and cytoplasmic retention of the pro-fission Drp1 (110). Since mitochondrial fusion is integral to cell survival in the autophagic pathway proteins that are central to this process are viable therapeutic targets. Mitofusins (Mfn1 and Mfn2) and Opa1 (Optic atrophy 1) are OMM and IMM localized proteins, respectively, that are essential for mitochondrial fusion (21). Mfn2 in particular has been focused on as a therapeutic target because of its role in mitochondrial metabolism and calcium homeostasis (41, 111).

The HIV Vpr (96 residues) has been shown to induce host cell death by increasing OMM permeability through interactions with VDAC and ANT (43) as well as by disturbing the OMM integrity (41), *see above*. However, HIV Vpr also depletes mitofusin 2 (Mfn2; essential GTPase for the fusion of mitochondrial membranes) leading to mitochondrial membrane deformation, loss of $\Delta\psi_m$ and cell death (41). The loss of functional Mfn2 via HIV Vpr and consequent reduction in the frequency of fusion among mitochondria suggest that Vpr may confer a unique therapeutic potential in the context of pathologic autophagy (41). The mitofusin proteins are also of interest because they help to coordinate mitochondria-to-mitochondria docking as well as tethering the mitochondria and endoplasmic reticulum together to coordinate calcium flow (41). The intersection between mitochondrial dynamics and apoptosis may be a central leverage point for inducing an immunogenic type of cell death (93).

Pro-apoptotic mitochondrial targeting proteins dysregulated in malignancy

p53

p53 is a critical tumor suppressor protein that is dysregulated in over 50% of cancers (112). Recapitulating its function is central to many anti-tumor therapies. Under a wide variety of cell stress conditions p53 accumulates in the nucleus and mitochondria (reviewed in (113)). At the mitochondria p53 is found within multiple compartments, such as the OMM, IMS, and matrix (114). Mitochondrial p53 regulates apoptosis by acting in different cellular compartments by: 1) directly modifying propensity for MOMP by interacting with proteins of Bcl-2 family, 2) inhibiting manganese superoxide dismutase (MnSOD) activity, and 3) regulating mitochondrial physiology in proliferative conditions via interaction with mitofilin (115). Mitofilin is a multifunctional regulator of mitochondrial architecture and protein biogenesis (116) and has critical functions in mitochondrial morphology and mitochondrial fusion and fission (as well as protein import), specifically in the formation of tubular cristae and cristae junctions (117). And finally, there is increasing evidence for the role of p53 in metabolism regulation and mitochondrial respiration, which could be a major component of p53 oncosuppressive function (114, 115). An advantage of targeting p53 to the mitochondria (versus the nucleus) may be the avoidance of nuclear negative regulators of p53 such as human double minute 2 (HDM2) and Fibroblast Growth Factor 1 (FGF1) which inhibit p53's nuclear function and are often highly expressed in certain types of cancer (118). Recent work in our laboratory has shown that targeting p53 to the OMM of a breast cancer cell line (T47D) using the MTS derived from Bcl-x_L triggered a rapid induction of apoptosis (58).

c-Abl

Chronic myelogenous leukemia (CML) is defined by the expression of the oncoprotein Bcr-Abl through a reciprocal chromosomal translocation in a hematopoietic stem cell fusing the ABL and BCR genes (119) creating the constitutively active Bcr-Abl tyrosine kinase. Bcr-Abl thwarts the normal pro-death functions of c-Abl. c-Abl has been termed a "mitochondrial wracking factor" (120) because active c-Abl translocation to the mitochondria induces cell death (121, 122). Artificially targeting c-Abl (as a fusion to a cryptic MTS) to the mitochondria of leukemia cells (K562) recapitulated c-Abl's pro-apoptotic function (59).

MTCH2

Recent work has demonstrated the importance of the mitochondrial carrier homologue 2/Met-induced mitochondrial protein (MTCH2/MIMP) that resides on the surface of the OMM in tBid-mediated apoptosis (55). MTCH2 facilitates mitochondrial recruitment of tBid (in conjunction with OMM cardiolipin, *see section 'Mitochondrial membranes'*) whereupon tBid activates Bax (21). MTCH2 is a conserved protein that belongs to the mitochondrial carrier protein (MCP) family, like ANT. Unlike ANT however, MTCH2 is localized to the OMM instead of the IMM (123). Peptides derived from the MTCH2 and tBid binding interface and fused to the Antennapedia CPP were able to induce apoptosis in cancer cells. While the mechanism of action is not yet clear, it is interesting that the tBid/MTCH2 interface-derived peptide does not include the BH3 domain of tBid (55, 123).

Upregulated mitochondrial survival factors

MnSOD

The exclusively mitochondrial manganese superoxide dismutase (MnSOD) is a key enzyme involved in superoxide radical scavenging (124). In the context of oncogenic progression MnSOD has a bimodal expression profile (permitting oncogenic levels of ROS to persist but preventing overwhelming ROS toxicity), where its expression is lower at early stages of malignancy and higher at later stages (125). Inhibition of aberrantly elevated MnSOD is considered an effective strategy to selectively kill cancer cells and diminish resistance to standard chemotherapy (126). Mitochondrial p53 inactivates MnSOD, leading to mitochondrial dysfunction and initiation of apoptosis (124, 127). Additionally, targeting NF-κB with an inhibitory peptide suppressed MnSOD expression in aggressive breast cancer cell lines MDA-MB231 and SKBR3 (126).

TRAP-1

Tumor necrosis factor receptor-associated protein-1 (TRAP-1) is a mitochondrial-compartmentalized Hsp90-like chaperone that is strongly cytoprotective (128). High expression of TRAP-1 is consistently associated with malignancy and with resistance to chemotherapy while corresponding healthy tissues exhibit very low to undetectable levels of TRAP-1 (128). TRAP-1 associates with cyclophilin D, a component of the PTP, and inhibits PTP opening (as does aberrantly localized mitochondrial Hsp90, (*Figure 2.2*)). The ATPase activity of TRAP-1 can be inhibited by small molecules (e.g., geldanamycin), however none of these inhibitors could access the mitochondrial compartment. However, a peptide (shepherdin, antagonist of the interaction between

Hsp90 and the IAP survivin) was able to target and inhibit mitochondrial TRAP-1 inducing MOMP and cell death selectively in cancer cells (128). Furthermore, the scope of TRAP-1/mitochondrial Hsp90 inhibition extended to the induction of a mitochondrial specific unfolded protein response (mUPR) program which can engage an autophagic type cell death mechanism (128).

PDK-1

In many cancers the transcription and survival factor HIF-1 increases expression of the mitochondrial pyruvate dehydrogenase kinase (PDK1) (11). PDK1 inhibits pyruvate dehydrogenase which suppresses the TCA cycle (12). Consequently this reinforces the Warburg effect or glycolytic shift in cancer cells and may also protect cells from cytotoxic levels of ROS (12). Inhibition of this mitochondrial kinase with a small molecule (dichloroacetate or DCA) has met with good success with low/no toxicity to non-malignant cells (11). DCA is an excellent example of an agent acting specifically on the mitochondria of cancer cells without perturbing the physiology of nonmalignant cells (29).

Survival factors that have special relevance when localized to the mitochondria.

Hsp90

Hsp90 is widely regarded as a pro-survival factor in cancer that affects multiple down-stream pathways (i.e., Hsp90 is a ‘nodal’ target (129)). Overexpression of Hsp90 is

typical in cancer cells in addition to an activity increase of nearly 100-fold (130). Hsp90 stabilizes inhibitors of apoptosis (IAPs) such as survivin, inhibits MOMP via cyclophilin D (128), stimulates nitric oxide production through association with nitric-oxide synthase (NOS) (131) and has a role in the mitochondrial unfolded protein response (mUPR) (132). However, small molecule antagonists targeting Hsp90 ATPase have a low clinical response in patients (133). It has been confirmed that this is primarily due to the inability of the agents to access the mitochondrial compartment (133). A pool of mitochondrial Hsp90 was unexpectedly found localized to the mitochondria in prostate cancer samples while investigating the differential expression of TRAP-1 in cancer and healthy tissue (128). As with TRAP-1, the mitochondrial Hsp90 was undetectable in the normal corresponding tissue. Several peptides have been developed to target Hsp90 including, shepherdin (modeled on the interface between Hsp90 and the IAP survivin (53)) and Antp-TPR (modeled on the interface between Hsp90 and Hsp90 cofactor, Hop (54)). It has become clear that targeting the mitochondrial pool of Hsp90 is key for therapeutic efficacy, with applicability in genetically disparate tumors and provides a basis for tumor versus normal tissue selectivity in vivo (132).

Peptides are uniquely suited to target malignant mitochondria

Current clinical cancer trials with agents targeting the mitochondria include obatoclax (small molecule BH3 mimetic) and the mitochondrial PDHK1 inhibitor DCA but as of yet, there are no peptides in this category (134). However, mitochondrial targeting antioxidant peptides are in phase 2 clinical trials for the indication of acute

myocardial infarction (135). Targeted peptides in cancer have primarily centered on tumor vasculature, inhibition of IAPs (136), monoclonal antibodies, anti-cancer vaccines (137), and plasma membrane disrupting peptides (138). Why are there no peptides targeted to the mitochondria for anti-cancer therapy? The technical problems of intracellular delivery and drug optimization are still formidable obstacles, and until recently intracellular protein-protein interactions have been considered to be "the most intractable of undruggable targets" (139).

Peptides have the distinct advantage of being able to discriminate between closely related targets with high affinity binding and low or no toxic effects (140). Evolutionarily refined natural peptides are a tremendous resource in the pursuit of selective anti-cancer agents that have the potential to extend the range of druggable targets beyond the scope of small molecules. The rapid development of synthetic peptides is a means to harness this evolutionarily cultivated specificity, subtlety, and low toxicity by bridging the problems of stability and delivery (139). Nonetheless, therapeutic peptide development is often complementary to improvement of targeted small molecules. In many cases, high affinity natural peptides (endogenous protein domains) already exist for many proteins of interest making libraries screening often unnecessary (140). Conversely, high affinity natural peptides can be used to efficiently screen small molecules for activity. For instance, a high-throughput screen for the anti-apoptotic Bcl-2 family member Bfl-1 used BH3-only domain binding to assess the displacement efficacy of small molecules (141). Going a step further, an iterative process of rational (e.g., BH3-only peptide) design can be used to refine and optimize target binding as a means to enhance screening for increasingly potent small molecules (142).

Targeting peptides intracellularly

In order to reach the mitochondria, peptides and proteins must have a means to penetrate the plasma membrane. Cell penetrating peptides (also called protein transduction domains or PTDs) are highly versatile non-toxic sequences (as compared to liposomes and polymers) for intracellular delivery (143). CPPs generally come in two flavors, either as short amino acid sequences that are mainly composed of arginine, lysine, and histidine (cationic character mediates the interaction of the peptide with anionic/acidic motifs on the plasma membrane in a receptor-independent fashion) or as amphipathic peptides (lipophilic and hydrophilic tails) that mediate peptide translocation across the plasma membranes. However, the exact mechanism of uptake is controversial for this type of CPP (143). Recently a new class of CPPs with delocalized lipophilic cations incorporated into the peptide sequence have been created to specifically facilitate drug delivery to the mitochondria (144). Finally, CPPs have been widely used in animal models and can achieve systemic delivery in vivo (therefore deliverable to any type of cancer) (143). However, optimization testing is required for every modification because the orientation of peptide, cargo, and linkages can have a significant impact on therapeutic peptide efficacy (81, 143).

Peptide toxicity: immunogenicity

Immunogenicity of protein (and to a limited degree, peptide) therapeutics pose a risk that can possibly compromise safety and alter pharmacokinetics and bioavailability of the agent (145). The fast growing number of therapeutic proteins and related immunogenicity data shows that most of them induce formation of anti-drug antibodies

(ADA). Additionally, *in silico* assessment of peptide immunogenicity risk is becoming more common (145). In the case where ADA takes the form of neutralizing antibodies (NAb), these NAbs have a direct effect on the effector-function of the therapeutic proteins (146). Of special concern are fusion proteins composed of a foreign and self-protein because of the potential of the foreign moiety to provoke an immune response to the self-protein (epitope spreading) (147). Risk of immunogenic response (esp. non-human peptides (e.g., enfuvirtide)) can be mitigated by re-engineering to reduce the size and/or elimination of MHC-II epitopes (147) through standard humanization techniques. Standard strategies for increasing half-life can also reduce immunogenicity such as pegylation or the introduction of non-natural amino acids (143).

Conclusion and future perspective

While it is unclear if mitochondrial dysfunction directly contributes to tumorigenesis (or if mitochondrial dysfunction is co-opted in the process of cancer metabolic transformation) the key clinical point is that the mitochondria of cancer cells, as opposed to normal cells, are ripe for selective therapeutic targeting to overcome common mechanisms of resistance and augment current anticancer strategies (1). Many of the current and emerging mitochondrial targets are dependent upon disruption of protein-protein interactions. There has been a general lack of progress in developing small molecules targeting protein-protein interactions and unlike therapeutic monoclonal antibodies, most peptides can function in an intracellular environment and are more amenable to synthesis/modification and delivery (148). Currently, an advancing developmental congruence exists between peptide drug design and delivery modalities

for peptides and proteins. Several recent reviews (3-6) cover important aspects of these advances and are illustrative of the creative energy being applied to the problems associated with peptide drug delivery.

Peptides can harness the culmination of evolutionary processes that dictate specificity of interaction (139). Using peptides as therapeutics meets the highest standard (and arguably the most natural) for candidates to achieve the specificity and subtlety of interaction small molecules cannot. Even between highly homologous binding targets, peptides can discriminate due to their high-level complexity (149). Discovery of locations of protein-protein interaction sites can lead to a further refinement of targeted peptides and/or new screening targets for small molecule intervention. Multifunctional (e.g., targeting moiety combined with bioactive domain) peptides or multi-valency (e.g., more than binding modality) can be readily engineered while undesirable features (e.g., immunogenicity) can be virtually eliminated (148). Peptides offer low toxicity and highly malleable formats for creating tunable, multi-functional therapeutics (148). Peptides have advantages over large proteins (avoiding the necessity to employ complex cellular systems, problems of characterization, and higher immunogenic potential), small molecules (toxicity, target promiscuity, poor ability to target protein-protein and protein-lipid interactions), and DNA/RNA aptamers (require rounds of screening using large libraries and purified target) (139).

Some of the most promising mitochondrial targeted peptides are derivatives of a parent protein (150). Moreover, tremendous effort has been channeled into industrial scale development and production of synthetic peptides in recent years ramping up the capability to make larger and more complex peptides with improved physiochemical

properties (148). Furthermore, proteins, especially enzymes, have been in use as drugs for many years, and biologics are making an increasing contribution to the number of new drug approvals (151). A variety of FDA approved biologics have been in use for over 3 decades, and the number of biologics continues to steadily increase (152).

Drug efficacy and drug resistance are ultimately reconciled at the level of the mitochondrion, and many therapeutic efforts define success by achieving Bak/Bax oligomerization and MOMP (1). Also, it is not uncommon for resistance to be exacerbated by the very agents used to try to kill the malignant cells (i.e., induction of EGFR mitochondrial localization (73) or radiation therapy-induced resistance via Mcl-1 stabilization (153)). Therefore strategies that engage the mitochondria directly bypass problems of resistance and upstream prosurvival pressures (11). For instance, if malignant cells overcome therapeutically induced ROS via up-regulated anti-oxidant mechanisms or RAF signaling, targeting MOMP using BH3-only peptides could restore cell death (154). Another complementary approach is to test the status of the mitochondria (e.g., overexpression of anti-apoptotic factors) to tailor therapeutic intervention. Recently, 'BH3 profiling' (originally defined as a pattern of mitochondrial apoptotic sensitivity based on peptides derived from BH3-only proteins (155)) has been performed as a companion diagnostic for determining the probability of drug efficacy (e.g., bortezomib) across cancer patients (19). Combining mitochondrially targeted peptides with conventional chemotherapy may be a powerful way to reduce the standard chemotherapeutic dose and associated toxicity, potentiate synergistic killing of tumor cells (156), reduce resistance, and elicit an immunogenic response to the malignant tissue (9).

The term ‘mitocan’ has recently been coined to describe therapeutic agents within the rapidly developing and burgeoning field of mitochondrial focused anti-cancer therapy (157). In the near future we can expect peptide therapeutics to comprise an ever larger segment of the mitocan arsenal.

Executive summary

1. *Mitochondrial cell death pathway and malignant mitochondria*

   Cancer therapy is dependent on permeabilization of the mitochondrial outer membrane (MOMP). Directly targeting the mitochondria in cancer is an excellent universal therapeutic strategy especially because there are ‘targetable’ differences between malignant and healthy mitochondria.

2. *Peptides are uniquely suited to target malignant mitochondria*

   Therapeutic peptide agents have the potential to open new vistas of traditionally “undruggable” targets (e.g., protein-protein interactions) and offer a subtlety and specificity of target interaction that cannot be matched by small molecules, all while decreasing side effects. Rapid advances in therapeutic peptide design are likely to soon surmount the major problems of stability and delivery.

3. *The mitochondria and immunogenic apoptosis*

   The type of death a cell dies may be central to achieving a durable response to anti-cancer therapy. Targeting the mitochondria may be a means to kill cancer cells but be able to modulate the killing to invoke an “immunogenic apoptosis.” Pairing peptide therapeutics with traditional chemotherapy may be a way to preserve the immune effector cells (by using a sub-immune toxic

chemotherapeutic dose) to achieve tumor killing while engaging an anti-tumor immune response.

Acknowledgements

This work was funded by NIH RO1 CA129528

Bibliography

1. S.J. Ralph, S. Rodriguez-Enriquez, J. Neuzil, E. Saavedra, and R. Moreno-Sanchez. The causes of cancer revisited: "mitochondrial malignancy" and ROS-induced oncogenic transformation - why mitochondria are targets for cancer therapy. Molecular Aspects of Medicine. 31:145-170 (2010).

2. M.F. McCarty. Targeting multiple signaling pathways as a strategy for managing prostate cancer: multifocal signal modulation therapy. Integr Cancer Ther. 3:349-380 (2004).

3. R.I. Mahato, A.S. Narang, L. Thoma, and D.D. Miller. Emerging trends in oral delivery of peptide and protein drugs. Crit Rev Ther Drug Carrier Syst. 20:153-214 (2003).

4. M.L. Tan, P.F. Choong, and C.R. Dass. Recent developments in liposomes, microparticles and nanoparticles for protein and peptide drug delivery. Peptides. 31:184-193 (2010).

5. E. Ieva, A. Trapani, N. Cioffi, N. Ditaranto, A. Monopoli, and L. Sabbatini. Analytical characterization of chitosan nanoparticles for peptide drug delivery applications. Anal Bioanal Chem. 393:207-215 (2009).

6. V.P. Torchilin. Tat peptide-mediated intracellular delivery of pharmaceutical nanocarriers. Adv Drug Deliv Rev. 60:548-558 (2008).

7. I. Martins, M. Michaud, A.Q. Sukkurwala, S. Adjemian, Y. Ma, S. Shen, O. Kepp, L. Menger, E. Vacchelli, L. Galluzzi, L. Zitvogel, and G. Kroemer. Premortem autophagy determines the immunogenicity of chemotherapy-induced cancer cell death. Autophagy. 8: (2012).

8. M. Wemeau, O. Kepp, A. Tesniere, T. Panaretakis, C. Flament, S. De Botton, L. Zitvogel, G. Kroemer, and N. Chaput. Calreticulin exposure on malignant blasts predicts a cellular anticancer immune response in patients with acute myeloid leukemia. Cell Death Dis. 1:e104 (2010).

9. D.R. Green, T. Ferguson, L. Zitvogel, and G. Kroemer. Immunogenic and tolerogenic cell death. Nat Rev Immunol. 9:353-363 (2009).

10. B.G. Bitler and J.A. Schroeder. Anti-cancer therapies that utilize cell penetrating peptides. Recent Pat Anticancer Drug Discov. 5:99-108 (2010).

11. S. Fulda, L. Galluzzi, and G. Kroemer. Targeting mitochondria for cancer therapy. Nat Rev Drug Discov. 9:447-464 (2010).

12. V. Gogvadze, B. Zhivotovsky, and S. Orrenius. The Warburg effect and mitochondrial stability in cancer cells. Molecular Aspects of Medicine. 31:60-74 (2010).

13. G.N. Hortobagyi. Trastuzumab in the treatment of breast cancer. N Engl J Med. 353:1734-1736 (2005).

14. I. Nakase, Y. Konishi, M. Ueda, H. Saji, and S. Futaki. Accumulation of arginine-rich cell-penetrating peptides in tumors and the potential for anticancer drug delivery in vivo. J Control Release. 159:181-188 (2012).

15. M. Mossalam, A.S. Dixon, and C.S. Lim. Controlling subcellular delivery to optimize therapeutic effect. Ther Deliv. 1:169-193 (2010).

16. T.N. Seyfried and L.M. Shelton. Cancer as a metabolic disease. Nutrition & Metabolism. 7:7 (2010).

17. H.R. Christofk, M.G. Vander Heiden, M.H. Harris, A. Ramanathan, R.E. Gerszten, R. Wei, M.D. Fleming, S.L. Schreiber, and L.C. Cantley. The M2 splice isoform of pyruvate kinase is important for cancer metabolism and tumour growth. Nature. 452:230-233 (2008).

18. L. Galluzziand G. Kroemer. Necroptosis: a specialized pathway of programmed necrosis. Cell. 135:1161-1163 (2008).

19. T. Ni Chonghaile, K.A. Sarosiek, T.T. Vo, J.A. Ryan, A. Tammareddi, G. Moore Vdel, J. Deng, K.C. Anderson, P. Richardson, Y.T. Tai, C.S. Mitsiades, U.A. Matulonis, R. Drapkin, R. Stone, D.J. Deangelo, D.J. McConkey, S.E. Sallan, L. Silverman, M.S. Hirsch, D.R. Carrasco, and A. Letai. Pretreatment mitochondrial priming correlates with clinical response to cytotoxic chemotherapy. Science. 334:1129-1133 (2011).

20. C. Atay, S. Ugurlu, and N. Ozoren. Shock the heat shock network. J Clin Invest. 119:445-448 (2009).

21. J.C. Martinou and R.J. Youle. Mitochondria in apoptosis: Bcl-2 family members and mitochondrial dynamics. Developmental Cell. 21:92-101 (2011).

22. J.E. Chipuk, T. Kuwana, L. Bouchier-Hayes, N.M. Droin, D.D. Newmeyer, M. Schuler, and D.R. Green. Direct activation of Bax by p53 mediates mitochondrial membrane permeabilization and apoptosis. Science. 303:1010-1014 (2004).

23. O. Kutuk and A. Letai. Regulation of Bcl-2 family proteins by posttranslational modifications. Curr Mol Med. 8:102-118 (2008).

24. I. Szabo, M. Soddemann, L. Leanza, M. Zoratti, and E. Gulbins. Single-point mutations of a lysine residue change function of Bax and Bcl-xL expressed in Bax- and Bak-less mouse embryonic fibroblasts: novel insights into the molecular mechanisms of Bax-induced apoptosis. Cell Death Differ. 18:427-438 (2011).

25. I. Szabo, J. Bock, H. Grassme, M. Soddemann, B. Wilker, F. Lang, M. Zoratti, and E. Gulbins. Mitochondrial potassium channel Kv1.3 mediates Bax-induced apoptosis in lymphocytes. Proc Natl Acad Sci U S A. 105:14861-14866 (2008).

26. S. Cipolat, T. Rudka, D. Hartmann, V. Costa, L. Serneels, K. Craessaerts, K. Metzger, C. Frezza, W. Annaert, L. D'Adamio, C. Derks, T. Dejaegere, L. Pellegrini, R. D'Hooge, L. Scorrano, and B. De Strooper. Mitochondrial rhomboid PARL regulates cytochrome c release during apoptosis via OPA1-dependent cristae remodeling. Cell. 126:163-175 (2006).

27. T. Liu, B. Hannafon, L. Gill, W. Kelly, and D. Benbrook. Flex-Hets differentially induce apoptosis in cancer over normal cells by directly targeting mitochondria. Mol Cancer Ther. 6:1814-1822 (2007).

28. C. Griffin, A. Karnik, J. McNulty, and S. Pandey. Pancratistatin selectively targets cancer cell mitochondria and reduces growth of human colon tumor xenografts. Mol Cancer Ther. 10:57-68 (2011).

29. S. Vella, M. Conti, R. Tasso, R. Cancedda, and A. Pagano. Dichloroacetate inhibits neuroblastoma growth by specifically acting against malignant undifferentiated cells. Int J Cancer. 130:1484-1493 (2012).

30. N. Bellance, P. Lestienne, and R. Rossignol. Mitochondria: from bioenergetics to the metabolic regulation of carcinogenesis. Front Biosci. 14:4015-4034 (2009).

31. S.C. Gupta, D. Hevia, S. Patchva, B. Park, W. Koh, and B.B. Aggarwal. Upsides and Downsides of Reactive Oxygen Species for Cancer: The Roles of Reactive Oxygen Species in Tumorigenesis, Prevention, and Therapy. Antioxid Redox Signal 11:1295-1322 (2012).

32. M. Diehn, R.W. Cho, N.A. Lobo, T. Kalisky, M.J. Dorie, A.N. Kulp, D. Qian, J.S. Lam, L.E. Ailles, M. Wong, B. Joshua, M.J. Kaplan, I. Wapnir, F.M. Dirbas, G. Somlo, C. Garberoglio, B. Paz, J. Shen, S.K. Lau, S.R. Quake, J.M. Brown, I.L. Weissman, and M.F. Clarke. Association of reactive oxygen species levels and radioresistance in cancer stem cells. Nature. 458:780-783 (2009).

33. K. Ishikawa, K. Takenaga, M. Akimoto, N. Koshikawa, A. Yamaguchi, H. Imanishi, K. Nakada, Y. Honma, and J. Hayashi. ROS-generating mitochondrial DNA mutations can regulate tumor cell metastasis. Science. 320:661-664 (2008).

34. J.S. Bair, R. Palchaudhuri, and P.J. Hergenrother. Chemistry and biology of deoxynyboquinone, a potent inducer of cancer cell death. J Am Chem Soc. 132:5469-5478 (2010).

35. A. Atlante, P. Calissano, A. Bobba, A. Azzariti, E. Marra, and S. Passarella. Cytochrome c is released from mitochondria in a reactive oxygen species (ROS)-dependent fashion and can operate as a ROS scavenger and as a respiratory substrate in cerebellar neurons undergoing excitotoxic death. The Journal of Biological Chemistry. 275:37159-37166 (2000).

36. I.S. Song, H.K. Kim, S.H. Jeong, S.R. Lee, N. Kim, B.D. Rhee, K.S. Ko, and J. Han. Mitochondrial Peroxiredoxin III is a Potential Target for Cancer Therapy. Int J Mol Sci. 12:7163-7185 (2011).

37. G.R. Yu, W.W. Qin, J.P. Li, W. Hua, Y.L. Meng, R. Chen, B. Yan, L. Wang, X. Zhang, L.T. Jia, J. Zhao, R. Zhang, and A.G. Yang. HIV-TAT-fused FHIT protein functions as a potential pro-apoptotic molecule in hepatocellular carcinoma cells. Biosci Rep. 32:271-279 (2011).

38. J. Martin, M.V. St-Pierre, and J.F. Dufour. Hit proteins, mitochondria and cancer. Biochim Biophys Acta. 1807:626-632 (2011).

39. H. Lecoeur, A. Borgne-Sanchez, O. Chaloin, R. El-Khoury, M. Brabant, A. Langonne, M. Porceddu, J.J. Briere, N. Buron, D. Rebouillat, C. Pechoux, A. Deniaud, C. Brenner, J.P. Briand, S. Muller, P. Rustin, and E. Jacotot. HIV-1 Tat protein directly induces mitochondrial membrane permeabilization and inactivates cytochrome c oxidase. Cell Death Dis. 3:e282 (2012).

40. F. Chiara, D. Castellaro, O. Marin, V. Petronilli, W.S. Brusilow, M. Juhaszova, S.J. Sollott, M. Forte, P. Bernardi, and A. Rasola. Hexokinase II detachment from mitochondria triggers apoptosis through the permeability transition pore independent of voltage-dependent anion channels. PloS One. 3:e1852 (2008).

41. C.Y. Huang, S.F. Chiang, T.Y. Lin, S.H. Chiou, and K.C. Chow. HIV-1 Vpr Triggers Mitochondrial Destruction by Impairing Mfn2-Mediated ER-Mitochondria Interaction. PloS One. 7:e33657 (2012).

42. E.N. Sabbah, S. Druillennec, N. Morellet, S. Bouaziz, G. Kroemer, and B.P. Roques. Interaction between the HIV-1 protein Vpr and the adenine nucleotide translocator. Chem Biol Drug Des. 67:145-154 (2006).

43. A. Borgne-Sanchez, S. Dupont, A. Langonne, L. Baux, H. Lecoeur, D. Chauvier, M. Lassalle, O. Deas, J.J. Briere, M. Brabant, P. Roux, C. Pechoux, J.P. Briand, J. Hoebeke, A. Deniaud, C. Brenner, P. Rustin, L. Edelman, D. Rebouillat, and E. Jacotot. Targeted Vpr-derived peptides reach mitochondria to induce apoptosis of alphaVbeta3-expressing endothelial cells. Cell Death Differ. 14:422-435 (2007).

44. V.R. Fantin, M.J. Berardi, H. Babbe, M.V. Michelman, C.M. Manning, and P. Leder. A bifunctional targeted peptide that blocks HER-2 tyrosine kinase and disables mitochondrial function in HER-2-positive carcinoma cells. Cancer Res. 65:6891-6900 (2005).

45. H.M. Ellerby, W. Arap, L.M. Ellerby, R. Kain, R. Andrusiak, G.D. Rio, S. Krajewski, C.R. Lombardo, R. Rao, E. Ruoslahti, D.E. Bredesen, and R. Pasqualini. Anti-cancer activity of targeted pro-apoptotic peptides. Nat Med. 5:1032-1038 (1999).

46. R. Smolarczyk, T. Cichon, K. Graja, J. Hucz, A. Sochanik, and S. Szala. Antitumor effect of RGD-4C-GG-D(KLAKLAK)2 peptide in mouse B16(F10) melanoma model. Acta Biochim Pol. 53:801-805 (2006).

47. J.K. Ko, K.H. Choi, J. Peng, F. He, Z. Zhang, N. Weisleder, J. Lin, and J. Ma. Amphipathic tail-anchoring peptide and Bcl-2 homology domain-3 (BH3) peptides from Bcl-2 family proteins induce apoptosis through different mechanisms. The Journal of Biological Chemistry. 286:9038-9048 (2010).

48. E.P. Holinger, T. Chittenden, and R.J. Lutz. Bak BH3 peptides antagonize Bcl-xL function and induce apoptosis through cytochrome c-independent activation of caspases. J Biol Chem. 274:13298-13304 (1999).

49. S.S. Dharap and T. Minko. Targeted proapoptotic LHRH-BH3 peptide. Pharm Res. 20:889-896 (2003).

50. J.L.L. S.G. Katz, M. Godes, J. Fisher, G.H. Bird & L.D. Walensky. A Stapled BIM BH3 Helix Restores Apoptosis In Bim-Null Mantle Cell Lymphoma. American Society of Hematology Annual Meeting, 2010.

51. R. Ponassi, B. Biasotti, V. Tomati, S. Bruno, A. Poggi, D. Malacarne, G. Cimoli, A. Salis, S. Pozzi, M. Miglino, G. Damonte, P. Cozzini, F. Spyraki, B. Campanini, L. Bagnasco, N. Castagnino, L. Tortolina, A. Mumot, F. Frassoni, A. Daga, M. Cilli, F. Piccardi, I. Monfardini, M. Perugini, G. Zoppoli, C. D'Arrigo, R. Pesenti, and S. Parodi. A novel Bim-BH3-derived Bcl-XL inhibitor: biochemical characterization, in vitro, in vivo and ex-vivo anti-leukemic activity. Cell cycle. 7:3211-3224 (2008).

52. F. Zhong, M.W. Harr, G. Bultynck, G. Monaco, J.B. Parys, H. De Smedt, Y.P. Rong, J.K. Molitoris, M. Lam, C. Ryder, S. Matsuyama, and C.W. Distelhorst. Induction of Ca(2)+-driven apoptosis in chronic lymphocytic leukemia cells by peptide-mediated disruption of Bcl-2-IP3 receptor interaction. Blood. 117:2924-2934 (2011).

53. J. Plescia, W. Salz, F. Xia, M. Pennati, N. Zaffaroni, M.G. Daidone, M. Meli, T. Dohi, P. Fortugno, Y. Nefedova, D.I. Gabrilovich, G. Colombo, and D.C. Altieri. Rational design of shepherdin, a novel anticancer agent. Cancer Cell. 7:457-468 (2005).

54. T. Horibe, M. Kawamoto, M. Kohno, and K. Kawakami. Cytotoxic activity to acute myeloid leukemia cells by Antp-TPR hybrid peptide targeting Hsp90. J Biosci Bioeng. Epub ahead of print (2012).

55. C. Katz, Y. Zaltsman-Amir, Y. Mostizky, N. Kollet, A. Gross, and A. Friedler. Molecular basis of the interaction between the pro apoptotic tBID protein and mitochondrial carrier homologue 2 (MTCH2): Key players in the mitochondrial death pathway. J Biol Chem (2012).

56. D. Park, J. Chiu, G.G. Perrone, P.J. Dilda, and P.J. Hogg. The tumour metabolism inhibitors GSAO and PENAO react with cysteines 57 and 257 of mitochondrial adenine nucleotide translocase. Cancer Cell Int. 12:11 (2012).

57. V. Shoshan-Barmatz and D. Ben-Hail. VDAC, a multi-functional mitochondrial protein as a pharmacological target. Mitochondrion. 12:24-34 (2012).

58. M. Mossalam, K.J. Matissek, A. Okal, J.E. Constance, and C.S. Lim. Direct Induction of Apoptosis Using an Optimal Mitochondrially Targeted P53. Mol Pharm 9:1449-58 (2012).

59. J.E. Constance, S.D. Despres, A. Nishida, and C.S. Lim. Selective Targeting of c-Abl via a Cryptic Mitochondrial Targeting Signal Activated by Cellular Redox Status in Leukemic and Breast Cancer Cells. Pharm Res. Epub ahead of print (2012).

60. L. Yin, M. Kosugi, and D. Kufe. Inhibition of the MUC1-C oncoprotein induces multiple myeloma cell death by down-regulating TIGAR expression and depleting NADPH. Blood. 119:810-816 (2011).

61. D. Svilar, E.M. Goellner, K.H. Almeida, and R.W. Sobol. Base excision repair and lesion-dependent subpathways for repair of oxidative DNA damage. Antioxid Redox Signal. 14:2491-2507 (2011).

62. M.A. Houston, L.H. Augenlicht, and B.G. Heerdt. Stable differences in intrinsic mitochondrial membrane potential of tumor cell subpopulations reflect phenotypic heterogeneity. Int J Cell Biol. 2011:978583 (2011).

63. X. Xue, S. You, Q. Zhang, Y. Wu, G.Z. Zou, P.C. Wang, Y.L. Zhao, Y. Xu, L. Jia, X. Zhang, and X.J. Liang. Mitaplatin increases sensitivity of tumor cells to Cisplatin by inducing mitochondrial dysfunction. Mol Pharm. 9:634-644 (2012).

64. R. Fukuda, H. Zhang, J.W. Kim, L. Shimoda, C.V. Dang, and G.L. Semenza. HIF-1 regulates cytochrome oxidase subunits to optimize efficiency of respiration in hypoxic cells. Cell. 129:111-122 (2007).

65. M. Nonaka, Y. Hashimoto, S.N. Takeshima, and Y. Aida. The human immunodeficiency virus type 1 Vpr protein and its carboxy-terminally truncated form induce apoptosis in tumor cells. Cancer Cell Int. 9:20 (2009).

66. A. Arcangeli, O. Crociani, E. Lastraioli, A. Masi, S. Pillozzi, and A. Becchetti. Targeting ion channels in cancer: a novel frontier in antineoplastic therapy. Curr Med Chem. 16:66-93 (2009).

67. I. Szabo, L. Leanza, E. Gulbins, and M. Zoratti. Physiology of potassium channels in the inner membrane of mitochondria. Pflugers Arch. 463:231-246 (2012).

68. A.R. Cardoso, B.B. Queliconi, and A.J. Kowaltowski. Mitochondrial ion transport pathways: role in metabolic diseases. Biochimica et biophysica acta. 1797:832-838 (2010).

69. A. Felipe, J. Bielanska, N. Comes, A. Vallejo, S. Roig, Y.C.S. Ramon, E. Condom, J. Hernandez-Losa, and J.C. Ferreres. Targeting the voltage-dependent k(+) channels kv1.3 and kv1.5 as tumor biomarkers for cancer detection and prevention. Curr Med Chem. 19:661-674 (2012).

70. L. Kosztka, Z. Rusznak, D. Nagy, Z. Nagy, J. Fodor, G. Szucs, A. Telek, M. Gonczi, O. Ruzsnavszky, N. Szentandrassy, and L. Csernoch. Inhibition of TASK-3 (KCNK9) channel biosynthesis changes cell morphology and decreases both DNA content and mitochondrial function of melanoma cells maintained in cell culture. Melanoma Res. 21:308-322 (2011).

71. D. De Stefani, A. Raffaello, E. Teardo, I. Szabo, and R. Rizzuto. A forty-kilodalton protein of the inner membrane is the mitochondrial calcium uniporter. Nature. 476:336-340 (2011).

72. R. Wong, C. Steenbergen, and E. Murphy. Mitochondrial permeability transition pore and calcium handling. Methods in molecular biology. 810:235-242 (2012).

73. X. Cao, H. Zhu, F. Ali-Osman, and H.W. Lo. EGFR and EGFRvIII undergo stress- and EGFR kinase inhibitor-induced mitochondrial translocalization: a potential mechanism of EGFR-driven antagonism of apoptosis. Mol Cancer. 10:26 (2011).

74. J. Ren, A. Bharti, D. Raina, W. Chen, R. Ahmad, and D. Kufe. MUC1 oncoprotein is targeted to mitochondria by heregulin-induced activation of c-Src and the molecular chaperone HSP90. Oncogene. 25:20-31 (2006).

75. S.V. Sharma, D.W. Bell, J. Settleman, and D.A. Haber. Epidermal growth factor receptor mutations in lung cancer. Nat Rev Cancer. 7:169-181 (2007).

76. H. Zhu, X. Cao, F. Ali-Osman, S. Keir, and H.W. Lo. EGFR and EGFRvIII interact with PUMA to inhibit mitochondrial translocalization of PUMA and PUMA-mediated apoptosis independent of EGFR kinase activity. Cancer Lett. 294:101-110 (2010).

77. N. Cruickshanks, H. Hamed, M.D. Bareford, A. Poklepovic, P.B. Fisher, S. Grant, and P. Dent. Lapatinib and Obatoclax kill tumor cells through blockade of ERBB1 / 3 / 4 and through inhibition of BCL-XL and MCL-1. Mol Pharm. 81:748-58 (2012).

78. L. Yin and D. Kufe. MUC1-C Oncoprotein Blocks Terminal Differentiation of Chronic Myelogenous Leukemia Cells by a ROS-Mediated Mechanism. Genes Cancer. 2:56-64 (2011).

79. T.H. Kim, Y. Zhao, W.X. Ding, J.N. Shin, X. He, Y.W. Seo, J. Chen, H. Rabinowich, A.A. Amoscato, and X.M. Yin. Bid-cardiolipin interaction at mitochondrial contact site contributes to mitochondrial cristae reorganization and cytochrome C release. Mol Biol Cell. 15:3061-3072 (2004).

80. P. Boya, A.L. Pauleau, D. Poncet, R.A. Gonzalez-Polo, N. Zamzami, and G. Kroemer. Viral proteins targeting mitochondria: controlling cell death. Biochimica et Biophysica Acta. 1659:178-189 (2004).

81. N. Papo and Y. Shai. New lytic peptides based on the D,L-amphipathic helix motif preferentially kill tumor cells compared to normal cells. Biochemistry. 42:9346-9354 (2003).

82. V. Madan, S. Sanchez-Martinez, L. Carrasco, and J.L. Nieva. A peptide based on the pore-forming domain of pro-apoptotic poliovirus 2B viroporin targets mitochondria. Biochimica et Biophysica Acta. 1798:52-58 (2010).

83. A. Szewczyk and L. Wojtczak. Mitochondria as a pharmacological target. Pharmacol Rev. 54:101-127 (2002).

84. L. Galluzzi, O. Kepp, C. Trojel-Hansen, and G. Kroemer. Non-apoptotic functions of apoptosis-regulatory proteins. EMBO Reports 13:322-30 (2012).

85. J. Rudner, S.J. Elsaesser, A.C. Muller, C. Belka, and V. Jendrossek. Differential effects of anti-apoptotic Bcl-2 family members Mcl-1, Bcl-2, and Bcl-xL on celecoxib-induced apoptosis. Biochem Pharmacol. 79:10-20 (2010).

86. S.M. Schoenwaelder and S.P. Jackson. Bcl-xL-inhibitory BH3 mimetics (ABT-737 or ABT-263) and the modulation of cytosolic calcium flux and platelet function. Blood. 119:1320-1321 (2012).

87. K. Pitter, F. Bernal, J. Labelle, and L.D. Walensky. Dissection of the BCL-2 family signaling network with stabilized alpha-helices of BCL-2 domains. Methods Enzymol. 446:387-408 (2008).

88. L. Gangoda, D. Moujalled, Y. Lee, A. Rahimi, and H. Puthalakath. Analysis of the role of Bim as a tumor suppressor in Carney Complex Syndrome, *Cell Death in Cancer*, De Rode Hoed, Amsterdam, The Netherlands, (2012).

89. Y.P. Rong, G. Bultynck, A.S. Aromolaran, F. Zhong, J.B. Parys, H. De Smedt, G.A. Mignery, H.L. Roderick, M.D. Bootman, and C.W. Distelhorst. The BH4 domain of Bcl-2 inhibits ER calcium release and apoptosis by binding the regulatory and coupling domain of the IP3 receptor. Proc Natl Acad Sci U S A. 106:14397-14402 (2009).

90. S. Iqbal, S. Zhang, A. Driss, Z.R. Liu, H.R. Kim, Y. Wang, C. Ritenour, H.E. Zhau, O. Kucuk, L.W. Chung, and D. Wu. PDGF upregulates Mcl-1 through activation of beta-catenin and HIF-1alpha-dependent signaling in human prostate cancer cells. PloS one. 7:e30764 (2012).

91. M. Elgendy, C. Sheridan, G. Brumatti, and S.J. Martin. Oncogenic Ras-induced expression of Noxa and Beclin-1 promotes autophagic cell death and limits clonogenic survival. Mol Cell. 42:23-35 (2011).

92. S. Cristofanon and S. Fulda. ABT-737 promotes tBid mitochondrial insertion to enhance TRAIL-induced apoptosis in glioblastoma cells, Cell Death in Cancer Conference, De Rode Hoed, Amsterdam, The Netherlands, (2012).

93. A.D. Garg, D.V. Krysko, T. Verfaillie, A. Kaczmarek, G.B. Ferreira, T. Marysael, N. Rubio, M. Firczuk, C. Mathieu, A.J. Roebroek, W. Annaert, J. Golab, P. de Witte, P. Vandenabeele, and P. Agostinis. A novel pathway combining calreticulin exposure and ATP secretion in immunogenic cancer cell death. Embo J (2012).

94. S.P. Glaser, E.F. Lee, E. Trounson, P. Bouillet, A. Wei, W.D. Fairlie, D.J. Izon, J. Zuber, A.R. Rappaport, M.J. Herold, W.S. Alexander, S.W. Lowe, L. Robb, and A. Strasser. Anti-apoptotic Mcl-1 is essential for the development and sustained growth of acute myeloid leukemia. Genes Dev. 26:120-125 (2012).

95. M.L. Stewart, E. Fire, A.E. Keating, and L.D. Walensky. The MCL-1 BH3 helix is an exclusive MCL-1 inhibitor and apoptosis sensitizer. Nat Chem Biol. 6:595-601 (2010).

96. L. Galluzzi, O. Kepp, N. Tajeddine, and G. Kroemer. Disruption of the hexokinase-VDAC complex for tumor therapy. Oncogene. 27:4633-4635 (2008).
97. C. Brenner and S. Grimm. The permeability transition pore complex in cancer cell death. Oncogene. 25:4744-4756 (2006).

98. V. Shoshan-Barmatz, V. De Pinto, M. Zweckstetter, Z. Raviv, N. Keinan, and N. Arbel. VDAC, a multi-functional mitochondrial protein regulating cell life and death. Molecular Aspects of Medicine. 31:227-285 (2010).

99. R. Rupprecht, V. Papadopoulos, G. Rammes, T.C. Baghai, J. Fan, N. Akula, G. Groyer, D. Adams, and M. Schumacher. Translocator protein (18 kDa) (TSPO) as a therapeutic target for neurological and psychiatric disorders. Nat Rev Drug Discov. 9:971-988 (2010).

100. S. Taliani, I. Pugliesi, and F. Da Settimo. Structural requirements to obtain highly potent and selective 18 kDa Translocator Protein (TSPO) Ligands. Curr Top Med Chem. 11:860-886 (2011).

101. I. Masgras, A. Rasola, and P. Bernardi. Induction of the permeability transition pore in cells depleted of mitochondrial DNA. Biochimica et Biophysica Acta. Epub ahead of print (2012).

102. P.J. Dilda, S. Decollogne, L. Weerakoon, M.D. Norris, M. Haber, J.D. Allen, and P.J. Hogg. Optimization of the antitumor efficacy of a synthetic mitochondrial toxin by increasing the residence time in the cytosol. Journal of Medicinal Chemistry. 52:6209-6216 (2009).

103. J. Banerjee and S. Ghosh. Bax increases the pore size of rat brain mitochondrial voltage-dependent anion channel in the presence of tBid. Biochemical and Biophysical Research Communications. 323:310-314 (2004).

104. G. Gergalova, O. Lykhmus, O. Kalashnyk, L. Koval, V. Chernyshov, E. Kryukova, V. Tsetlin, S. Komisarenko, and M. Skok. Mitochondria Express alpha7 Nicotinic Acetylcholine Receptors to Regulate Ca Accumulation and Cytochrome c Release: Study on Isolated Mitochondria. PloS one. 7:e31361 (2012).

105. M. Karbowski, K.L. Norris, M.M. Cleland, S.Y. Jeong, and R.J. Youle. Role of Bax and Bak in mitochondrial morphogenesis. Nature. 443:658-662 (2006).
106. M.T. Rosenfeldt and K.M. Ryan. The multiple roles of autophagy in cancer. Carcinogenesis. 32:955-963 (2011).

107. E.J. White, V. Martin, J.L. Liu, S.R. Klein, S. Piya, C. Gomez-Manzano, J. Fueyo, and H. Jiang. Autophagy regulation in cancer development and therapy. Am J Cancer Res. 1:362-372 (2011).

108. M. Hoyer-Hansen and M. Jaattela. Autophagy: an emerging target for cancer therapy. Autophagy. 4:574-580 (2008).

109. L.C. Gomes, G. Di Benedetto, and L. Scorrano. During autophagy mitochondria elongate, are spared from degradation and sustain cell viability. Nat Cell Biol. 13:589-598 (2011).

110. C. Blackstone and C.R. Chang. Mitochondria unite to survive. Nat Cell Biol. 13:521-522 (2011).

111. A. Zorzano, D. Sebastian, J. Segales, and M. Palacin. The molecular machinery of mitochondrial fusion and fission: An opportunity for drug discovery? Curr Opin Drug Discov Devel. 12:597-606 (2009).

112. M. Mossalam, K.J. Matissek, A. Okal, J.E. Constance, and C.S. Lim. Direct induction of apoptosis using an optimal mitochondrially targeted p53. Mol Pharm. 9:1449-1458 (2012).

113. J.E. Chipuk and D.R. Green. Dissecting p53-dependent apoptosis. Cell Death Differ. 13:994-1002 (2006).

114. I. Ferecatu, M. Bergeaud, A. Rodriguez-Enfedaque, N. Le Floch, L. Oliver, V. Rincheval, F. Renaud, F.M. Vallette, B. Mignotte, and J.L. Vayssiere. Mitochondrial localization of the low level p53 protein in proliferative cells. Biochemical and Biophysical Research Communications. 387:772-777 (2009).

115. M. Bergeaud, L. Mathieu, N. Le Floch, B. Mignotte, V. Rincheval, and J.L. Vayssiere. Localization and function of p53 protein at mitochondria in proliferative cells, Cell Death in Cancer Conference, De Rode Hoed, Amsterdam, The Netherlands, (2012).

116. K. von der Malsburg, J.M. Muller, M. Bohnert, S. Oeljeklaus, P. Kwiatkowska, T. Becker, A. Loniewska-Lwowska, S. Wiese, S. Rao, D. Milenkovic, D.P. Hutu, R.M. Zerbes, A. Schulze-Specking, H.E. Meyer, J.C. Martinou, S. Rospert, P. Rehling, C. Meisinger, M. Veenhuis, B. Warscheid, I.J. van der Klei, N. Pfanner, A. Chacinska, and M. van der Laan. Dual role of mitofilin in mitochondrial membrane organization and protein biogenesis. Developmental Cell. 21:694-707 (2011).

117. E. Alirol and J.C. Martinou. Mitochondria and cancer: is there a morphological connection? Oncogene. 25:4706-4716 (2006).

118. S. Bouleau, I. Parvu-Ferecatu, A. Rodriguez-Enfedaque, V. Rincheval, H. Grimal, B. Mignotte, J.L. Vayssiere, and F. Renaud. Fibroblast Growth Factor 1 inhibits p53-dependent apoptosis in PC12 cells. Apoptosis.12:1377-1387 (2007).

119. D.J. Barnes, D. Palaiologou, E. Panousopoulou, B. Schultheis, A.S. Yong, A. Wong, L. Pattacini, J.M. Goldman, and J.V. Melo. Bcr-Abl expression levels determine the rate of development of resistance to imatinib mesylate in chronic myeloid leukemia. Cancer Res. 65:8912-8919 (2005).

120. J.Y. Wang. Nucleo-cytoplasmic communication in apoptotic response to genotoxic and inflammatory stress. Cell Res. 15:43-48 (2005).

121. Y. Ito, P. Pandey, N. Mishra, S. Kumar, N. Narula, S. Kharbanda, S. Saxena, and D. Kufe. Targeting of the c-Abl tyrosine kinase to mitochondria in endoplasmic reticulum stress-induced apoptosis. Mol Cell Biol. 21:6233-6242 (2001).

122. M. Lasfer, L. Davenne, N. Vadrot, C. Alexia, Z. Sadji-Ouatas, A.F. Bringuier, G. Feldmann, D. Pessayre, and F. Reyl-Desmars. Protein kinase PKC delta and c-Abl are required for mitochondrial apoptosis induction by genotoxic stress in the absence of p53, p73 and Fas receptor. FEBS Lett. 580:2547-2552 (2006).

123. Y. Zaltsman, L. Shachnai, N. Yivgi-Ohana, M. Schwarz, M. Maryanovich, R.H. Houtkooper, F.M. Vaz, F. De Leonardis, G. Fiermonte, F. Palmieri, B. Gillissen, P.T. Daniel, E. Jimenez, S. Walsh, C.M. Koehler, S.S. Roy, L. Walter, G. Hajnoczky, and A. Gross. MTCH2/MIMP is a major facilitator of tBID recruitment to mitochondria. Nat Cell Biol. 12:553-562 (2010).

124. A.K. Holley, S.K. Dhar, Y. Xu, and D.K. St Clair. Manganese superoxide dismutase: beyond life and death. Amino Acids. 42:139-158 (2012).

125. A. Pedram, M. Razandi, D.C. Wallace, and E.R. Levin. Functional estrogen receptors in the mitochondria of breast cancer cells. Mol Biol Cell. 17:2125-2137 (2006).

126. M. Ennen, V. Minig, S. Grandemange, N. Touche, J.L. Merlin, V. Besancenot, E. Brunner, L. Domenjoud, and P. Becuwe. Regulation of the high basal expression of the manganese superoxide dismutase gene in aggressive breast cancer cells. Free Radic Biol Med. 50:1771-1779 (2011).

127. Y. Zhao, L. Chaiswing, J.M. Velez, I. Batinic-Haberle, N.H. Colburn, T.D. Oberley, and D.K. St Clair. p53 translocation to mitochondria precedes its nuclear translocation and targets mitochondrial oxidative defense protein-manganese superoxide dismutase. Cancer Res. 65:3745-3750 (2005).

128. D.C. Altieri, G.S. Stein, J.B. Lian, and L.R. Languino. TRAP-1, the mitochondrial Hsp90. Biochimica et Biophysica Acta. 1823:767-773 (2011).

129. C. Dai and L. Whitesell. HSP90: a rising star on the horizon of anticancer targets. Future Oncol. 1:529-540 (2005).

130. A. Kamal, L. Thao, J. Sensintaffar, L. Zhang, M.F. Boehm, L.C. Fritz, and F.J. Burrows. A high-affinity conformation of Hsp90 confers tumour selectivity on Hsp90 inhibitors. Nature. 425:407-410 (2003).

131. H. Xu, Y. Shi, J. Wang, D. Jones, D. Weilrauch, R. Ying, B. Wakim, and K.A. Pritchard, Jr. A heat shock protein 90 binding domain in endothelial nitric-oxide synthase influences enzyme function. The Journal of Biological Chemistry. 282:37567-37574 (2007).

132. M.D. Siegelin, T. Dohi, C.M. Raskett, G.M. Orlowski, C.M. Powers, C.A. Gilbert, A.H. Ross, J. Plescia, and D.C. Altieri. Exploiting the mitochondrial unfolded protein response for cancer therapy in mice and human cells. J Clin Invest. 121:1349-1360 (2011).

133. B.H. Kang, M. Tavecchio, H.L. Goel, C.C. Hsieh, D.S. Garlick, C.M. Raskett, J.B. Lian, G.S. Stein, L.R. Languino, and D.C. Altieri. Targeted inhibition of mitochondrial Hsp90 suppresses localised and metastatic prostate cancer growth in a genetic mouse model of disease. Br J Cancer. 104:629-634 (2011).

134. R. Seigneuric, J. Gobbo, P. Colas, and C. Garrido. Targeting cancer with peptide aptamers. Oncotarget. 2:557-561 (2011).

135. H.H. Szeto and P.W. Schiller. Novel therapies targeting inner mitochondrial membrane--from discovery to clinical development. Pharm Res. 28:2669-2679 (2011).

136. A. Weiss, B. Brill, C. Borghouts, N. Delis, L. Mack, and B. Groner. Survivin inhibition by an interacting recombinant peptide, derived from the human ferritin heavy chain, impedes tumor cell growth. J Cancer Res Clin Oncol (2012).

137. T. Shirakata, Y. Oka, S. Nishida, N. Hosen, A. Tsuboi, Y. Oji, A. Murao, H. Tanaka, S. Nakatsuka, H. Inohara, and H. Sugiyama. WT1 peptide therapy for a patient with chemotherapy-resistant salivary gland cancer. Anticancer Res. 32:1081-1085 (2012).

138. C. Sinthuvanich, A.S. Veiga, K. Gupta, D. Gaspar, R. Blumenthal, and J.P. Schneider. Anticancer ss-hairpin peptides: membrane-induced folding triggers activity. J Am Chem Soc (2012).

139. G.L. Verdine. Drugging the "undruggable". Harvey Lect. 102:1-15 (2006).

140. C. Borghouts, C. Kunz, and B. Groner. Current strategies for the development of peptide-based anti-cancer therapeutics. J Pept Sci. 11:713-726 (2005).

141. D. Zhai, P. Godoi, E. Sergienko, R. Dahl, X. Chan, B. Brown, J. Rascon, A. Hurder, Y. Su, T.D. Chung, C. Jin, P. Diaz, and J.C. Reed. High-Throughput

Fluorescence Polarization Assay for Chemical Library Screening against Anti-Apoptotic Bcl-2 Family Member Bfl-1. J Biomol Screen. 17:350-360 (2012).

142. G.L. Verdine and L.D. Walensky. The challenge of drugging undruggable targets in cancer: lessons learned from targeting BCL-2 family members. Clinical Cancer Research.13:7264-7270 (2007).

143. A. Bolhassani. Potential efficacy of cell-penetrating peptides for nucleic acid and drug delivery in cancer. Biochimica et Biophysica Acta. 1816:232-246 (2011).

144. S.O. Kelley, K.M. Stewart, and R. Mourtada. Development of novel peptides for mitochondrial drug delivery: amino acids featuring delocalized lipophilic cations. Pharmaceutical Research. 28:2808-2819 (2011).

145. V. Moreau, C. Fleury, D. Piquer, C. Nguyen, N. Novali, S. Villard, D. Laune, C. Granier, and F. Molina. PEPOP: computational design of immunogenic peptides. BMC Bioinformatics. 9:71 (2008).

146. I. Van Walle, Y. Gansemans, P.W. Parren, P. Stas, and I. Lasters. Immunogenicity screening in protein drug development. Expert Opin Biol Ther. 7:405-418 (2007).

147. A.J. Chirino, M.L. Ary, and S.A. Marshall. Minimizing the immunogenicity of protein therapeutics. Drug Discov Today. 9:82-90 (2004).

148. P.M. Watt. Screening for peptide drugs from the natural repertoire of biodiverse protein folds. Nat Biotechnol. 24:177-183 (2006).

149. C.R. Braun, J. Mintseris, E. Gavathiotis, G.H. Bird, S.P. Gygi, and L.D. Walensky. Photoreactive stapled BH3 peptides to dissect the BCL-2 family interactome. Chem Biol. 17:1325-1333 (2010).

150. J.G. Valero, L. Sancey, J. Kucharczak, Y. Guillemin, D. Gimenez, J. Prudent, G. Gillet, J. Salgado, J.L. Coll, and A. Aouacheria. Bax-derived membrane-active peptides act as potent and direct inducers of apoptosis in cancer cells. J Cell Sci. 124:556-564 (2011).

151. A.M. Trusheim MR, and Berndt ER. Characterizing markets for biopharmaceutical innovations: Do biologics differ from small molecules? Forum for Health Economics and Policy. 13:4 (2010).

152. S. Kozlowski, J. Woodcock, K. Midthun, and R.B. Sherman. Developing the nation's biosimilars program. N Engl J Med. 365:385-388 (2011).

153. D. Trivigno, F. Essmann, S. Huber, and J. Rudner. The deubiquitinase USP9x controls Mcl-1 levels in response to ionizing radiation, Cell Death in Cancer Conference, De Rode Hoed, Amsterdam, The Netherlands, (2012).

154. I. Naumann, R. Kappler, D. von Schweinitz, K.M. Debatin, and S. Fulda. Bortezomib primes neuroblastoma cells for TRAIL-induced apoptosis by linking the death receptor to the mitochondrial pathway. Clinical Cancer Research.17:3204-3218 (2011).

155. M. Certo, V. Del Gaizo Moore, M. Nishino, G. Wei, S. Korsmeyer, S.A. Armstrong, and A. Letai. Mitochondria primed by death signals determine cellular addiction to antiapoptotic BCL-2 family members. Cancer Cell. 9:351-365 (2006).

156. J. Vrielink, M.S. Heins, R. Setroikromo, E. Szegezdi, M.M. Mullally, A. Samali, and W.J. Quax. Synthetic constrained peptide selectively binds and antagonizes death receptor 5. Febs J. 277:1653-1665 (2010).

157. J. Neuzil, X.F. Wang, L.F. Dong, P. Low, and S.J. Ralph. Molecular mechanism of 'mitocan'-induced apoptosis in cancer cells epitomizes the multiple roles of reactive oxygen species and Bcl-2 family proteins. FEBS Lett. 580:5125-5129 (2006).

CHAPTER 3

SELECTIVE TARGETING OF C-ABL VIA A CRYPTIC MITOCHONDRIAL TARGETING SIGNAL ACTIVATED BY CELLULAR REDOX STATUS IN LEUKEMIC AND BREAST CANCER CELLS

Abstract

The tyrosine kinase c-Abl localizes to the mitochondria under cell stress conditions and promotes apoptosis. However, c-Abl has not been directly targeted to the mitochondria. Fusing c-Abl to a mitochondrial translocation signal (MTS) that is activated by reactive oxygen species (ROS) will selectively target the mitochondria of cancer cells exhibiting an elevated ROS phenotype. Mitochondrially targeted c-Abl will thereby induce malignant cell death. Confocal microscopy was used to determine mitochondrial colocalization of ectopically expressed c-Abl-EGFP/cMTS fusion across three cell lines (K562, Cos-7, and 1471.1) with varying levels of basal (and pharmacologically modulated) ROS. ROS were quantified by indicator dye assay. The

Reprinted with permission from J.E. Constance, S.D. Despres, A. Nishida, and C.S. Lim. Selective targeting of c-Abl via a cryptic mitochondrial targeting signal activated by cellular redox status in leukemic and breast cancer cells. Pharm Res. 29:2317-2328 (2012). Copyright 2012 Springer.

functional consequences of mitochondrial c-Abl were assessed by DNA accessibility to 7-AAD using flow cytometry. The cMTS and cMTS/c-Abl fusions colocalized to the mitochondria in leukemic (K562) and breast (1471.1) cancer phenotypes (but not Cos-7 fibroblasts) in a ROS- and PKC-dependent manner. We confirm and extend oxidative stress-activated translocation of the cMTS by demonstrating that the cMTS and Abl/cMTS fusion selectively target the mitochondria of K562 leukemia and mammary adenocarcinoma 1471.1 cells. c-Abl-induced K562 leukemia cell death when targeted to the matrix but not the outer membrane of the mitochondria.

Introduction

A hyper-oxidative environment is a pathophysiologic hallmark of many disease states, including cancer (1). Cell fate often rests on proteins (e.g., antioxidant enzymes or pro-apoptotic factors) that are responsive to oxidative stress and translocate to the mitochondria (2). However, oncoprotein signaling can disrupt, directly or indirectly, pro-apoptotic signal transduction at the level of the mitochondria (3). For instance, the ubiquitously expressed non-receptor tyrosine kinase c-Abl has been termed a "mitochondrial wracking factor" (4) since active c-Abl translocation to the mitochondria induces cell death (5). In the context of chronic myelogenous leukemia (CML) though, the pro-death functions of c-Abl are prevented by the aberrantly active tyrosine kinase fusion oncoprotein Bcr-Abl (6).

The functional specificity of c-Abl is dictated by subcellular location (7). The majority (70%) of c-Abl resides in the nucleus, with about 20% in the ER, 5-8% in the cytoplasm, and the remainder (~4%) found in the mitochondria (8). c-Abl can promote

mitogenesis when located in the cytoplasm, cell cycle arrest when activated in the nucleus, and upon translocation to the mitochondria c-Abl can induce the loss of mitochondrial membrane potential (ψ_{MIT}), depletion of ATP, and apoptotic/necrotic cell death (8, 9). Additionally, c-Abl was the first tyrosine kinase found to associate with the mitochondria (10) and is considered to be the key apoptotic tyrosine kinase (11). At present the submitochondrial location and substrates for c-Abl are unidentified (12). To our knowledge the consequences of c-Abl to mitochondrial targeting has only been examined in the context of a cellular insult (e.g., H_2O_2, genotoxic agents, and endoplasmic reticulum toxins), and direct targeting of c-Abl to the mitochondria through fusion to a mitochondrial targeting signal (MTS) has not been studied.

Protein localization to different subcellular compartments is often directed by signal sequences encoded in the protein itself. Normally, death-directed c-Abl requires association with a chaperone protein (i.e., PKCδ) to reach the mitochondria as it does not contain an MTS of its own (9). MTSs are usually found at the N- or C-terminus of proteins (13) but fusions to the N-terminus of c-Abl (e.g., Bcr-Abl) disrupt its normal conformation (14). Therefore, in order to permit c-Abl to adopt its native conformation a C-terminal fusion is required. One such C-terminal MTS, that conditionally targets the mitochondria, is derived from murine glutathione-S-transferase A4-4 (GSTA4-4; C-terminal residues 172-222) (15).

The GSTA4-4 MTS is considered a ‘cryptic’ MTS (cMTS) and was previously shown to translocate from the cytosol to the mitochondria in Cos cells under pharmacological stimulation of oxidative stress or protein kinase activators (15, 16). The mitochondrial translocation of the cMTS is dependent upon activation, via

phosphorylation. Key cMTS residues, S189 and T193, are phosphorylated by the protein kinase A (PKA) and/or protein kinase C (PKC) family of ser/thr kinases, respectively. A dihydrofolate reductase/cMTS fusion was previously shown to localize in the mitochondria of Cos cells upon protein kinase activator stimulation (15). Therefore, this study aims to determine if the cMTS could provide a means to selectively target pro-apoptotic c-Abl to the mitochondria based on the inherent level of intracellular reactive oxygen species (ROS) as a discriminating factor across cell types.

Elevated intracellular ROS can lead to the activation of transcription factors (e.g., HIF-1 and NF-κB) leading to a host of protein expression profiles that contribute to malignancy such as, proliferation, survival, and metastasis. This situation leads to a seeming 'ROS paradox' where many antineoplastic agents, like imatinib, exert their cytotoxic effects through the generation of ROS. The underlying mechanisms for (the essential) ROS-mediated killing by chemotherapeutics and radiation therapy is not well understood (17). However, an increase in magnitude of the already elevated ROS in cancer cells is likely to exceed the antioxidant capacity of the cancer and cause cell death (18).

A small selection of cell lines exhibiting different levels of basal ROS were used to test the selective mitochondrial accumulation of cMTS containing constructs. First, human leukemia K562 cells are characterized by elevated ROS and serve as a representative of a cell type in a pathologic pro-oxidative state. K562 cells have high basal levels of ROS due to Bcr-Abl's stimulation of the PI3K/mTOR pathway leading to overactivation of the mitochondrial electron transport chain (19). The oncogenic Bcr-Abl (present in K562) engages signaling pathways that result in the production of ROS,

causing CML cells to have a high cellular oxidative stress background (20). Therefore, ROS levels are chronically elevated due to the presence of Bcr-Abl. Even when Bcr-Abl activity is blocked by tyrosine kinase inhibitor therapy, ROS production is induced via another (apoptotic) route (21). Secondly, both chronic ROS and PKC over-activation have been associated with breast cancer (22, 23), therefore, the murine mammary adenocarcinoma 1471.1 cell line was included. Finally, the transformed monkey kidney fibroblast Cos-7 cell line was used as a negative control for background ROS. Within the context of the elevated ROS K562 cell line, antioxidants (α-tocopherol and N-acetylcysteine) and an antineoplastic (imatinib) were used to modulate the level of ROS and the consequent effects on mitochondrial localization of constructs was determined.

Materials and methods

Materials

RPMI-1640 medium, MitoTracker Red CM-H_2XRos (MitoTracker CMXros), 7-aminoactinomycin D (7-AAD; DNA intercalating dye permeable to dying or dead cells), 5-(and-6)-carboxy-2',7'-dichlorofluoroescein (carboxy-H_2DCFDA; general oxidative stress indicator), Lipofectamine LTX with Plus reagent, and phosphate-buffered saline (PBS) were purchased from Invitrogen (Carlsbad, CA). Penicillin-streptomycin-L-glutamine (P-S-G; 100U/mL), DMEM media and trypsin were purchased from Gibco BRL (Grand Island, NY). Fetal bovine serum (FBS) and gentamycin were purchased from Hyclone Laboratories (Logan, UT). The (+)-α-tocopherol type VI (α-Toc), N-acetyl-L-cysteine (NAC), and poly-L-lysine (0.01% solution) were purchased from

Sigma-Aldrich (St. Louis, MO). Imatinib (CT-IM001) was purchased from ChemieTek (Indianapolis, IN). QuikChange II XL Site-Directed Mutagenesis Kit was purchased from Agilent Technologies (Santa Clara, CA). Cell Line Nucleofector Kit V was purchased from Lonza Group (Basel, Switzerland).

Cell lines and culture conditions

K562 cells (non-adherent human chronic myelogenous leukemia cell line), gift from Dr. K. Elenitoba-Johnson, University of Michigan, and Cos-7 (monkey kidney fibroblast adherent cell line; ATCC) were cultured in RPMI 1640 supplemented with 10% FBS, 1% P-S-G (GIBCO BRL, Grand Island, NY), and 0.1% gentamycin. Murine mammary adenocarcinoma 1471.1 cells, (gift from Gordon Hager, PhD, NCI, NIH) were grown as monolayers in DMEM supplemented with 10% FBS, 1% P-S-G and 0.1% gentamycin. K562 cells were passaged at a density of 0.5×10^5/mL every other day, and discontinued at the tenth passage. Cos-7 and 1471.1 cells were passaged at 80% confluency and split 1:10 in fresh media and discontinued after passage 15. All cells were maintained in a 5% CO_2 incubator at 37 ^oC.

Expression of constructs in K562 leukemia, Cos-7 fibroblast, and 1471.1 breast cancer cells

Constructs were transiently transfected into K562 cells using the Amaxa Nucleofector II, as described previously (24). Briefly, 2×10^6 K562 cells, between passages 5 to 10, were pelleted prior to a 48 hour initial seed density of 0.5×10^5

cells/mL. Cells were resuspended in 100 µL Amaxa Solution V, combined with 2 µg of DNA and transfected in an Amaxa cuvette under program T-013. Transfected cells were immediately transferred to a 25 cm^2 flask with 7 mL of pre-warmed complete RPMI. Transient transfections of 1471.1 and Cos-7 cells were carried out in two-well live-cell chambers (Lab-Tek chamber slide system, Nalge NUNC International, Naperville, IL) or sterile 6-well tissue culture plates (Greiner CellStar, Greiner Bio-one GmbH) using Lipofectamine LTX as per manufacturers' instructions between passages 3 and 15 in antibiotic free media.

Subcloning and construction of plasmids

The murine glutathione S-transferase A4-4 [Swiss-Prot:P24472.3] cMTS (N-terminal residues, 172-222 (15); 51% sequence homology to human wherein S189 and T193 are conserved) was constructed by annealing four oligonucleotides (**1**: (5'phosphorylated) 5' –AATTCCGCCCCCGTGCTGAGCGACTTCCCCCTGCTGCA-GGCCTTCAAGACCAGAATCAGCAACATCCCCACCATCAAGAAGTTCCTGCAG CCC-3', **2**: 5' –CTGCCGGGCTGCAGGAACTTCTTGATGGTGGGGATGTTGCTGA-TTCTGGTCTTGAAGGCCTGCAGCAGGGGGAAGTCGCTCAGCACGGGGGCGG-3', **3**: 5' –GGCAGCCAGAGAAAGCCCCCCCCCGACGGCCCCTACGTGGAGGTG-GTGAGAACCGTGCTGAAGTTCGGCGCCGGCTGCTGCCCCGGCTGCTGCTGA-3', **4**: (5' phosphorylated) 5' –AATTTCAGCAGCAGCCGGGGCAGCAGCCGGCGC-CGAACTTCAGCACGGTTCTCACCACCTCCACGTAGGGGCCGTCGGGGGGGGG CTTTCTCTGG-3') simultaneously and then inserting the annealed product into the multiple cloning site (MCS) of EGFP-C1 vector (Promega Biotech, Madison, WI) at the

EcoRI (New England Biolabs, Ipswich, MA) site creating pE-cMTS. The pE-cMTS-SY (T186E/R187A/S189Y) and pE-cMTS-TY (P192I/T193Y) were created using site-directed mutagenesis using primers, 5'-GCTGCAGGCCTCAAGGAGGCCATCTACA-ACATCCCCACC-3' and 5'-GACCAGAATCAGCAACATCATCTACATCAAGAAG-TTCCTGCAGCCCGGCAGCCAGAGAA-3', respectively, with corresponding reverse complements. Additionally, a tetracysteine motif tag present in the annealed oligonucleotide cMTS insert, was eliminated from being expressed by site-directed mutagenesis to incorporate a stop codon (Primer: 5'-CCGTGCTGAAGTTCTGAGCCG-GCTGCTGCC-3' and reverse complement). Human c-Abl (ABL1 isoform a; NM_005157) was purchased from DF/HCC DNA Resource Core (http://dnaseq.med.harvard.edu/) as plasmid DNA in vector pJP1563 (clone ID HsCD00039065). DNA encoding c-Abl was amplified through PCR using the primers 5'-CGACGACACCGGTCGCCACCATGTTGGAGATCTGCCTG-3' (includes Kozak sequence) and 5'- CAGTGACATAGTGCAGAGGGGCGCCGGCGGACCGGTCGAC-GAC-3' and subcloned into pEGFP-C1 (Clontech, Mountain View, CA, USA) and pE-cMTS at the blunted (Quick Blunting Kit, New England Biolabs Inc., Ipswich, MA, USA) *Age1* restriction enzyme site. The pAbl-E-cMTS KD (kinase dead; isoform 1a K271A mutation (25)) mutant was created using site-directed mutagenesis with the primer 5'-CTGACGGTGGCCGTGGCGACCTTGAAGGAGGAC-3' and its reverse complement. The MOM targeting sequence derived from Bcl-X_L was constructed by annealing two complementary 5' phosphorylated oligonucleotides each containing *BamHI* sticky ends (XL oligonucleotide 5′-AGAAAGGGCCAGGAGAGATTCAACA-

GATGGTTCCTGACCGGCATGACCGTGGCCGGCGTGGTGCTGCTGGGCAGCCT GTTCAGCAGAAAGTGA-3′) and inserting into the *BamHI* restriction enzyme site of pEGFP-C1 and pAbl-E to create pE-MOM and pAbl-E-MOM, respectively. All constructs were verified by sequence analysis.

Mitochondrial staining

Aliquots of transfected K562 suspension cells (400µL) were plated into poly-L-lysine coated 4-well live-cell chambers at least 4 hours in advance of microscopy. Cells were incubated with MitoTracker Red CM-H_2XRos (K562; 100nM, Cos-7 and 1471.1; 325nM) for 45 minutes at 37 ^{o}C and protected from light prior to imaging.

Confocal microscopy

All images of K562, Cos-7, and 1471.1 live cells were acquired on an Olympus IX81 FV1000-XY spectral confocal microscope (Imaging Core Facility, University of Utah) equipped with 405 nm diode, 488 nm argon, and 543 nm HeNe lasers using a 60X PlanApo oil immersion objective (NA 1.45) using Olympus FluoView software. Excitation and emission filters were as follows: EGFP, 488 nm excitation, emission filter 500-530 nm; MitoTracker Red CM-H_2XRos, 543 nm excitation, emission filter 555-655 nm. Images were collected in sequential line mode with exposure and gain of laser kept constant and below detected pixel saturation for each group of cells. No channel crosstalk was observed. Pixel resolution was kept at 1024 x 1024 (0-2.5-fold digital zoom) with a pixel dwell time of 12.5 µs.

Image analysis

Images were analyzed as previously described (26). Briefly, original images were saved as 16-bit files preserving meta-data. Images were converted to 8-bit, stacked as separate channels, and corrected for background noise using ImageJ plugin 'BG subtraction from background' in default mode (i.e., mean background intensity outside of cells was subtracted) (27). All experiments were completed in at least triplicate. ROIs, to be compared for colocalization, were constructed using individual cells to control for cell-to-cell intensity variation in colocalization analysis. Image and statistical analysis was performed with JACoP in ImageJ (28). Pearson's correlation coefficient (PCC) was generated using Costes' automatic threshold algorithm to eliminate manual thresholding bias, increase the accuracy in quantifying low level colocalization, and ensure reproducibility (29, 30). The PCC is dependent upon both the pixel intensity and overlap of signal and has a range of +1 (complete colocalization) to -1 (anti-correlation) with zero correlating with random distribution between comparators (28). The PCC threshold for defining colocalization (i.e., colocalization due to co-compartmentalization) is 0.6 as per Bolte and Cordelières (28) (see *Fig. 3.1*). Channel one (EGFP) and channel two (MitoTracker CMXros) have been false colored, using ImageJ LUT, cyan and magenta, respectively, for increased visual clarity. Additionally, spatial representation of intensity correlation was included between EGFP-tagged proteins and the mitochondria (stained with MitoTracker Red CM-H_2XRos) using the Colocalization Colormap ImageJ plugin. 'Colormap' displays positively correlated pixels in hot colors and negatively correlated pixels in cold colors that can be visually interpreted using the color scale bar (31).

Figure 3.1. Degree of colocalization. The degree of colocalization is based on Pearson's correlation coefficient (PCC) generated using the method of Costes'. PCC values above 0.6 (top dashed line) can be considered either co-compartmentalized or colocalized as established by Bolte and Cordelières while PCC values 0.5 or above (bottom dashed line) meet the threshold for co-compartmentalization only. The term colocalization is defined more stringently and implies that two fluorescent entities are associated based on both spatial overlap of pixels and matching intensity co-variation. Co-compartmentalization (also 'partial-colocalization') can be synonymous with colocalization however, if a comparator channel signal is from a compartment specific stain that is not expected to have any stoichiometric relationship or interaction with the other fluor then the PCC threshold value is adjusted down to 0.5 to compensate for the expected lack in intensity correlation. The interpretation of values between 0.5 and -0.5 (PCC range is from 1 to -1) is difficult.

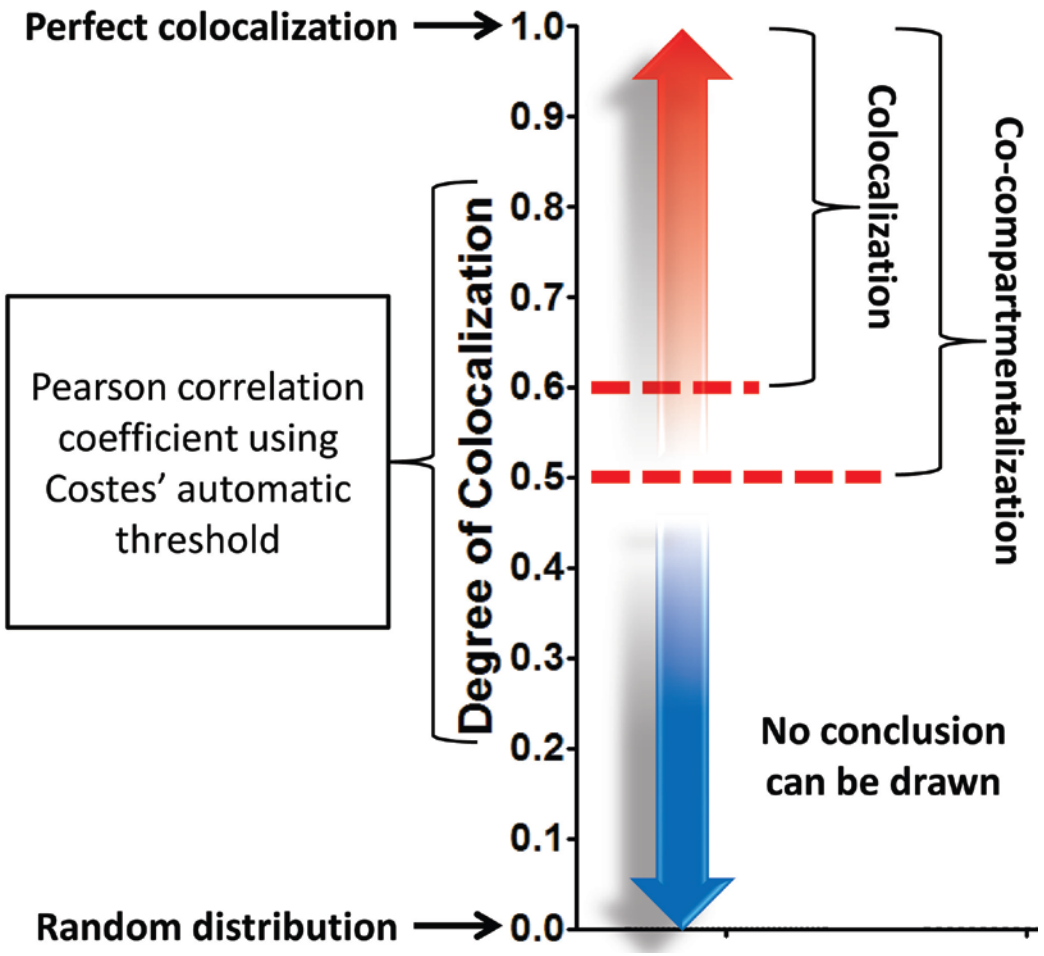
Perfect colocalization
1.0
0.9
0.8
0.7
0.6
0.5
0.4
0.3
0.2
0.1
0.0
Random distribution
Degree of Colocalization
Pearson correlation coefficient using Costes' automatic threshold
Colocalization
Co-compartmentalization
No conclusion can be drawn

Antioxidant treatment of K562 cells

Complete RPMI media containing 50 μM (+)-α-tocopherol or N-acetyl-L-cysteine (300 μM or 5 mM (dissolved in RPMI at 80 mM stock concentration (pH adjusted to 7.4)) was added to freshly transfected cells.

ROS detection assay

ROS production was measured according to the manufacturer's instructions. Briefly, the cellular ROS level was measured by incubating approximately 10^6 cells with 25 μM carboxy-H_2DCFDA for 45 minutes and protected from light at 37˚C in a 5% CO_2 incubator in PBS. Immediately following incubation cells were pelleted via centrifugation and resuspended in 400 μL warmed PBS, split into two wells on a black Corning Costar 96-well plate and measured on a SpectraMax M2 fluorescence plate reader (Molecular Devices, Sunnyvale, CA) with excitation at 485 nm and emission collected at 530 nm wavelengths. Either raw arbitrary fluorescence units were reported or expressed as percent control. Positive controls were H_2O_2 (500 μM) treated cell lines (with and without carboxy-H_2DCFDA) and negative controls were cells in PBS without carboxy-H_2DCFDA and also PBS with carboxy-H_2DCFDA.

Cell death assay

Flow cytometric assay of cell death was done as previously described (32). Briefly, K562, Cos-7, and 1471.1 cells were collected 48 hours posttransfection and resuspended in 500 μL ice cold PBS containing 1 μM 7-aminoactinomycin D (7-AAD) for 30 minutes prior to analysis. Media from adherent Cos-7 and 1471.1 cells was

collected prior to trypsinization of cell monolayer and recombined with the enzymatically released cell population for centrifugation and subsequent resuspension. Analysis and gating was performed on a BD FACSCanto II (Flow Cytometry Core Facility, University of Utah) on BD FACSDiva software (BD Biosciences, Franklin Lakes, NJ). At least three separate experiments in duplicate were performed. Compensation controls were included with each experiment.

Statistical analyses

Data are shown as mean ± S.E.M. Unpaired t-test, one-way ANOVA with Tukey's (or Dunnett's) post-test, two-way ANOVA with Bonferroni post-test, or two-tailed correlation (as indicated in figure legends), were used to evaluate measurements between experimental data with an N of 3 or greater. Statistical significance was set at $P<0.05$ or adjusted lower in instances of multiple comparisons (by convention $P<0.05$ is represented with *; $P< 0.01$ with **; $P< 0.001$ with ***). GraphPad Prism Graph 4 (GraphPad, La Jolla, CA) software was used for generating statistics.

Results

K562 leukemia and 1471.1 mammary adenocarcinoma cells exhibit elevated ROS backgrounds and cMTS mitochondrial localization compared to Cos-7

To assess differences in basal ROS level between K562 leukemia, mammary adenocarcinoma 1471.1, and the Cos-7 (negative control for oxidative stress (15, 33))

Figure 3.2. The cMTS is mitochondrial in K562 and 1471.1 cells but cytosolic in Cos-7. *A*) Leukemic (K562) and Breast cancer (1471.1) cells exhibit elevated background ROS as compared to Cos-7. ROS detection assay using the general oxidative stress indicator carboxy-H_2DCFDA conversion to DCF was monitored on a fluorescent plate reader with excitation at 485nm and emission at 530nm. Fluorescence signal was stable across samples and over time when the endpoint reading was collected. One-way ANOVA with Tukey's post-test (error bars are ±S.E.M, N=3).

B) Representative images of E-cMTS in K562, Cos-7 and 1471.1 cells. The cMTS is selectively targeted to the mitochondria in cells with elevated oxidative stress. ROS activate PKC kinases that, in turn, activate, via phosphorylation, the cMTS. The phosphorylated "active" cMTS translocates from the cytoplasm to the mitochondria. Channel one (EGFP) and channel two (MitoTracker) have been false colored, cyan and magenta, respectively, for increased visual clarity. Colocalized pixels in merged cyan and magenta images show as white. The 'Colormap' (far right column) displays positively correlated pixels in hot colors and negatively correlated pixels in cold colors that can be interpreted using the color scale bar (shown at bottom of the 'Colormap' column). Scale bars are 5 μm (mean Pearson correlation coefficient (PCC) values are ±S.E.M, N=3).

C) Individual cell ROIs were selected from confocal images taken with live cells and analyzed using the PCC to quantify the degree of E-cMTS mitochondrial colocalization in K562, 1471.1 and Cos-7 cells. Signal from EGFP (tagged to cMTS) and MitoTracker Red CM-H_2XRos staining were compared. One-way ANOVA with Tukey's post-test (error bars are ±S.E.M, N=3, $P<0.01$**, $P<0.001$***).

A.

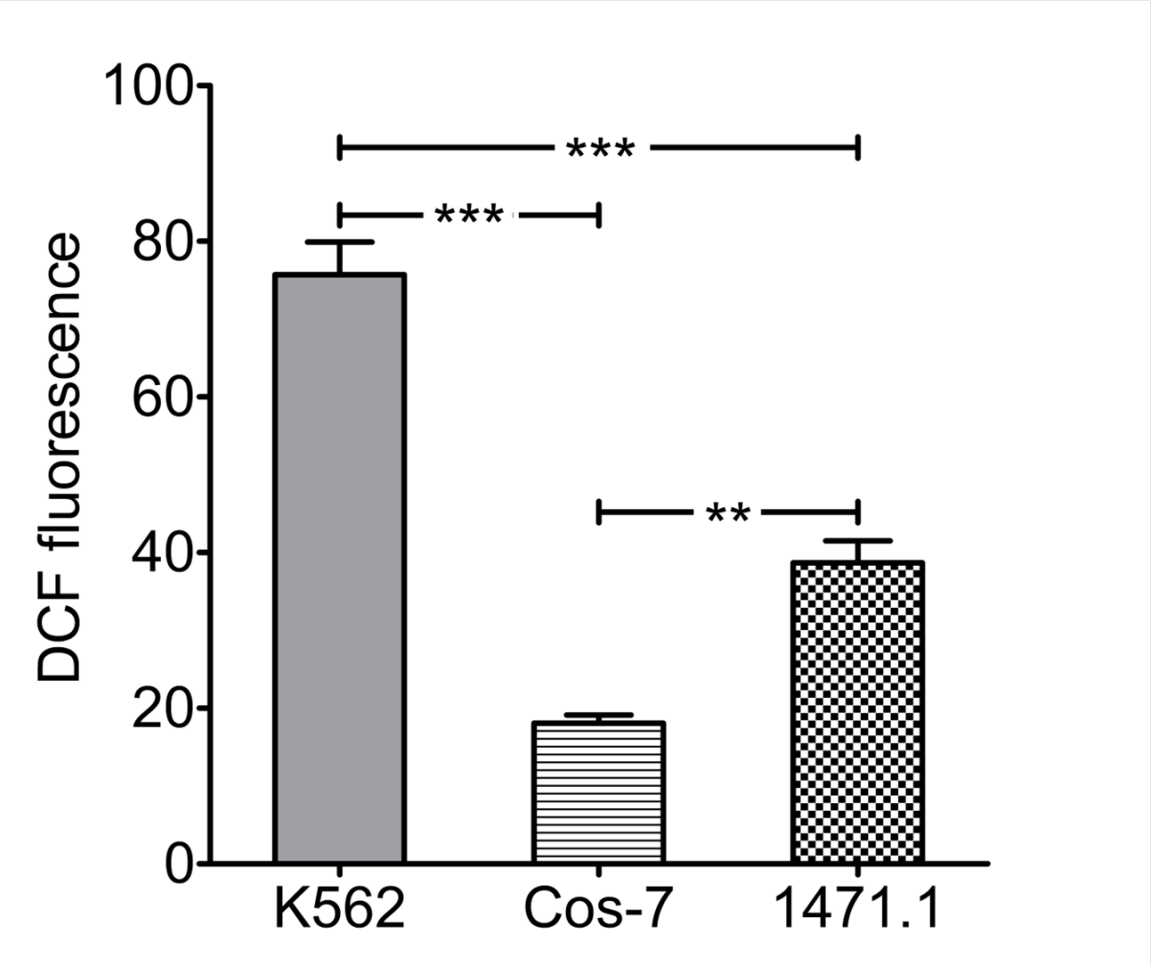

B.

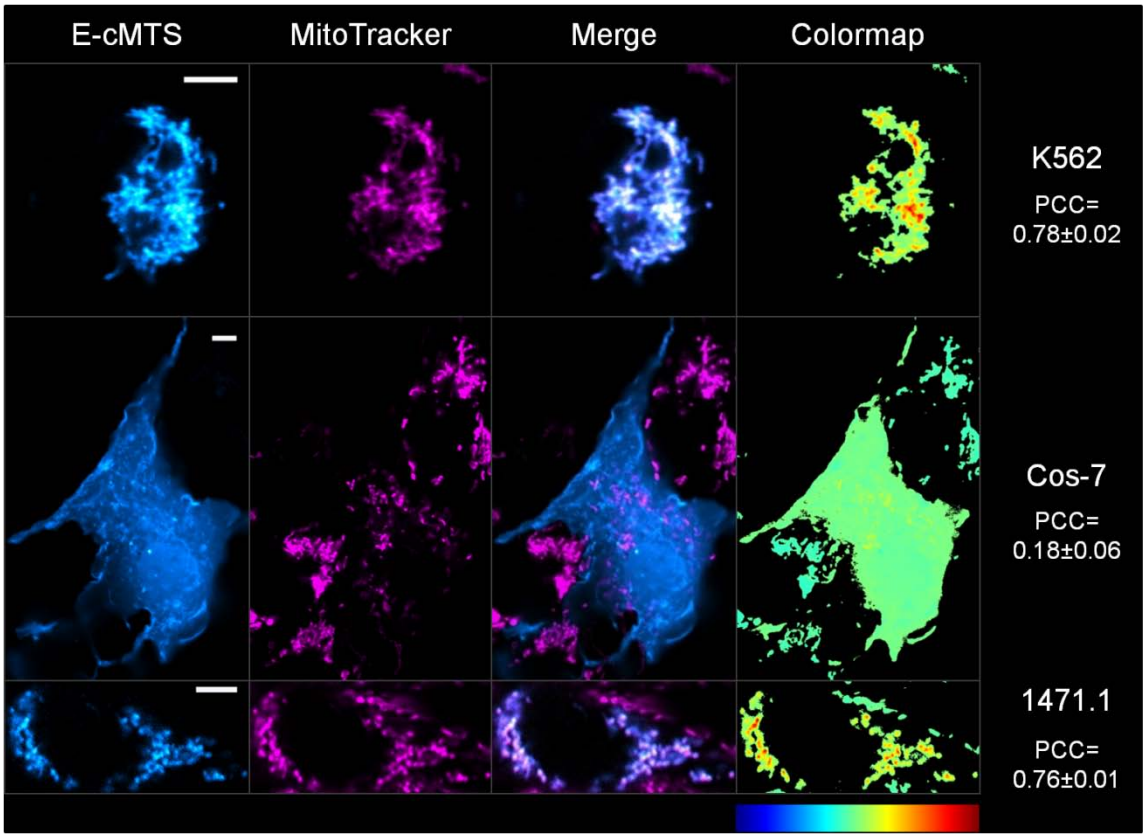
E-cMTS
MitoTracker
Merge
Colormap
K562
PCC=
0.78±0.02
Cos-7
PCC=
0.18±0.06
1471.1
PCC=
0.76±0.01

C.

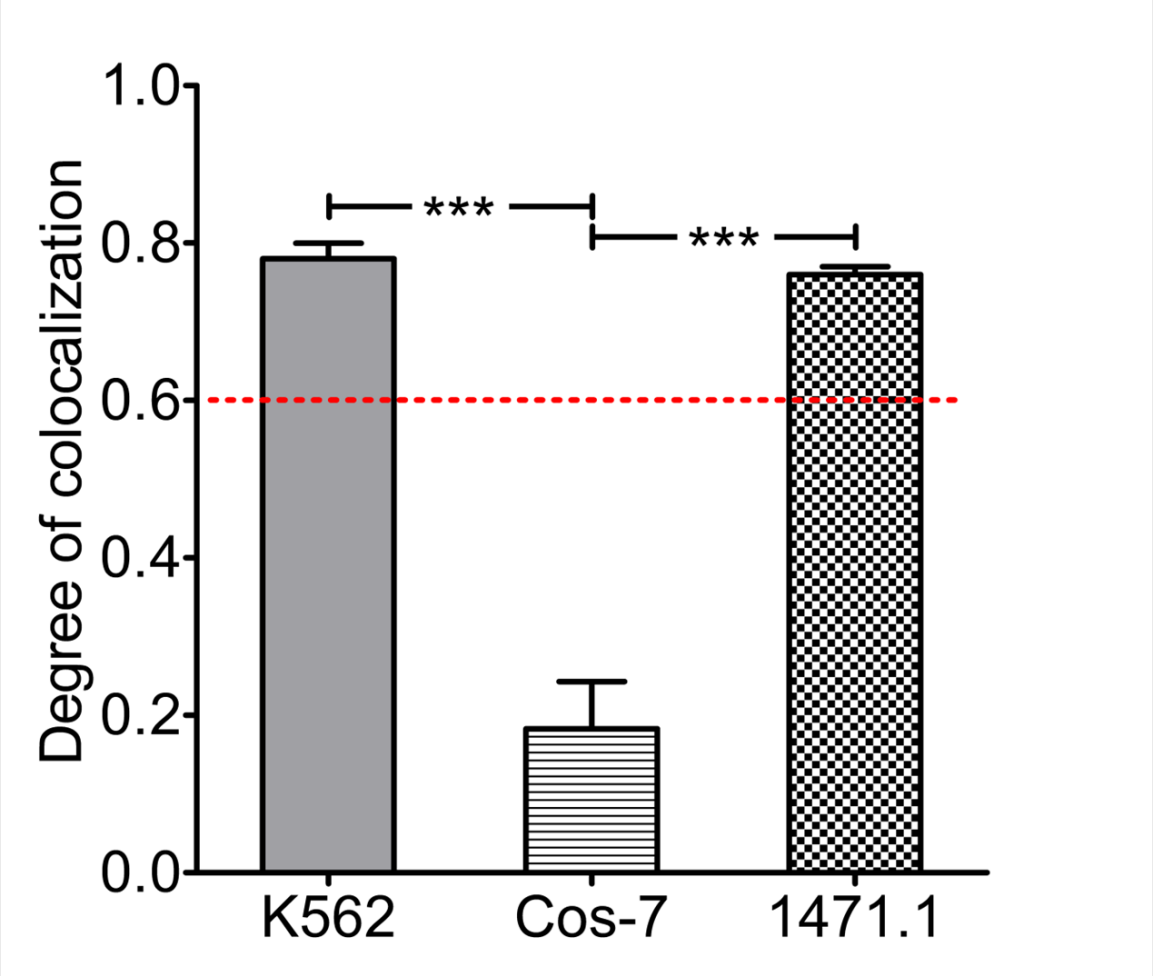

monkey kidney fibroblast cell lines, the conversion of carboxy-H_2DCFDA to DCF was measured (*Fig. 3.2*; y-axis in arbitrary fluorescence units). K562 (*left column, Fig. 3.2A*) and 1471.1 mammary adenocarcinoma (*right column, Fig. 3.2A*) cells demonstrated an elevated background ROS compared to Cos-7 (*middle column, Fig. 3.2A*). The basal ROS level of 1471.1 cells fell between the K562 and Cos-7 reference cell lines.

Confocal fluorescence microscopy (*Figure 3.2B*) paired with statistical analysis was used to determine mitochondrial localization of the cryptic MTS derived from GSTA4-4 (cMTS), fused to EGFP, across cell types. Despite the nearly two-fold higher basal ROS level of K562 over the 1471.1 cell line, the E-cMTS was equally colocalized to the mitochondria of both K562 (*left column, Fig. 3.2C*) and 1471.1 (*right column, Fig. 3.2C*) cells 24 hours post-transfection whereas the E-cMTS remained cytosolic in Cos-7 (*Fig. 3.2C, middle column*). *Figure 3.2B* shows representative images for each cell line transfected with E-cMTS (cyan) and stained with MitoTracker Red (magenta) with white scale bars in the E-cMTS images measuring 5 μm. Image analysis, from at least three separate experiments quantifying the degree of colocalization of the E-cMTS with the mitochondria was used to construct *Figure 3.2C*. The 'degree of colocalization' is represented by Pearson's correlation coefficient (PCC) (29). EGFP-C1 was used as a negative control for colocalization studies (thresholded PCC values of EGFP-C1 and MitoTracker CMXros in the different cell lines were, K562: -0.20 ± 0.13, Cos-7: 0.04 ± 0.03, and 1471.1: 0.12 ± 0.03). Mitochondrial colocalization of constructs was verified to be consistent at different cell depths (i.e., z-plane sections; data not shown). Although overlay of the E-cMTS and MitoTracker CMXros signals are provided ('Merge' column) for visual assessment of pixel overlap, a superior visual representation of colocalization,

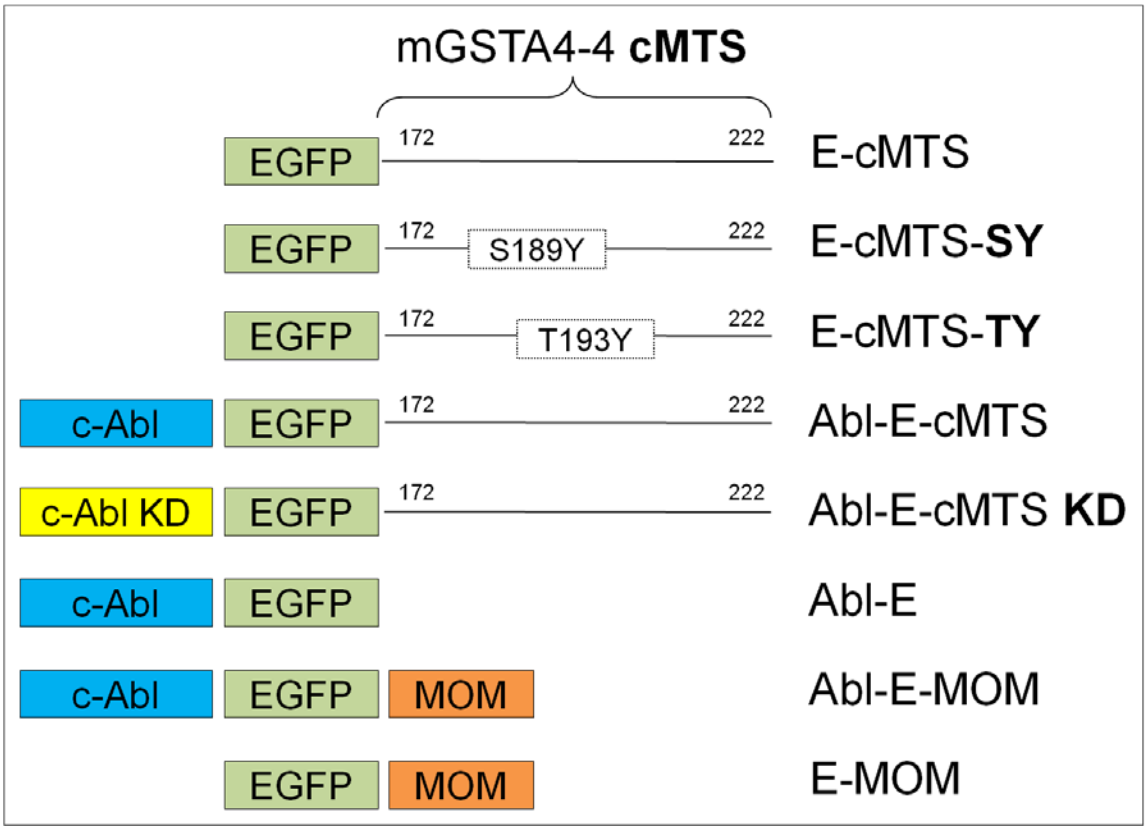

Figure 3.3. Diagram of constructs. The C-terminal 50-amino acid sequence of mGSTA4-4 was fused to the C-terminus of EGFP to create, E-cMTS. The PKA and PKC phosphorylation site-mutants are E-cMTS-SY and E-cMTS-TY, respectively. Abl-E serves as a negative control for mitochondrial translocation and a baseline for cell death upon mitochondrial targeting of c-Abl/MTS constructs. Abl-E was constructed with c-Abl positioned N-terminally to the EGFP tag in order to maintain c-Abl's ability to adopt a native auto-inhibitory conformation (14). Abl-E-MOM and E-MOM contain a canonical MTS derived from Bcl-X_L that targets to the mitochondrial outer membrane (MOM). Abl-E-cMTS KD is the cMTS fused to a kinase dead c-Abl.

showing spatial depiction of pixel overlap and relative intensity, can be seen in the 'colormap' column (31).

As a control for baseline translocation efficiency across cell types, in a PKC- and PKA-independent manner, a canonical MTS derived from Bcl-X_L was subcloned into EGFP-C1 (E-MOM), *Figure 3.3*. The Bcl-X_L has been demonstrated to efficiently translocate heteroproteins to the mitochondrial outer membrane (MOM) (34). The MTSs from both the cMTS and Bcl-X_L are C-terminal sequences. The Bcl-X_L MTS targets to the MOM (35) whereas the cMTS targets to the mitochondrial matrix (15). Images in *Figure 3.4A* display the robust mitochondrial targeting efficiencies of E-MOM in each of the three cell lines used. Analysis of images evaluating E-MOM mitochondrial localization collected in three separate experiments (*Fig. 3.4B*) confirm that the translocation machinery of K562, 1471.1 and Cos-7 cells is sufficiently proficient for comparison of cMTS localization in these cell types.

Requirement for threonine 193 but not serine 189 for mitochondrial translocation of cMTS in K562 and 1471.1 cells

Two cMTS mutants were made in order to determine the importance, in K562 and 1471.1 cells, of previously determined PKA (S189) and PKC (T193) phosphorylation sites that lead to the activation and mitochondrial accumulation of the cMTS (*Table 3.1*, E-cMTS-SY and E-cMTS-TY, respectively) (15). The mutations to the PKA and PKC phosphorylation sites were changed to minimal c-Abl tyrosine kinase recognition sequences because of the possibility that Bcr-Abl tyrosine kinase activity in K562 cells

A.

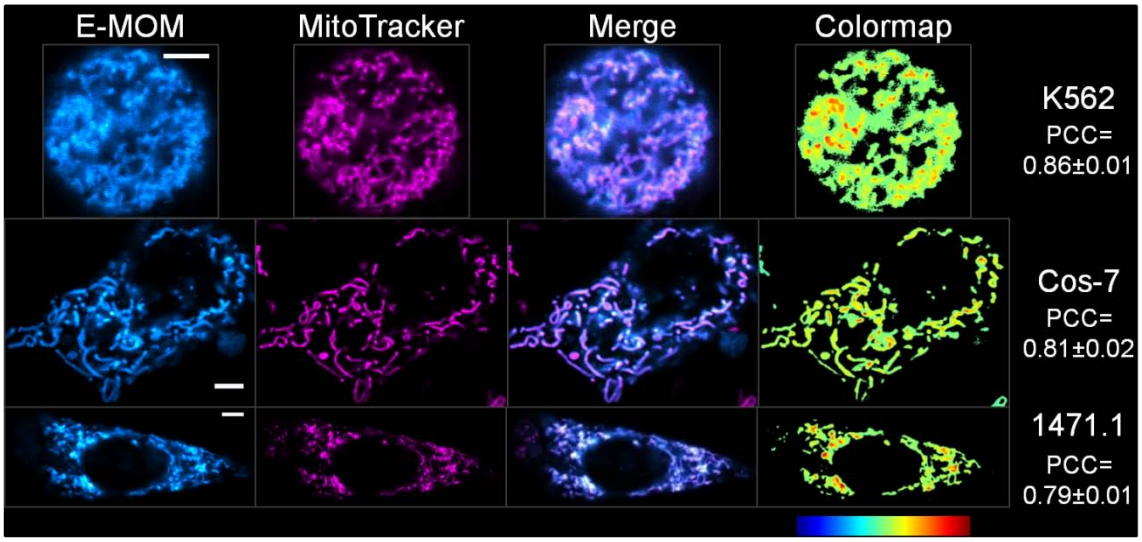

Figure 3.4. The translocation efficiency for the cell types tested is sufficient to determine mitochondrial localization of constructs. Using a canonical MTS derived from Bcl-X_L fused to EGFP, the relative capability of each cell type was determined.

A) Representative images of K562, Cos-7, and 1471.1 cells transfected with E-MOM construct at 24 hours.

B) Signal from E-MOM and MitoTracker Red CM-H_2XRos staining were compared. One-way ANOVA with Tukey's post-test (error bars are ±S.E.M, N=3, P<0.05*).

B.

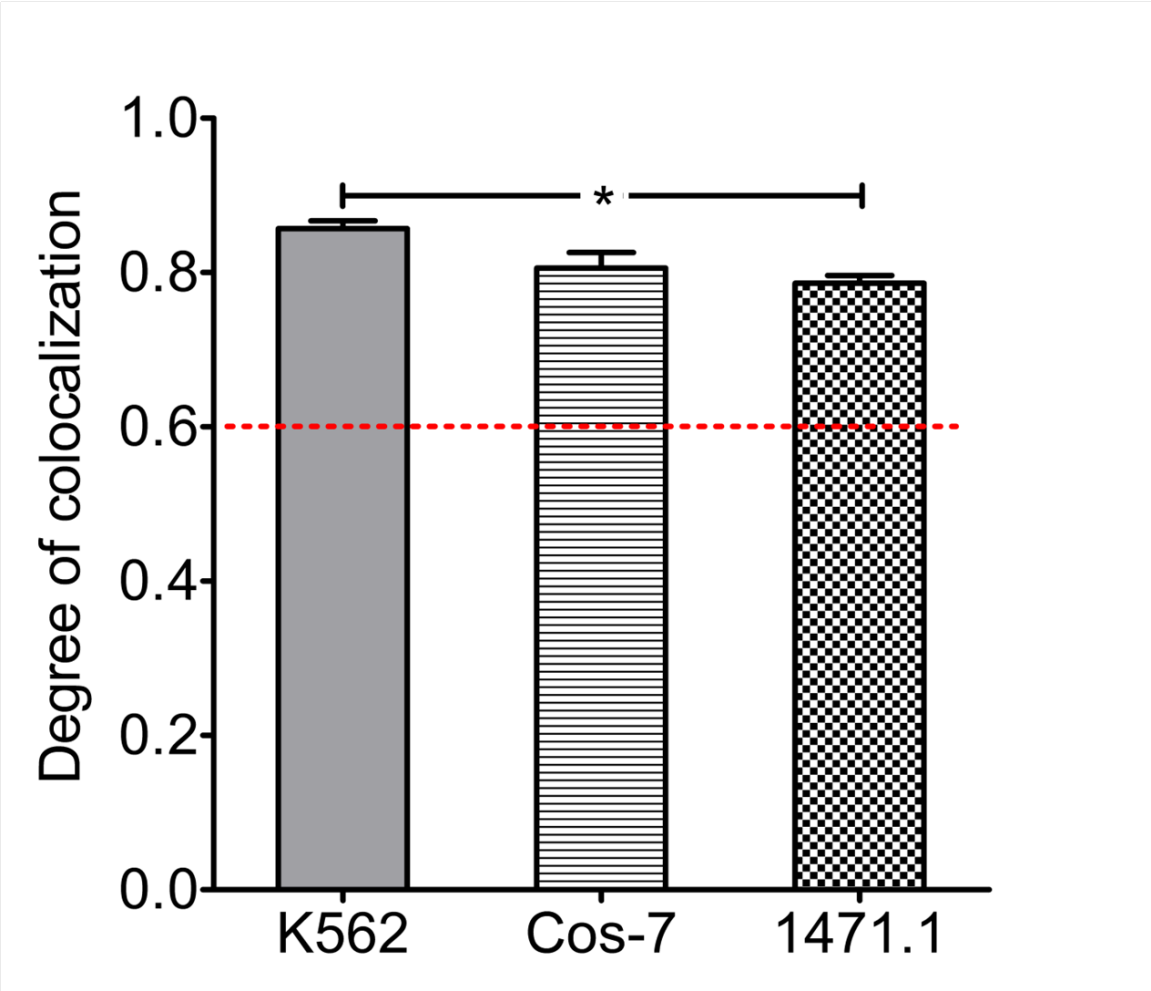

Figure 3.4: Continued

Table 3.1. Names of cMTS constructs, corresponding residue sequences, relevant protein kinase, and key residue mutations. cMTS constructs names, corresponding residue sequences, relevant protein kinase, and key residue mutations. PKA (S189) and PKC (T193) phosphorylation sites are bolded. cMTS-SY has a key mutation (S189Y) creating a PKA-null site-mutant whereas cMTS-TY contains a key mutation (T193Y) creating a PKC-null site-mutant. Residues underlined in black were also mutated to incorporate the minimal c-Abl phosphorylation consensus recognition sequence while simultaneously ablating either the PKA or PKC phosphorylation sites. The cMTS-SY and cMTS-TY mutations, computationally analyzed for potential changes to the secondary structure via the MPI Bioinformatics Toolkit (36), did not alter the secondary structure (i.e., α-helicity, disordered regions, or solvent accessibility) as compared to wild-type cMTS. Incorporation of both the S189Y and T193Y mutations into the cMTS resulted in a strictly cytosolic distribution of the cMTS-SY/TY mutant generating a thresholded PCC of 0.14 ± 0.2 in K562 cells when compared to MitoTracker CMXros.

Construct	**cMTS Sequence:** **mGSTA4-4 C-terminal residues 172-222**	**Phosphorylation by:**	**Key residue mutation**
cMTS	APVLSDFPLLQAFKTRI**S**NIP**T**IKKFLQPGSQRKPPPDGP YVEVVRTVLKF	PKA/PKC	none
cMTS-SY	APVLSDFPLLQAFKEAI**Y**NIPTIKKFLQPGSQRKPPPDG PYVEVVRTVLKF	PKC only	S189Y
cMTS-TY	APVLSDFPLLQAFKTRISNII**Y**IKKFLQPGSQRKPPPDGP YVEVVRTVLKF	PKA only	T193Y

Figure 3.5. The conserved threonine 193 is critical for mediating mitochondrial localization under oxidative conditions.

A) EGFP-tagged cMTS-SY and cMTS-TY were compared to MitoTracker Red CM-H_2XRos staining in live cells. EGFP and MitoTracker channels were false-colored cyan and magenta, respectively, for increased visual clarity. Colormap displays spatial intensity correlation between channels. Scale bar is 5 μm. (mean PCC values are ±S.E.M, N=3)

B) Mitochondrial localization of wild-type E-cMTS as compared to mutated E-cMTS-SY (S189Y) and E-cMTS-TY (T193Y) in K562 and 1471.1 cells. In both 1471.1 and K562 cells the cMTS was not statistically different from E-cMTS-SY. Two-way ANOVA with Bonferroni post-test (error bars are ±S.E.M, N=3, $P<0.01$**, $P<0.001$***).

A.

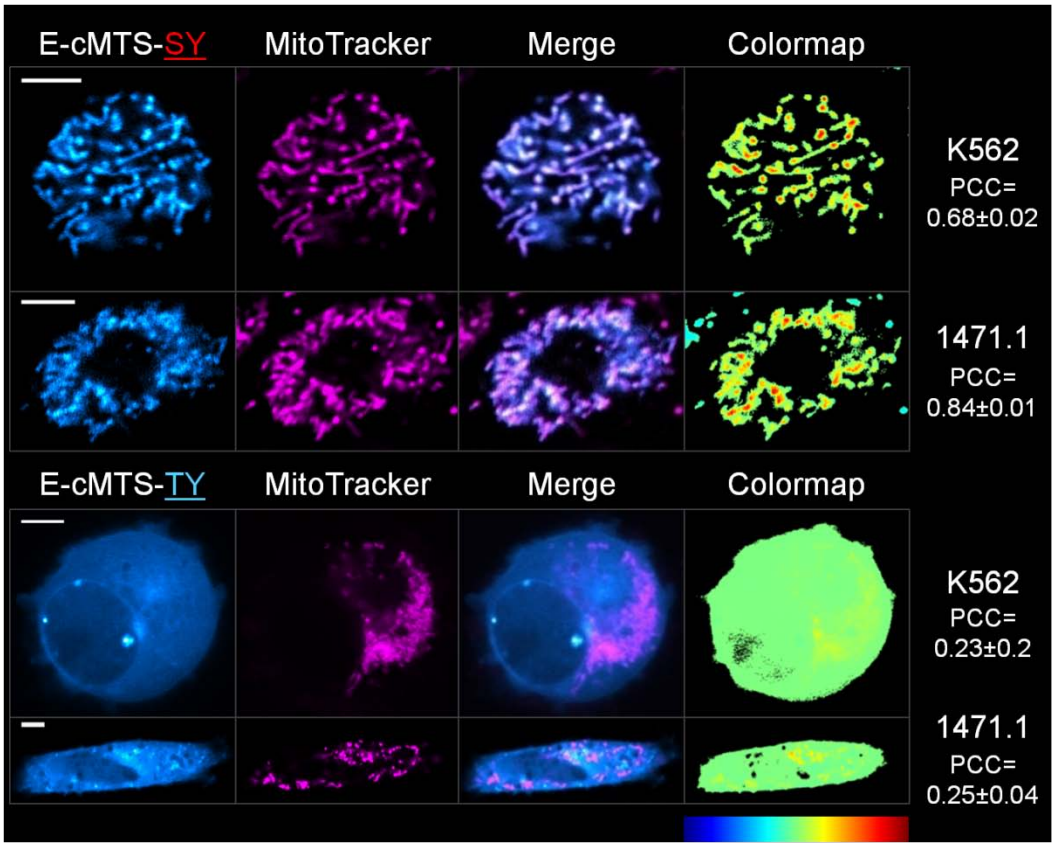
E-cMTS-SY
MitoTracker
Merge
Colormap
K562
PCC=
0.68±0.02
1471.1
PCC=
0.84±0.01
E-cMTS-TY
MitoTracker
Merge
Colormap
K562
PCC=
0.23±0.2
1471.1
PCC=
0.25±0.04

B.

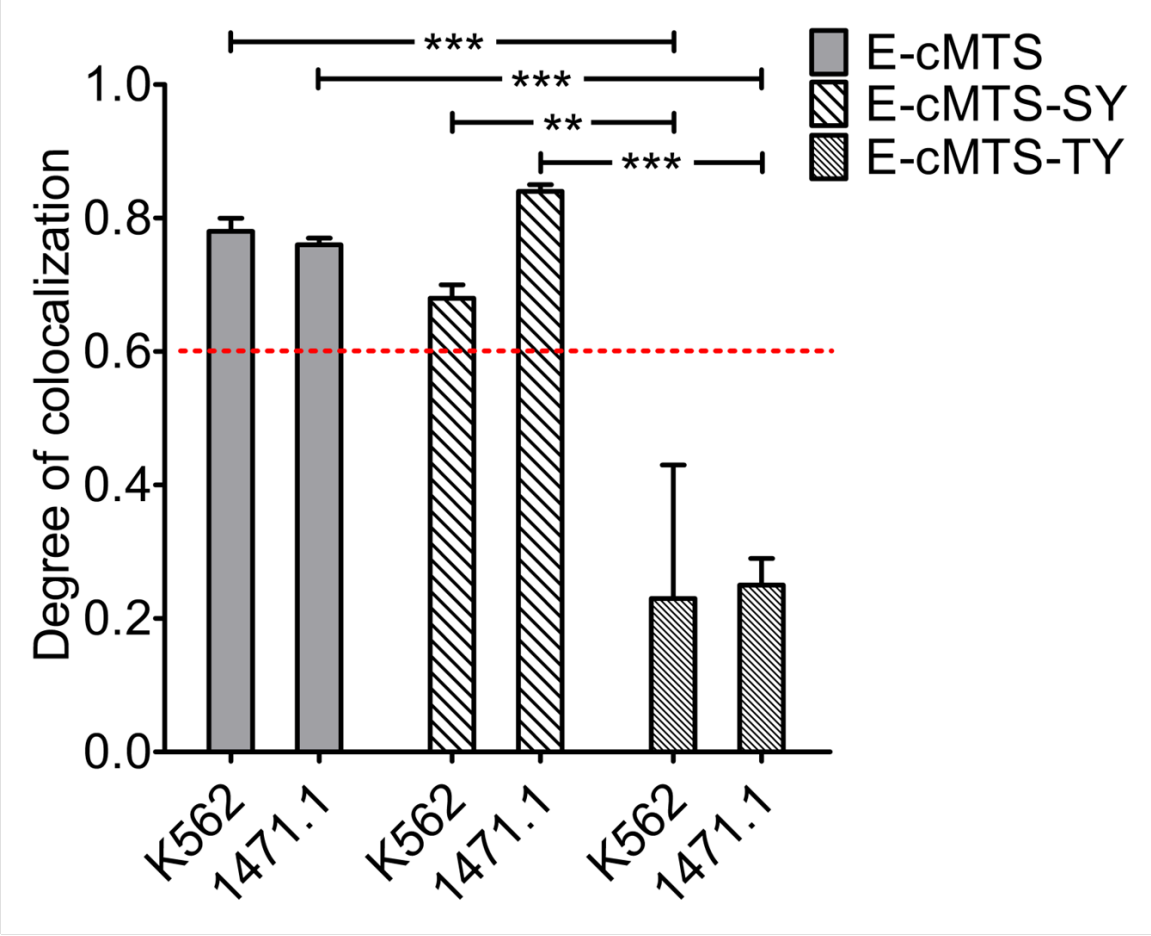
***
***
**
***
E-cMTS
E-cMTS-SY
E-cMTS-TY
Degree of colocalization
1.0
0.8
0.6
0.4
0.2
0.0
K562
1471.1
K562
1471.1
K562
1471.1

Figure 3.6. Imatinib increases, while antioxidants α-tocopherol and N-acetylcysteine attenuate, ROS and E-cMTS mitochondrial colocalization in K562 cells.

A) Comparison of ROS levels between K562 cells treated with imatinib (10 μM, IM), α-tocopherol (50 μM, α-toc), or N-acetylcysteine (300 μM or 5 mM, NAC) for 24 hours. Values are expressed as a percent of untreated K562 cells. Significance was determined using one-way ANOVA with Dunnett's post-test (error bars are ±S.E.M, N=3).

B) Representative images of live K562 cells transfected with E-cMTS and treated with imatinib, α-tocopherol, or NAC compared to MitoTracker Red CM-H_2XRos staining. Scale bar is 5 μm. (mean thresholded PCC values are ±S.E.M, N=3)

C) Mitochondrial association of the E-cMTS or E-cMTS-SY in K562 cells after 24 hours of treatment with imatinib (10 μM) or E-cMTS with α-tocopherol (50 μM) and N-acetylcysteine (NAC; 300 μM and 5 mM). The imatinib induced ROS in K562 cells corresponds to the increased mitochondrial accumulation of both E-cMTS and E-cMTS-SY (mutant with PKC phosphorylation site only). Likewise, α-tocopherol and 5 mM NAC treated cells demonstrated lower overall mitochondrial association which corresponds to lower ROS levels. Statistical analysis for the E-cMTS transfected groups was (*A* and *C*): one-way ANOVA with Tukey's post-test and E-cMTS-SY group (*C*): two-tailed unpaired t-test (error bars are ±S.E.M, N=3, $P<0.05$*, $P<0.01$**, $P<0.001$***).

A.

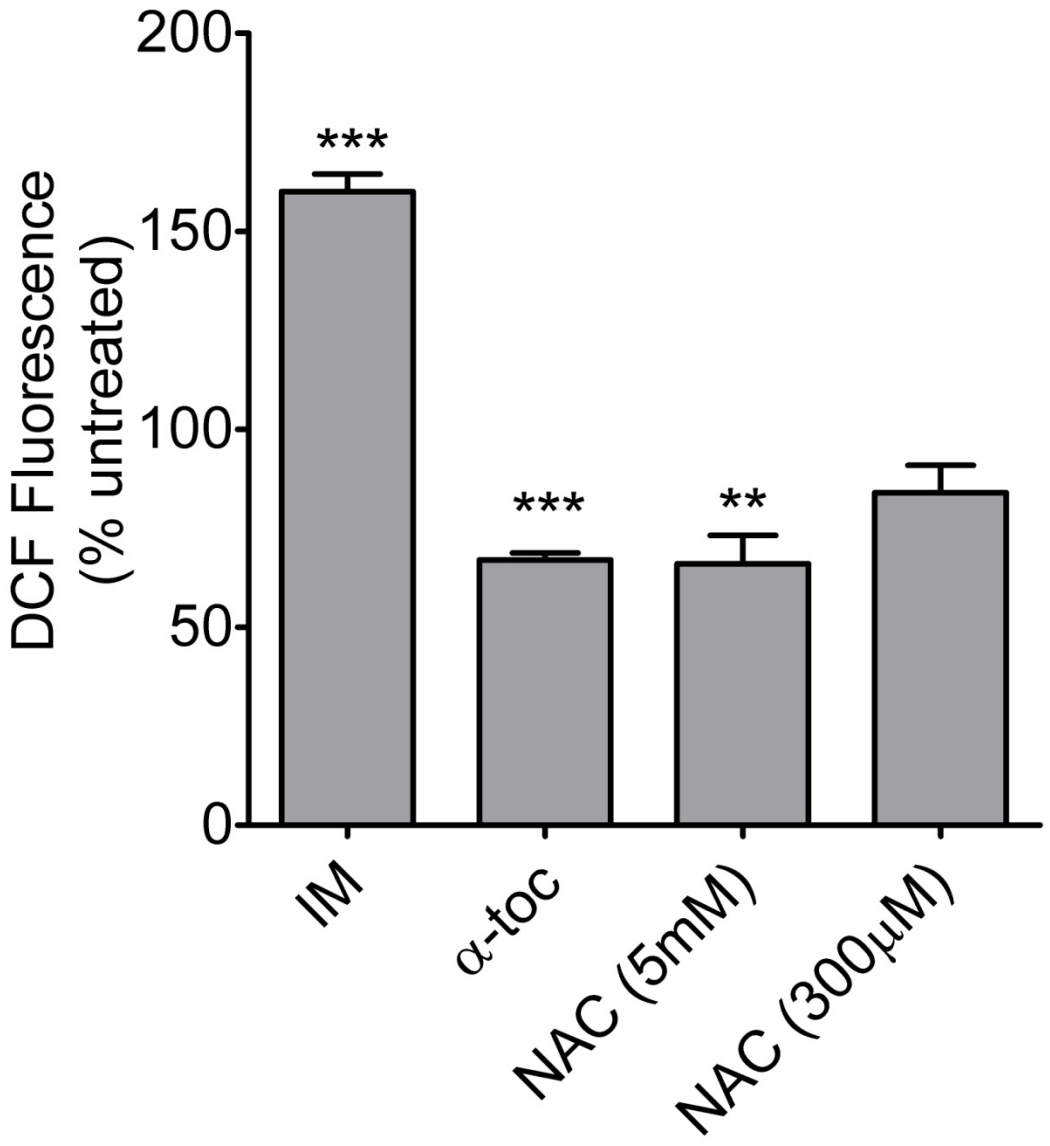
200
150
100
50
0
DCF Fluorescence
(% untreated)
***
***
**
IM
α-toc
NAC (5mM)
NAC (300μM)

B.

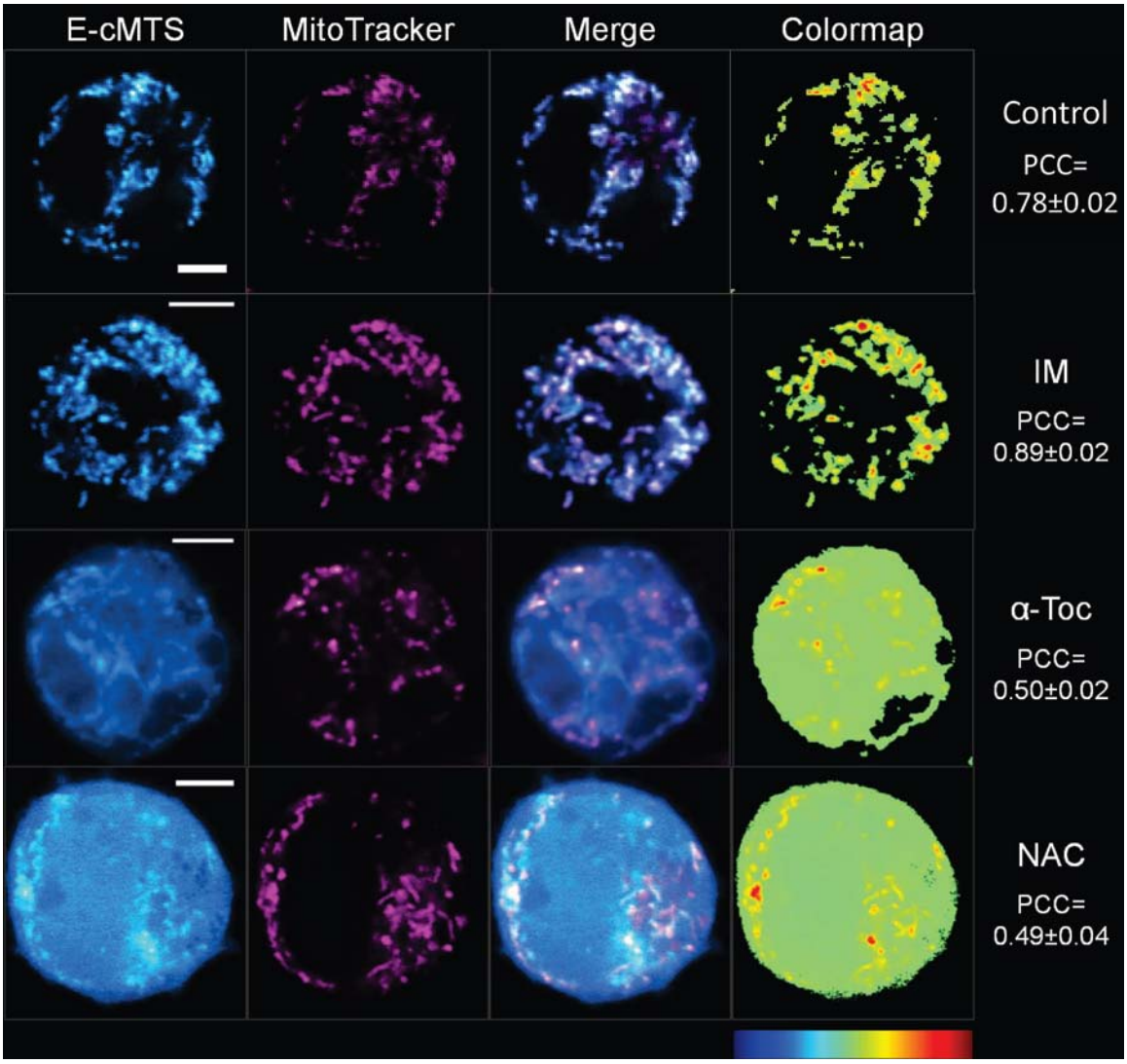
E-cMTS
MitoTracker
Merge
Colormap
Control
PCC=
0.78±0.02
IM
PCC=
0.89±0.02
α-Toc
PCC=
0.50±0.02
NAC
PCC=
0.49±0.04

C.

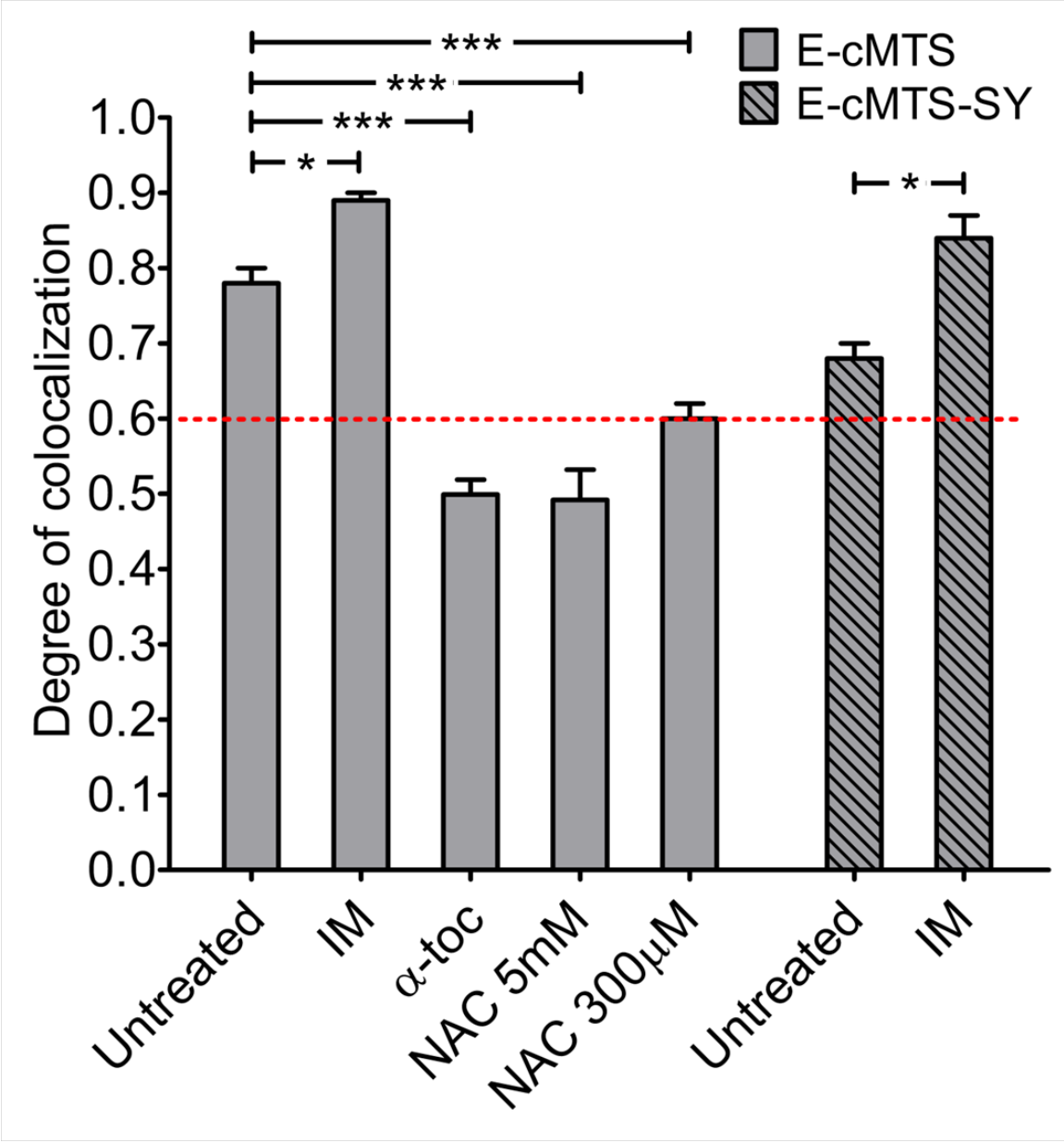
E-cMTS
E-cMTS-SY
***
***
***
*
*
Degree of colocalization
1.0
0.9
0.8
0.7
0.6
0.5
0.4
0.3
0.2
0.1
0.0
Untreated
IM
α-toc
NAC 5mM
NAC 300μM
Untreated
IM

could modulate the mitochondrial localization of a mutant cMTS via tyrosine phosphorylation. However, Bcr-Abl does not activate the mutant cMTSs (*Fig. 3.5B, 5th column to the right* (E-cMTS-TY does not accumulate in the mitochondria of Bcr-Abl positive K562 cells) and *Fig. 3.6C, 7th column* (the kinase inhibitor imatinib does not prevent the mitochondrial accumulation of E-cMTS-SY)). Mutating the PKA phosphorylation site, S189 to tyrosine and further altering the three residues proceeding the serine at position at 189 (E-cMTS-SY, see *Table 3.1, underlined*) did not have an effect on mitochondrial localization in either 1471.1 or K562 cells as compared to E-cMTS (*Fig. 3.5B, compare 1st and 2nd set of columns*). However, the T193Y mutation (E-cMTS-TY), interrupting the PKC phosphorylation site, ablated mitochondrial localization in both K562 and 1471.1 cell lines (*Fig. 3.5B, compare 1st and 3rd set of columns*). The cMTS mutant data implicate PKC, and not PKA, as a critical activator of the cMTS in K562 leukemia and 1471.1 breast cancer cell lines. Qualitatively, the differences in mitochondrial localization between the E-cMTS-SY (*Fig. 3.5A, top two rows*) and E-cMTS-TY (*Fig. 3.5A, bottom two rows*) mutants in K562 and 1471.1 cells can be seen. Instead of tyrosine mutations we also tested alanine mutations (as done previously (15)) at positions 189 and 193 and obtained similar results (data not shown).

ROS and mitochondrial localization of the E-cMTS in K562 cells

It is well established that imatinib (IM) treatment induces ROS production (37). Imatinib treatment (10 μM) produced a 160% rise in ROS after 24 hours in K562 cells (versus untreated K562 cells, *Fig. 3.6A, compare 2nd to 1st column*). The converse was

seen with antioxidant treatment, using either 50 μM α-tocopherol (α-Toc) or 5 mM N-acetylcysteine (NAC) for 24 hours, which brought about a decline (~30%) in measured ROS relative to control K562 (*Fig. 3.6A, compare 3rd and 4th columns to 1st*). A concentration of 300 μM NAC was also used in K562 cells but it did not result in a significant decrease in ROS (*Fig. 3.6A, 5th column*). In addition to its antioxidant effects, α-tocopherol also has an independent inhibitory effect on PKC family members (38). Previously, a physiological concentration of α-tocopherol (50 μM) reduced phorbol ester-stimulated cell adhesion in K562 cells to the same degree as a specific PKC inhibitor, Calphostin C (39). Hydrogen peroxide (500 μM, 24 hours), as a positive control, generated a 3-fold induction of ROS (data not shown) above that of untreated K562 cells.

Imatinib and antioxidant treatment altered E-cMTS mitochondrial localization corresponding to the assessed ROS levels (*compare Fig. 3.6A, for the ROS level difference between imatinib- and antioxidant-treated K562 and corresponding degree of mitochondrial localization in Fig. 3.6C*). Correlation analysis between E-cMTS mitochondrial localization and ROS level (*Fig. 3.7*) generated an $R^2 = 0.62$ ($P<0.05$) across each cell type and K562 cells treated with imatinib and antioxidants. The correlation between E-cMTS mitochondrial localization and basal ROS level for the 1471.1 breast cancer cell line falls outside of the 95% confidence band (dotted lines). This is not unexpected as high PKC activity or expression is associated with rapidly proliferating breast cancer cell lines (40). Higher mitochondrial localization of E-cMTS (PCC: 0.89 ± 0.01) was seen with imatinib while α-tocopherol (PCC: 0.50 ± 0.02) lowered E-cMTS mitochondrial localization as compared to untreated (PCC: 0.78 ± 0.02) in K562 cells (*Fig. 3.6C*). Similar to α-tocopherol treatment of K562 cells, the E-cMTS

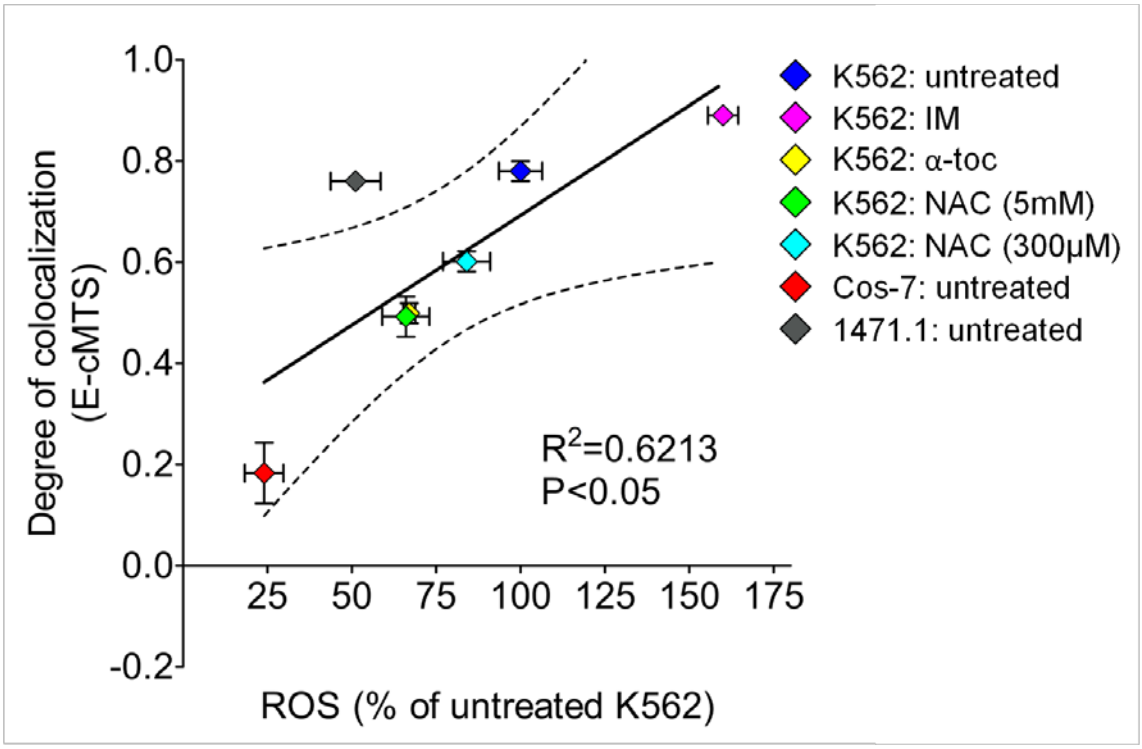

Figure 3.7. Correlation analysis between ROS level and the 'degree of colocalization'. Correlation analysis demonstrated a positive correlation between ROS level and mitochondrial localization of the E-cMTS. Since PKC mediates the ROS activation of the E-cMTS an altered ROS-to-mitochondrial localization relationship for E-cMTS, is to be expected to be contingent upon the varying level of PKC expression and activity of PKC within a given cell type. The R^2 shown in the graph represents all points with the dotted lines indicating the 95% confidence interval. The R^2 value for K562 data points only was 0.877 ($P<0.05$).

decreased mitochondrial association when treated with either 5 mM NAC (*Fig 3.6C, 4th column* (PCC: 0.49±0.04)) or 300 μM NAC (*Fig. 3.6C, 5th column* (PCC: 0.60 ± 0.02)). The imatinib-related increase in mitochondrial association was also seen with the E-cMTS-SY mutant (*Fig 3.6C, compare 6th and 7th columns*) but not with the E-cMTS-TY mutant which remained cytoplasmic (PCC: 0.35 ± 0.2 and 0.23 ± 0.2, with and without imatinib, respectively) in K562 cells. There was no difference in the mitochondrial distribution of E-cMTS-TY in imatinib-treated and untreated K562 cells. The E-cMTS-SY mutant is exclusively phosphorylated by PKC at the T193 position (15). The contrast in mitochondrial localization between the E-cMTS-SY and E-cMTS-TY mutants, in the presence of imatinib, further clarifies the relative importance of PKC- over PKA-mediated activation of the cMTS by antineoplastic-induced ROS.

As noted above, the mutants incorporating the minimal c-Abl tyrosine kinase consensus sequence (either at or around residue position 189 (E-cMTS-SY) or 193 (E-cMTS-TY); *Table 3.1*) are not targeted to the mitochondria by the activity of Bcr-Abl (c-Abl). This is confirmed by the increased mitochondrial colocalization of the E-cMTS-SY in the presence of the tyrosine kinase inhibitor, imatinib at a saturating concentration of 10 μM. Representative images of E-cMTS mitochondrial localization in K562 cells upon imatinib (*Fig. 3.6B, top row*), α-tocopherol (*Fig. 3.6B, middle row*), or N-acetylcysteine (NAC 5 mM: *Fig. 3.6B, bottom row*) treatment show the different intracellular distribution profiles.

Abl-E-cMTS selectively targets the mitochondria of cells with higher oxidative backgrounds

The c-Abl protein was fused to the N-terminus of the cMTS (Abl-E-cMTS) (see *Fig. 3.4*) and transiently transfected into K562, Cos-7, and 1471.1 cells. The Abl-E construct (no MTS) was used as a negative control in K562 (*Fig. 3.8A, top row and 3.8B, first column*) and Cos-7 cells (PCC: -0.26±0.06). The c-Abl fusion to the cMTS colocalized with the mitochondria in K562 and 1471.1 cells similar to cMTS alone (*compare Fig. 3.2C, 1st and 3rd columns with Fig. 3.8B, 2nd and 4th columns*). This was not expected for the c-Abl-E-cMTS because c-Abl has many cytosolic and nuclear binding partners (41). Also, as with the cMTS alone the Abl-E-cMTS remained cytosolic in Cos-7 cells (*Fig. 3.2C, 2nd row (PCC = 0.18±0.06) and Fig. 3.8B, 3rd row (PCC = 0.13±0.08), respectively*).

The same C-terminal canonical MTS derived from Bcl-X_L as used above, was also fused to c-Abl-E (*Fig. 3.3*) as a control for mitochondrial translocation efficiency of c-Abl across cell types and to assess of functional consequences accompanying ROS selective mitochondrial targeting via the cMTS. Although there was a significant difference in mitochondrial colocalization coefficients between K562 and Cos-7 (*Fig. 3.8D, compare 1st and 2nd columns*; $P<0.05$), the PCC values for all three cell lines exceeded the 0.6 colocalization threshold for Abl-E-MOM. Importantly, there was no difference between E-MOM and Abl-E-MOM colocalization for any of the cell lines as expected. Representative images of K562, Cos-7, and 1471.1 cells transfected with Abl-

Figure 3.8. The cMTS selectively targets c-Abl to the mitochondria of cells that have elevated oxidative backgrounds.

A) Abl-E-cMTS and Abl-E were compared to MitoTracker Red CM-H_2XRos staining in live cells. EGFP and MitoTracker channels were false-colored cyan and magenta, respectively, for increased visual clarity. Scale bar is 5 μm. (mean thresholded PCC values are ±S.E.M, N=3)

B) Abl-E-cMTS localized to the mitochondria of 1471.1 and K562 but not Cos-7 cells. Without the cMTS, Abl-E does not localize to the mitochondria of K562 cells.

C & D) In contrast to the cMTS, the MOM robustly directs c-Abl to the mitochondria of each cell type. *C*) Representative images of K562, Cos-7, and 1471.1 cells transfected with Abl-E-MOM construct at 24 hours. One-way ANOVA with Tukey's post-test (error bars are ±S.E.M, N=3, $P<0.05$*, $P<0.001$***).

A.

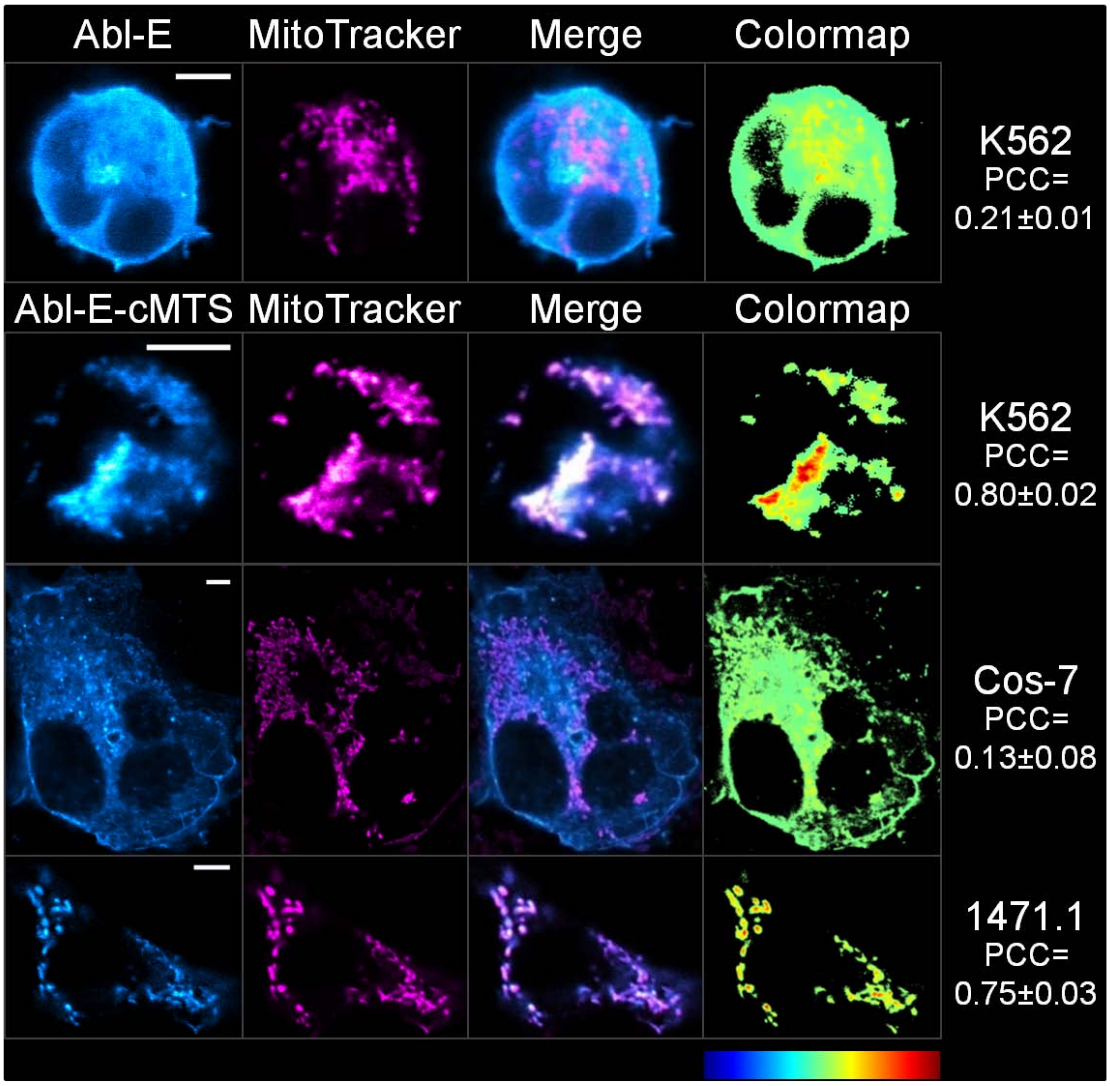
Abl-E
MitoTracker
Merge
Colormap
K562
PCC=
0.21±0.01
Abl-E-cMTS
MitoTracker
Merge
Colormap
K562
PCC=
0.80±0.02
Cos-7
PCC=
0.13±0.08
1471.1
PCC=
0.75±0.03

B.

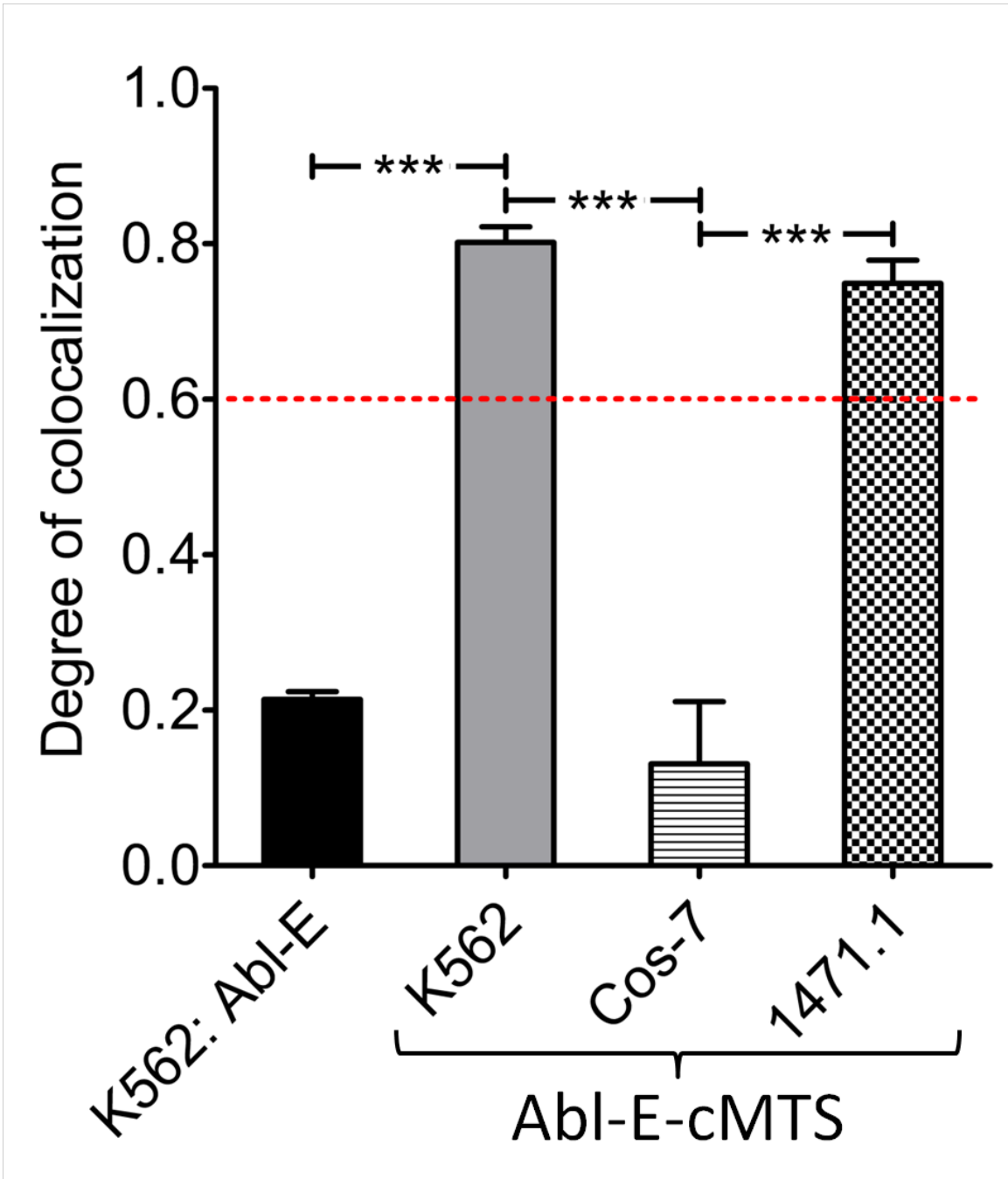
1.0
0.8
0.6
0.4
0.2
0.0
Degree of colocalization
***
***
***
K562: Abl-E
K562
Cos-7
1471.1
Abl-E-cMTS

C.

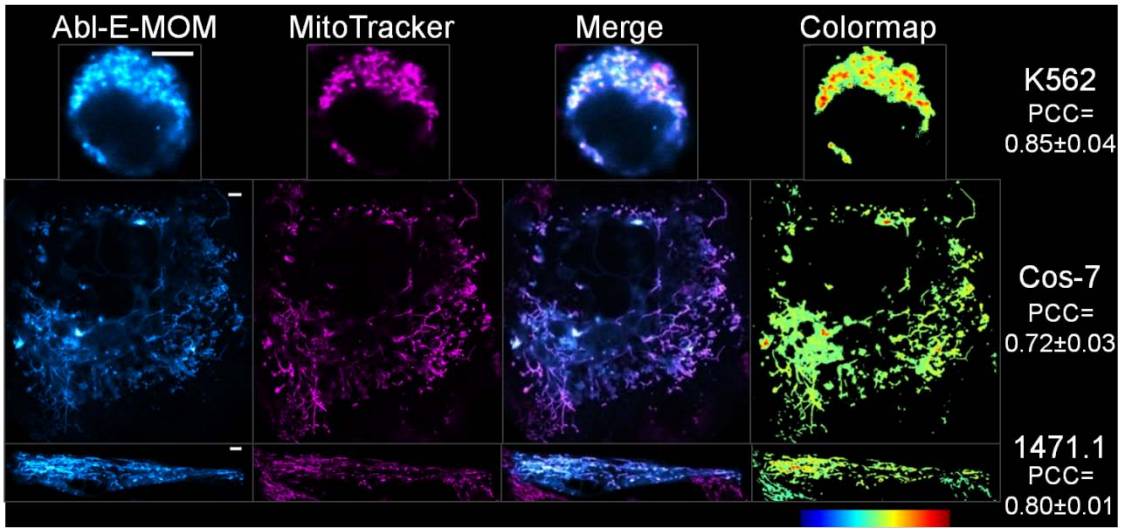
Abl-E-MOM
MitoTracker
Merge
Colormap
K562
PCC=
0.85±0.04
Cos-7
PCC=
0.72±0.03
1471.1
PCC=
0.80±0.01

D.

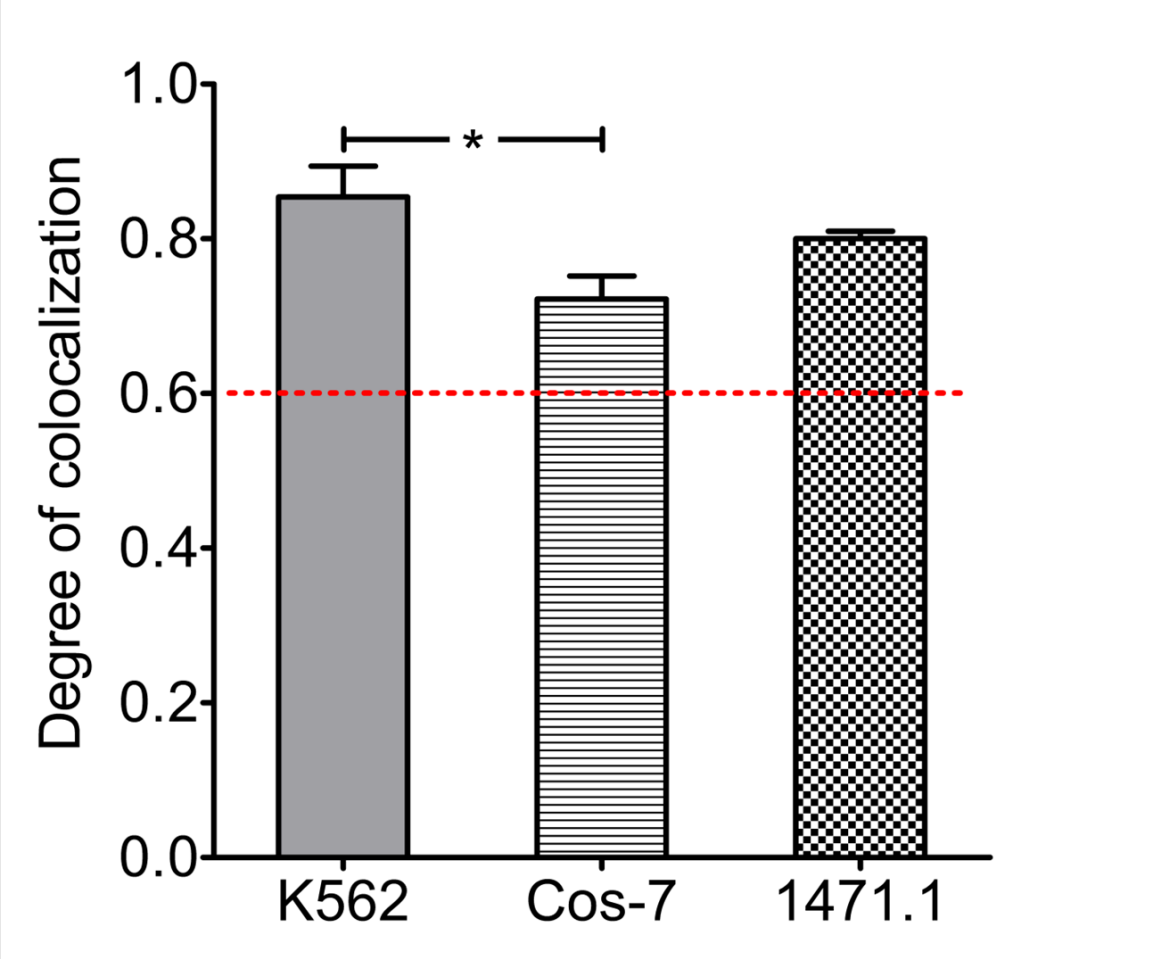

E-MOM and stained with MitoTracker CMXros showing mitochondrial localization can be seen in *Figure 3.8C*.

Targeting c-Abl to the mitochondrial matrix is toxic to K562 leukemia but not 1471.1 breast cancer cell lines

To assess the functional significance at the level of cell death induction from mitochondrial c-Abl, cell lines were transiently transfected with the c-Abl-containing constructs or controls (*Fig. 3.3*), stained with 7-AAD, and fluorescence measured via flow cytometry at 48 hours after transfection. The effects of the constructs were analyzed for each cell type (*Fig. 3.9, A-C*). First, there was no difference between any of the constructs and measured cell death in Cos-7 cells (*Fig. 3.9B*). Secondly, 1471.1 cells (*Fig. 3.9C*) did not exhibit any significant difference in cell death between cytoplasmic c-Abl (i.e., Abl-E) and mitochondrially localized c-Abl (i.e., Abl-E-MOM and Abl-E-cMTS). Finally, K562 cells (*Fig. 3.9A*) are killed by mitochondrial c-Abl but only if targeted to the matrix (Abl-E-cMTS). Targeting c-Abl to the outer membrane induces death to the same level as either cytoplasmic c-Abl (Abl-E) or the cMTS alone (E-cMTS). A kinase dead mutant (25) of c-Abl (Abl-E-cMTS KD) trended lower but did not reach significance from Abl-E-cMTS nor was it different from cytoplasmic Abl-E. Taken together the data suggest a cell type dependent susceptibility to the cell death effects of c-Abl targeted to the mitochondrial matrix. Although there is no statistical difference between the EGFP control and the E-cMTS (*Fig. 3.9A, compare 1st and 2nd columns*) in K562 cells, this "trend" in mild toxicity associated with the mitochondrial targeting of

Figure 3.9. c-Abl selectively induces cell death in K562 leukemia cells when targeted to the mitochondrial matrix.

A) *K562 leukemia cells*: K562 leukemia cells were highly susceptible to cell death caused by c-Abl in the mitochondrial matrix (Abl-E-cMTS) but not at the mitochondrial outer membrane (Abl-E-MOM).

B) *Cos-7 fibroblast cells*: In Cos-7 cells, neither cytoplasmic nor mitochondrially targeted c-Abl induced cell death.

C) *1471.1 breast cancer cells*: There was an increase ($P<0.01$) in cell death for Abl-E-cMTS over the 'non-toxic' EGFP and E-MOM controls in 1471.1 cells. However, there was no difference between the mitochondrially localized c-Abl and cMTS. (B-D: One-way ANOVA with Tukey's post-test; A-D: error bars are ±S.E.M., $N\geq3$, $P<0.05$*, $P<0.01$**, $P<0.001$***).

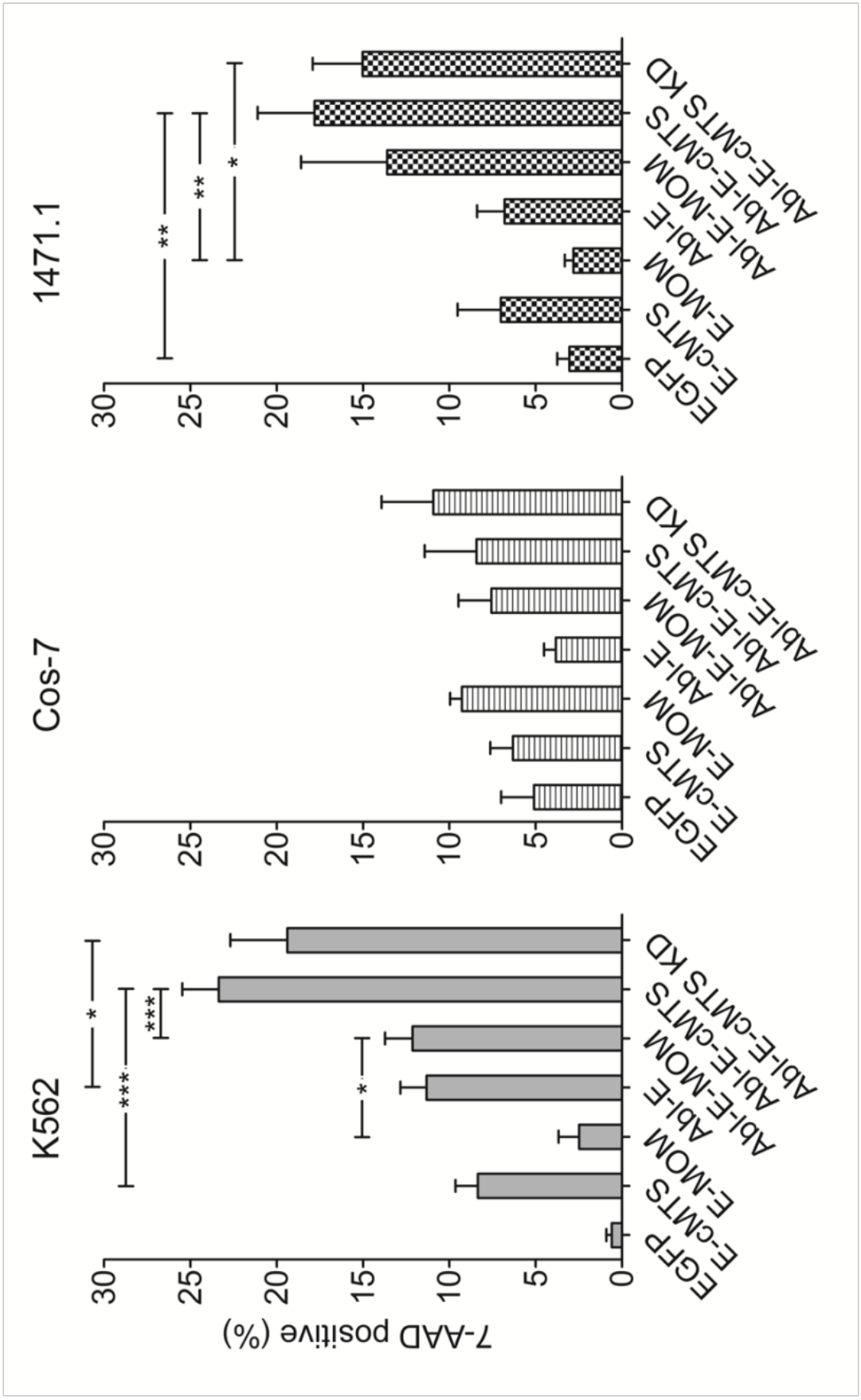
K562
Cos-7
1471.1
7-AAD positive (%)
0
5
10
15
20
25
30
EGFP
E-cMTS
E-MOM
Abl-E
Abl-E-MOM
Abl-E-cMTS
Abl-E-cMTS KD
*
***
***
*
**
**
*

EGFP regardless of MTS is a common occurrence that we have noticed in several of our studies across multiple cell types (42). This trend, when viewed between K562 and 1471.1 cells (*Fig. 3.9, A and C*) may be indicative of a phenomenon termed 'mitochondrial priming' whereby the mitochondria set the cell death threshold via a balance between pro-survival and pro-apoptotic Bcl-2 family members, in a rheostat like manner (43). Cell death exhibited across constructs in 1471.1 cells was lower than expected (as compared to K562). However, overall profiles for cell death between K562 and 1471.1 look very similar but the scale of cell death is reduced in 1471.1 cells. It is possible that the mitochondria of K562 cells are more susceptible to a mitochondrial insult such as c-Abl. Future studies investigating the level of 'primed' mitochondrial status between K562 and 1471.1 would be very useful for optimizing therapeutic agents targeted to the mitochondria.

This study represents (to our knowledge) the first time c-Abl has been directly targeted to the mitochondria (instead of indirectly by a pharmacological or UV/IR insult). Furthermore, we show that c-Abl may exert its pro-apoptotic effect at the mitochondrial matrix. Our laboratory has developed an intracellular chaperone designed to bind and target the oncoprotein Bcr-Abl to the mitochondria. This study served as a proof of concept for using the central etiologic agent of chronic myelogenous leukemia (Bcr-Abl) to, in essence, self-destruct the diseased cells via the mitochondrial apoptotic pathway.

Discussion

Our laboratory has previously developed a protein switch capable of translocating a protein from the cytoplasm to the nucleus upon ligand induction (44). Here we show

that, the cMTS acts as a mitochondrial protein switch, translocating from the cytoplasm to the mitochondria as a condition of elevated ROS inherent in K562 leukemic and 1471.1 breast cancer line phenotypes. The C-terminal cMTS is particularly useful for targeting the sensitive proto-oncoprotein c-Abl to the mitochondria of K562 cells because any fusion to the N-terminus will disrupt the ability of c-Abl to adopt its native conformation (45). The fusion of the BCR gene to the ABL gene creates Bcr-Abl, etiological cause of chronic myelogenous leukemia, disrupting c-Abl's autoinhibitory conformation and generating a constitutively active Abl tyrosine kinase (45). The kinase activity of c-Abl is necessary and sufficient for the induction of apoptosis and c-Abl has a critical role at the mitochondria in apoptotic induction (46, 47). Previous studies of c-Abl translocating to the mitochondria have been indirect, through the induction of apoptosis/cell stress (e.g., hydrogen peroxide, etoposide, tunicamycin (46)). This study investigated the *in vitro* cell death consequences of direct mitochondrial targeting of c-Abl using MTSs in the context of varying levels of basal oxidative stress.

Likewise, protein kinase stimulators (e.g., cAMP and phorbol ester) were used previously for activating the mitochondrial targeting of the cMTS fused to a heteroprotein (dihydrofolate reductase) in Cos cells (15). However, we demonstrate that the cMTS can robustly target the mitochondria of K562 and 1471.1 cancer cell lines without pharmacological induction. Therefore, the cMTS may confer specific targeting of heteroproteins (c-Abl) to the mitochondria in cells exhibiting elevated ROS/PKC activity. Further work will need to be done to identify which PKC isoforms are contributing the phosphorylation of the cMTS and if these are the same isoforms that are often overexpressed in cancer (e.g., breast). Yet, the mitochondrial targeting of the cMTS can

be attenuated or enhanced by antioxidant or antineoplastic treatment, respectively. We are interested in elucidating the functional consequences of targeting c-Abl to the mitochondria in a leukemia-specific context, and the cMTS provides an effective way to accomplish this in a selective manner. To this end, we were intrigued to find the difference in cell death induction efficacy between c-Abl targeted to the mitochondrial matrix versus the outer membrane of the leukemia cell line. A similar cell death phenomenon occurred when p53 was directly targeted to the mitochondrial matrix and outer membrane using MTSs (48). There may be a correspondence between susceptibility to cell death when c-Abl is localized to the mitochondrial matrix and ROS level (1). However, this will require further investigation.

We used the cMTS as a vehicle to selectively deliver c-Abl under conditions of oxidative stress in a cancer context but the implications of the cMTS utility could be expanded upon. For instance, c-Abl's role at the mitochondria is currently being investigated in other conditions with pathological ROS such as neurodegenerative disease (49) and diabetes (50). Additionally, the cMTS may be of benefit to selectively target either pro-apoptotic or pro-survival factors (e.g., BH3 mimetics or antioxidant enzymes) to the mitochondria to elicit or prevent cell death, respectively.

Considering future directions, if the Abl-cMTS were delivered *in vivo,* perhaps via adenoviral vector delivery, it would confer a level of selectivity for mitochondrial accumulation in cells with elevated oxidative stress. Additionally, our results indicate that the Abl-cMTS is toxic to leukemic cells and much less so in nonleukemic cell lines.

Acknowledgements

We acknowledge the use of the University of Utah, School of Medicine, Cell Imaging Facility and would like to thank the Director, Chris Rodesch, PhD, for scientific discussions. We would also like to thank Karina Matissek, Geoffrey Miller, and Dr. Andy Dixon for scientific discussions. The Core Facilities described in this project were supported by Award Number P30CA042014 from the National Cancer Institute. The content is solely the responsibility of the authors and does not necessarily represent the official views of the National Cancer Institute or the National Institutes of Health. The authors declare that they have no competing interests. This work was funded by NIH R01-CA129528 and by an AFPE Pre-Doctoral Fellowship (JEC).

References

1. S.J. Ralph, S. Rodriguez-Enriquez, J. Neuzil, E. Saavedra, and R. Moreno-Sanchez. The causes of cancer revisited: "mitochondrial malignancy" and ROS-induced oncogenic transformation - why mitochondria are targets for cancer therapy. Mol Aspects Med. 31:145-170 (2010).

2. G. Szabadkai and R. Rizzuto. Chaperones as parts of organelle networks. Adv Exp Med Biol. 594:64-77 (2007).

3. M. Certo, V. Del Gaizo Moore, M. Nishino, G. Wei, S. Korsmeyer, S.A. Armstrong, and A. Letai. Mitochondria primed by death signals determine cellular addiction to antiapoptotic BCL-2 family members. Cancer Cell. 9:351-365 (2006).

4. J.Y. Wang. Nucleo-cytoplasmic communication in apoptotic response to genotoxic and inflammatory stress. Cell Res. 15:43-48 (2005).

5. Y. Ito, P. Pandey, N. Mishra, S. Kumar, N. Narula, S. Kharbanda, S. Saxena, and D. Kufe. Targeting of the c-Abl tyrosine kinase to mitochondria in endoplasmic reticulum stress-induced apoptosis. Mol Cell Biol. 21:6233-6242 (2001).

6. M. Gupta, L. Milani, M. Hermansson, B. Simonsson, B. Markevarn, A.C. Syvanen, and G. Barbany. Expression of BCR-ABL1 oncogene relative to ABL1 gene changes overtime in chronic myeloid leukemia. Biochem Biophys Res Commun. 366:848-851 (2008).

7. A. Sirvent, C. Benistant, and S. Roche. Cytoplasmic signalling by the c-Abl tyrosine kinase in normal and cancer cells. Biol Cell. 100:617-631 (2008).

8. S. Kumar, A. Bharti, N.C. Mishra, D. Raina, S. Kharbanda, S. Saxena, and D. Kufe. Targeting of the c-Abl tyrosine kinase to mitochondria in the necrotic cell death response to oxidative stress. J Biol Chem. 276:17281-17285 (2001).

9. X. Qi and D. Mochly-Rosen. The PKCdelta -Abl complex communicates ER stress to the mitochondria - an essential step in subsequent apoptosis. J Cell Sci. 121:804-813 (2008).

10. M. Salvi, A.M. Brunati, and A. Toninello. Tyrosine phosphorylation in mitochondria: a new frontier in mitochondrial signaling. Free Radical Biology & Medicine. 38:1267-1277 (2005).

11. S. Kumar, N. Mishra, D. Raina, S. Saxena, and D. Kufe. Abrogation of the cell death response to oxidative stress by the c-Abl tyrosine kinase inhibitor STI571. Molecular Pharmacology. 63:276-282 (2003).

12. C. Horbinski and C.T. Chu. Kinase signaling cascades in the mitochondrion: a matter of life or death. Free Radical Biology & Medicine. 38:2-11 (2005).

13. M.C. Sangar, S. Bansal, and N.G. Avadhani. Bimodal targeting of microsomal cytochrome P450s to mitochondria: implications in drug metabolism and toxicity. Expert Opin Drug Metab Toxicol. 6:1231-1251 (2010).

14. A. Quintas-Cardama and J. Cortes. Molecular biology of bcr-abl1-positive chronic myeloid leukemia. Blood. 113:1619-1630 (2009).

15. M.A. Robin, S.K. Prabu, H. Raza, H.K. Anandatheerthavarada, and N.G. Avadhani. Phosphorylation enhances mitochondrial targeting of GSTA4-4 through increased affinity for binding to cytoplasmic Hsp70. J Biol Chem. 278:18960-18970 (2003).

16. H. Raza, M.A. Robin, J.K. Fang, and N.G. Avadhani. Multiple isoforms of mitochondrial glutathione S-transferases and their differential induction under oxidative stress. Biochemical J. 366:45-55 (2002).

17. S.C. Gupta, D. Hevia, S. Patchva, B. Park, W. Koh, and B.B. Aggarwal. Upsides and downsides of reactive oxygen species for cancer: the roles of reactive oxygen species in tumorigenesis, prevention, and therapy. Antioxid Redox Signal. 16:1295-322 (2012).

18. J.S. Bair, R. Palchaudhuri, and P.J. Hergenrother. Chemistry and biology of deoxynyboquinone, a potent inducer of cancer cell death. J Am Chem Soc. 132:5469-5478 (2010).

19. J.H. Kim, S.C. Chu, J.L. Gramlich, Y.B. Pride, E. Babendreier, D. Chauhan, R. Salgia, K. Podar, J.D. Griffin, and M. Sattler. Activation of the PI3K/mTOR pathway by BCR-ABL contributes to increased production of reactive oxygen species. Blood. 105:1717-1723 (2005).

20. M. Sattler, S. Verma, G. Shrikhande, C.H. Byrne, Y.B. Pride, T. Winkler, E.A. Greenfield, R. Salgia, and J.D. Griffin. The BCR/ABL tyrosine kinase induces production of reactive oxygen species in hematopoietic cells. J Biol Chem. 275:24273-24278 (2000).

21. S.P. Chang, S.C. Shen, W.R. Lee, L.L. Yang, and Y.C. Chen. Imatinib mesylate induction of ROS-dependent apoptosis in melanoma B16F0 cells. J Dermatol Sci. 62:183-191 (2011).

22. N.S. Brown and R. Bicknell. Hypoxia and oxidative stress in breast cancer. Oxidative stress: its effects on the growth, metastatic potential and response to therapy of breast cancer. Breast Cancer Res. 3:323-327 (2001).

23. M. Morse-Gaudio, J.M. Connolly, and D.P. Rose. Protein kinase C and its isoforms in human breast cancer cells: relationship to the invasive phenotype. Int J Oncol. 12:1349-1354 (1998).

24. A.S. Dixon, M. Kakar, K.M. Schneider, J.E. Constance, B.C. Paullin, and C.S. Lim. Controlling subcellular localization to alter function: Sending oncogenic Bcr-Abl to the nucleus causes apoptosis. J Control Release. 140:245-249 (2009).

25. H.S. Ko, Y. Lee, J.H. Shin, S.S. Karuppagounder, B.S. Gadad, A.J. Koleske, O. Pletnikova, J.C. Troncoso, V.L. Dawson, and T.M. Dawson. Phosphorylation by the c-Abl protein tyrosine kinase inhibits parkin's ubiquitination and protective function. Proc Natl Acad Sci U S A. 107:16691-16696 (2010).

26. A.S. Dixon, J.E. Constance, T. Tanaka, T.H. Rabbitts, and C.S. Lim. Changing the subcellular location of the oncoprotein Bcr-Abl using rationally designed capture motifs. Pharm Res. 29(4):1098-109 (2012).

27. W.S. Rasband. BG subtraction from ROI plugin. Available from: www.uhnres.utoronto.ca/facilities/wcif/imagej/image_intensity_proce.htm#intensity_BG. (2004).

28. S. Bolte and F.P. Cordelieres. A guided tour into subcellular colocalization analysis in light microscopy. J Microsc. 224:213-232 (2006).

29. S.V. Costes, D. Daelemans, E.H. Cho, Z. Dobbin, G. Pavlakis, and S. Lockett. Automatic and quantitative measurement of protein-protein colocalization in live cells. Biophys J. 86:3993-4003 (2004).

30. A.L. Barlow, A. Macleod, S. Noppen, J. Sanderson, and C.J. Guerin. Colocalization analysis in fluorescence micrographs: verification of a more accurate calculation of pearson's correlation coefficient. Microsc Microanal. 16:710-724 (2010).

31. F. Jaskolski, C. Mulle, and O.J. Manzoni. An automated method to quantify and visualize colocalized fluorescent signals. J Neurosci Methods. 146:42-49 (2005).

32. A.S. Dixon, G.D. Miller, B.J. Bruno, J.E. Constance, D.W. Woessner, T.P. Fidler, J.C. Robertson, T.E. Cheatham, and C.S. Lim. Improved coiled-coil design enhances interaction with bcr-abl and induces apoptosis. Mol Pharm. 9:187-195 (2012).

33. M.G. Mediavilla, G.A. Di Venanzio, E.E. Guibert, and C. Tiribelli. Heterologous ferredoxin reductase and flavodoxin protect Cos-7 cells from oxidative stress. PLoS One. 5:e13501 (2010).

34. T.W. Owens, A.J. Valentijn, J.P. Upton, J. Keeble, L. Zhang, J. Lindsay, N.K. Zouq, and A.P. Gilmore. Apoptosis commitment and activation of mitochondrial Bax during anoikis is regulated by p38MAPK. Cell Death Differ. 16:1551-1562 (2009).

35. T. Kaufmann, S. Schlipf, J. Sanz, K. Neubert, R. Stein, and C. Borner. Characterization of the signal that directs Bcl-x(L), but not Bcl-2, to the mitochondrial outer membrane. J Cell Biol. 160:53-64 (2003).

36. A. Biegert, C. Mayer, M. Remmert, J. Soding, and A.N. Lupas. The MPI Bioinformatics Toolkit for protein sequence analysis. Nucleic Acids Res. 34:W335-339 (2006).

37. S.P. Chang, S.C. Shen, W.R. Lee, L.L. Yang, and Y.C. Chen. Imatinib mesylate induction of ROS-dependent apoptosis in melanoma B16F0 cells. J Dermatol Sci. 62:183-191 (2011).

38. R. Ricciarelli, A. Tasinato, S. Clement, N.K. Ozer, D. Boscoboinik, and A. Azzi. alpha-Tocopherol specifically inactivates cellular protein kinase C alpha by changing its phosphorylation state. Biochem J. 334 (Pt 1):243-249 (1998).

39. I. Breyer and A. Azzi. Differential inhibition by alpha- and beta-tocopherol of human erythroleukemia cell adhesion: role of integrins. Free Radical Biology & Medicine. 30:1381-1389 (2001).

40. G.K. Lonne, L. Cornmark, I.O. Zahirovic, G. Landberg, K. Jirstrom, and C. Larsson. PKCalpha expression is a marker for breast cancer aggressiveness. Mol Cancer. 9:76 (2010).

41. A. Mitra and V. Radha. F-actin-binding domain of c-Abl regulates localized phosphorylation of C3G: role of C3G in c-Abl-mediated cell death. Oncogene. 29:4528-4542 (2010).

42. M. Mossalam, K.J. Matissek, A. Okal, J.E. Constance, and C.S. Lim. Direct induction of apoptosis using an optimal mitochondrially targeted P53. Mol Pharm. 9:1449-58 (2012).

43. J.C. Reed. Cancer. Priming cancer cells for death. Science. 334:1075-1076 (2011).

44. M. Kakar, J.R. Davis, S.E. Kern, and C.S. Lim. Optimizing the protein switch: altering nuclear import and export signals, and ligand binding domain. J Control Release. 120:220-232 (2007).

45. O. Hantschel and G. Superti-Furga. Regulation of the c-Abl and Bcr-Abl tyrosine kinases. Nat Rev Mol Cell Biol. 5:33-44 (2004).

46. X. Qi and D. Mochly-Rosen. The PKCdelta -Abl complex communicates ER stress to the mitochondria - an essential step in subsequent apoptosis. J Cell Sci. 121:804-813 (2008).

47. Y. Ito, P. Pandey, N. Mishra, S. Kumar, N. Narula, S. Kharbanda, S. Saxena, and D. Kufe. Targeting of the c-Abl tyrosine kinase to mitochondria in endoplasmic reticulum stress-induced apoptosis. Mol Cell Biol. 21:6233-6242 (2001).

48. G. Palacios, H.C. Crawford, A. Vaseva, and U.M. Moll. Mitochondrially targeted wild-type p53 induces apoptosis in a solid human tumor xenograft model. Cell Cycle. 7:2584-2590 (2008).

49. S.D. Schlatterer, C.M. Acker, and P. Davies. c-Abl in neurodegenerative disease. J Mol Neurosci. 45:445-52 (2011).

50. R. Hagerkvist, S. Sandler, D. Mokhtari, and N. Welsh. Amelioration of diabetes by imatinib mesylate (Gleevec): role of beta-cell NF-kappaB activation and anti-apoptotic preconditioning. Faseb J. 21:618-628 (2007).

CHAPTER 4

ENHANCED AND SELECTIVE KILLING OF CHRONIC MYELOGENOUS LEUKEMIA CELLS WITH AN ENGINEERED BCR-ABL BINDING PROTEIN AND IMATINIB

Abstract

The oncoprotein Bcr-Abl stimulates pro-survival pathways and suppresses apoptosis from its exclusively cytoplasmic locale (1), but when forced to the mitochondrial compartment of leukemia cells, Bcr-Abl was potently cytotoxic. Therefore, we designed a protein construct to act as a mitochondrial chaperone to move Bcr-Abl to the mitochondria. The chaperone (i.e., intracellular cryptic escort (iCE)) consists of two previously characterized motifs: 1) An optimized Bcr-Abl binding motif that interacts with the coiled-coil domain of Bcr (2), and 2) A cryptic mitochondrial targeting signal that selectively targets the mitochondria in oxidatively stressed cells (i.e., Bcr-Abl positive leukemic cells) via phosphorylation at a key residue (T193) by protein kinase C (3). While the iCE colocalized with Bcr-Abl it did not significantly re-localize to the mitochondria. However, the iCE was selectively toxic to Bcr-Abl positive K562 cells as compared to Bcr-Abl negative Cos-7

Reprinted with permission from J.E. Constance, D.W. Woessner, K.J. Matissek, M. Mossalam, and C.S. Lim. Enhanced and Selective Killing of Chronic Myelogenous Leukemia Cells with an Engineered Bcr-Abl Binding Protein and Imatinib. Molecular pharmaceutics (2012).

fibroblasts and 1471.1 murine breast cancer cells. The toxicity of the iCE to leukemic cells was equivalent to 10 μM imatinib at 48 hours and the iCE combined with imatinib potentiated cell death beyond imatinib or the iCE alone. Substitution of either the ccmut3 or the cMTS with another Bcr-Abl binding domain (derived from the tight binding Ras/Rab interaction protein 1 (RIN1)) or MTS (i.e., the canonical IMS derived from Smac/Diablo) could not recapitulate the cytotoxicity of the iCE. Additionally, a phosphorylation null mutant of the iCE also abolished the cytotoxic effect. The mitochondrial toxicity of Bcr-Abl and the iCE in Bcr-Abl positive K562 leukemia cells was confirmed by flow cytometric analysis of 7-AAD, TUNEL, and annexin-V staining. DNA segmentation and cell viability were assessed by microscopy. Subcellular localization of constructs was determined using confocal microscopy (including statistical colocalization analysis) (3). *Figure 4.1* is the graphical abstract.

Introduction

The fusion oncoprotein, and constitutively active tyrosine kinase, Bcr-Abl (autoinhibition of c-Abl kinase activity is lost in Bcr-Abl fusion) is the central etiologic agent of chronic myelogenous leukemia (CML) and is exclusively localized in the cytoplasmic space at the plasma membrane through interactions with cytoskeletal actin (1). Forcing a change in Bcr-Abl's subcellular location can change Bcr-Abl from an oncogenic agent into a pro-apoptotic factor (4, 5).

Normal c-Abl fulfills a terminal role as a pro-apoptotic factor when targeted to the mitochondria under a variety of cellular insults (6, 7). We previously demonstrated that direct targeting of c-Abl to the mitochondria is toxic to leukemia cells (3). Therefore, forcing Bcr-

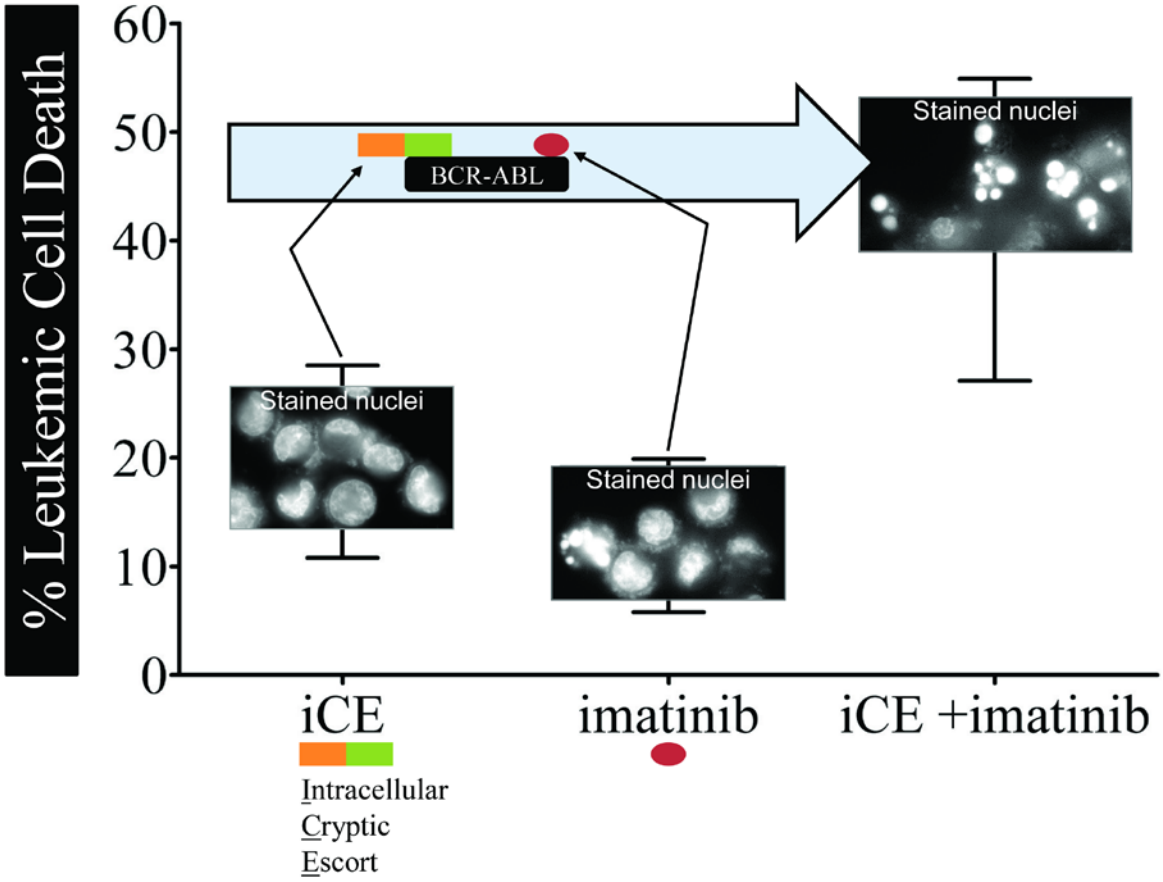

Figure 4.1. Graphical abstract

Abl to the mitochondria would reinstate a version of death-directed mitochondrial c-Abl that is largely defunct in CML cells (8, 9). In this paper, as with c-Abl (3), the direct mitochondrial targeting of Bcr-Abl (by fusion to canonical MTSs targeting the mitochondrial matrix (10), inner mitochondrial membrane (11), and the intermitochondrial membrane space (12)) was potently cytotoxic.

In light of this, we designed a small protein, the intracellular cryptic escort (iCE), for the purpose of capturing and translocating Bcr-Abl to the mitochondria. The Bcr-Abl capture motif employed for the iCE, was a previously optimized coiled-coil (i.e., the ccmut3) (2) which demonstrated both the ability to bind and, when fused to four nuclear localization signals (NLS), move endogenous Bcr-Abl to the nucleus (13). The ccmut3 oligomerizes with the coiled-coil domain of the Bcr portion of Bcr-Abl while possessing a reduced affinity for homodimer formation (2). Since coupling the ccmut3 with a targeting signal (i.e., NLS) efficiently relocalized endogenous Bcr-Abl (to the nucleus), we paired the ccmut3 with a 'cryptic' mitochondrial targeting signal (cMTS) (3) to operate on a similar principle.

Despite the lack of iCE/Bcr-Abl mitochondrial localization the iCE alone was selectively toxic to Bcr-Abl positive K562 cells to the same degree as 10 μM imatinib at 48 hours. The killing capacity of the iCE was ablated by substitution of either the ccmut3 (with the Bcr-Abl binding domain of Ras and Rab interactor 1 (RIN1-BD) (14)) or the cMTS (with the canonical intermitochondrial membrane space targeting sequence (IMS) from Smac/Diablo (12)) in two 'mock' iCEs, the RIN-cMTS or the IMS-ccmut3, respectively. The combination of the iCE with imatinib was the most potent inducer of leukemic cell death. This work demonstrates the selective and enhanced killing of Bcr-Abl positive cells by a designed

Bcr-Abl coiled-coil interacting protein where phosphorylation (via PKC or PKA) is coincident with the cell death effect.

Materials and methods

Subcloning and construction of plasmids

pEGFP-Bcr-Abl was constructed as previously (5). Bcr-Abl DNA was also cloned into pmCherry-C1 (Clonetech, Mountain View, CA, USA) and pTagBFP-C (Evrogen, Moscow, Russia) at the *EcoR1* site on both vectors creating pmCherry-Bcr-Abl and pBFP-Bcr-Abl, respectively. The pOTC-EGFP-Bcr-Abl was created using an oligonucleotide encoding the MTS from OTC (incorporating the Kozak sequence), 5′-CCGGTCGCCACCATGCTGTTTAATCTGAGGATCCTGTTAAACAATGCAGCTTTTAGAAATGGTCACAACTTCATGGTTCGAAATTTTCGGTGTGGACAACCACTACAAAATAAAGTGCAGCGA-3′ which was annealed to its complementary strand and subsequently cloned into the *Age1* site of EGFP-Bcr-Abl. The pIMS-EGFP-Bcr-Abl, pIMS-EGFP, and pIMS-EGFP-ccmut3 were made by annealing and ligating four oligonucleotides encoding the Kozak sequence and IMS signal (**1**: (5'phosphorylated) 5'-CCGGTGCCACCATGAGAAGCGTGTGCAGCCTGTTCAGATACAGACAGAGATTCCCCGTGCTGGCCAACAGCAA – 3', **2**: 5'- GAAGAGATGCTTCAGCGAGCTGATCAAGCCCTGGCACAAGACCGTGCTGACCGGCTTCGGCATGACCCTGTGCGCCGTGCCCATCGGA-3', **3**: 5'- TGCCACCATGAGAAGCGTGTGCAGCCTGTTCAGATACAGACAGAGATTCCCCGTGCTGGCCAACAGCAAGAAGAG-3', **4**: (5' phosphorylated) 5'- ATGCTTCAGCGAGCTGATCAAGCCCT

GGCACAAGACCGTGCTGACCGGCTTCGGCATGACCCTGTGCGCCGTGCCCATCAG GACCGG-3') followed by insertion into the *Age1* site of pEGFP-Bcr-Abl, pEGFP, or pEGFP-ccmut3 (2), respectively. The inner mitochondrial membrane targeting sequence (IMM) was incorporated into the pIMM-EGFP-Bcr-Abl and pIMM-EGFP by annealing the 5' phosphorylated oligonucleotide encoding the Kozak sequence and IMM signal, 5'-CCGGTCGCCACCATGTCCGTCCTGACGCCGCTGCTGCTGCGGGGCTTGACAGGCT CGGCCCGGCGGCTCCCAGTGCCGCGCGCCAAGATCCATTCGTTGA-3' with its reverse compliment followed by ligation into the *Age1* site of pEGFP-Bcr-Abl and pEGFP-C1, respectively. The kinase dead mutant of pIMM-EGFP-Bcr-Abl (i.e., pIMM-EGFP-Bcr-Abl-KD) was made using site directed mutagenesis with the primer 5'-CTGACGGTGGCCGTGGCGACCTTGAAGGAGGAC-3' and its reverse compliment. The pRIN-cMTS construct was made by PCR amplifying the binding domain of the human RIN1 gene (NM_004292, OriGene, Rockville, MD, USA) with the primers 5′- GCGCGCGCGATC TATGGAAAGCCCTGGAGAGTCAGGCGCG-3′ and 5′- GCGCGCGAATTCCCGTACCC CACTGAGCTCTCCCTCCGTAGCAGCTGGC-3′ and inserted into pEGFP-cMTS using the *BglII* and *EcoR1* sites. The murine glutathione S-transferase A4-4 [Swiss-Prot:P24472.3] cMTS (N-terminal residues, 172-222 (15); 51% sequence homology to human wherein S189 and T193 are conserved) was constructed by annealing four oligonucleotides encoding the cMTS (**1**: (5'phosphorylated) 5' –AATTCCGCCCCCGTGCTGAGCGACTTCCCCCTGCTG CAGGCCTTCAAGACCAGAATCAGCAACATCCCCACCATCAAGAAGTTCCTGCAGC CC-3', **2**: 5' –CTGCCGGGCTGCAGGAACTTCTTGATGGTGGGGATGTTGCTGATTCT GGTCTTGAAGGCCTGCAGCAGGGGGAAGTCGCTCAGCACGGGGGCGG-3', **3**: 5' – GGCAGCCAGAGAAAGCCCCCCCCCGACGGCCCCTACGTGGAGGTGGTGAGA

ACCGTGCTGAAGTTCGGCGCCGGCTGCTGCCCCGGCTGCTGCTGA-3', **4**: (5' phosphorylated) 5' –AATTTCAGCAGCAGCCGGGGCAGCAGCCGGCGCCGAACTTCA GCACGGTTCTCACCACCTCCACGTAGGGGCCGTCGGGGGGGGGCTTTCTCTGG-3') simultaneously and then inserting the annealed product into the multiple cloning site (MCS) of EGFP-C1 vector (Promega Biotech, Madison, WI), with or without the ccmut3 sequence present, at the *EcoRI* site creating pEGFP-cMTS (3) (cMTS) and pEGFP-ccmut3-cMTS (iCE), respectively. The pEGFP-ccmut3-cMTS null (S189A and T193A) was created using site-directed mutagenesis using primers, 5'- GACCAGAATCGCCAACATCCCCGCCATCA AGAAGTTCCTGCAGCCCGGCAGCCAGAGAA-3' and its reverse complement. All constructs were verified by sequence analysis.

Materials

RPMI-1640 medium, MitoTracker Red CM-H_2XRos (MitoTracker CMXros), Hoechst 33342 (cell permeable nuclear stain), 7-aminoactinomycin D (7-AAD; DNA intercalating dye permeable in dying or dead cells), annexin-APC (annexin-V conjugated to allophycocyanin), staurosporine, Lipofectamine LTX with Plus Reagent, trypan blue 0.4%, phosphate-buffered saline (PBS), fetal bovine serum (FBS), and gentamycin were purchased from Invitrogen (Carlsbad, CA). Penicillin-streptomycin-L-glutamine (P-S-G; 100 U/mL), DMEM media, and trypsin were purchased from Gibco BRL (Grand Island, NY). The poly-L-lysine (0.01% solution) was purchased from Sigma-Aldrich (St. Louis, MO). Imatinib (CT-IM001) was purchased from ChemieTek (Indianapolis, IN). QuikChange II XL Site-Directed Mutagenesis Kit was purchased from Agilent Technologies (Santa Clara, CA). Cell Line

Nucleofector Kit V was purchased from Lonza Group (Basel, Switzerland). Restriction enzymes (*EcoRI, AgeI, and BglII*) were purchased from New England Biolabs (Ipswich, MA).

Cell lines and culture conditions

As previously described (3), K562 cells (non-adherent human chronic myelogenous leukemia cell line), gift from Dr. K. Elenitoba-Johnson, University of Michigan, and Cos-7 (monkey kidney fibroblast adherent cell line; ATCC) were cultured in RPMI 1640 supplemented with 10% FBS, 1% P-S-G, and 0.1% gentamycin. Murine mammary adenocarcinoma 1471.1 cells, (gift from Gordon Hager, PhD, NCI, NIH) were grown as monolayers in DMEM supplemented with 10% FBS, 1% P-S-G and 0.1% gentamycin. K562 cells were passaged at a density of 0.5 x 10^5/mL every other day, for ten passages. Cos-7 and 1471.1 cells were passaged at 80% confluency and split 1:10 in fresh media and discontinued after passage 15. All cells were maintained in a 5% CO_2 incubator at 37 ^oC.

Expression of constructs in K562 leukemia, Cos-7 fibroblast, and 1471.1 breast cancer cells

Constructs were transiently transfected into K562 cells using the Amaxa Nucleofector II, as described previously (5). Briefly, 1 x 10^6 K562 cells, (initially seeded at a density of 0.5 x 10^5 cells/mL) between passages 5 to 10, were pelleted and resuspended in 100 µL Amaxa Solution V, combined with 2 µg of DNA and transfected in an Amaxa cuvette under program T-013. Transfected cells were immediately transferred to a 25 cm^2 flask with 7 mL of pre-warmed complete RPMI. Transient transfection of 1471.1 and Cos-7 were carried out in two-well live-cell chambers (Lab-Tek chamber slide system, Nalge NUNC

International, Naperville, IL) or sterile 6-well tissue culture plates (Greiner CellStar, Greiner Bio-one GmbH) using Lipofectamine LTX as per manufacturers' instructions between passages 3 and 15 in antibiotic free media.

Cell proliferation

Trypan blue exclusion was used to determine cell proliferation (cell viability)(16) in K562 cells 48 hours posttransfection of EGFP-C1, cMTS, ccmut3, cMTS, and iCE, with and without the presence of imatinib (10 μM).

Western blotting

As described previously (17), cell lysates were prepared by suspending 1 x 10^6 cells in 200 μL lysis buffer (62.5 mM Tris-HCl, 2% w/v SDS, 10% glycerol, 50 mM DTT, 0.01% w/v bromophenol blue) followed by standard western blotting procedures using antibodies to detect the total and/or phosphorylated forms of Bcr-Abl, Crk-L, STAT5, and elF4E as the protein loading control. Primary antibody labels (anti-pAbl (Y245), anti-pCrk-L (Y207), and anti-elF4E, Cell Signaling Technology; anti-pSTAT5 (Y694), Abcam) were detected with anti-rabbit (#7074, Cell Signaling Technology) HRP-conjugated secondary antibodies prior to the addition of ChemiGlo (AlphaInnotech, Cell Biosciences, Santa Clara, CA, USA) chemiluminescent substrate and detection using a FluorChem FC2 imager (AlphaInnotech). Densitometry and quantification was performed on the appropriate bands with normalization to elF4E.

Mitochondrial staining

As described previously (3), aliquots of transfected K562 suspension cells (400 µL) were plated into poly-L-lysine coated 4-well live-cell chambers at least 4 hours in advance of microscopy. Cells were incubated with MitoTracker Red CM-H_2XRos (K562; 100 nM, Cos-7 and 1471.1; 325 nM) for 45 minutes at 37 ^{o}C and protected from light prior to imaging.

Microscopy

Fluorescent images of K562, Cos-7, and 1471.1 live cells were acquired on an Olympus IX81 FV1000-XY spectral confocal microscope (Imaging Core Facility, University of Utah) equipped with 405 nm diode, 488 nm argon, and 543 nm HeNe lasers using a 60X PlanApo oil immersion objective (NA 1.45) using Olympus FluoView software, as previously described (3). Excitation and emission filters were as follows: EGFP, 488 nm excitation, emission filter 500-530 nm; MitoTracker Red CM-H_2XRos, 543 nm excitation, emission filter 555-655 nm. Images were collected in sequential line mode with exposure and gain of laser kept constant and below detected pixel saturation for each group of cells. No channel crosstalk was observed. Pixel resolution was kept at 1024 x 1024 (0-2.5-fold digital zoom) with a pixel dwell time of 12.5 µs. Imaging of K562 cells for the analysis of DNA segmentation was acquired on an Olympus IX71F fluorescence microscope (Scientific Instrument Company, Aurora, CO) with a 60X PlanApo oil immersion objective (NA 1.4) on an F-view monochrome CCD camera. K562 cells were stained with the nuclear dye Hoechst 33342 (Invitrogen, Carlsbad, CA) at a concentration of 4 µM.

Image analysis

Images were analyzed as described previously (3). Briefly, original images were converted to 8-bit, then stacked as separate channels, and corrected for background noise using ImageJ plugin 'BG subtraction from background' in default mode (i.e., mean background intensity outside of cells was subtracted) (18). Image and statistical analysis was performed with JACoP plugin in ImageJ (19). Pearson's correlation coefficient (PCC) was generated using Costes' automatic threshold algorithm (20, 21). The PCC is dependent upon both the pixel intensity and overlap of signal and has a range of +1 (complete colocalization) to -1 (anti-correlation) with zero correlating with random distribution between comparators (19). The PCC threshold for defining colocalization (i.e., colocalization due to co-compartmentalization) is 0.6 as per Bolte and Cordelières (19). Channels have been false-colored (cyan and magenta) using ImageJ LUT for increased visual clarity. Additionally, spatial representation of intensity correlation was included using the Colocalization Colormap ImageJ plugin. 'Colormap' displays positively correlated pixels in hot colors and negatively correlated pixels in cold colors that can be visually interpreted using the color scale bar (22). Identification of segmented nuclei was performed using the nuclear dye H33342 on K562 cells displaying green fluorescence 24 hours posttransfection.

7-AAD assay

Flow cytometric assay of cell death was done as previously described (2). Briefly, K562, Cos-7, or 1471.1 cells were resuspended in 500 µL ice cold PBS containing 1 µM 7-aminoactinomycin D (7-AAD) for 30 minutes prior to analysis. Cells that have compromised membrane integrity (late apoptosis/necrosis) are permeable to 7-AAD (23). Media from

adherent Cos-7 and 1471.1 cells was collected prior to trypsinization of cell monolayer and recombined with the enzymatically released cell population for centrifugation and subsequent resuspension. Analysis and gating was performed on a BD FACSCanto II (Flow Cytometry Core Facility, University of Utah) using BD FACSDiva software (BD Biosciences, Franklin Lakes, NJ). At least three separate experiments ($n \geq 3$) in duplicate were performed. Compensation controls were included with each experiment.

TUNEL assay

As previously described (24), detection of DNA strand breaks in the K562 cell line was performed using the In Situ Death Detection Kit, TMR red (Roche, Mannheim, Germany) as per the manufacturers' protocol. Terminal deoxynucleotidyl transferase (TdT) dUTP nick-end labeling (TUNEL) detects cells that have extensive DNA degradation in late stage apoptosis/necrosis (25). Samples were run on a Becton-Dickinson FACSAria-II (BD-BioSciences, University of Utah Core Facility) using the 488 nm (for EGFP) and 563 nm (TMR red) laser lines with FACSDiva software. Analysis was performed on EGFP positive cells using preset gates. The TMR red positive cells were detected in the PE (phycoerythrin) channel. Each construct was assayed in at least triplicate ($n \geq 3$).

Annexin-V assay

Annexin-V binding was assessed, as previously described (24), 48 hours post-transfection in K562 cells. Externalized phosphatidylserine in the plasma membrane is indicative of early apoptosis and is bound specifically by annexin V (26). K562 cells were suspended in 100 µl Annexin binding buffer (Invitrogen) and incubated with 5 µl Annexin-V

conjugated to allophycocyanin (Annexin-APC, Invitrogen) for 10 minutes. The incubated cells were then diluted in 400 µl Annexin binding buffer and analyzed using the FACSCanto-II (BD-BioSciences, University of Utah Core Facility) with FACSDiva software. EGFP (ex. 488 nm and em. 507 nm) and APC (ex. 635 nm and em. 660 nm) fluorescence was collected. Analysis was conducted on EGFP-positive cells using preset EGFP gates. Each construct was tested in triplicate (n=3).

Statistics

Data are shown as mean ± S.E.M., with one-way ANOVA using Tukey's post-test or two-way ANOVA using Bonferroni post-test (as indicated in figure legends) to compare measurements between experimental data with an N of 3 or greater. Statistical significance was set at $p<0.05$ (by convention $p<0.05$ is represented with *; $p<0.01$ with **; $p<0.001$ with ***). GraphPad Prism Graph 4 (GraphPad, La Jolla, CA) software was used for generating statistics.

Results

Targeting Bcr-Abl to the mitochondria induces cell death in K562 leukemia cells

Previously, we demonstrated that directly targeting c-Abl to the mitochondria is toxic to K562 leukemia cells (3). Based on this we have directly targeted the constitutively active and oncogenic form of c-Abl (i.e., Bcr-Abl) to the mitochondria. The IMM-Bcr-Abl was created by fusing Bcr-Abl to a canonical mitochondrial targeting signal (MTS; derived

from cytochrome c oxidase subunit VIII) that is widely used to direct proteins to the mitochondria and the inner mitochondrial membrane in particular (IMM; see *Table 4.1*) (11). Cell death evaluated by flow cytometric analysis of 7-AAD (DNA accessibility) and annexin-APC (phosphatidylserine externalization) staining (*Fig. 4.2*) showed the toxic consequences of mitochondrially targeted Bcr-Abl (*Fig. 4.2A, 3rd column*) at 24 hours posttransfection in K562 cells. DNA segmentation analysis of mitochondrially targeted Bcr-Abl also revealed the same pattern (data not shown). Interestingly, the kinase dead version (i.e., mutation of a single critical lysine ablates the capacity for kinase activity) of mitochondrially targeted Bcr-Abl (IMM-Bcr-Abl-KD; see *Table 4.1*) yields no statistical difference in cell death to that of IMM-Bcr-Abl (*compare Fig. 4.2, 3rd and 4th columns*). Furthermore, mitochondrially targeted Bcr-Abl and Bcr-Abl-KD (*Fig.4.2, 3rd and 4th columns*) significantly induce more cell death as compared to the gold standard of current CML therapy, imatinib (IM; 10 μM) (*Fig. 4.2B, 2nd column*) at 24 hours.

Yet, the mitochondrial target(s) and submitochondrial localization of the pro-apoptotic c-Abl are not known (3, 7). Therefore, in order to further investigate the potential toxicity of a 'surrogate death-directed c-Abl,' in the form of mitochondrial Bcr-Abl, we targeted exogenous Bcr-Abl to multiple submitochondrial regions (*Table 4.1*). *Figure 4.3A* shows representative images of E-Bcr-Abl or mitochondrially targeted Bcr-Abl in K562 cells compared to MitoTracker CMXros (MitoTracker) dye. The E-Bcr-Abl construct was not associated with the mitochondria (*Fig. 4.3A, compare 1st column with 2nd 'MitoTracker' column*) but each of the mitochondrially targeted Bcr-Abl constructs did localize (*Fig. 4.3A, 2nd through 4th rows*) to the mitochondria. The corresponding EGFP-only constructs (i.e., IMM-EGFP, IMS-EGFP, and OTC-EGFP) were also tested and exhibited robust

Table 4.1. Canonical MTSs used to target Bcr-Abl to the mitochondria. MTSs targeting different mitochondrial compartments were fused to Bcr-Abl and tested for cellular toxicity. KD represents a kinase dead version of Bcr-Abl where a so-called 'essential lysine' residue is mutated at the ATP binding site, abolishing all kinase activity (27).

Construct	**Target compartment**	**Kinase**	**Reference**
OTC-Bcr-Abl	mitochondrial matrix	active	(10)
IMS-Bcr-Abl	mitochondrial intermembrane space	active	(12)
IMM-Bcr-Abl	mitochondrial inner membrane	active	(11)
IMM-Bcr-Abl-KD	mitochondrial inner membrane	inactive	(27)
IMM-EGFP	mitochondrial inner membrane	N/A	(24)
E-Bcr-Abl	cytoplasmic (nontargeted)	active	(5)

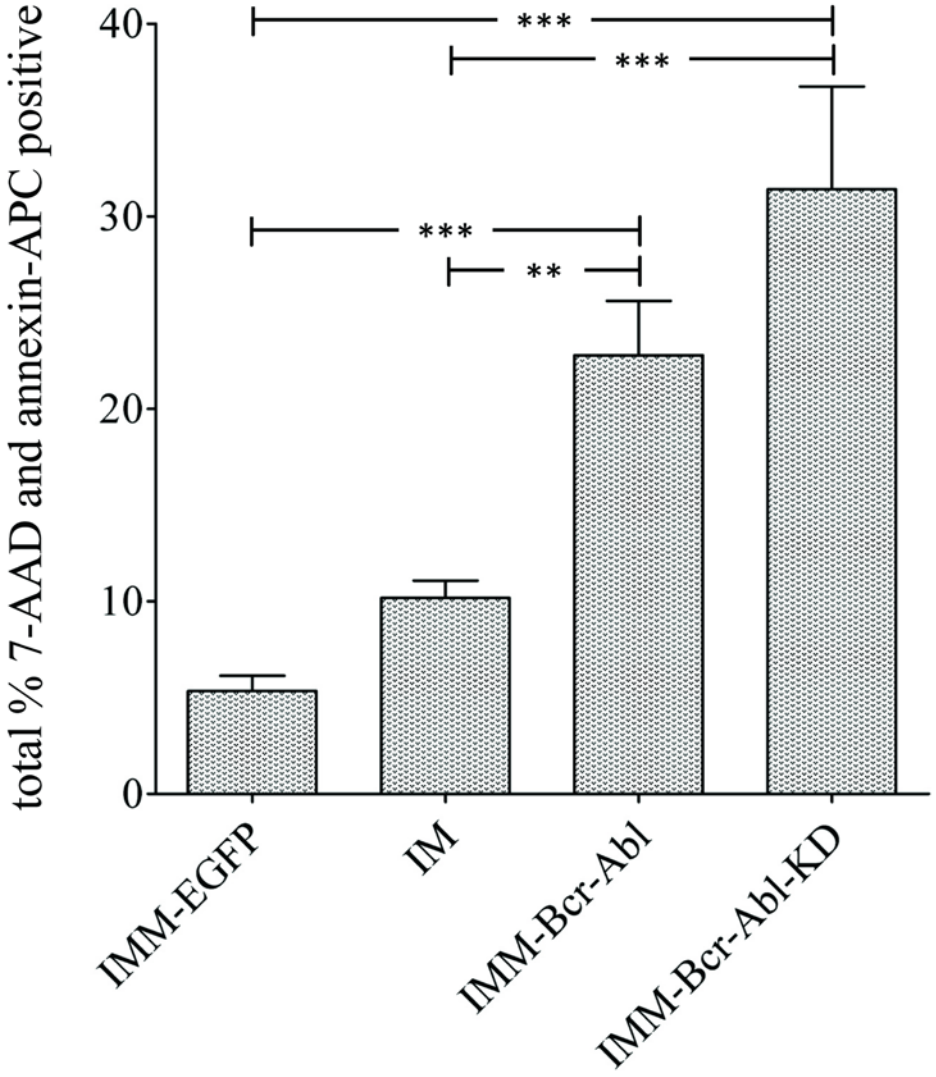

Figure 4.2. Direct targeting of Bcr-Abl to the mitochondria causes leukemic cell death. Flow cytometric analysis of GFP positive K562 cells 24 hours posttransfection stained with 7-AAD and annexin-APC. Both IMM-Bcr-Abl and the kinase dead version (IMM-Bcr-Abl-KD) displayed higher cell death than imatinib or mitochondrially targeted EGFP (IMM-EGFP). Significance was determined using one-way ANOVA with Tukey's post-test (error bars are ±S.E.M., $N \geq 4$; $p<0.01$**, $p<0.001$***).

Figure 4.3. Submitochondrial targeting of Bcr-Abl in K562 leukemia cells.

A) Representative images of E-Bcr-Abl or Bcr-Abl fused to a canonical MTS in K562 cells and compared to MitoTracker CMXros staining. Each of the MTS-Bcr-Abl constructs localize to the mitochondria while the E-Bcr-Abl (no targeting signal) remains cytosolic. Channel one (EGFP) and channel two (MitoTracker) have been false-colored, cyan and magenta. Colocalized cyan and magenta pixels show as white in merged ('composite' column) images. The 'Colormap' (*far right column*) is a visual representation of pixel correlation both in space and intensity with positive correlation as hot colors and negative correlation in cooler colors and can be interpreted using the color scale bar (shown at bottom of the 'Colormap' column). Scale bars are 5 μm.

B) Cell death in K562 cells 48 hours post-transfection. Each of the submitochondrially targeted Bcr-Abl species caused significantly more cell death than EGFP but only OTC and IMM conjugated Bcr-Abl were different from EGFP-Bcr-Abl. Significance was determined using one-way ANOVA with Tukey's post-test (error bars are S.E.M., $n \geq 3$, $p<0.05$*, $p<0.01$**, $p<0.001$***).

A.

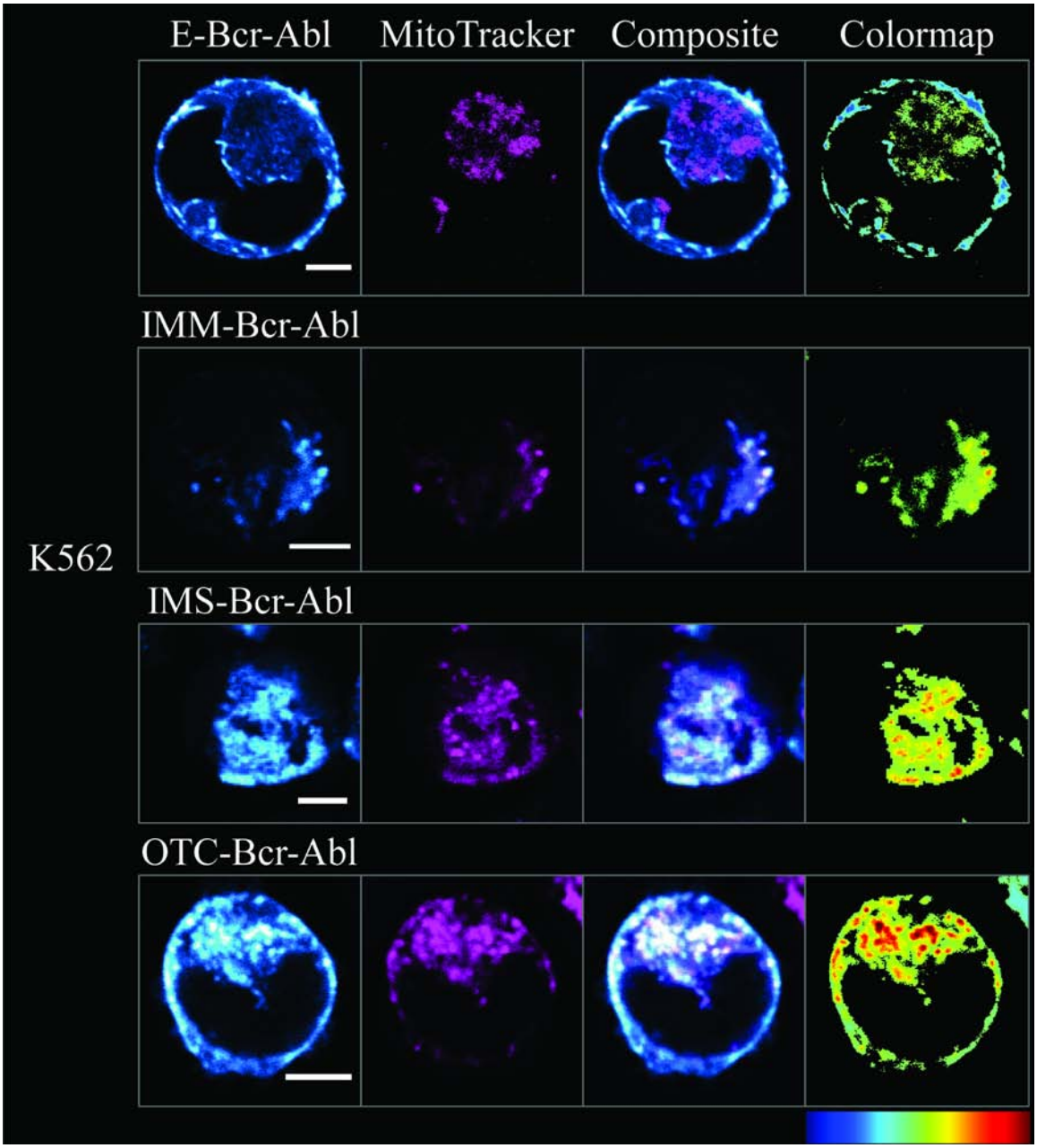
E-Bcr-Abl
MitoTracker
Composite
Colormap
IMM-Bcr-Abl
K562
IMS-Bcr-Abl
OTC-Bcr-Abl

B.

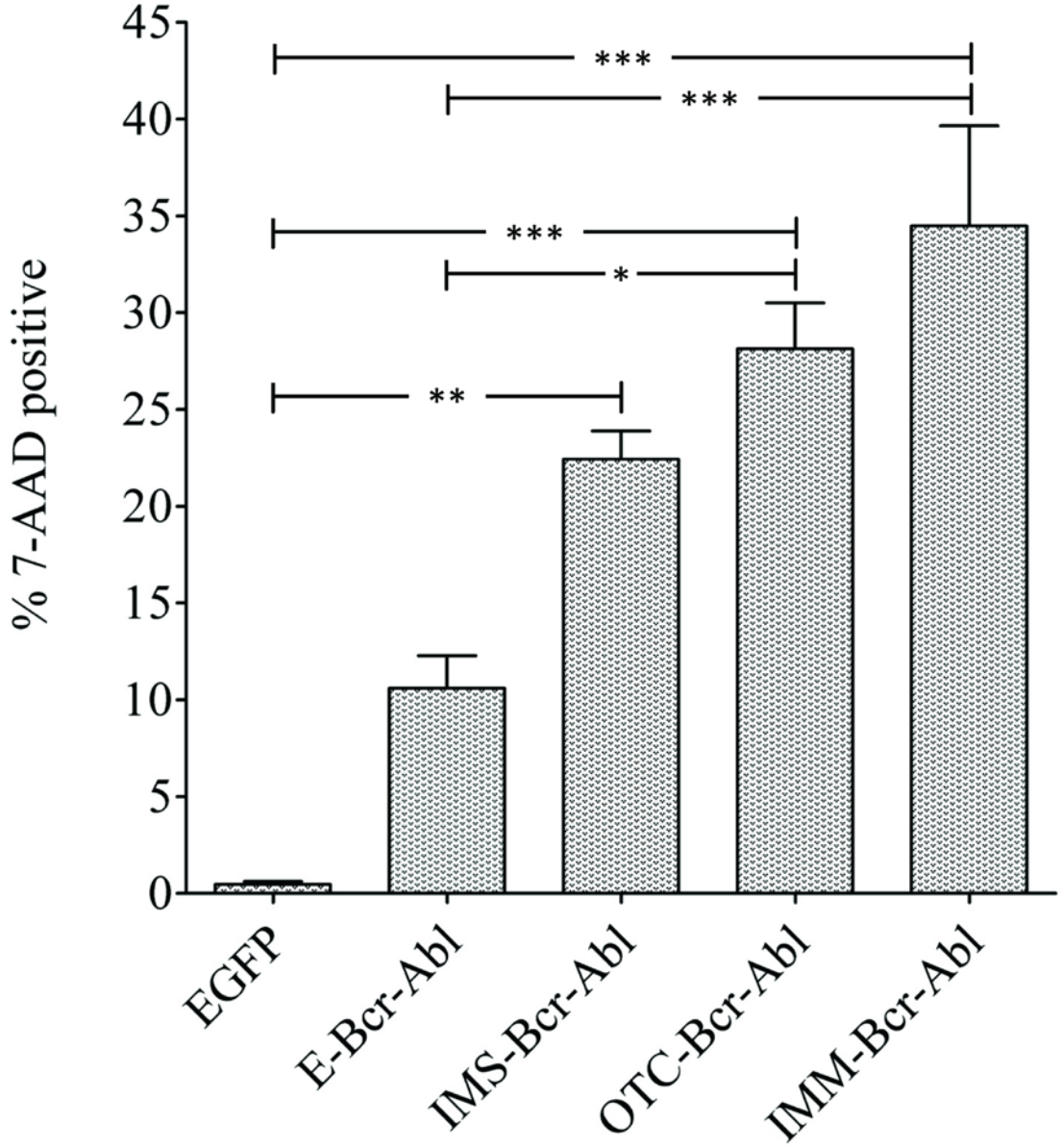
% 7-AAD positive
45
40
35
30
25
20
15
10
5
0
***
***
***
*
**
EGFP
E-Bcr-Abl
IMS-Bcr-Abl
OTC-Bcr-Abl
IMM-Bcr-Abl

mitochondrial localization and low-toxicity. Therefore, only data on the IMM-EGFP are shown (*Fig. 4.2, IMM-EGFP*). We further characterized the effects of targeting Bcr-Abl to the mitochondrial matrix with the OTC MTS in Cos-7 and 1471.1 cells (*Fig. 4.4*).

In K562 cells, the OTC and the IMM fused Bcr-Abl constructs were significantly more toxic (7-AAD positive) than the E-Bcr-Abl (*Fig. 4.3B, compare 4^{th} and 5^{th} columns to 2^{nd} column*) at 48 hours posttransfection. Yet, there was no difference in toxicity between the individual MTS-Bcr-Abl constructs (*Fig. 4.3B, compare 3^{rd}, 4^{th}, and 5^{th} columns*).

Designing a protein chaperone to bind and force Bcr-Abl to the mitochondria of leukemia cells

Since Bcr-Abl targeted to the mitochondria is toxic (*Fig. 4.2, 3^{rd} column*), we designed a bimodal construct (intracellular cryptic escort (iCE)) using a previously characterized cMTS (that we used to directly target c-Abl to the mitochondria) (3) and our optimized Bcr-Abl binding domain, ccmut3 (2) (*see Fig. 4.5 for description of constructs*). The mitochondrial targeting of the cMTS is limited to cell types with an elevated ROS phenotype (3). K562 cells exhibit high basal levels of ROS which is a common pathophysiological feature of malignancy (28, 29). The elevated oxidative stress level leads to an increase in PKA and PKC activity which, in turn, phosphorylate and thereby 'activate' the cMTS at S189 (PKA) and/or T193 (PKC) to induce mitochondrial translocation in a Hsp70 dependent manner (3, 15).

The ccmut3 Bcr-Abl binding protein oligomerizes in an antiparallel orientation with the coiled-coil domain of Bcr-Abl (2). Previously, the ccmut3 was shown to efficiently bind

A.

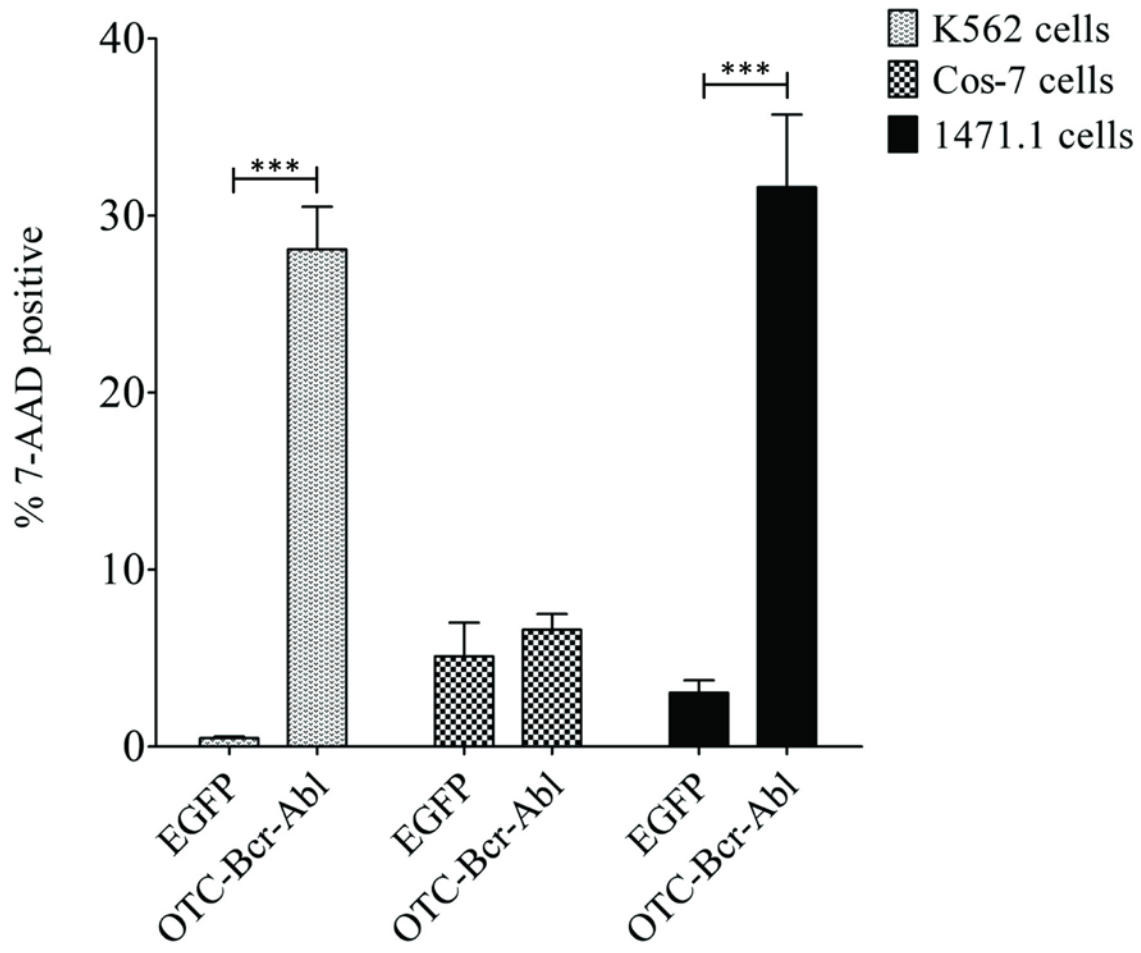

Figure 4.4. Bcr-Abl targeted to the mitochondria of K562, Cos-7, and 1471.1 cells.

A) K562 leukemia and 1471.1 breast cancer cells were sensitive to mitochondrial Bcr-Abl whereas Cos-7 fibroblast cells were not. The OTC MTS was used because it is reportedly the 'stronger' MTS as compared to the IMM sequence) (24). One-way ANOVA with Tukey's post-test was performed on individual cell types (error bars are S.E.M., $N \geq 3$; $p < 0.001$***).

B) Representative images showing OTC-Bcr-Abl colocalizing with the mitochondria (MitoTracker CMXros) in Cos-7 and 1471.1 cells (OTC-Bcr-Abl localizes to the mitochondria in K562 cells; *Fig. 2A, bottom row*). Scale bar is 5µM.

B.

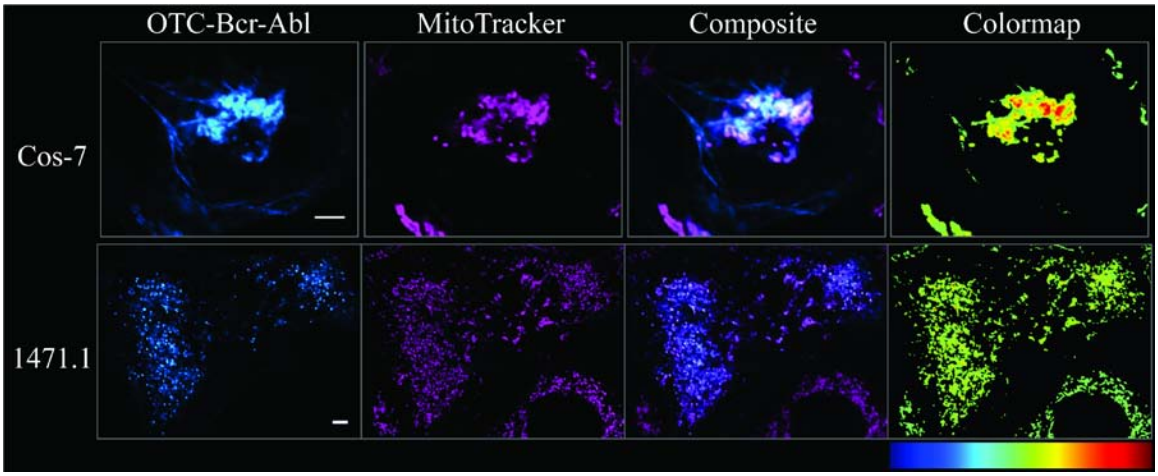

Figure 4.4: Continued

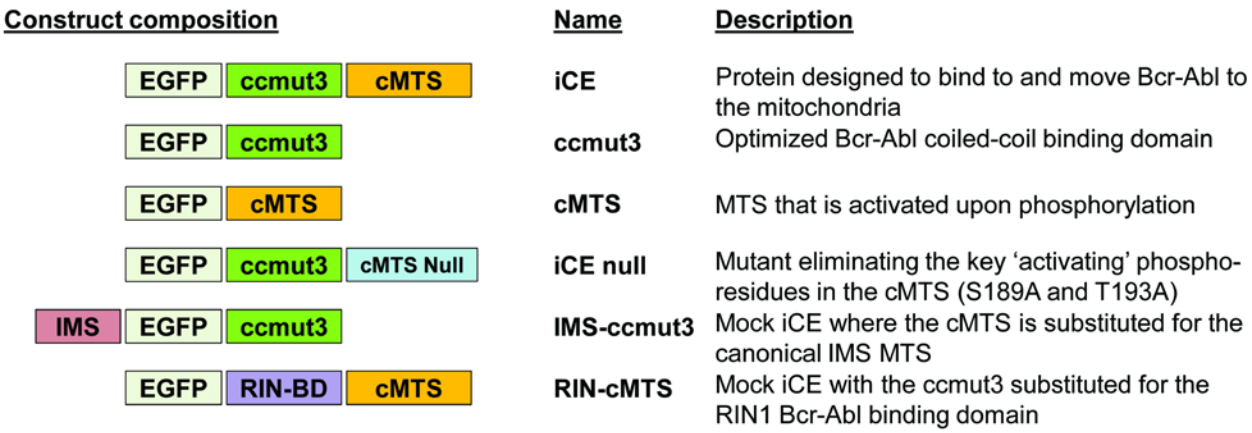

Figure 4.5. Domain arrangement of constructs. RIN-BD = Abl binding domain from the Ras and Rab interactor 1 (RIN1; binds the SH3/SH2 domains of Bcr-Abl), CC = coiled-coil domain, IMS = intermitochondrial membrane space, ccmut3 = coiled-coil mutation set 3, cMTS = cryptic mitochondrial translocation sequence, Bcr = breakpoint cluster region, Abl = Abelson proto-oncogene, EGFP = enhanced green fluorescent protein. See *Figure 4.6* for domain residue sequences.

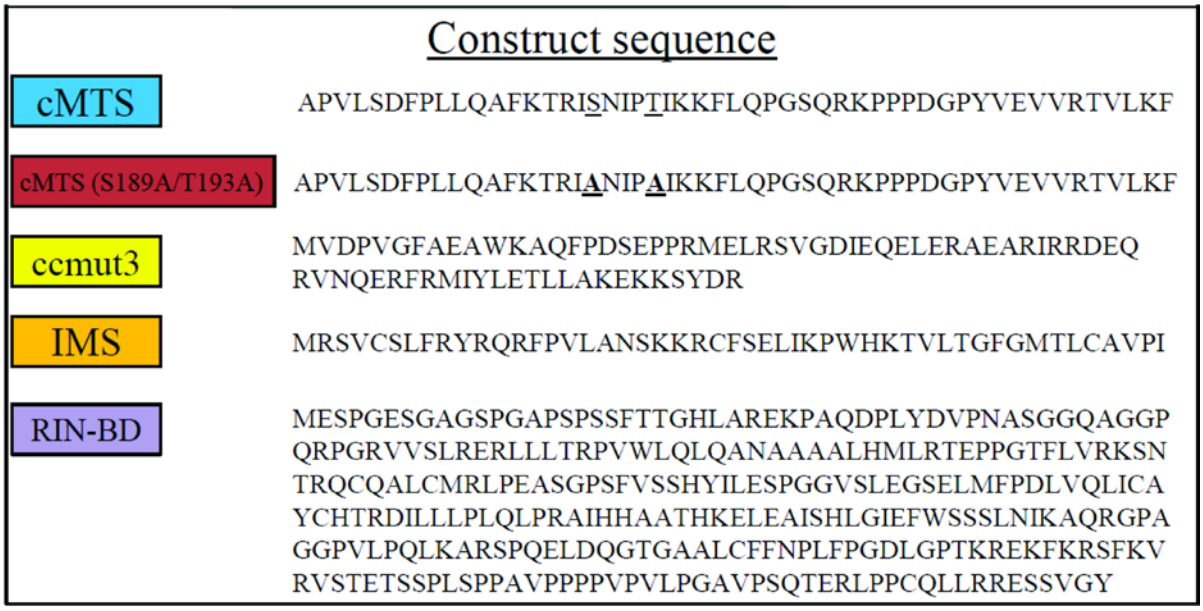

Figure 4.6. Residue sequences for the construct domains.

and force Bcr-Abl to the nucleus when fused to four strong nuclear localization signals (NLS) (13). However, cell death from nuclear entrapment or nuclear targeting of Bcr-Abl is relatively modest when compared to mitochondrially targeted Bcr-Abl. For instance, cell death assessed by nuclear segmentation analysis 24 hours post-transfection with 4NLS-Bcr-Abl versus IMM-Bcr-Abl yielded a mean of 12% (5) versus 88%, respectively (data not shown).

The iCE is designed to bind Bcr-Abl in the cytoplasm and upon activation of the cMTS, translocate the Bcr-Abl/iCE complex to the mitochondria. Mutating the key phospho-residues (i.e., S189A and T193A) on the cMTS ablates the capacity for mitochondrial translocation (3) and these mutations have been incorporated into the iCE Null (*Fig. 4.5*). The IMS-ccmut3 and RIN-cMTS are 'mock' iCEs where a canonical MTS (IMS) (12) has been substituted for the cMTS in the IMS-ccmut3 construct while the well known Bcr-Abl binding domain from RIN1 (i.e., RIN-BD) (14) has been substituted for the ccmut3 in the RIN-cMTS construct.

The iCE exhibits selective and potent toxicity to Bcr-Abl positive K562 cells

The iCE and its component parts (i.e., EGFP, ccmut3, and cMTS; *Fig. 4.5*) were transfected into Bcr-Abl positive K562 and Bcr-Abl negative Cos-7 and 1471.1 cell lines. The cell death profiles, as measured by flow cytometric analysis of 7-AAD staining, demonstrated a cell type-dependent response to the constructs. The iCE was toxic only in the K562 cell line (*Fig. 4.7A, K562, iCE column*) as was imatinib (*Fig. 4.7A, K562, IM column*). There was no significant difference in Cos-7 or 1471.1 between treatment with imatinib or the constructs

Figure 4.7. Cell death in Bcr-Abl positive (K562 leukemia) and Bcr-Abl negative (Cos-7 fibroblast and 1471.1 breast cancer) cells 48 hours post-transfection or treatment with 10 μM imatinib. Cell death was assessed by flow cytometric analysis of 7-AAD.

A) K562 cells were sensitive to imatinib as expected but also to the iCE. The combination of the iCE with imatinib led to a significant increase in cell death over either imatinib or the iCE alone.

B) In Bcr-Abl negative Cos-7 cells there was no significant toxicity from imatinib treatment or the constructs.

C) In 1471.1 breast cancer cells there was no significant toxicity from imatinib or the constructs individually. Yet, the combination of the iCE and imatinib did cause toxicity when compared to imatinib or EGFP but not the iCE alone. One-way ANOVA with Tukey's post-test performed on individual cell types (error bars are S.E.M., $N \geq 3$; $p<0.05$*, $p<0.01$**, $p<0.001$***).

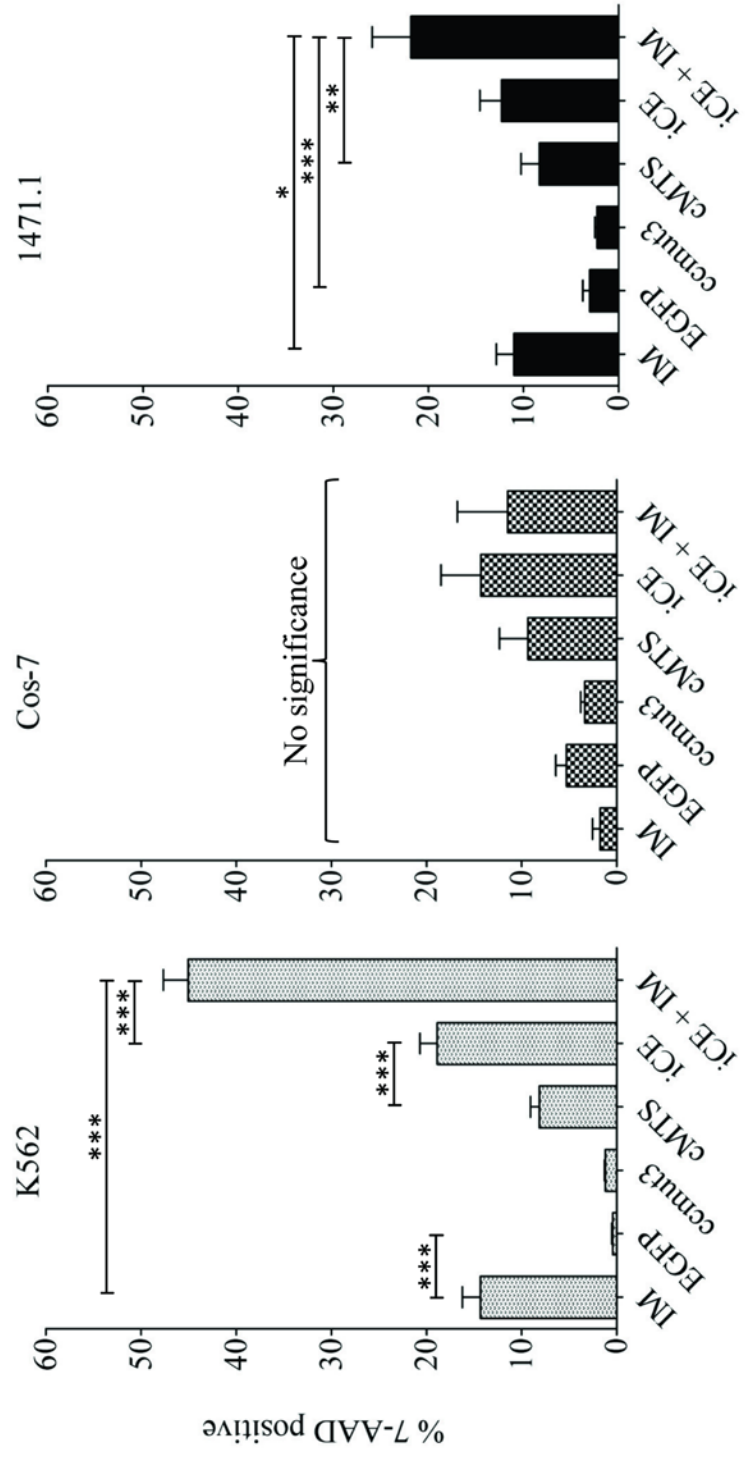
% 7-AAD positive
K562
Cos-7
1471.1
No significance
IM
EGFP
ccmut3
cMTS
iCE
iCE + IM
***
***
***
***
**
*
0
10
20
30
40
50
60

individually with the exception of 1471.1 cells with the iCE combined with imatinib (*Fig. 4.7C, 1471.1, iCE+IM column*). This was not evidenced in Cos-7 where combining imatinib and the iCE were not toxic (*Fig. 4.7B, Cos-7, iCE+IM column*). In contrast, within K562 cells imatinib and the iCE were not different from one another (*Fig. 4.7A, K562, compare iCE to IM columns*) but both were different from the EGFP control and the iCE components (*Fig. 4.7A, K562, EGFP, ccmut3, and cMTS columns*). When the iCE was combined with imatinib (*Fig. 4.7A, K562, iCE+IM column*) an enhanced killing effect was observed.

Figure 4.8A includes the components comprising the iCE (i.e., EGFP, ccmut3, and cMTS) combined with imatinib. There was no difference between imatinib alone and the individual components of the iCE combined with imatinib (*Fig. 4.8A, compare IM with EGFP+IM, ccmut3+IM, and cMTS+IM*). As mentioned above the iCE alone was not different from imatinib (*Fig. 4.8A, compare IM with iCE*). The cMTS alone was not different from imatinib, however when compared to the iCE alone (*Fig. 4.8A, compare cMTS to iCE*) the difference was extremely significant ($P<0.001$). Overall, the iCE+IM was extremely significant in its killing potential when compared to all constructs regardless of imatinib treatment (*Fig. 4.8A, compare iCE+IM to EGFP+IM, ccmut3+IM, and cMTS+IM*).

Representative histograms (*Fig. 4.8B*) from a set of K562 cells transfected and/or treated (imatinib (10 μM) or positive control staurosporine (1 μM)) samples at 48 hours demonstrate the difference in dead cells when the iCE and imatinib are combined (*Fig. 4.8B, compare staurosporine or imatinib to iCE+imatinib*). The vertical line within the plot is the gate for 7-AAD positive cells for which the percent is listed in the shaded box. As expected, a similar cell death pattern was seen using a different cell permeable nuclear stain (H33342) to identify nuclear segmentation by microscopy (5) (*Fig. 4.8C, compare imatinib only (top right*

Figure 4.8. The iCE combined with imatinib is highly toxic to K562 cells.

A) This figure is an expansion of the data set seen in *Figure 4.7A, K562* (cell death in K562 at 48 hours). Box and whisker plot showing percent 7-AAD positive cells 48 hours post-transfection and/or treatment with imatinib. The darker shaded boxes (of the box plot) represent the presence of imatinib (10 μM). One-way ANOVA with Tukey's post-test (error bars are S.E.M., $N \geq 4$; $p<0.05$*, $p<0.01$**, $p<0.001$***).

B) Representative set of flow cytometric histograms displaying cell count on the y-axis and 7-AAD intensity on the x-axis. The percent 7-AAD positive population represents cells to the right of the vertical line and is listed in the shaded box. As each histogram only depicts a single sample, the mean (*Fig. 4.7A, K562*) and median values (*Fig. 4.8A*) across the entire experimental set are included for reference below the shaded box. 'GFP Gated' refers to the transfected subset of cells (> 10^3 intensity in the GFP channel) that were analyzed for 7-AAD staining analysis (staurosporine and imatinib samples were not subject to a GFP gate).

C) Phase-contrast paired with fluorescent images using the nuclear dye, H33342, at 48 hours post-transfection (iCE) or imatinib treatment. Upper left, control K562 cells; lower left, cells transfected with iCE construct; upper right, cells treated with imatinib only; lower right, cells transfected with the iCE and treated with imatinib. White arrow in bottom, rightmost panel indicates a cell with a segmented nucleus. Scale bar is 20 μm.

D) Evaluation of 7-AAD positive K562 cells at 8, 24, and 48 hours posttransfection and/or imatinib treatment. Two-way ANOVA with Bonferroni posttest (error bars are S.E.M., $N \geq 3$; $p<0.05$*, $p<0.001$***).

A.

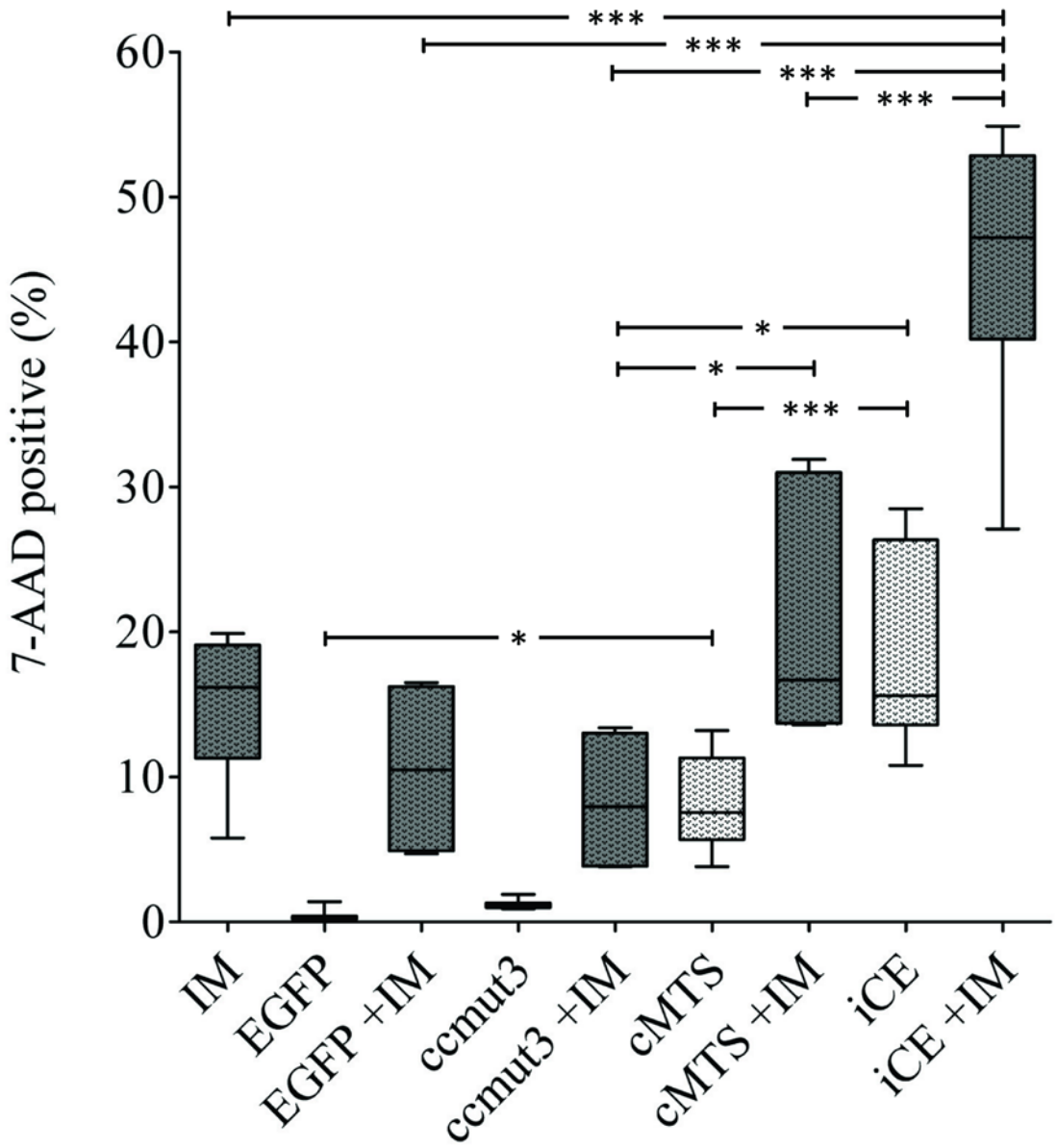
7-AAD positive (%)
60
50
40
30
20
10
0
***
***
***
***
*
*
***
*
IM
EGFP
EGFP +IM
ccmut3
ccmut3 +IM
cMTS
cMTS +IM
iCE
iCE +IM

B.

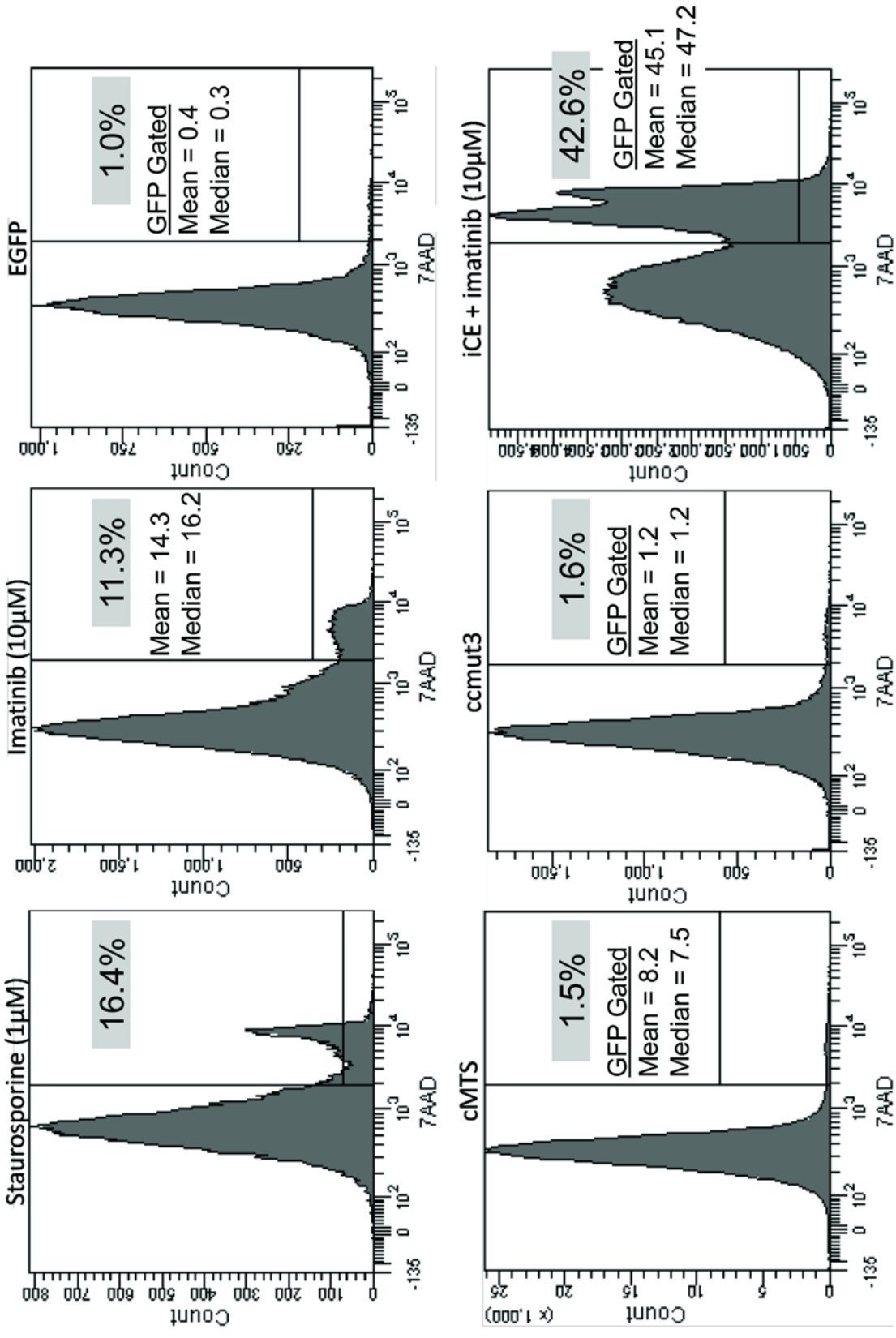
EGFP
1.0%
GFP Gated
Mean = 0.4
Median = 0.3
Imatinib (10μM)
11.3%
Mean = 14.3
Median = 16.2
Staurosporine (1μM)
16.4%
iCE + imatinib (10μM)
42.6%
GFP Gated
Mean = 45.1
Median = 47.2
ccmut3
1.6%
GFP Gated
Mean = 1.2
Median = 1.2
cMTS
1.5%
GFP Gated
Mean = 8.2
Median = 7.5
Count
7AAD

C.

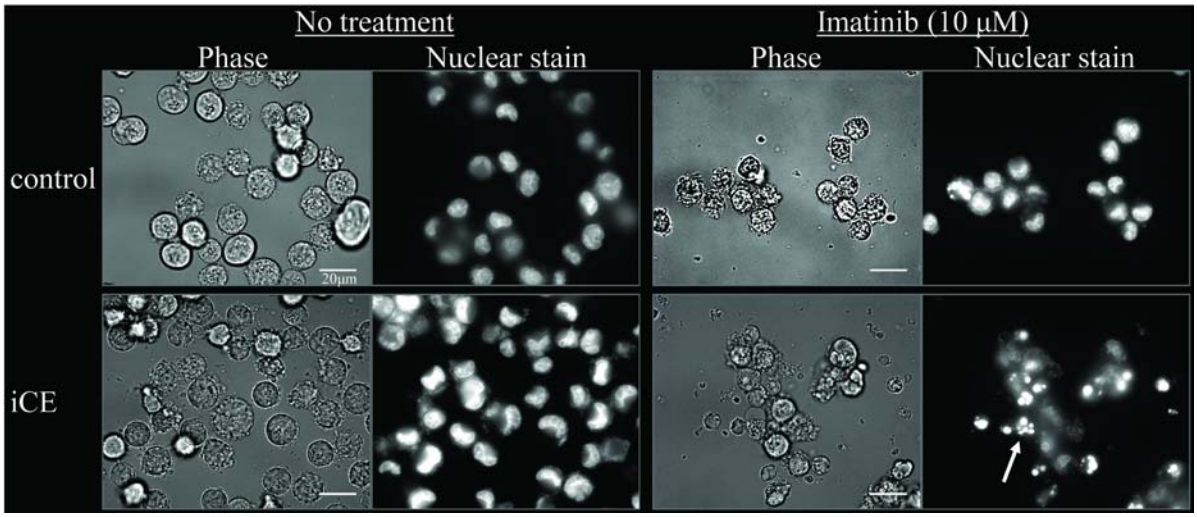
No treatment
Imatinib (10 μM)
Phase
Nuclear stain
Phase
Nuclear stain
control
iCE
20μm

D.

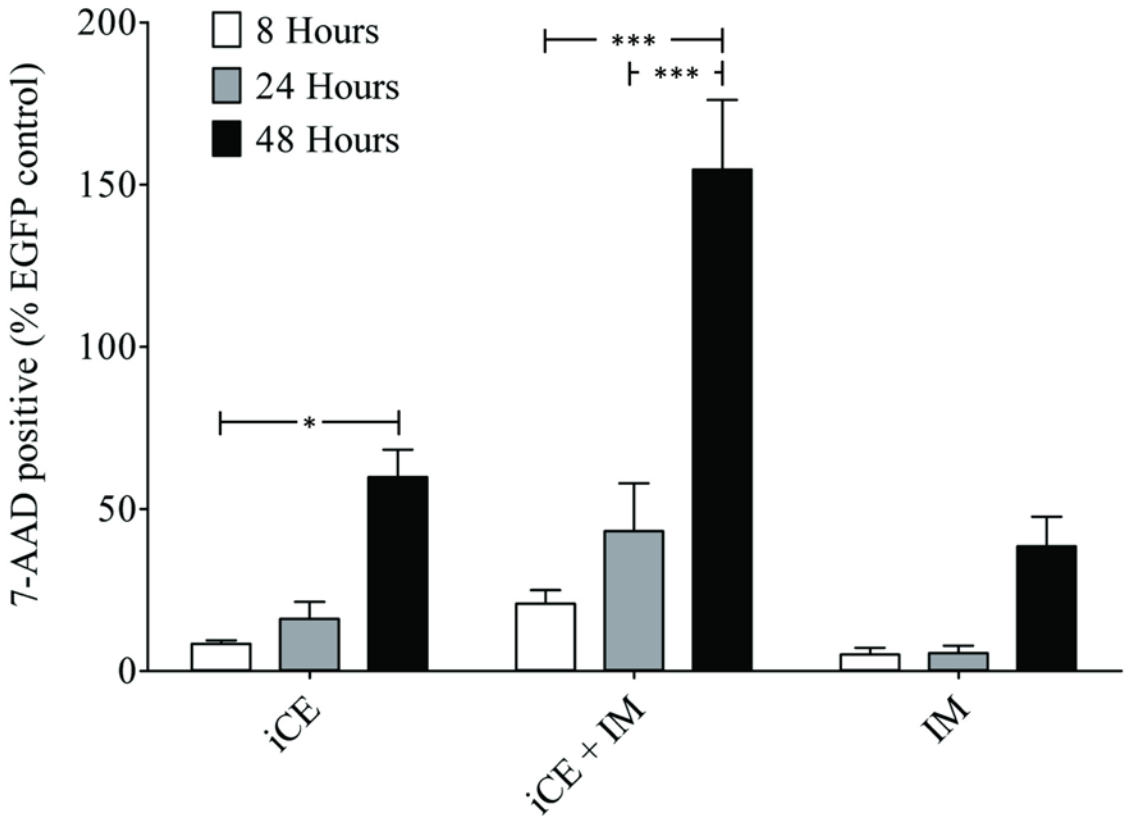
200
150
100
50
0
7-AAD positive (% EGFP control)
8 Hours
24 Hours
48 Hours
*
***
***
iCE
iCE + IM
IM

set) to iCE + imatinib (lower right set)). The relative health of the cells was revealed by phase contrast as well, where the cells treated with imatinib and the iCE evidence the sequelae of apoptosis/necrosis (e.g., cell shrinkage/swelling and membrane blebbing) (5) in comparison to the untreated control (e.g., round cells with intact membranes) (*Fig. 4.8C, compare 'Phase' of iCE, 'no treatment' and 'imatinib' to control, 'no treatment'*). The combined treatment of imatinib and the iCE accelerates the progression to full blown DNA segmentation (*Fig. 4.8C, compare the stained nuclei of the iCE, 'no treatment' and 'imatinib' to iCE, with 'imatinib'*). The peak time for iCE+IM killing of K562 is 48 hours (*Fig. 4.8D*) whereas it is later for imatinib alone (10 µM imatinib kills most K562 cells by approximately 72 to 96 hours, our unpublished observations).

Cell viability decreases and apoptosis increases when the iCE is combined with imatinib

Trypan blue exclusion (cell viability), terminal deoxynucleotidyl transferase dUTP nick end labeling (TUNEL), and phosphatidylserine (PS) externalization (annexin-V binding) demonstrated the antileukemic activity associated with the iCE in K562 cells (*Figs. 4.9A, 4.9B, and 4.9C, respectively*). Cell viability was significantly decreased for the iCE compared to EGFP and ccmut3 but not the cMTS (*Fig. 4.9A, compare 'no treatment', iCE to EGFP and ccmut3 data points*). However, the decline in cell viability with imatinib present (*Fig. 4.9A, 'IM'*) was extremely significant for the iCE when compared to the other component constructs. The cell viability assessment was completed 48 hours post-transfection but 24 hours post-addition of imatinib (IM). Reducing the incubation time, for this assay, with imatinib to 24 instead of 48 hours allowed better discernment of viable cells since the full 48

A.

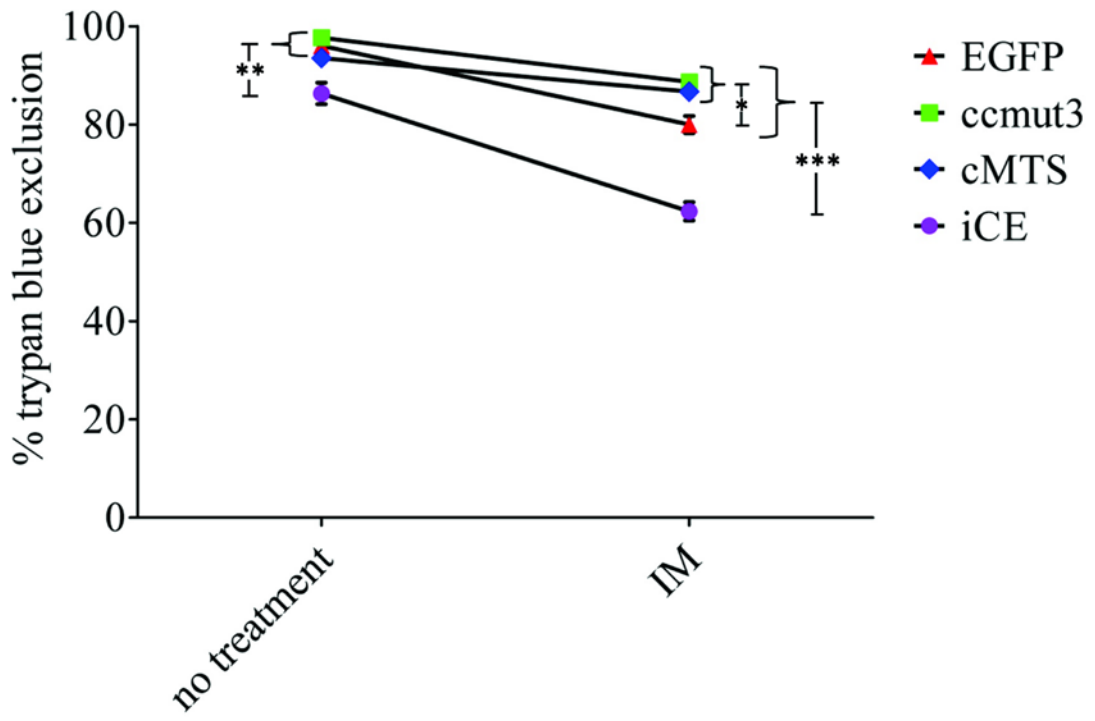

Figure 4.9. Assessment of cell viability and apoptotic induction in K562 cells.

A) Viability 48 hours posttransfection and 24 hours after addition of imatinib. One-way ANOVA with Tukey's posttest was performed within each treatment type (i.e., 'no treatment and 'IM').

B) Terminal deoxynucleotidyl transferase dUTP nick end labeling (TUNEL) was assessed 48 hours posttransfection and/or with imatinib treatment (dark shaded columns indicate with imatinib) by flow cytometry. One-way ANOVA with Tukey's posttest.

C) Phosphatidylserine externalization detection using annexin-APC and flow cytometric analysis 48 hours posttransfection and/or imatinib treatment. Dark shaded columns indicate imatinib treatment. One-way ANOVA with Tukey's posttest (for all assays here, error bars are S.E.M., $N \geq 3$; $p<0.05$*, $p<0.01$**, $p<0.001$***).

B.

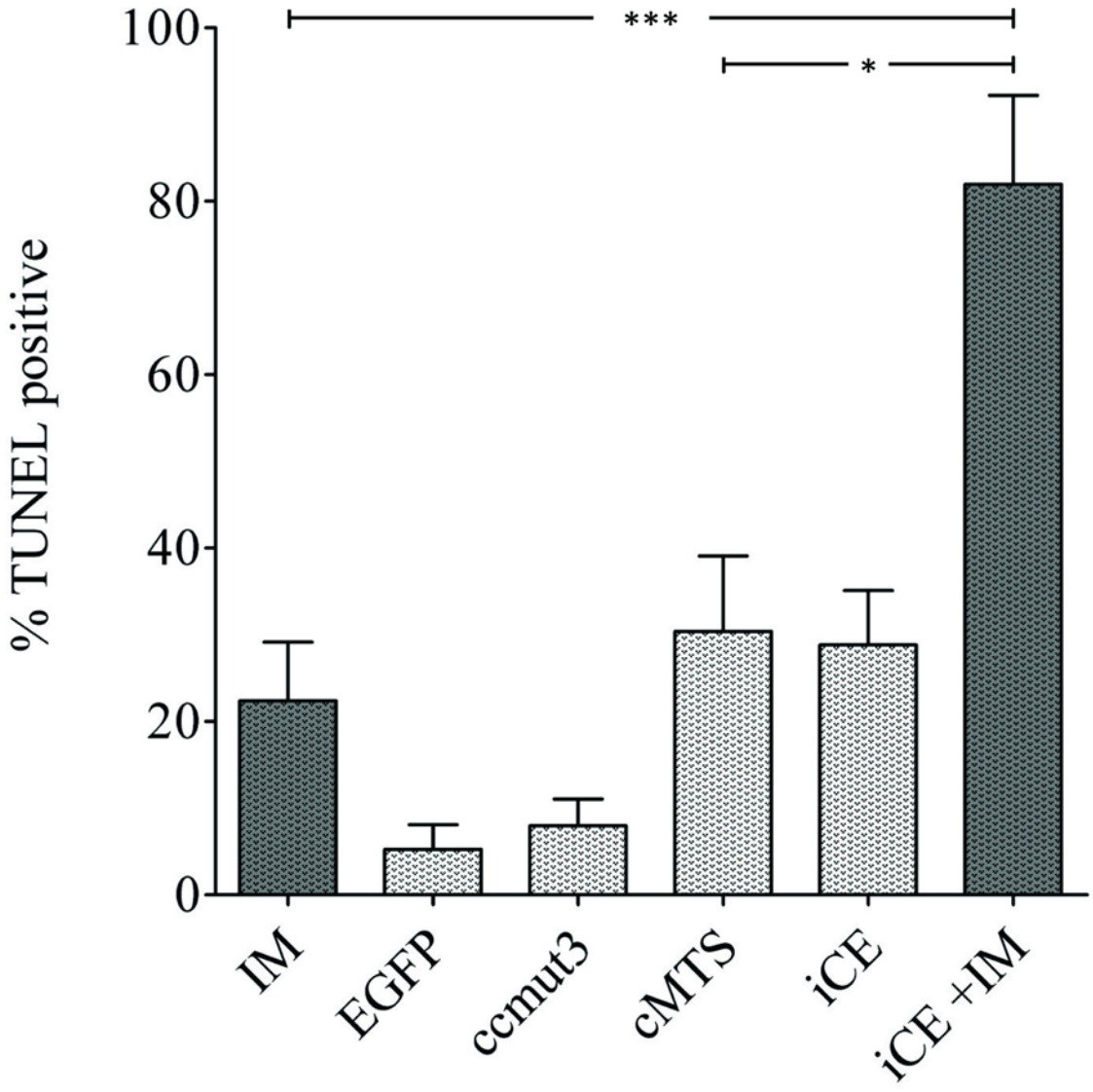

Figure 4.9: Continued

C.

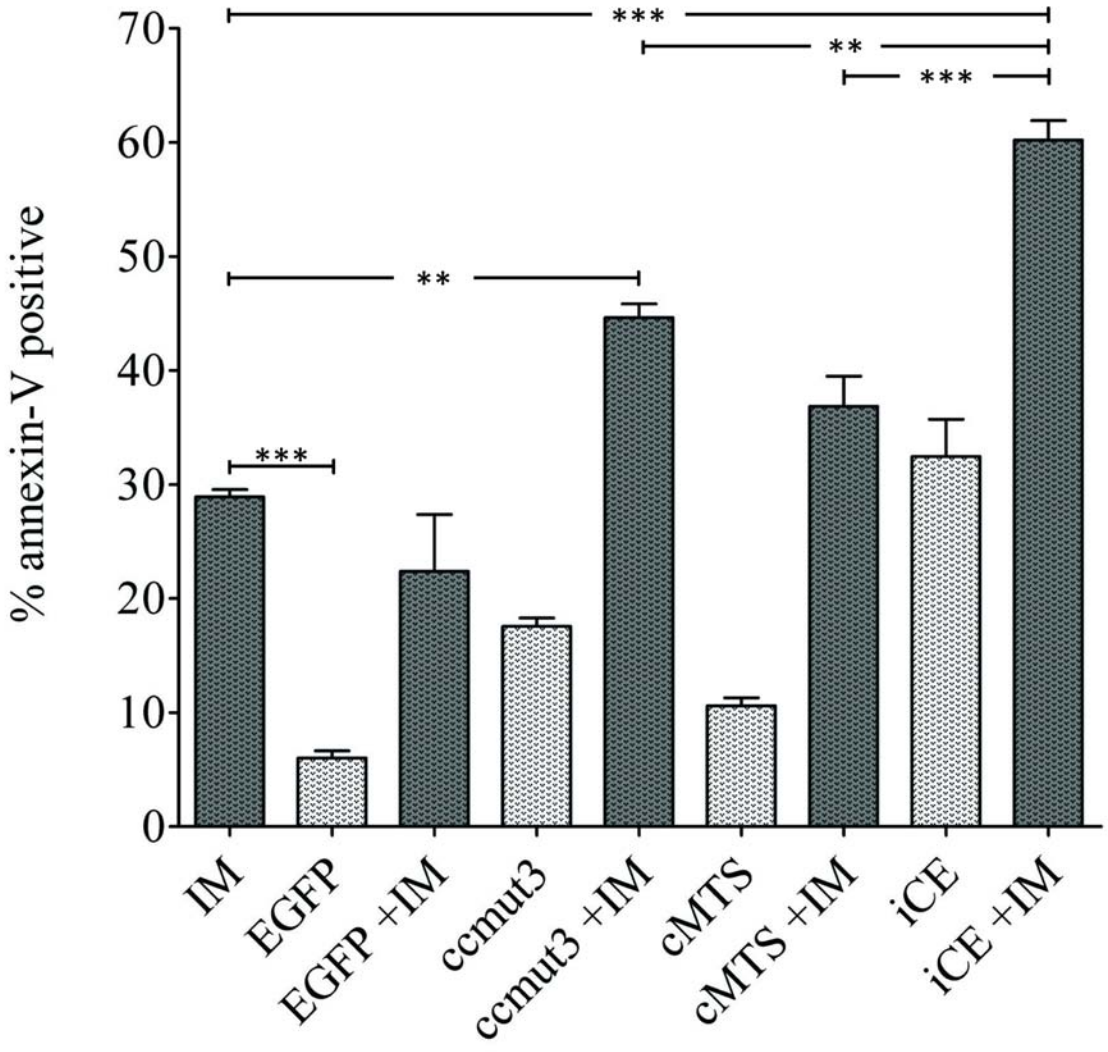

Figure 4.9: Continued

hour incubation period leaves very few cells to count in the iCE+IM treatment group (*Fig. 4.8C, bottom row, third column, 'Phase' for iCE + imatinib demonstrates the lack of cells with intact plasma membranes*). The level of apoptosis as determined by TUNEL and annexin-APC staining (in contrast to 7-AAD staining which detects late-stage necrotic/apoptotic cells) (30) was extremely significant for the combined iCE+IM when compared to IM treated K562 cells (*Fig. 4.9B, iCE+IM vs. IM; or Fig.4.9C compare iCE+IM to ccmut3+IM and cMTS+IM*). Both assays were completed 48 hours post-transfection and/or imatinib (10μM) treatment and analyzed by flow cytometry.

The iCE colocalizes with Bcr-Abl

Figure 4.10A shows the cellular localization of the EGFP-tagged iCE or its components (*see Fig. 4.5 for domain arrangement of constructs*) co-expressed with exogenous Bcr-Abl (either labeled with blue or mCherry fluorescent proteins) in Cos-7 cells. The iCE, like the ccmut3 alone, colocalizes (defined as a Pearson correlation coefficient (PCC) greater than 0.6) (19) with Bcr-Abl (Cos-7: *Fig. 4.10A, 4th row*; PCC=0.63±0.04 and 1471.1: *Fig. 4.10B*; PCC=0.83±0.05). The colocalized iCE/Bcr-Abl exhibits a distinct punctate pattern in both Cos-7 and 1471.1 cells which was different from the typical diffuse pattern of colocalized ccmut3/Bcr-Abl (*Fig. 4.10A, compare 2nd row, 1st column (Bcr-Abl with ccmut3 present) to 4th row, 1st column (Bcr-Abl with iCE present)*). In contrast, the cMTS or EGFP, as expected, do not colocalize with Bcr-Abl in either Cos-7 or 1471.1 cells (Cos-7: *Fig. 4.10A, 3rd row, PCC=0.3±0.1, for cMTS and Bcr-Abl and Fig. 4.10A, 1st row, PCC=0.02±0.03, for EGFP and Bcr-Abl*: 1471.1 data not shown). As we previously demonstrated the cMTS alone robustly localizes to the mitochondria (*Fig. 4.10C, cMTS in K562 (top) and 1471.1 (bottom)*

Figure 4.10. Representative images of exogenous Bcr-Abl coexpressed with the iCE or its individual components and cMTS mitochondrial localization. Scale bars are 5 μm.

A) Comparison of subcellular localization and association between Bcr-Abl (first column, cyan) and the iCE or iCE component parts (second column, magenta) in Cos-7 cells. The PCC values in the 'Composite' column represent the degree of colocalization between Bcr-Abl and the given construct.

B) Co-expression of Bcr-Abl (first column, cyan) and the iCE (second column, magenta) in 1471.1 cells with PCC value below the 'composite' image.

C) The cMTS (first column, cyan) strongly localizes to the mitochondria (second column, magenta) in both K562 and 1471.1 (but does not in Cos-7; not shown), as previously described (3).

A.

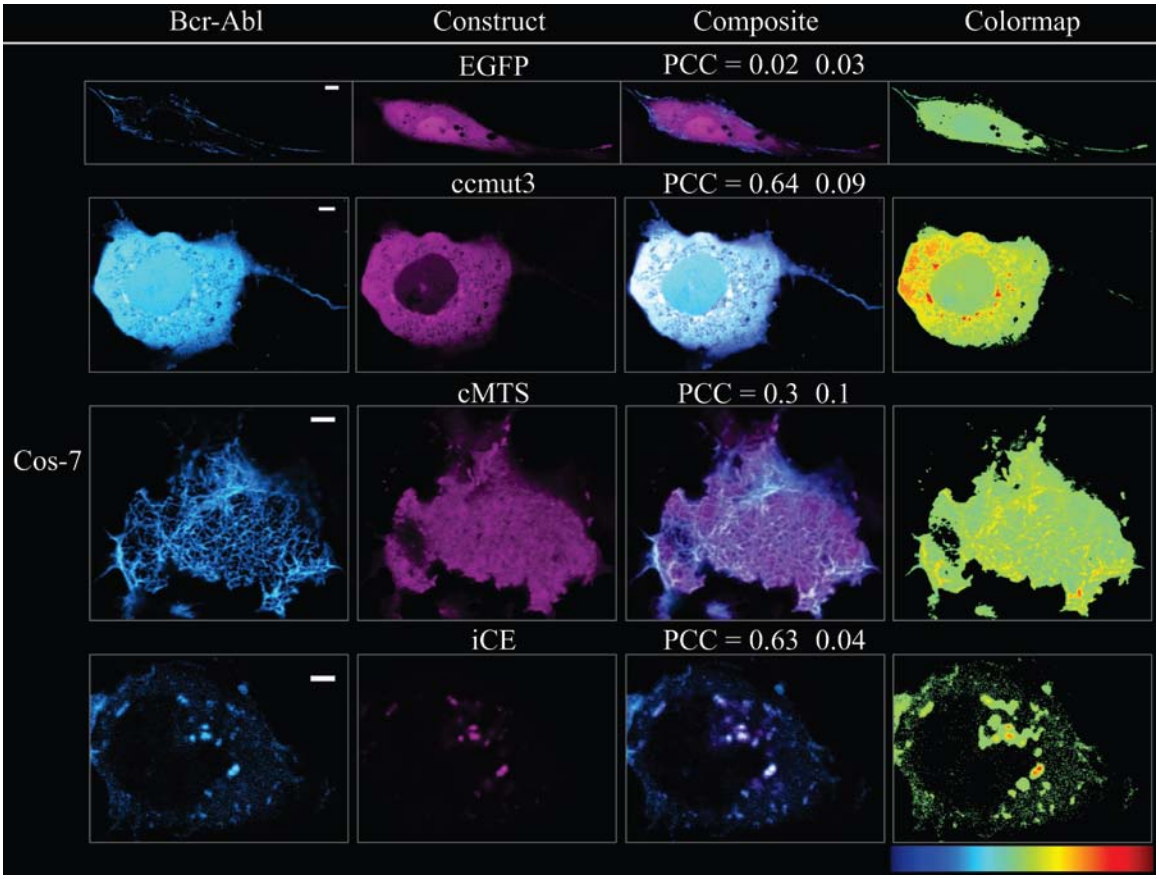
Bcr-Abl
Construct
Composite
Colormap
EGFP
PCC = 0.02 0.03
ccmut3
PCC = 0.64 0.09
cMTS
PCC = 0.3 0.1
Cos-7
iCE
PCC = 0.63 0.04

B.

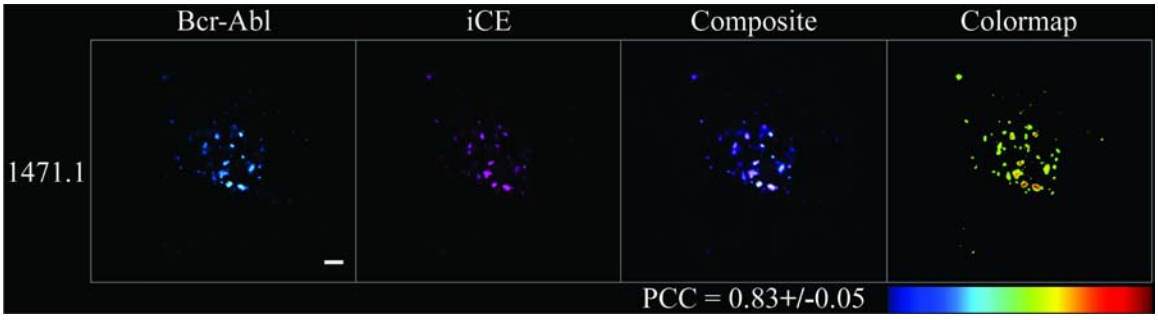
Bcr-Abl
iCE
Composite
Colormap
1471.1
PCC = 0.83+/-0.05

C.

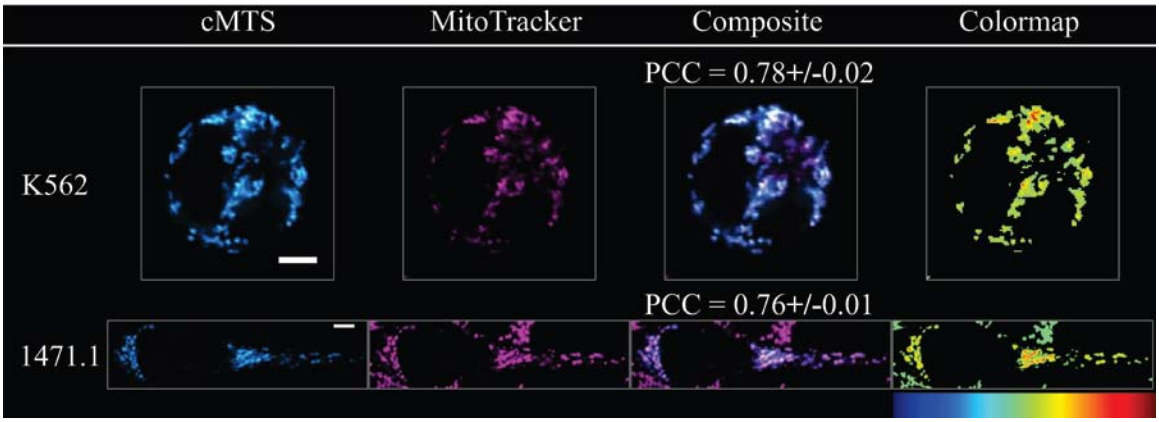
cMTS
MitoTracker
Composite
Colormap
PCC = 0.78+/-0.02
K562
PCC = 0.76+/-0.01
1471.1

compared to MitoTracker) in K562 and 1471.1 cells with higher oxidative backgrounds but not in the 'low ROS' Cos-7 (3).

The iCE did not associate with the mitochondria

Unlike the cMTS alone which strongly colocalized with the mitochondria in both K562 and 1471.1 cells (3) (*Fig. 4.10C*) the iCE remained cytoplasmic in its distribution across all three cell types (*Fig. 4.11, compare 'iCE' column to 'MitoTracker' column, 1st through 3rd rows*). Within the context of the Cos-7 cells (which have low inherent ROS levels and therefore do not activate the cMTS) (3), as with the cMTS, the iCE was not expected to localize to the mitochondria. However, the cMTS alone translocates to the mitochondria in the Bcr-Abl negative 1471.1 cell line that features an elevated level of basal ROS (3). Therefore, without Bcr-Abl to 'keep' the iCE cytoplasmic it was expected that the iCE would robustly localize to the mitochondria in this cell line. This was not the case however, and the iCE did not localize to the mitochondria of 1471.1 cells (*Fig. 4.11, 3rd row*). In K562 cells the ccmut3 alone colocalized with Bcr-Abl and the cMTS alone colocalized with the mitochondria, but the iCE did not localize to the mitochondria (*Fig. 4.11, 1st row*).

Earlier studies have demonstrated the importance of the two conserved cMTS residues S189 and T193 for activating cytoplasmic-to-mitochondrial trafficking (3, 15). When these key phospho-acceptor residues are substituted with either tyrosine or alanine the cMTS no longer translocates to the mitochondria (3, 15). Incorporating S189A and T193A mutations (i.e., iCE-Null, *see Fig. 4.5*) led to a change in the qualitative distribution difference between the iCE (punctate looking) and the diffuse iCE Null (*Fig. 4.11, compare 'iCE' in the 1st row with 'iCE Null' in the bottom row*). The only difference between the iCE and the iCE Null are

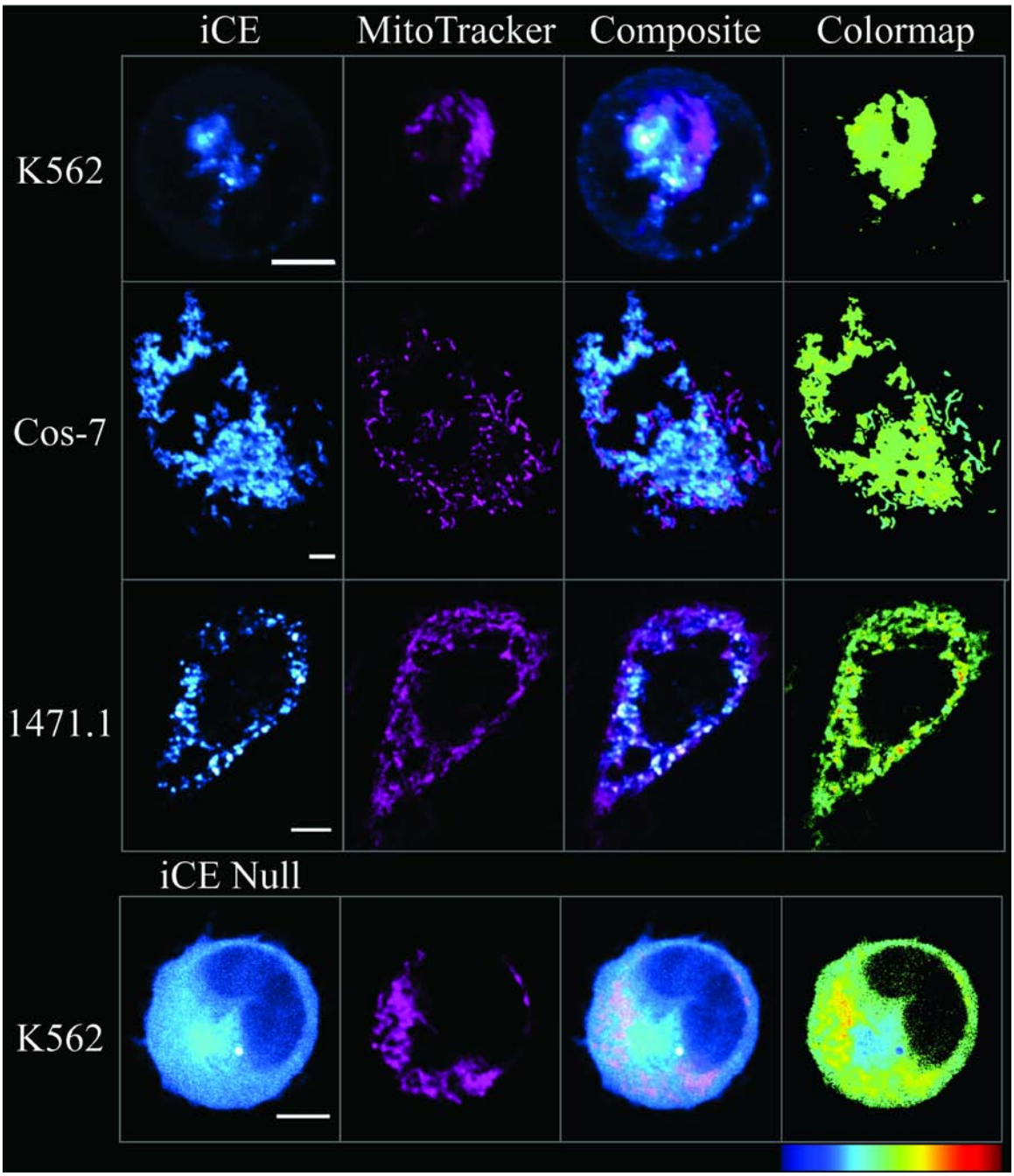

Figure 4.11. Representative images of the subcellular localization of the iCE (or iCE Null, *see Fig. 4.5*) in K562, Cos-7, and 1471.1 cells and compared to MitoTracker CMXros. The iCE did not localize to the mitochondria of K562, Cos-7 or 1471.1 cells. Scale bars are 5 µm.

the S189A and T193A mutations preventing phosphorylation at these sites in the cMTS domain of the iCE Null (*Fig. 4.5*).

The toxic effect of the iCE on K562 cells is not recapitulated upon substitution of the cMTS or the ccmut3 with another canonical MTS or Bcr-Abl binding domain

The ccmut3 and cMTS paired together uniquely confer the toxic effects of the iCE in K562 cells. When the ccmut3 is substituted for another Bcr-Abl binding domain (i.e., RIN-BD) (14) to create a mock iCE (*Fig. 4.5, RIN-cMTS*), the cytotoxic effect remains equivalent to the cMTS alone, and the concomitant use of imatinib does not potentiate toxicity beyond that of imatinib alone (*Fig. 4.12A, RIN-cMTS and RIN-cMTS+IM columns*). Furthermore, substituting the cMTS with a canonical IMS MTS (12), (*Fig. 4.5, IMS-ccmut3*) diminished the induced toxicity to that of the ccmut3 alone, or upon the addition of imatinib, no more toxicity than imatinib alone (*Fig. 4.12A, IMS-ccmut3 and IMS-ccmut3+IM columns*). The mock iCEs localize to different subcellular compartments (*Fig. 4.12B, compare top (IMS-ccmut3) and bottom (RIN-cMTS) rows*). The IMS-ccmut3 colocalizes to the mitochondria (*Fig. 4.12B, top row, compare 'IMS-ccmut3' to 'MitoTracker' columns*) while the RIN-cMTS remains cytoplasmic (*Fig. 4.12B, bottom row, compare 'RIN-cMTS' to 'MitoTracker' column*). The cellular distribution of IMS-ccmut3 (mitochondrial) and RIN-cMTS (cytoplasmic) remained the same in the presence of 10 μM imatinib (data not shown).

Figure 4.12. Domain substitution of either the ccmut3 or the cMTS in the iCE.

A) The combination of the ccmut3 and cMTS to create the iCE is toxic to K562 cells and the substitution of the Bcr-Abl binding domain, ccmut3 with RIN-BD or the cMTS with a canonical MTS (IMS MTS) does not reproduce the toxicity of the original iCE. Flow cytometric analysis for 7-AAD positivity was measured 48 hours posttransfection and/or treatment. IM, iCE, iCE+IM, ccmut3, and cMTS values are also in *Fig. 4A*. Imatinib is 10 μM. One-way ANOVA with Tukey's post-test (error bars are S.E.M., $N \geq 3$; $p < 0.001$***).

B) Representative images of the subcellular localization of the mock iCE constructs, IMS-ccmut3 (top) and RIN-cMTS (bottom), in K562 cells. Top row, the IMS-ccmut3 colocalizes with the mitochondria whereas, the RIN-cMTS, bottom row, remains cytoplasmic. Scale bars are 5μm.

A.

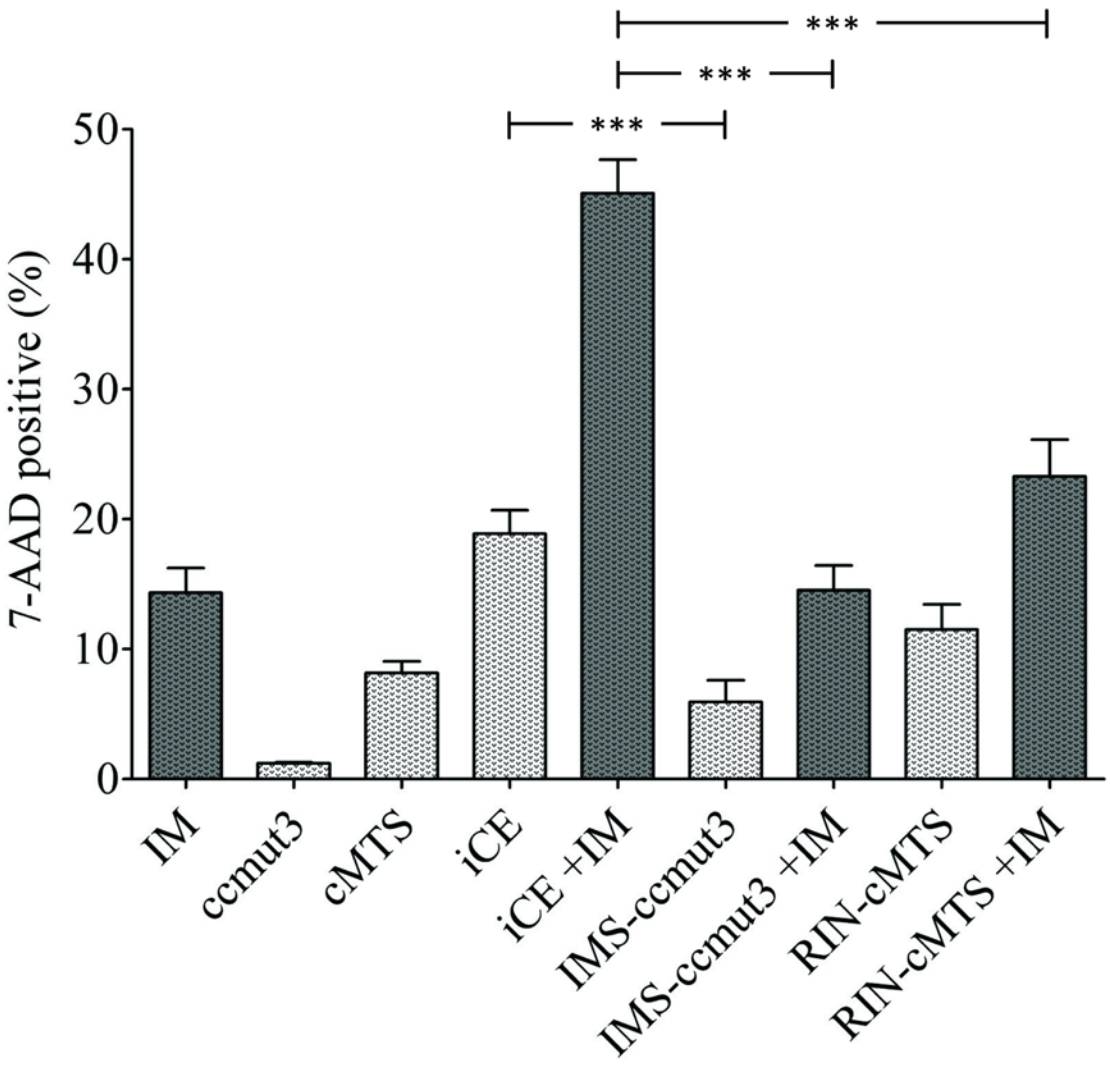
***
***
***
7-AAD positive (%)
50
40
30
20
10
0
IM
ccmut3
cMTS
iCE
iCE +IM
IMS-ccmut3
IMS-ccmut3 +IM
RIN-cMTS
RIN-cMTS +IM

B.

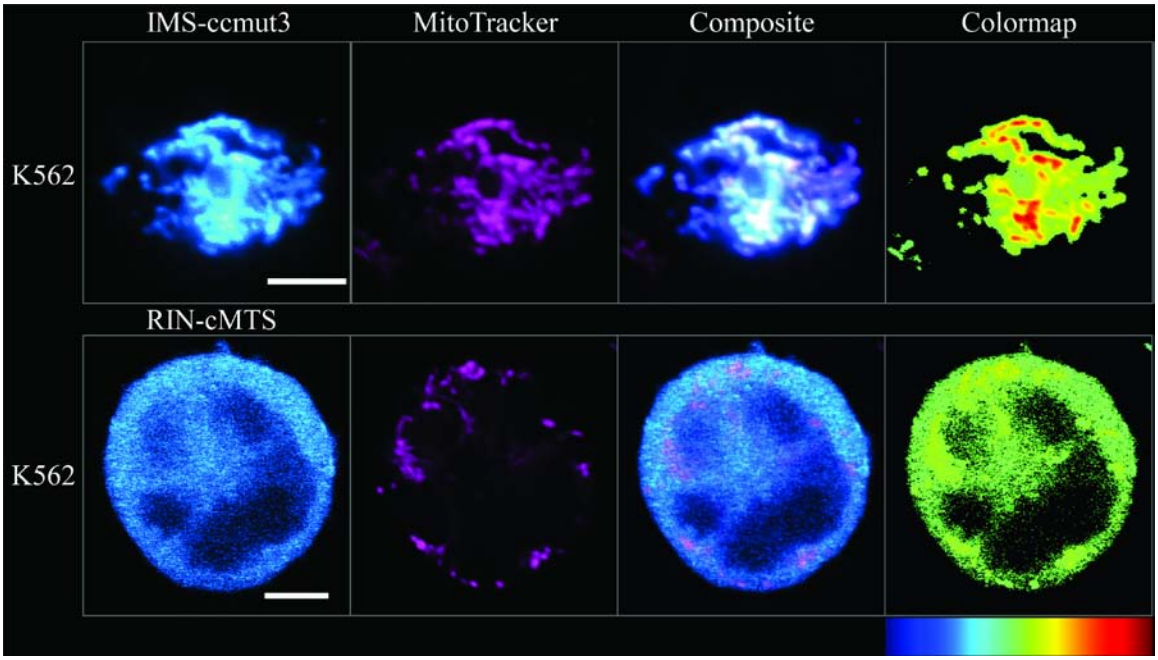
IMS-ccmut3
MitoTracker
Composite
Colormap
K562
RIN-cMTS
K562

Altering the key phospho-residues in the cMTS domain of the iCE ablates toxic effect

We and others have shown that the cMTS no longer translocates to the mitochondria when the key phospho-acceptor residues of the cMTS are substituted with either tyrosine or alanine (3, 15). Incorporating S189A and T193A mutations (i.e., iCE-Null, *see Fig. 4.5*) into the cMTS domain of the iCE leads to a significant reduction in cell death (i.e., 7-AAD) and apoptosis (e.g., annexin-APC) in K562 cells at 48 hours (*Figs. 4.13A and C, compare iCE to iCE Null columns*). However, this effect is more pronounced in combination with imatinib (*Figs. 4.13A and C, compare iCE+IM to iCE Null+IM columns*). The trend is similar for TUNEL staining but did not reach significance (*Fig. 4.13B*).

Discussion

The oncogenic Bcr-Abl protein, a causative agent for the vast majority of CML cases, was directly targeted to the mitochondria by fusion with different MTSs as a proof of concept that Bcr-Abl directed to the mitochondria could effectively be used to destroy diseased cells. Bcr-Abl was targeted to three submitochondrial regions, since the mitochondrial locations and substrates of mitochondrially death-directed c-Abl are not known (3). Similar to mitochondrial c-Abl, Bcr-Abl was highly toxic when targeted to the mitochondria of CML cells (*Fig. 4.2, 3rd column*). Interestingly, and unlike c-Abl (31), Bcr-Abl's mitochondrial cytotoxic effect was independent of its kinase activity (*Fig. 4.2, 4th column*). However, there are instances where the kinase activity of c-Abl is dispensable for the induction of apoptosis (e.g., via p38 MAPK) (32). Overall, the tyrosine kinase-independent killing of CML cells is compelling because it suggests that the strategy of targeting Bcr-Abl to

Figure 4.13. Reduction in cell death and apoptosis at 48 hours in K562 cells with phospho-residue substitutions in the iCE. Cell death (7-AAD) and apoptosis (annexin-APC and TUNEL) were measured by flow cytometric analysis. Imatinib is 10 μM.

A) 7-AAD staining reveals a marked attenuation in the iCE's cell death effect with and without the presence of imatinib (10 μM). IM, EGFP, iCE, and iCE+IM, values are also in *Fig. 4.7A*. One-way ANOVA with Tukey's post-test.

B) Apoptosis as measured by TUNEL shows a similar trend to 7-AAD and annexin-APC. IM, EGFP, iCE, and iCE+IM, values are also in *Fig. 4.9B*. One-way ANOVA with Tukey's post-test.

C) Annexin-APC staining corroborated cell death analysis (7-AAD) to show that S189 and T193 are essential for the toxic effect of the iCE. IM, EGFP, iCE, and iCE+IM, values are also in *Fig. 4.9C*. One-way ANOVA with Tukey's post-test (for all assays here, error bars are S.E.M., $N \geq 3$; $p<0.05$*, $p<0.01$**, $p<0.001$***).

A.

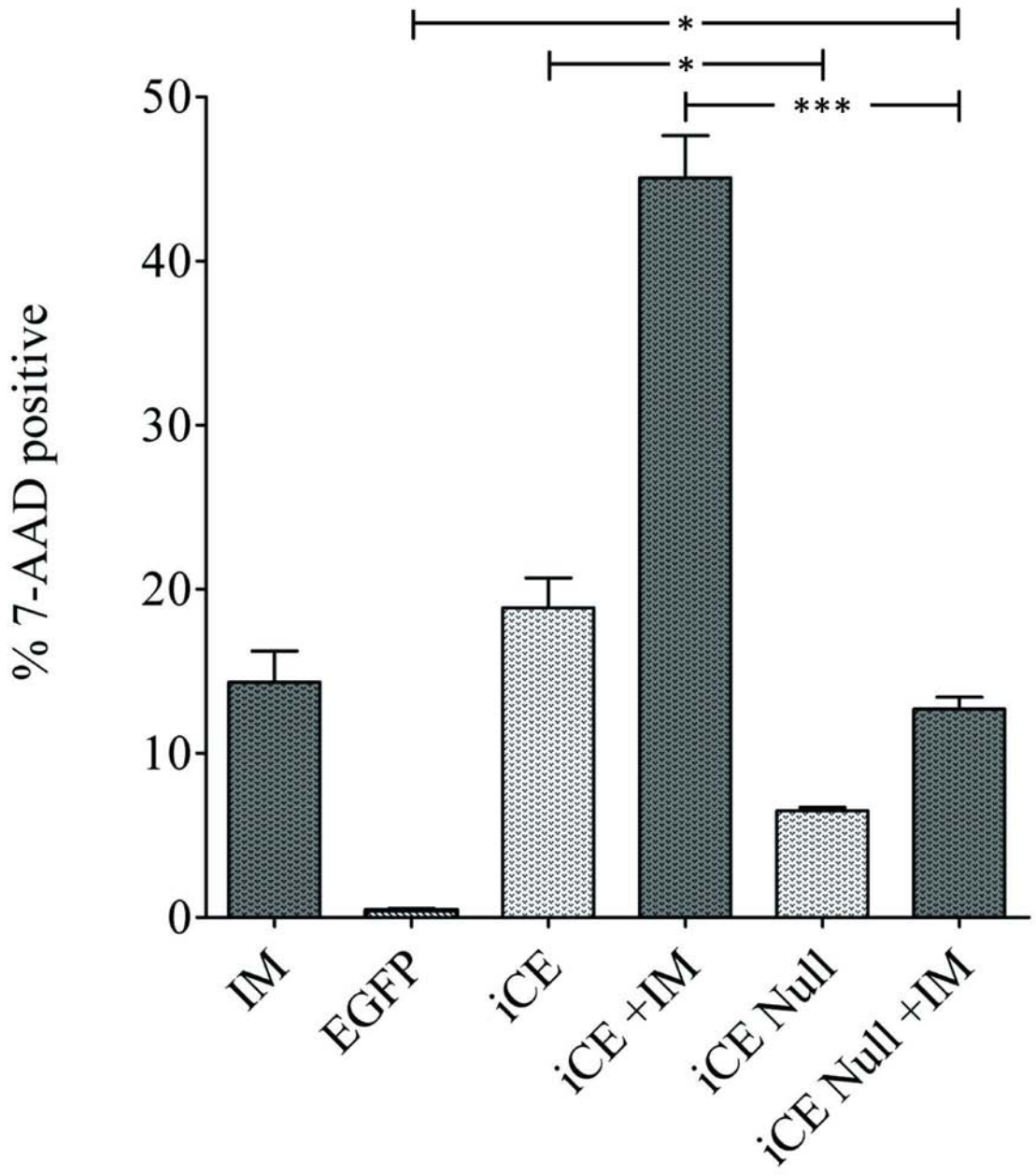
*
*
***
50
40
30
20
10
0
% 7-AAD positive
IM
EGFP
iCE
iCE +IM
iCE Null
iCE Null +IM

B.

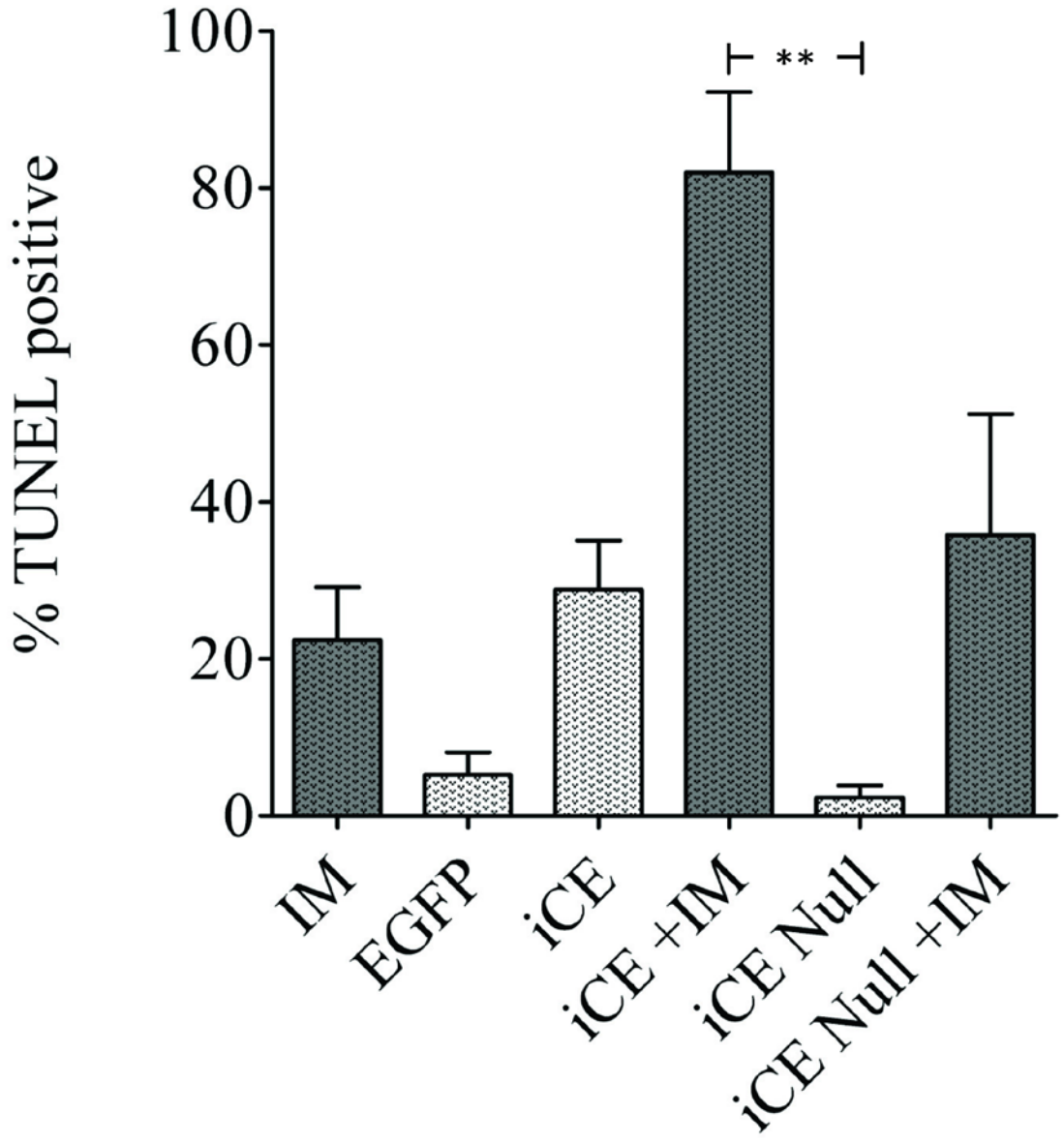
% TUNEL positive
100
80
60
40
20
0
**
IM
EGFP
iCE
iCE +IM
iCE Null
iCE Null +IM

C.

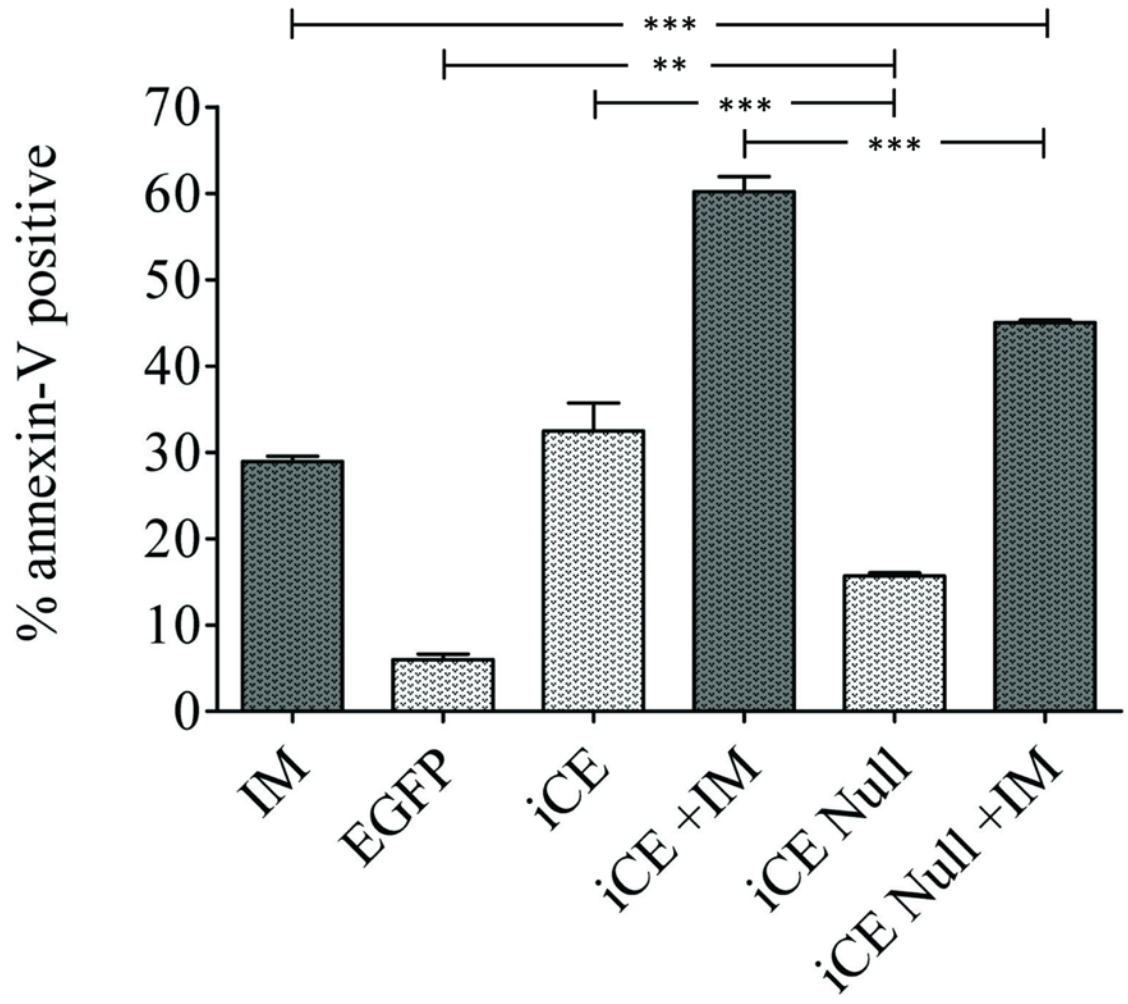
***
**
***
***
% annexin-V positive
70
60
50
40
30
20
10
0
IM
EGFP
iCE
iCE +IM
iCE Null
iCE Null +IM

the mitochondria would be compatible with and complementary to current tyrosine kinase inhibitor (TKI) therapy.

This led to an attempt to forcibly translocate endogenous Bcr-Abl by means of a designed chaperone protein to exploit the toxicity of mitochondrial Bcr-Abl (*Fig. 4.5, schematic of constructs*). The intracellular cryptic escort (iCE) was constructed to bind to and move endogenous Bcr-Abl to the mitochondria. We have previously characterized two domains comprising the iCE (ccmut3 and cMTS) (2, 3). The ccmut3 Bcr-Abl binding domain demonstrated efficient relocalization of Bcr-Abl to the nuclear compartment when fused to four NLSs (i.e., 4NLS-ccmut3) (13) and the cMTS was used to directly and selectively target c-Abl to the mitochondria in K562 cells (i.e., Abl-cMTS) (3).

Consistent with the cytotoxicity (7-AAD positivity) elicited by the direct mitochondrial targeting of Bcr-Abl at 48 hours (*Fig. 4.3B, 3^{rd} – 5^{th} columns*), the iCE also induced cell death (*Fig. 4.7A, iCE column*) within a similar time range. However, subcellular compartmental analysis of confocal images comparing between the mitochondria (stained with MitoTracker) and fluorescent protein tagged iCE fluorescence and/or Bcr-Abl did not indicate any mitochondrial accumulation of the iCE or iCE/Bcr-Abl (*Fig. 4.12, compare iCE column to MitoTracker column, K562 cells*). Therefore, the cytoplasmically localized iCE and the mitochondrially targeted Bcr-Abl (MTS-Bcr-Abl) are likely inducing cell death by different mechanisms.

Our experience with NLSs (e.g., 1 NLS was insufficient to move Bcr-Abl but four NLSs were) (5) suggest that the ‘strength’ of the cMTS (within the iCE) was not sufficient to overcome the cytoplasmic interactions of Bcr-Abl for efficient translocation to the mitochondria. Anticipating that this could happen, we employed imatinib to better facilitate

iCE-to-mitochondrial targeting for two reasons. First, imatinib treatment increases the level of ROS/PKC activity which in turn leads to more robust mitochondrial localization of the cMTS (3). Secondly, imatinib bound Bcr-Abl undergoes a conformational change that decreases actin binding and frees Bcr-Abl for relocalization (33). Yet, even with the addition of 10 μM imatinib the iCE did not localize to the mitochondria in K562 cells. Furthermore, the iCE did not localize to the mitochondria in the elevated ROS, but Bcr-Abl-negative 1471.1 cell line revealing that the ccmut3 fusion to the cMTS may compromise the capacity for iCE mitochondrial translocation.

Nonetheless, the cell death effect caused by the iCE appears to be entirely dependent upon the combination of the ccmut3 and cMTS. Mock 'iCE's' substituting either the ccmut3 with RIN-BD (RIN-cMTS; RIN-BD binds SH3/SH2 domains of Bcr-Abl) (14) or the cMTS with the canonical IMS MTS (IMS-ccmut3; IMS targets the intermitochondrial membrane space) (12) failed to restore cell death beyond control levels. The RIN-cMTS and IMS-ccmut3 results suggest that the toxicity of the iCE is not propagated by either ccmut3 localization to the mitochondria or the cMTS remaining bound to Bcr-Abl (at least to the SH2/SH3 domains via RIN-BD, which would put the cMTS domain of the iCE on Bcr-Abl but at a different location) in the cytoplasm. Moreover, a phosphorylation null mutant version of the cMTS domain of the iCE lost cytotoxic potency.

The ccmut3 alone and imatinib, as expected (2), both reduced the level of phospho-Bcr-Abl and Bcr-Abl substrate phosphorylation (i.e., p-Stat5 and p-Crk-L), but the iCE and iCE Null were unchanged from control in K562 cells (western blot; data not shown). Therefore, the iCE is not acting as a dominant-negative for Bcr-Abl kinase activity. Yet since the iCE colocalizes with Bcr-Abl it may be disrupting nonkinase Bcr-Abl

survival/antiapoptotic function. For instance, the iCE may increase the steric hindrance of kinase-independent signaling from Bcr-Abl such as Src kinase Hck phosphorylation of the Grb2 binding site on Bcr-Abl or Bcr's RhoGEF activity (34, 35).

Alternatively, it may be possible that the ccmut3 (binding in an anti-parallel coiled-coil) (17) positions the cMTS where the phosphorylation of the S189 (PKA) and/or T193 (PKC) is central to the mechanism for cell death induction. Interestingly, cMTS mitochondrial translocation (i.e., not cytotoxic) must be 'activated', via phosphorylation (S189 and/or T193), and subsequently chaperoned to the mitochondria by Hsp70 (15). However, in K562 cells only phosphorylation of the T193 is critical for mitochondrial translocation whereas S189 is not (3). Perhaps the cytotoxic nature of the iCE is also primarily a function of PKC phosphorylation. Although beyond the scope of this paper, a negative feedback coupling of PKC and Bcr-Abl involving transient calcium influx may play a role in the essential nature of cMTS phospho-residues, and T193 in particular. Increased transient calcium influx can stimulate cellular proliferation while blocking calcium influx via PKC activation is toxic to Ph^+ leukemia cells (36). Inhibition of Bcr-Abl activity with imatinib relieves negative regulation of PKC and thereby diminishes intracellular calcium flux (36). Perhaps increased stimulation or altered localization of PKC (due to the presence of the iCE) could further diminish transient calcium influx. A fascinating possibility that connects calcium homeostasis and iCE toxicity is depicted in *Fig. 4.14*. (36).

In this report, we demonstrate that direct targeting of Bcr-Abl to the mitochondria elicits potent cell death induction in a cell type specific and kinase-independent manner. Additionally, we attempted to the harness Bcr-Abl's mitochondrial death induction activity with the use of a designed protein chaperone (i.e., iCE) in order to restore the defunct

Figure 4.14. Possible mechanisms for iCE induced toxicity to K562 leukemia cells. With imatinib (IM) present, Bcr-Abl kinase activity is eliminated (1) and the iCE may be potentiating leukemic cell death by altering calcium status and/or blocking kinase-independent oncogenic functions of Bcr-Abl. Bcr-Abl tyrosine kinase (Y kinase) activity stimulates transient calcium influx (which stimulates proliferation) while PKC activation, at the plasma membrane, can have the opposite effect on calcium transients which has been shown to be toxic to leukemia cells (36-38). Another cause of iCE enhanced cell death may be through a more complete blockade of Bcr-Abl signaling by steric restriction of kinase-independent pathways (34, 39). Steric effects may be caused by the presence of PKA and/or PKC, a conformational change in the cMTS domain, and/or binding of Hsp70 to the phosphorylated cMTS (15). iCE toxicity requires interaction with Bcr-Abl via the CC domain and the cMTS (S/T phospho-residues). The ccmut3 competes with Bcr-Abl for oligomerization at the N-terminal portion of the Bcr to Abl fusion (2) at the CC, blocking Bcr-Abl transautophosphorylation (17).

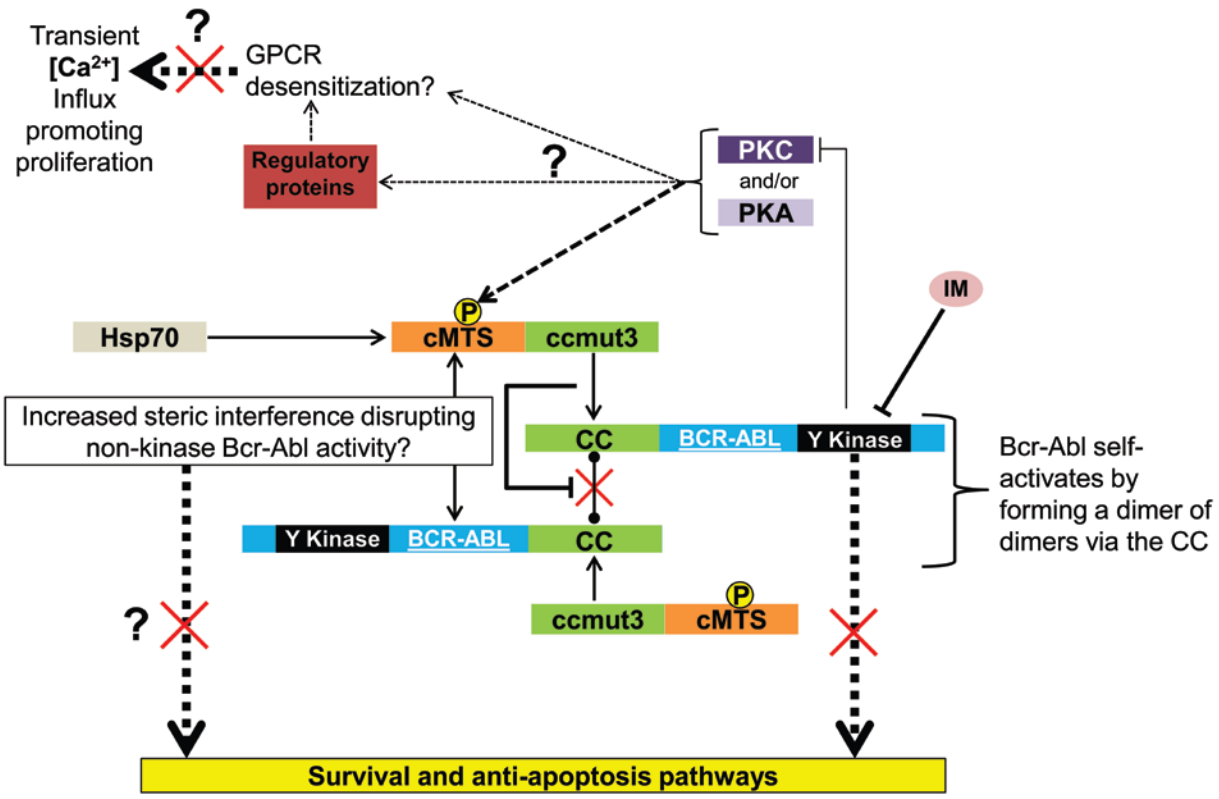
Transient
[Ca2+]
Influx
promoting
proliferation
?
GPCR
desensitization?
Regulatory
proteins
?
PKC
and/or
PKA
IM
Hsp70
P
cMTS
ccmut3
Increased steric interference disrupting
non-kinase Bcr-Abl activity?
CC
BCR-ABL
Y Kinase
Bcr-Abl self-
activates by
forming a dimer of
dimers via the CC
Y Kinase
BCR-ABL
CC
?
ccmut3
P
cMTS
Survival and anti-apoptosis pathways

apoptotic avenue of ‘mitochondrially death directed c-Abl’ in CML cells. Though the iCE bound to Bcr-Abl, the iCE/Bcr-Abl complex did not translocate to the mitochondria. However, the iCE combined with imatinib treatment is a potent killer of leukemic cells. We observed robust killing as measured by 7-AAD (late apoptosis/necrosis), TUNEL (apoptosis/necrosis), annexin-V (apoptosis) and trypan blue exclusion assay (cell viability).

Acknowledgements

We acknowledge the use of the University of Utah, School of Medicine, Cell Imaging Facility and would like to thank the Director, Chris Rodesch, PhD, for scientific discussions. We would also like to thank Dr. Andy Dixon, J. Rian Davis, Ben Bruno, and Geoff Miller for scientific discussions. The Core Facilities described in this project were supported by Award Number P30CA042014 from the National Cancer Institute. The content is solely the responsibility of the authors and does not necessarily represent the official views of the National Cancer Institute or the National Institutes of Health. The authors declare that they have no competing interests. This work was funded by NIH R01-CA129528 and by an AFPE Pre-Doctoral Fellowship (JEC). This work was supported in part by a grant to University of Utah from the Howard Hughes Medical Institute through the Med into Grad Initiative (DW).

References

1. O. Hantschel, S. Wiesner, T. Guttler, C.D. Mackereth, L.L. Rix, Z. Mikes, J. Dehne, D. Gorlich, M. Sattler, and G. Superti-Furga. Structural basis for the cytoskeletal association of Bcr-Abl/c-Abl. Mol Cell. 19:461-473 (2005).

2. A.S. Dixon, G.D. Miller, B.J. Bruno, J.E. Constance, D.W. Woessner, T.P. Fidler, J.C. Robertson, T.E. Cheatham, and C.S. Lim. Improved coiled-coil design enhances interaction with Bcr-Abl and induces apoptosis. Mol Pharm. 9:187-195 (2012).

3. J.E. Constance, S.D. Despres, A. Nishida, and C.S. Lim. Selective Targeting of c-Abl via a Cryptic Mitochondrial Targeting Signal Activated by Cellular Redox Status in Leukemic and Breast Cancer Cells. Pharmaceutical Research (2012).

4. P. Vigneri and J.Y. Wang. Induction of apoptosis in chronic myelogenous leukemia cells through nuclear entrapment of BCR-ABL tyrosine kinase. Nature Medicine. 7:228-234 (2001).

5. A.S. Dixon, M. Kakar, K.M. Schneider, J.E. Constance, B.C. Paullin, and C.S. Lim. Controlling subcellular localization to alter function: Sending oncogenic Bcr-Abl to the nucleus causes apoptosis. J Control Release. 140:245-249 (2009).

6. X. Qi and D. Mochly-Rosen. The PKCdelta -Abl complex communicates ER stress to the mitochondria - an essential step in subsequent apoptosis. J Cell Sci. 121:804-813 (2008).

7. S. Kumar, A. Bharti, N.C. Mishra, D. Raina, S. Kharbanda, S. Saxena, and D. Kufe. Targeting of the c-Abl tyrosine kinase to mitochondria in the necrotic cell death response to oxidative stress. The Journal of Biological Chemistry. 276:17281-17285 (2001).

8. M. Gupta, L. Milani, M. Hermansson, B. Simonsson, B. Markevarn, A.C. Syvanen, and G. Barbany. Expression of BCR-ABL1 oncogene relative to ABL1 gene changes overtime in chronic myeloid leukemia. Biochem Biophys Res Commun. 366:848-851 (2008).

9. M. Mancini, N. Veljkovic, V. Corradi, E. Zuffa, P. Corrado, E. Pagnotta, G. Martinelli, E. Barbieri, and M.A. Santucci. 14-3-3 ligand prevents nuclear import of c-ABL protein in chronic myeloid leukemia. Traffic. 10:637-647 (2009).

10. G. Isaya, W.A. Fenton, J.P. Hendrick, K. Furtak, F. Kalousek, and L.E. Rosenberg. Mitochondrial import and processing of mutant human ornithine transcarbamylase precursors in cultured cells. Molecular and Cellular Biology. 8:5150-5158 (1988).

11. R. Rizzuto, A.W. Simpson, M. Brini, and T. Pozzan. Rapid changes of mitochondrial Ca2+ revealed by specifically targeted recombinant aequorin. Nature. 358:325-327 (1992).

12. T. Ozawa, Y. Natori, Y. Sako, H. Kuroiwa, T. Kuroiwa, and Y. Umezawa. A minimal peptide sequence that targets fluorescent and functional proteins into the mitochondrial intermembrane space. ACS Chem Biol. 2:176-186 (2007).

13. A.S. Dixon, J.E. Constance, T. Tanaka, T.H. Rabbitts, and C.S. Lim. Changing the Subcellular Location of the Oncoprotein Bcr-Abl Using Rationally Designed Capture Motifs. Pharm Res (2011).

14. D.E. Afar, L. Han, J. McLaughlin, S. Wong, A. Dhaka, K. Parmar, N. Rosenberg, O.N. Witte, and J. Colicelli. Regulation of the oncogenic activity of BCR-ABL by a tightly bound substrate protein RIN1. Immunity. 6:773-782 (1997).

15. M.A. Robin, S.K. Prabu, H. Raza, H.K. Anandatheerthavarada, and N.G. Avadhani. Phosphorylation enhances mitochondrial targeting of GSTA4-4 through increased affinity for binding to cytoplasmic Hsp70. J Biol Chem. 278:18960-18970 (2003).

16. W. Strober. Trypan blue exclusion test of cell viability. Curr Protoc Immunol. Appendix 3:Appendix 3B (2001).

17. A.S. Dixon, S.S. Pendley, B.J. Bruno, D.W. Woessner, A.A. Shimpi, T.E. Cheatham, 3rd, and C.S. Lim. Disruption of Bcr-Abl coiled coil oligomerization by design. J Biol Chem. 286:27751-27760.

18. W.S. Rasband. BG subtraction from ROI plugin. Available from: www.uhnres.utoronto.ca/facilities/wcif/imagej/image_intensity_proce.htm#intensity_BG. (2004).

19. S. Bolte and F.P. Cordelieres. A guided tour into subcellular colocalization analysis in light microscopy. J Microsc. 224:213-232 (2006).

20. S.V. Costes, D. Daelemans, E.H. Cho, Z. Dobbin, G. Pavlakis, and S. Lockett. Automatic and quantitative measurement of protein-protein colocalization in live cells. Biophys J. 86:3993-4003 (2004).

21. A.L. Barlow, A. Macleod, S. Noppen, J. Sanderson, and C.J. Guerin. Colocalization analysis in fluorescence micrographs: verification of a more accurate calculation of pearson's correlation coefficient. Microsc Microanal. 16:710-724 (2010).

22. F. Jaskolski, C. Mulle, and O.J. Manzoni. An automated method to quantify and visualize colocalized fluorescent signals. J Neurosci Methods. 146:42-49 (2005).

23. H. Lecoeur, L.M. de Oliveira-Pinto, and M.L. Gougeon. Multiparametric flow cytometric analysis of biochemical and functional events associated with apoptosis and oncosis using the 7-aminoactinomycin D assay. J Immunol Methods. 265:81-96 (2002).

24. M. Mossalam, K.J. Matissek, A. Okal, J.E. Constance, and C.S. Lim. Direct induction of apoptosis using an optimal mitochondrially targeted p53. Mol Pharm. 9:1449-1458 (2012).

25. K. Kyrylkova, S. Kyryachenko, M. Leid, and C. Kioussi. Detection of Apoptosis by TUNEL Assay. Methods Mol Biol. 887:41-47 (2012).

26. M. van Engeland, L.J. Nieland, F.C. Ramaekers, B. Schutte, and C.P. Reutelingsperger. Annexin V-affinity assay: a review on an apoptosis detection system based on phosphatidylserine exposure. Cytometry. 31:1-9 (1998).

27. X. Zhang and R. Ren. Bcr-Abl efficiently induces a myeloproliferative disease and production of excess interleukin-3 and granulocyte-macrophage colony-stimulating factor in mice: a novel model for chronic myelogenous leukemia. Blood. 92:3829-3840 (1998).

28. S.J. Ralph, S. Rodriguez-Enriquez, J. Neuzil, E. Saavedra, and R. Moreno-Sanchez. The causes of cancer revisited: "mitochondrial malignancy" and ROS-induced oncogenic transformation - why mitochondria are targets for cancer therapy. Mol Aspects Med. 31:145-170 (2010).

29. M. Sattler, S. Verma, G. Shrikhande, C.H. Byrne, Y.B. Pride, T. Winkler, E.A. Greenfield, R. Salgia, and J.D. Griffin. The BCR/ABL tyrosine kinase induces production of reactive oxygen species in hematopoietic cells. The Journal of Biological Chemistry. 275:24273-24278 (2000).

30. G. Kroemer, L. Galluzzi, P. Vandenabeele, J. Abrams, E.S. Alnemri, E.H. Baehrecke, M.V. Blagosklonny, W.S. El-Deiry, P. Golstein, D.R. Green, M. Hengartner, R.A. Knight, S. Kumar, S.A. Lipton, W. Malorni, G. Nunez, M.E. Peter, J. Tschopp, J. Yuan, M. Piacentini, B. Zhivotovsky, and G. Melino. Classification of cell death: recommendations of the Nomenclature Committee on Cell Death 2009. Cell Death and Differentiation. 16:3-11 (2009).

31. S. Kumar, N. Mishra, D. Raina, S. Saxena, and D. Kufe. Abrogation of the cell death response to oxidative stress by the c-Abl tyrosine kinase inhibitor STI571. Molecular Pharmacology. 63:276-282 (2003).

32. E.M. Galan-Moya, J. Hernandez-Losa, C.I. Aceves Luquero, M.A. de la Cruz-Morcillo, C. Ramirez-Castillejo, J.L. Callejas-Valera, A. Arriaga, A.F. Aranburo, S. Ramon y Cajal, J. Silvio Gutkind, and R. Sanchez-Prieto. c-Abl activates p38

MAPK independently of its tyrosine kinase activity: Implications in cisplatin-based therapy. Int J Cancer. 122:289-297 (2008).

33. M. Preyer, P. Vigneri, and J.Y. Wang. Interplay between kinase domain autophosphorylation and F-actin binding domain in regulating imatinib sensitivity and nuclear import of BCR-ABL. PLoS One. 6:e17020 (2011).

34. M. Warmuth, M. Bergmann, A. Priess, K. Hauslmann, B. Emmerich, and M. Hallek. The Src family kinase Hck interacts with Bcr-Abl by a kinase-independent mechanism and phosphorylates the Grb2-binding site of Bcr. J Biol Chem. 272:33260-33270 (1997).

35. D. Vigil, J. Cherfils, K.L. Rossman, and C.J. Der. Ras superfamily GEFs and GAPs: validated and tractable targets for cancer therapy? Nat Rev Cancer. 10:842-857 (2010).

36. A. Vichalkovski, I. Kotevic, N. Gebhardt, R. Kaderli, and H. Porzig. Tyrosine kinase modulation of protein kinase C activity regulates G protein-linked Ca2+ signaling in leukemic hematopoietic cells. Cell Calcium. 39:517-528 (2006).

37. F. Pellicano, M. Copland, H.G. Jorgensen, J. Mountford, B. Leber, and T.L. Holyoake. BMS-214662 induces mitochondrial apoptosis in chronic myeloid leukemia (CML) stem/progenitor cells, including CD34+38- cells, through activation of protein kinase Cbeta. Blood. 114:4186-4196 (2009).

38. G. Robert, I. Ben Sahra, A. Puissant, P. Colosetti, N. Belhacene, P. Gounon, P. Hofman, F. Bost, J.P. Cassuto, and P. Auberger. Acadesine kills chronic myelogenous leukemia (CML) cells through PKC-dependent induction of autophagic cell death. PLoS One. 4:e7889 (2009).

39. J.A. Wertheim, K. Forsythe, B.J. Druker, D. Hammer, D. Boettiger, and W.S. Pear. BCR-ABL-induced adhesion defects are tyrosine kinase-independent. Blood. 99:4122-4130 (2002).

CHAPTER 5

CONCLUSIONS AND FUTURE WORK

Conclusions

Chronic myelogenous leukemia (CML) is the disease for which the first triumph of rational drug design turned a near certain death sentence at diagnosis into a manageable chronic condition for many people (1). Nonetheless, the following decade has revealed that instances of resistance and relapse necessitate continued vigilance and effort on behalf of CML researchers (1). Toward this effort, we confirm our hypothesis that *forcing Bcr-Abl to the mitochondria will selectively induce the death of leukemic cells by converting Bcr-Abl into an apoptotic factor*.

While remaining embedded in the cytoplasmic space Bcr-Abl exerts proliferative, survival, and anti-apoptotic signaling via its multifunctional domain structure and aberrantly active tyrosine kinase domain (2). However, the c-Abl portion of Bcr-Abl is an inducer of apoptosis when it is active and localized to the mitochondria (3) (Chapter 3). Following this we have shown that Bcr-Abl can be turned into a potent mitochondriotoxic agent (Chapter 4). Our ultimate goal was to transition from proof of concept (i.e., mitochondrial Bcr-Abl is toxic to leukemia cells) to a therapeutic entity (the intracellular cryptic escort (iCE)) that could move endogenous Bcr-Abl to the mitochondria. The iCE was modeled after the normal mitochondrial ‘death-directed’ c-Abl chaperone mechanism (4). However, the attempt to relocate Bcr-Abl with the iCE

failed. Still, we discovered that the Bcr-Abl binding iCE had an unexpected leukemia specific toxicity which was potentiated by imatinib. We conclude that the iCE kills (at least in part) by a tyrosine kinase-independent mechanism and also that mitochondrial Bcr-Abl is toxic regardless of kinase status. Both of these findings have implications for opening new angles of attack on CML.

Cryptic mitochondrial translocation signal (cMTS)

The cMTS sequence is derived from the C-terminal 50-amino acid sequence from glutathione S-transferase A4-4 (GSTA4-4) and is only revealed for mitochondrial targeting upon phosphorylation by PKA at Ser-189 and/or PKC at Thr-193. This cMTS is sensitive to the cellular oxidative state and readily translocates from the cytoplasm to the mitochondria under conditions of oxidative stress, as found in CML cells (5). Ph^+ cells have elevated levels of ROS and consequently increased levels of active PKC (6).

Therefore, it was hypothesized that the oxidative background in Ph^+ cells would better facilitate iCE cytoplasmic-to-mitochondrial targeting, over cells with normal homeostatic control, while permitting sufficient iCE/Bcr-Abl interaction time. Results from other studies had previously demonstrated that unless stimulated, with PKA or PKC inducers/activators, the cMTS translocates to the mitochondria only modestly (~6% actually being imported into the matrix at 48 hours posttransfection) (5). We initially expected that some level of optimization (between PKA/PKC stimulation/inhibition) may be required to find a balance between sufficient binding and mitochondrial targeting. However, the robust level of activation and mitochondrial localization of the cMTS just from the inherent conditions in K562 (and in 1471.1 breast cancer cells) was unexpected.

Moreover, our study revealed that T193 (PKC) was the critical residue for mitochondrial targeting in K562 and 1471.1 cells. Therefore, we were able to confirm and extend the oxidative stress activated translocation of the cMTS (and cMTS fused to c-Abl) in K562 and 1471.1 cells.

c-Abl targeted to the mitochondria

In order to target native c-Abl to the mitochondria any MTS fusion must be located at the C-terminus to prevent disruption of c-Abl's autoinhibitory conformation (2). The cMTS is a C-terminal MTS as is the MTS derived from Bcl-X_L. Therefore, these two MTSs allowed the direct targeting of native c-Abl to the mitochondrial matrix and outer membrane, respectively (5, 7). While c-Abl has been stimulated to localize to the mitochondria by myriad cellular insults (8), it has not, to our knowledge, ever been directly targeted to the mitochondria. We were able to confirm that c-Abl is a pro-apoptotic factor when localized to the mitochondrial matrix but not the OMM in K562 cells (9). The mitochondrial matrix-localized c-Abl was relatively (compared to controls) more toxic to K562 than 1471.1 cells (c-Abl did not accumulate in the mitochondria of Cos-7 because the cMTS is not activated in this cell line (5, 9)). The difference in toxicity, from mitochondrial matrix-targeted c-Abl, may be may be due to a different balance in inhibitory (protein-protein) interactions in the matrix (leading to a less inhibited c-Abl) (10) or perhaps be connected to the level of endogenous ROS in these cell lines (9).

With respect to the OMM-targeted c-Abl, we reasoned that by using an MTS derived from Bcl-X_L it would put c-Abl in the right 'neighborhood' of the OMM for

apoptotic activity. Full length c-Abl (in complex with PKCδ) associates with Bcl-X_L at the OMM under genotoxic stress (11). However, a c-Abl/Bcl-X_L interaction at the mitochondria may not be pro-apoptotic without PKCδ present as Bcl-X_L is likely a substrate of PKCδ and not c-Abl (Bcl-X_L was shown to be phosphorylated on serine) (11). Additionally, since both c-Abl and PKCδ lack any known MTS the OMM seemed the more likely site for pro-apoptotic activity. c-Abl's lack of toxicity at the OMM may have been due to a lack of activity. Perhaps direct targeting of the constitutively active Bcr-Abl would yield a different result (an OMM direct targeted version of Bcr-Abl was attempted but the MTS (from BCS protein (12)) was insufficient to translocate Bcr-Abl to the mitochondria).

c-Abl is also proteolytically processed by caspases (*Fig. 5.1*). It is highly likely that two different forms (full length and a truncated version) of c-Abl are translocated to the mitochondria under conditions of cell stress (13). Even so, the probability of c-Abl being mitochondrially imported appears to be low. Using MITOPROT (14) to calculate the probability of a functional MTS, full length c-Abl yields a probability of 0.154 and the truncated c-Abl (non-NLS containing version) was 0.215. For reference, OTC-EGFP got a probability score of 0.995 while the EGFP-cMTS was 0.072, yet both of these proteins are imported into the mitochondrial matrix (5, 15).

Mitochondrial Bcr-Abl is toxic to cancer cells

By using previously characterized (i.e., canonical) MTSs demonstrated to target various heteroproteins to specific submitochondrial regions, we established the apoptotic potential of mitochondrially targeted Bcr-Abl in K562 cells. Since cytoplasmic Bcr-Abl

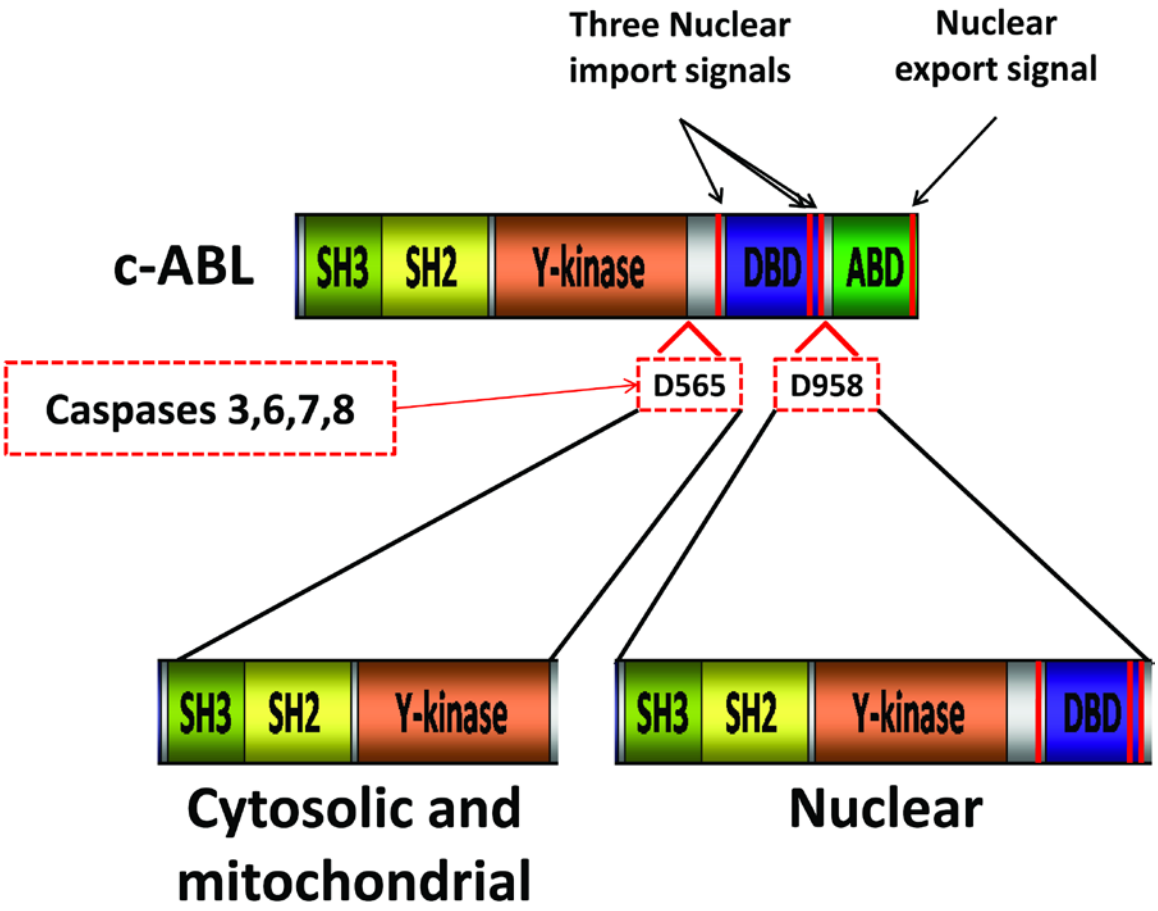

Figure 5.1. Caspases and c-Abl. Caspase cleavage of c-Abl at residues D565 and D958 create either a nuclear targeted version of c-Abl or a cytosolic version that could also be targeted to the mitochondria (via PKCδ).

obstructs the apoptotic pathway at so many levels (16, 17) we assessed late stage apoptosis/necrosis (e.g., 7-AAD and DNA segmentation) in order to ensure that MTS-Bcr-Abl apoptotic induction was irreversible and can be carried all the way through to the destruction of the leukemic cell. Targeting the IMM with Bcr-Abl induced cell death as early as 20 hours posttransfection as measured by annexin-APC and 7-AAD (*Fig. 5.2*). Since there are reports that the apoptosis-resistant K562 cell line can appear 'normal' 24 hours after treatment with DNA damaging agents (18) it was a little surprising to find that targeting Bcr-Abl to the mitochondria of K562 cells so robustly induced cell death even before 24 hours using a construct that requires time (as early as ~4 - 6 hours (19)) for protein expression. Bcr-Abl (OTC-Bcr-Abl) and c-Abl (Abl-cMTS) targeted to the mitochondrial matrix were similar in their toxicities in both K562 and 1471.1 cells at 48 hours (*Fig 5.3*) with no statistical difference using a two-way ANOVA. Nonetheless, it is unclear if OTC-Bcr-Abl (or Abl-cMTS) is acting as an authentic surrogate for death-directed c-Abl. The kinase activity has been reported to be essential for the pro-apoptotic function of c-Abl at the mitochondria (20). Yet death induction from kinase-dead forms of mitochondrial targeted c-Abl and Bcr-Abl were not statistically different from the wild-type versions.

The K562, 1471.1, and Cos-7 cell lines were differentially susceptible to death by mitochondrial c-Abl and Bcr-Abl. This may possibly reflect an underlying state of mitochondrial apoptotic 'priming' (i.e., BH3 profiles) where the Bcl-2 family proteins (with over a dozen members) are arrayed to trigger MOMP in certain types of cancer cell but not in most normal cells (21). However, K562 are considered a chemoresistant cell type that do not exhibit much of a 'primed' status and require exogenous priming with a

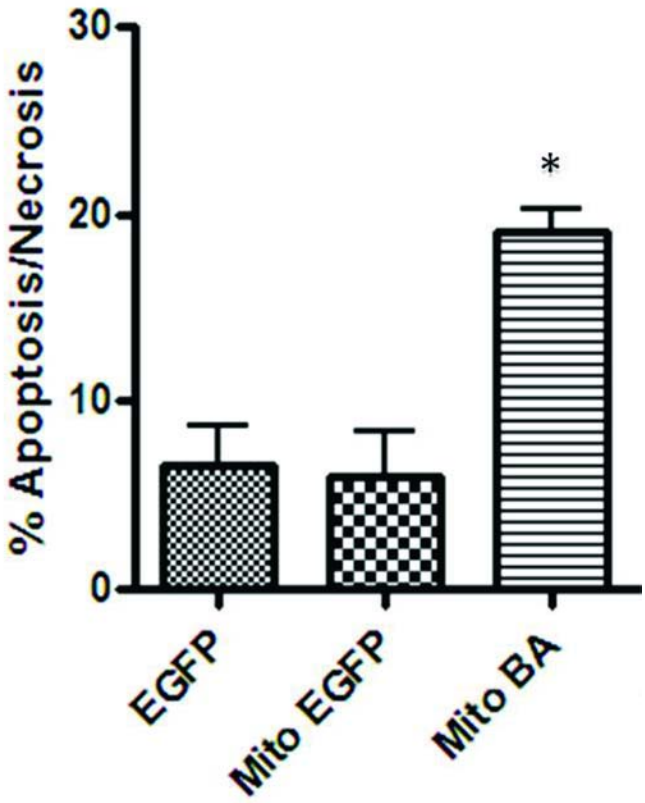

Figure 5.2. Cell death in K562 at 20 hours posttransfection with IMM targeted Bcr-Abl (Mito BA). 'Mito' label indicates the IMM targeting MTS derived from cytochrome c oxidase subunit VIII (i.e., the IMM MTS).

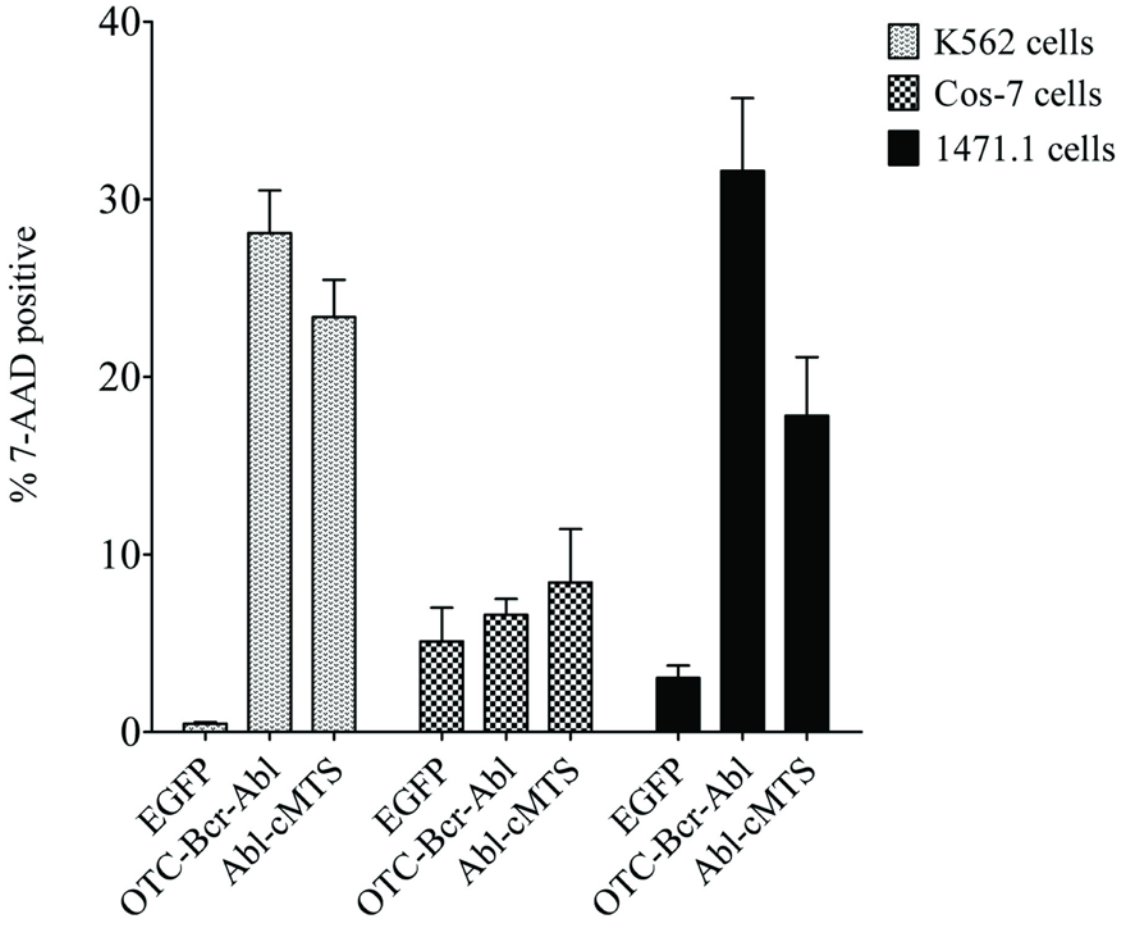

Figure 5.3. Comparison of cell death from mitochondrial matrix targeted c-Abl and Bcr-Abl in K562, Cos-7, and 1471.1 cells.

BH3 mimetic (ABT-737) in order to achieve chemotherapeutic sensitivity (21). The priming status of 1471.1 and Cos-7 cells is not known and could be lower than K562. Nonetheless, unlike the response to standard chemotherapeutics (e.g., etoposide and vincristine) K562 seem uniquely vulnerable to mitochondrial matrix targeted c-Abl and Bcr-Abl. Alternatively, the level of cell death across these cell types may have some correspondence to inherent ROS levels (*Fig 5.4*).

iCE is selectively toxic to leukemia cells

The iCE selectively induced leukemic K562 cell death (as compared to 1471.1 breast cancer and Cos-7 cell lines) to the same level as imatinib alone and had a more than additive killing effect when combined with imatinib (*Fig. 5.5*). Imatinib showed similar absolute toxicity to 1471.1 cells as to K562. To this point, imatinib has been shown to be effective in killing certain breast cancer cell lines that are dependent on the expression of c-Kit or PDGFR (22). Though, the expression of receptor tyrosine kinases in 1471.1 cells has yet to be characterized. Therefore, the 1471.1 cell line may be susceptible to imatinib either due to receptor (e.g., c-Kit or PDGFR) or non-receptor (c-Abl) tyrosine kinase inhibition. However, the added cell death (e.g., 7-AAD) values of imatinib and iCE were greater than that for the combination of iCE and imatinib demonstrating the lack of potentiation in the 1471.1 cell line.

Despite the killing effect of the iCE in K562, colocalization analysis demonstrated that Bcr-Abl and the iCE were not targeted to the mitochondria as expected. The mechanism of leukemic cell killing by the iCE remains obscure. Since the iCE colocalized with Bcr-Abl, the mechanism for iCE toxicity may be from the subcellular

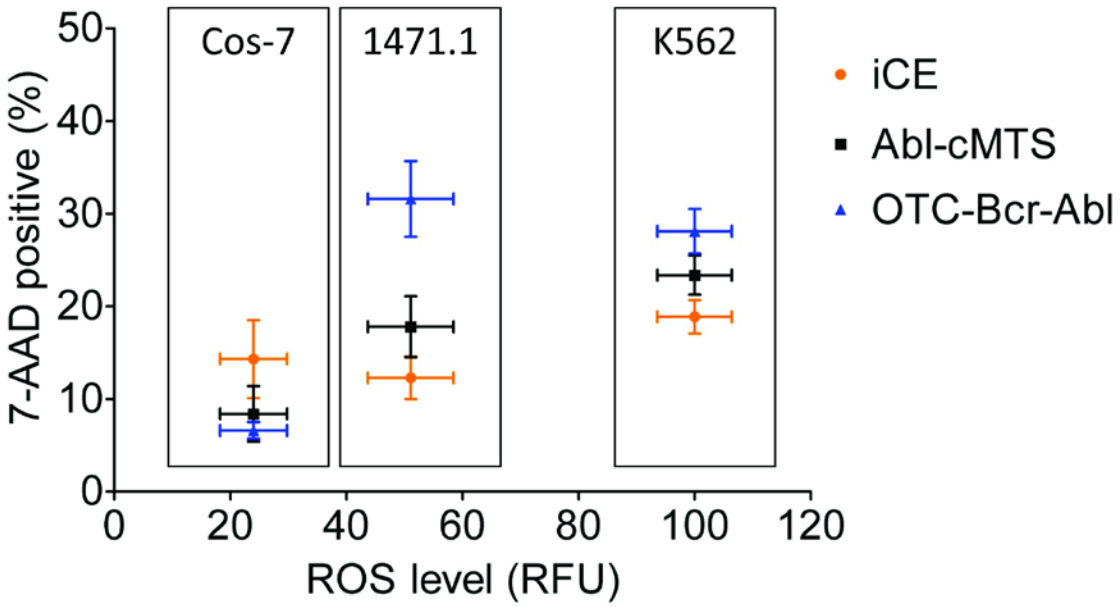

Figure 5.4. Level of cell death compared to ROS level. The iCE is not targeted to the mitochondria and cell death does not trend with ROS level. Error bars are S.E.M.

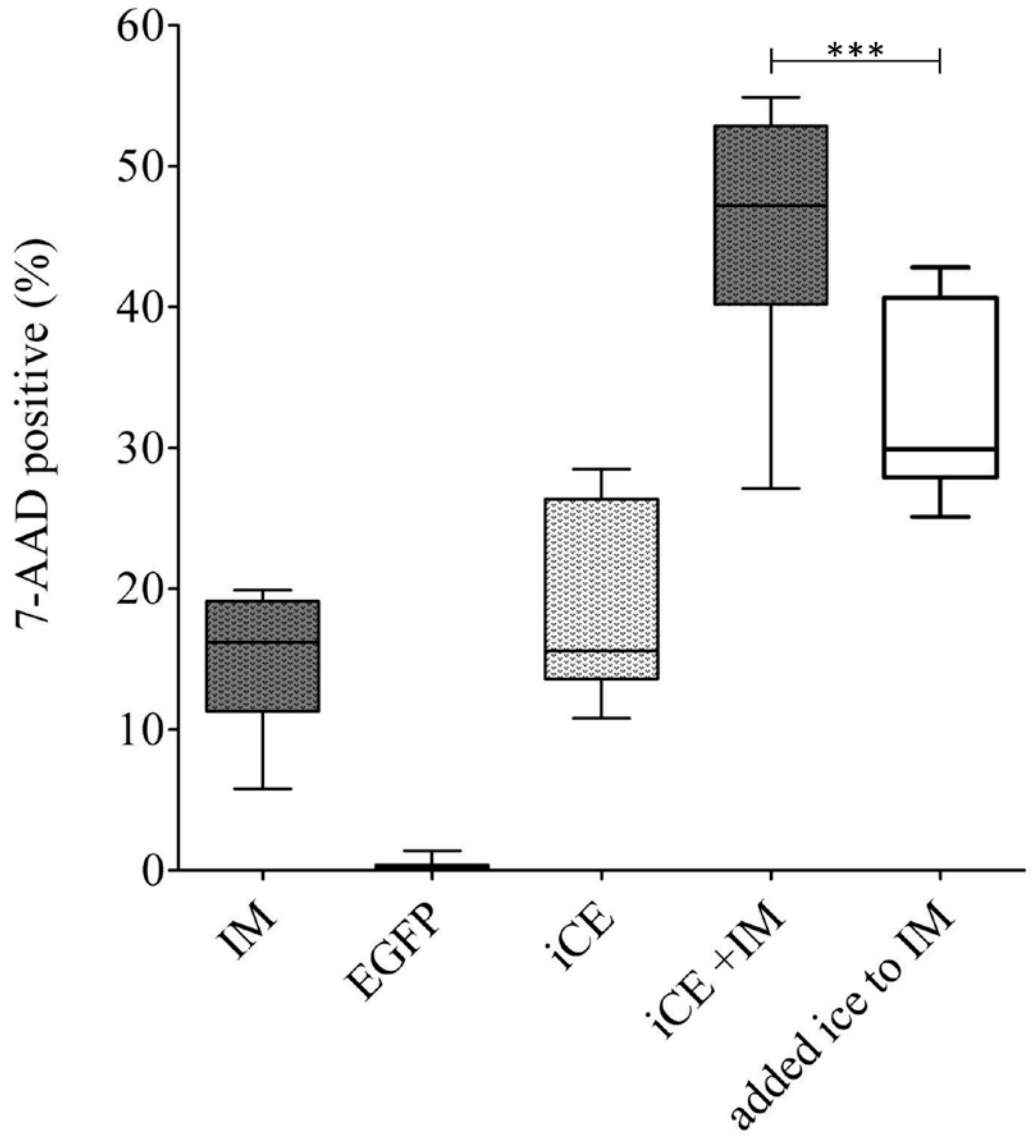

Figure 5.5. The combination of the iCE+IM has a more than additive killing effect on K562 cells. The IM treated K562 7-AAD values (first column) were added to those of iCE alone (third column) to generate the 'added ice to IM' column. Statistical difference was determined by one-way ANOVA with Tukey post-hoc test (***P<0.001).

localization of the iCE itself or from a Bcr-Abl/iCE interaction. We suspect that the iCE may exert its killing activity by more than a one mechanism. While the iCE does not significantly inhibit the tyrosine kinase activity of Bcr-Abl itself, the ccmut3 domain disruption of Bcr-Abl homo-oligomerization may reinforce imatinib efficacy by shifting Bcr-Abl's conformational equilibrium to one in which imatinib is more readily bound. Additionally, the iCE, through the cMTS domain, possibly recruits a PKC (perhaps PKCβ) or PKA isoform to the plasma membrane which results in reduced pro-proliferative calcium transients (via G-protein coupled receptor desensitization) (23) PKCβ upregulation and activity was uniquely toxic for CML cells compared to normal stem cells (24) and the leukemia-specific toxicity occurs upon PKCβ translocation to the plasma membrane (25). Moreover, iCE binding to Bcr-Abl may interfere with tyrosine kinase independent oncogenic signal transduction through Bcr-Abl (e.g., disruption of signaling from Src kinase phosphorylation of Y177 on the Bcr portion of Bcr-Abl that leads to Grb2 binding and ultimately Ras activation) (26, 27) or block Bcr-Abl RhoGEF domain activity (28).

Alternatively, wild-type Bcr should also be considered as a potential source for mediating the iCE's killing effect since the ccmut3 binds to the Bcr portion of Bcr-Abl. Targeting Bcr has not been well studied in leukemia but the overexpression of Bcr reduces the leukemogenicity of Bcr-Abl. The novel S/T kinase activity of Bcr is required for the antileukemic activity of overexpressed Bcr. In addition, the tyrosine kinase activity of Bcr-Abl suppresses the S/T kinase activity of Bcr (29). It may be possible that the iCE binds to Bcr and prevents Bcr-Abl phosphorylation of Bcr thereby creating a condition of disinhibition for a negative regulator of Bcr-Abl.

While cell death may be effectively recapitulated in the Ph^+ and not in Ph^- cell lines used in this study, these cell lines are not be meant to model all of Ph^- or Ph^+ cells and it is unlikely that the results obtained with the iCE in this study can be extrapolated too broadly. Two of the most important Ph^+ cell populations to target in a curative design for CML will be the TKI refractory stem cell population and CML cells expressing TKI-resistant Bcr-Abl (e.g., T315I). Until these unique cell populations can be tested it will remain uncertain whether or not iCE type therapy would confer benefits beyond current CML therapies. Although the K562 line is a considered to be a blast phase cell it is still dependent upon Bcr-Abl for survival and therefore, more closely serves as a model of chronic phase CML. Nonetheless, the activity of the iCE and mitochondrial Bcr-Abl may represent two separate and selectively leukemotoxic mechanisms compared to 1471.1 breast cancer and Cos-7 fibroblast cell lines (*Fig 5.6*). Moreover, each of these mechanisms may have particular relevance in CML stem or TKI resistant cells due to the kinase-independent killing activity they both exhibit.

The iCE (in combination with imatinib) and mitochondrially targeted Bcr-Abl killing modalities may yet be highly relevant in chronic phase CML. After more than a decade of experience with TKI therapy, current clinical strategies are largely focused on gaining better long-term patient outcomes and preventing TKI resistance from emerging. The durability of a patient's response is thought to correspond to achieving a critical threshold level of CML cell burden elimination with the initial TKI therapeutic challenge. The potentiation of imatinib efficacy when combined with the iCE may offer an avenue to achieving a better 'up-front' patient response and lead to improved rates of sustained remission in patients with CML.

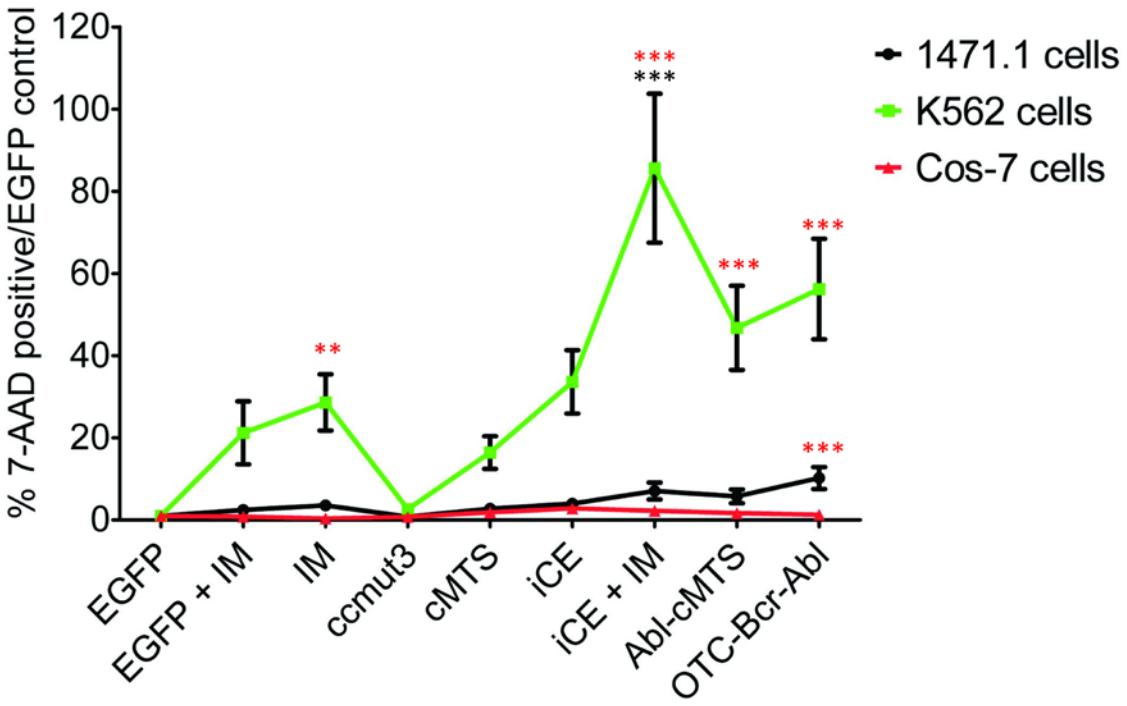

Figure 5.6. K562 cells are more susceptible to the iCE and mitochondrial c-Abl/Bcr-Abl than Cos or 1471.1 cells. Overall, the K562 cell line demonstrated selective sensitivity to imatinib (as expected) and the targeting of Bcr-Abl or c-Abl to the mitochondria. The iCE, through an unknown mechanism is also selectively and highly toxic to K562 cells. Red asterisks indicate difference from Cos-7 cell line and Black asterisks indicate difference from 1471.1 cell line. Two-way ANOVA with Bonferroni post-test (error bars are S.E.M., $N \geq 3$; $P<0.01$**, $P<0.001$***)

Future work

Mitochondrial Bcr-Abl and c-Abl

There are several questions that could be addressed now that Bcr-Abl has been demonstrated to be a mitochondrial toxin. For instance, the intention to mimic c-Abl's "mitochondrial wracking factor" (MWF) (30) potential is complicated by not knowing c-Abl's mitochondrial substrate(s) and submitochondrial translocation site (31). Determining the submitochondrial location of death-directed wild-type c-Abl is an important next step. The use of endoplasmic reticulum toxins (e.g., tunicamycin) that have been shown to target c-Abl to mitochondria and immunoelectron microscopy to determine Abl submitochondrial localization (immunocytochemical staining for transmission electron microscopy (TEM)) could resolve this question. Furthermore, once the optimal (or correct) submitochondrial location and protein interactions are determined, a refinement of the amount of c-Abl (Bcr-Abl) that is required to meet a particular 'death induction threshold' could be explored. Once the question of submitochondrial compartment is resolved, truncation or point mutants that disable specific domains could be used to determine the essential components of c-Abl (Bcr-Abl) mediated toxicity.

iCE

Since the iCE failed to relocalize Bcr-Abl it could be re-engineered for that end. The ccmut3 was selected from a set of binding domains to Bcr-Abl because it had been the most effective in moving Bcr-Abl from the cytoplasmic space to the nucleus (32). This indicates that the MTS (i.e., cMTS) was the limiting factor. However, other Bcr-Abl

binding domains may be better at ‘dislodging’ Bcr-Abl from its cytoplasmic interactions. The cytoplasmic retention of Bcr-Abl is primarily determined by the C-terminal actin binding domain (ABD) in the Abl portion of Bcr-Abl (33). The ABD is also central to Bcr-Abl’s transformative potential (34). Interrupting Bcr-Abl’s actin interaction leads to the release and nuclear translocation (through the NLSs (*Fig 1.3*) of Bcr-Abl (35). Andy Dixon, PhD of the Lim Laboratory developed a Bcr-Abl actin binding domain specific iDab (i.e. single domain antibody) (36, 37) that colocalizes with and can facilitate Bcr-Abl nuclear localization (32).

iDabs take advantage of the ability of a single variable fragment of an antibody (heavy or light chain) to bind an antigen with the same specificity and affinity as a full size (e.g. IgG) antibody but at a tenth the size (38, 39). Furthermore, iDabs do not require, as do full antibodies, disulfide bonds that are incompatible with the intracellular reducing environment (40). An iDab has been generated (41) against the ABD of Bcr-Abl (Andy Dixon, Lim Laboratory (32)). The ABD-iDab could be fused to the C-terminal cMTS before the EGFP (or other fluorescent tag) and this will produce a relatively small ~36-37 kDa protein.

Creating a multi-valent binding protein is almost certainly necessary to achieve translocation of Bcr-Abl to the mitochondria (32). Since the nuclear trafficking of Bcr-Abl was increased when the 4NLS-ccmut3 was paired with the 4NLS-ABD iDab (32), a set of iCEs with different Bcr-Abl binding moieties may be effective in mitochondrially relocating Bcr-Abl.

A potential limitation concerning the ABD-iDab containing iCE is that since the ABD pertains to the Abl portion of Bcr-Abl there exists the possibility that there may be

binding (and mitochondrial translocation) of both Bcr-Abl and c-Abl. As c-Abl activation is carefully controlled and our results show that c-Abl is not toxic at the OMM it is unlikely that, if it is translocated to the mitochondria of CML or non-CML cells, it would induce apoptosis (20).

An interesting alternative approach is the substitution of the two PKA/PKC (S189 and T193) target residues with tyrosine creating the condition that Bcr-Abl may be able to 'activate' its own chaperone (just like active c-Abl phosphorylates PKCδ for translocation(4)). This may allow for both increased selectivity (i.e., no iCE transport of inactive c-Abl) and (perhaps) improved rates of mitochondrial targeting of Bcr-Abl post-binding of the iCE.

If the iCE were made to function as intended, the amount of Bcr-Abl in a given cell will not be a limiting factor to iCE therapeutic efficacy but rather a condition leading to an intensification of apoptotic pressure. Likewise, an iCE would not be as vulnerable to mutations in Bcr-Abl or cellular efflux mechanisms and likely to have a minimal side effect profile (42). On the other hand if an iDab/cMTS construct (like the ccmut3) does not localize to the mitochondria it may help to elucidate the mechanism behind the toxicity of the iCE.

In vivo studies: cMTS

Koeffler and Golde, in a 1980 review of leukemia cell lines, predicted that K562 cells as a model of CML would "shed new light on the cell biology and perhaps lead to new therapeutic modalities." (43) However, CML is a disease of hematopoietic stem cells and can therefore give rise to multiple lineages of tumor cells. Cell line lineage is

considered to be a central factor in the determination of therapeutic response to TKIs (imatinib) (44). This necessitates prudent caution when extrapolating experiences with immortalized cell lines in culture to potential *in vivo* activities. Our work *in vitro* demonstrates that the cMTS can be activated by the physiologically relevant inherent levels of oxidative stress found in transformed cells. However, it will be necessary to replicate the findings for the cMTS (inherent ROS level-activated translocation) *in vivo*. An *in vivo* approach would most likely employ a mouse xenograft model of leukemia (45). The cMTS is small enough (and could potentially be further truncated) to be viable as a peptide therapeutic when conjugated to a cell-penetrating peptide motif (e.g., HIV TAT). However if conjugated to, say c-Abl, it would be better to adopt a gene therapy strategy for delivery.

We used the cMTS as a vehicle to selectively deliver c-Abl under conditions of oxidative stress but the implications of the cMTS utility could be expanded upon. For instance, in many pathophysiological conditions (e.g., neurodegeneration (46) and diabetes (47)) that manifest increased oxidative stress the cMTS could be used to selectively target the mitochondria with an antioxidant payload/enzyme. The cMTS may be of benefit to selectively target either pro-apoptotic or pro-survival factors to the mitochondria to elicit or prevent cell death, respectively. Additionally, the cMTS may find utility beyond conditions of elevated ROS but also in many breast cancers where PKC (of various isoforms) are overexpressed (48).

The genetic diversity of CML cells has dampened the early optimism surrounding targeted therapeutics (49). Turning Bcr-Abl back on itself to cause leukemic cell death is

more likely to circumvent the ‘newer’ problems brought about by genetic diversity in CML; quiescent LSC populations and TKI resistant forms of Bcr-Abl.

References

1. S. Roychowdhury and M. Talpaz. Managing resistance in chronic myeloid leukemia. Blood Rev. 25:279-290 (2011).

2. O. Hantschel, S. Wiesner, T. Guttler, C.D. Mackereth, L.L. Rix, Z. Mikes, J. Dehne, D. Gorlich, M. Sattler, and G. Superti-Furga. Structural basis for the cytoskeletal association of Bcr-Abl/c-Abl. Mol Cell. 19:461-473 (2005).

3. S. Kumar, A. Bharti, N.C. Mishra, D. Raina, S. Kharbanda, S. Saxena, and D. Kufe. Targeting of the c-Abl tyrosine kinase to mitochondria in the necrotic cell death response to oxidative stress. J Biol Chem. 276:17281-17285 (2001).

4. X. Qi and D. Mochly-Rosen. The PKCdelta -Abl complex communicates ER stress to the mitochondria - an essential step in subsequent apoptosis. J Cell Sci. 121:804-813 (2008).

5. M.A. Robin, S.K. Prabu, H. Raza, H.K. Anandatheerthavarada, and N.G. Avadhani. Phosphorylation enhances mitochondrial targeting of GSTA4-4 through increased affinity for binding to cytoplasmic Hsp70. J Biol Chem. 278:18960-18970 (2003).

6. P. Storz. Reactive oxygen species in tumor progression. Front Biosci. 10:1881-1896 (2005).

7. T.W. Owens, A.J. Valentijn, J.P. Upton, J. Keeble, L. Zhang, J. Lindsay, N.K. Zouq, and A.P. Gilmore. Apoptosis commitment and activation of mitochondrial Bax during anoikis is regulated by p38MAPK. Cell Death and Differentiation. 16:1551-1562 (2009).

8. Y. Ito, P. Pandey, N. Mishra, S. Kumar, N. Narula, S. Kharbanda, S. Saxena, and D. Kufe. Targeting of the c-Abl tyrosine kinase to mitochondria in endoplasmic reticulum stress-induced apoptosis. Mol Cell Biol. 21:6233-6242 (2001).

9. J.E. Constance, S.D. Despres, A. Nishida, and C.S. Lim. Selective targeting of c-Abl via a cryptic mitochondrial targeting signal activated by cellular redox status in leukemic and breast cancer cells. Pharm Res. 29:2317-2328 (2012).

10. O. Hantschel and G. Superti-Furga. Regulation of the c-Abl and Bcr-Abl tyrosine kinases. Nat Rev Mol Cell Biol. 5:33-44 (2004).

11. M. Lasfer, L. Davenne, N. Vadrot, C. Alexia, Z. Sadji-Ouatas, A.F. Bringuier, G. Feldmann, D. Pessayre, and F. Reyl-Desmars. Protein kinase PKC delta and c-Abl are required for mitochondrial apoptosis induction by genotoxic stress in the absence of p53, p73 and Fas receptor. FEBS Lett. 580:2547-2552 (2006).

12. T. Stan, J. Brix, J. Schneider-Mergener, N. Pfanner, W. Neupert, and D. Rapaport. Mitochondrial protein import: recognition of internal import signals of BCS1 by the TOM complex. Mol Cell Biol. 23:2239-2250 (2003).

13. D. Barila, A. Rufini, I. Condo, N. Ventura, K. Dorey, G. Superti-Furga, and R. Testi. Caspase-dependent cleavage of c-Abl contributes to apoptosis. Molecular and Cellular Biology. 23:2790-2799 (2003).

14. M.G. Claros and P. Vincens. Computational method to predict mitochondrially imported proteins and their targeting sequences. Eur J Biochem. 241:779-786 (1996).

15. A.L. Horwich, F. Kalousek, W.A. Fenton, R.A. Pollock, and L.E. Rosenberg. Targeting of pre-ornithine transcarbamylase to mitochondria: definition of critical regions and residues in the leader peptide. Cell. 44:451-459 (1986).

16. K. Piwocka, S. Vejda, T.G. Cotter, G.C. O'Sullivan, and S.L. McKenna. Bcr-Abl reduces endoplasmic reticulum releasable calcium levels by a Bcl-2-independent mechanism and inhibits calcium-dependent apoptotic signaling. Blood. 107:4003-4010 (2006).

17. Y. Kawabata, M. Hirokawa, A. Kitabayashi, T. Horiuchi, J. Kuroki, and A.B. Miura. Defective apoptotic signal transduction pathway downstream of caspase-3 in human B-lymphoma cells: A novel mechanism of nuclear apoptosis resistance. Blood. 94:3523-3530 (1999).

18. L. Diomede, B. Piovani, F. Re, P. Principe, F. Colotta, E.J. Modest, and M. Salmona. The induction of apoptosis is a common feature of the cytotoxic action of ether-linked glycerophospholipids in human leukemic cells. Int J Cancer. 57:645-649 (1994).

19. Lonza. Amaxa Cell Line Nucleofector Kit V, for K562. Lonza Cologne AG (2009).

20. S. Kumar, N. Mishra, D. Raina, S. Saxena, and D. Kufe. Abrogation of the cell death response to oxidative stress by the c-Abl tyrosine kinase inhibitor STI571. Mol Pharmacol. 63:276-282 (2003).

21. T. Ni Chonghaile, K.A. Sarosiek, T.T. Vo, J.A. Ryan, A. Tammareddi, G. Moore Vdel, J. Deng, K.C. Anderson, P. Richardson, Y.T. Tai, C.S. Mitsiades, U.A. Matulonis, R. Drapkin, R. Stone, D.J. Deangelo, D.J. McConkey, S.E. Sallan, L. Silverman, M.S. Hirsch, D.R. Carrasco, and A. Letai. Pretreatment mitochondrial priming correlates with clinical response to cytotoxic chemotherapy. Science. 334:1129-1133 (2011).

22. A.E. Roussidis, A.D. Theocharis, G.N. Tzanakakis, and N.K. Karamanos. The importance of c-Kit and PDGF receptors as potential targets for molecular therapy in breast cancer. Curr Med Chem. 14:735-743 (2007).

23. A. Vichalkovski, I. Kotevic, N. Gebhardt, R. Kaderli, and H. Porzig. Tyrosine kinase modulation of protein kinase C activity regulates G protein-linked Ca2+ signaling in leukemic hematopoietic cells. Cell Calcium. 39:517-528 (2006).

24. F. Pellicano, M. Copland, H.G. Jorgensen, J. Mountford, B. Leber, and T.L. Holyoake. BMS-214662 induces mitochondrial apoptosis in chronic myeloid leukemia (CML) stem/progenitor cells, including CD34+38- cells, through activation of protein kinase Cbeta. Blood. 114:4186-4196 (2009).

25. L.C. David Hoekstra, Kelvin P Lee. Rewiring the Protein Kinase C Beta 2 and Bcr/Abl Signal Transduction Pathways. 53rd ASH Annual Meeting and Exposition (2011).

26. E.M. Galan-Moya, J. Hernandez-Losa, C.I. Aceves Luquero, M.A. de la Cruz-Morcillo, C. Ramirez-Castillejo, J.L. Callejas-Valera, A. Arriaga, A.F. Aranburo, S. Ramon y Cajal, J. Silvio Gutkind, and R. Sanchez-Prieto. c-Abl activates p38 MAPK independently of its tyrosine kinase activity: Implications in cisplatin-based therapy. Int J Cancer. 122:289-297 (2008).

27. M. Preyer, C.W. Shu, and J.Y. Wang. Delayed activation of Bax by DNA damage in embryonic stem cells with knock-in mutations of the Abl nuclear localization signals. Cell Death Differ. 14:1139-1148 (2007).

28. S. Sahay, N.L. Pannucci, G.M. Mahon, P.L. Rodriguez, N.J. Megjugorac, E.V. Kostenko, H.L. Ozer, and I.P. Whitehead. The RhoGEF domain of p210 Bcr-Abl activates RhoA and is required for transformation. Oncogene. 27:2064-2071 (2008).

29. B. Perazzona, H. Lin, T. Sun, Y. Wang, and R. Arlinghaus. Kinase domain mutants of Bcr enhance Bcr-Abl oncogenic effects. Oncogene. 27:2208-2214 (2008).

30. B.N. Chau, T.T. Chen, Y.Y. Wan, J. DeGregori, and J.Y. Wang. Tumor necrosis factor alpha-induced apoptosis requires p73 and c-ABL activation downstream of RB degradation. Mol Cell Biol. 24:4438-4447 (2004).

31. M. Salvi, A.M. Brunati, and A. Toninello. Tyrosine phosphorylation in mitochondria: a new frontier in mitochondrial signaling. Free Radic Biol Med. 38:1267-1277 (2005).

32. A.S. Dixon, J.E. Constance, T. Tanaka, T.H. Rabbitts, and C.S. Lim. Changing the subcellular location of the oncoprotein Bcr-Abl using rationally designed capture motifs. Pharm Res. 29:1098-1109 (2011).

33. J.R. McWhirter and J.Y. Wang. Activation of tyrosinase kinase and microfilament-binding functions of c-abl by bcr sequences in bcr/abl fusion proteins. Mol Cell Biol. 11:1553-1565 (1991).

34. J.R. McWhirter and J.Y. Wang. An actin-binding function contributes to transformation by the Bcr-Abl oncoprotein of Philadelphia chromosome-positive human leukemias. EMBO J. 12:1533-1546 (1993).

35. M. Preyer, P. Vigneri, and J.Y. Wang. Interplay between kinase domain autophosphorylation and F-actin binding domain in regulating imatinib sensitivity and nuclear import of BCR-ABL. PLoS One. 6:e17020 (2011).

36. T. Tanaka, G.T. Chung, A. Forster, M.N. Lobato, and T.H. Rabbitts. De novo production of diverse intracellular antibody libraries. Nucleic Acids Res. 31:e23 (2003).

37. E. Tse, M.N. Lobato, A. Forster, T. Tanaka, G.T. Chung, and T.H. Rabbitts. Intracellular antibody capture technology: application to selection of intracellular antibodies recognising the BCR-ABL oncogenic protein. J Mol Biol. 317:85-94 (2002).

38. B. Serruys, F. Van Houtte, P. Verbrugghe, G. Leroux-Roels, and P. Vanlandschoot. Llama-derived single-domain intrabodies inhibit secretion of hepatitis B virions in mice. Hepatology. 49:39-49 (2009).

39. T. Tanaka, R.L. Williams, and T.H. Rabbitts. Tumour prevention by a single antibody domain targeting the interaction of signal transduction proteins with RAS. EMBO J. 26:3250-3259 (2007).

40. F. Kishida, T. Azuma, and K. Hamaguchi. Formation of interchain disulfide bonds in Bence Jones proteins and immunoglobulins. J Biochem. 79:91-105 (1976).

41. M. Visintin, M. Quondam, and A. Cattaneo. The intracellular antibody capture technology: towards the high-throughput selection of functional intracellular antibodies for target validation. Methods. 34:200-214 (2004).

42. K. Nihira, N. Taira, Y. Miki, and K. Yoshida. TTK/Mps1 controls nuclear targeting of c-Abl by 14-3-3-coupled phosphorylation in response to oxidative stress. Oncogene. 27:7285-7295 (2008).

43. H.P. Koeffler and D.W. Golde. Human myeloid leukemia cell lines: a review. Blood. 56:344-350 (1980).

44. R. Wetzel, V.L. Goss, B. Norris, L. Popova, M. Melnick, and B.L. Smith. Evaluation of CML model cell lines and imatinib mesylate response: determinants of signaling profiles. J Immunol Methods. 305:59-66 (2005).

45. G. Robert, I. Ben Sahra, A. Puissant, P. Colosetti, N. Belhacene, P. Gounon, P. Hofman, F. Bost, J.P. Cassuto, and P. Auberger. Acadesine kills chronic myelogenous leukemia (CML) cells through PKC-dependent induction of autophagic cell death. PLoS One. 4:e7889 (2009).

46. S.D. Schlatterer, C.M. Acker, and P. Davies. c-Abl in neurodegenerative disease. J Mol Neurosci. 45:445-52 (2011).

47. R. Hagerkvist, S. Sandler, D. Mokhtari, and N. Welsh. Amelioration of diabetes by imatinib mesylate (Gleevec): role of beta-cell NF-kappaB activation and anti-apoptotic preconditioning. Faseb J. 21:618-628 (2007).

48. M. Tan, P. Li, M. Sun, G. Yin, and D. Yu. Upregulation and activation of PKC alpha by ErbB2 through Src promotes breast cancer cell invasion that can be blocked by combined treatment with PKC alpha and Src inhibitors. Oncogene. 25:3286-3295 (2006).

49. M. Greaves. Cancer stem cells: back to Darwin? Semin Cancer Biol. 20:65-70 (2010).

APPENDIX A

BCR-ABL ACTIVATED CRYPTIC MTS

Introduction

Exploiting the aberrant tyrosine kinase activity of Bcr-Abl to control a cryptic mitochondrial targeting peptide

The optimized Bcr-Abl peptide substrate EAIY[XX]PFAKKK (also called Abltide (1)) is routinely used as a sensor for Bcr-Abl activity *in vitro* and has been suggested as a highly selective reporter for use in an activity-based diagnostic for CML (2-4). The phosphorylation of Abltide can be significantly increased by linking Abltide to modular recognition domains (e.g., such as a proline rich region, as found in the cMTS) that can interact with Bcr-Abl's SH2/SH3 domains (2, 5). The cMTS translocates from the cytoplasm to the mitochondria upon PKA/PKC mediated phosphorylation at key residues (S189/T193, respectively). We hypothesized that by altering the substrate consensus sequence and phosphoresidue (i.e., the enzyme-substrate specificity) at S189 and/or T193 of the cMTS we could uncouple ROS/PKA/PKC induced phosphorylation of the cMTS and, generate a peptide that is predominantly cytoplasmic unless phosphorylated by Bcr-Abl. Our therapeutic goal is to subvert Bcr-Abl's oncogenic activity and convert it into a pro-apoptotic agent. Engineering a Bcr-Abl inducible mitochondrial targeting peptide may convert Bcr-Abl into the switch that activates a pro-apoptotic factor.

Materials and methods

Subcloning and construction of plasmids

Each MTS plasmid construct is derived from the wild-type cryptic mitochondrial translocation sequence (N-terminal residues, 172-222) from glutathione S-transferase A4-4 (cMTS-wt) with iterative mutations to introduce tyrosines with minimal or strict v-Abl consensus phospho-substrate sequence specificity at the critical 189 or 193 residue positions (6), *see Table A.1*. The cMTS-wt was constructed cloned into the pEGFP-C1 vector as previously (7). Cell lines and culture conditions, expression of constructs, mitochondrial staining, microscopy, image, and statistical analysis were all as previously (7).

Summary of results

In a measure to alter the activating phosphorylation of the cryptic mitochondrial translocation sequence (cMTS) from the protein kinase A and C family of kinases to Bcr-Abl itself, several cMTS mutants were made (*Table A.1*). However, few of the cMTS mutants target the mitochondria (*Fig. A.1, A*). The mutations seem to influence an equilibrium between mitochondrial translocation and binding to Bcr-Abl. In a few mutants the equilibrium is strongly shifted to association with Bcr-Abl (*Fig. A.1, A and B*). The Bcr-Abl binding protein RIN1 (RIN1 binding domain (RIN-BD) was used as a positive control for Bcr-Abl binding domain optimization in our previous studies (i.e. ccmut3) (8)) sets a mechanistic precedent for the type of binding hypothesized to be occurring with the cMTS mutants (*Fig. A.2*). RIN1 is phosphorylated on tyrosine by Bcr-Abl leading to binding to the SH2 domain of Bcr-Abl. The interaction between RIN1 and

Bcr-Abl is further stabilized through a poly-proline rich region in RIN1 binding to the SH3 domain of Bcr-Abl (*Fig A.2, D*) (9). A few of the cMTS mutants achieved equal colocalization with RIN-BD to Bcr-Abl and even led to the displacement of RIN-BD from Bcr-Abl (i.e., OPT MTS '2'; *Fig. A.3 and Table A.2*).

Substitution of glutamate at positions 189 or 193 as a phosphomimetic (10) may provide a means to balance mitochondrial targeting and Bcr-Abl binding with the cMTS mutants. This would be an important future direction to pursue in light of our current results.

Table A.1. Residue mutation sets and mutagenesis primers for cMTS mutants.

Name	Mutation	Sequence	'activation domain'	Template
Y-mut	T186E R187A S189Y	5'-gctgcaggccttcaaggagg ccatctacaacatccccacc – 3'	EAIYNIPTIKKFLQPG	pEGFP-wt-cMTS
Y-OPT	T186E R187A S189Y T193F I194A F197K	5'-catctacaacatccccttcgc caagaagaagctgcagcccggcag – 3'	EAIYNIPFAKKKLQPG	pEGFP-Y-mut
OPT MTS 2	P192I T193Y	5'- gaccagaatcagcaaca tcatctacatcaagaagttcctg cagcccggcagccagagaa -3'	TRISNIIYIKKFLQPG	pEGFP-wt-cMTS
Round 1 of 2X	S189Y N190E I191A	5'- ccttcaagaccagaatctacg aagccatctacatcaagaagtt cctgcagaagaagagccagagaa agcccccc-3'	TRIYEAIYIKKFLQKK	pEGFP-OPT-MTS2
2X MTS	P192I T193Y K196P L198A Q199K P200K G201K	5'- ccttcaagaccagaatctacgaa gccatctacatcaagccgtt cgccaagaagaagagccagaga aagcccccc-3'	TRIYEAIYIKPFAKKK	pEGFP-round1-2x

Figure A.1. cMTS mutant subcellular associations and Bcr-Abl activity.

A) Comparison of cMTS mutant association with either Bcr-Abl (exogenously co-expressed with cMTS mutant or EGFP constructs in Cos-7 cells) or the mitochondria (in K562 cells). All experiments were completed in at least triplicate ($n \geq 3$) and images were collected in ≥ 4 fields with ≥ 10 cells per z-plane.,

B) Bcr-Abl activity is essential for association of the cMTS mutants. Bcr-Abl-KD and Bcr-Abl were co-expressed in Cos-7 cells with the cMTS mutants or EGFP. Error bars are S.E.M. for all studies. Dashed red lines indicate threshold for defining association (colocalization).

A.

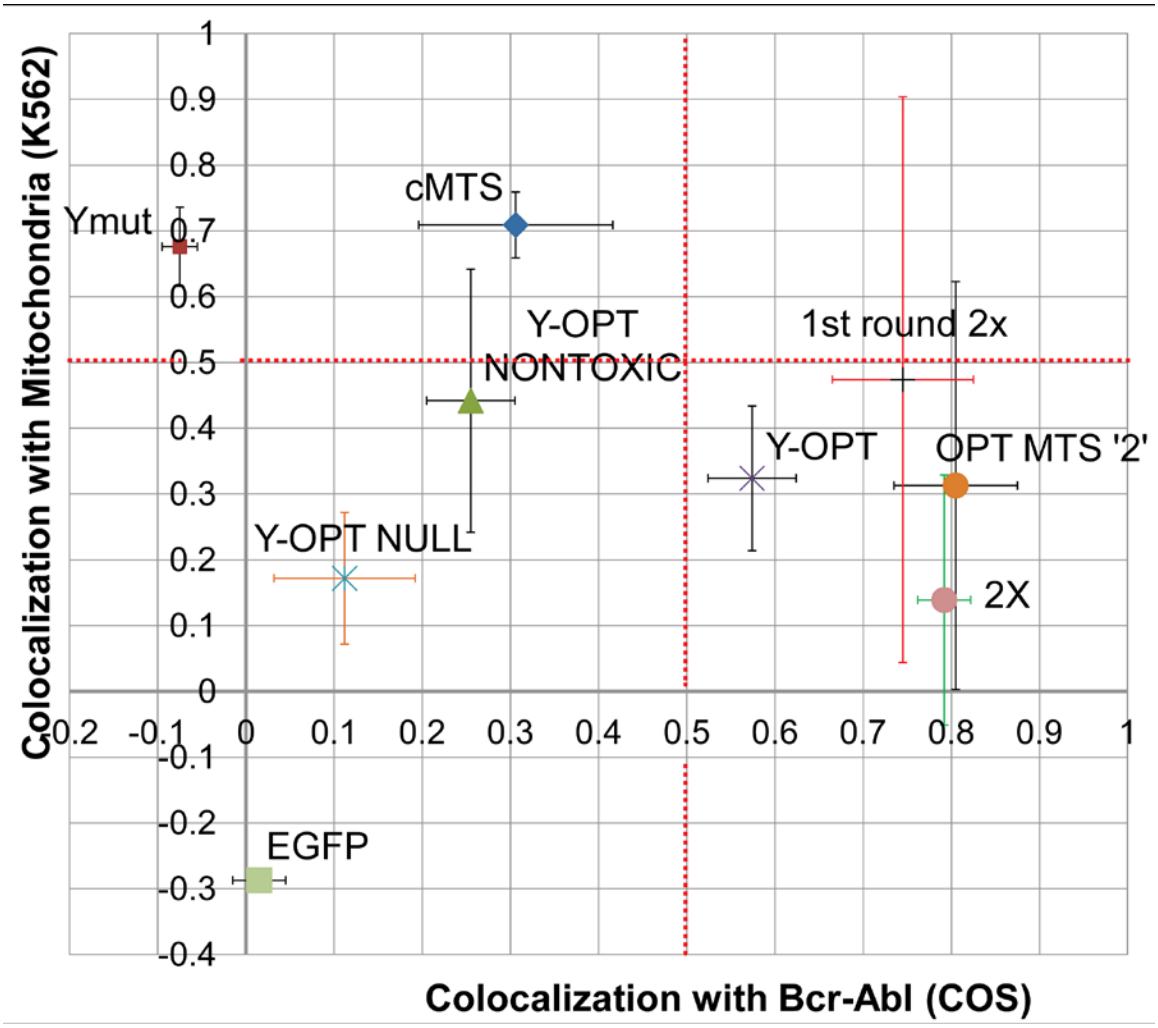
Colocalization with Mitochondria (K562)
Colocalization with Bcr-Abl (COS)
cMTS
Ymut
Y-OPT NONTOXIC
1st round 2x
Y-OPT
OPT MTS '2'
Y-OPT NULL
2X
EGFP
1
0.9
0.8
0.7
0.6
0.5
0.4
0.3
0.2
0.1
0
-0.1
-0.2
-0.3
-0.4
-0.2
-0.1
0
0.1
0.2
0.3
0.4
0.5
0.6
0.7
0.8
0.9
1

B.

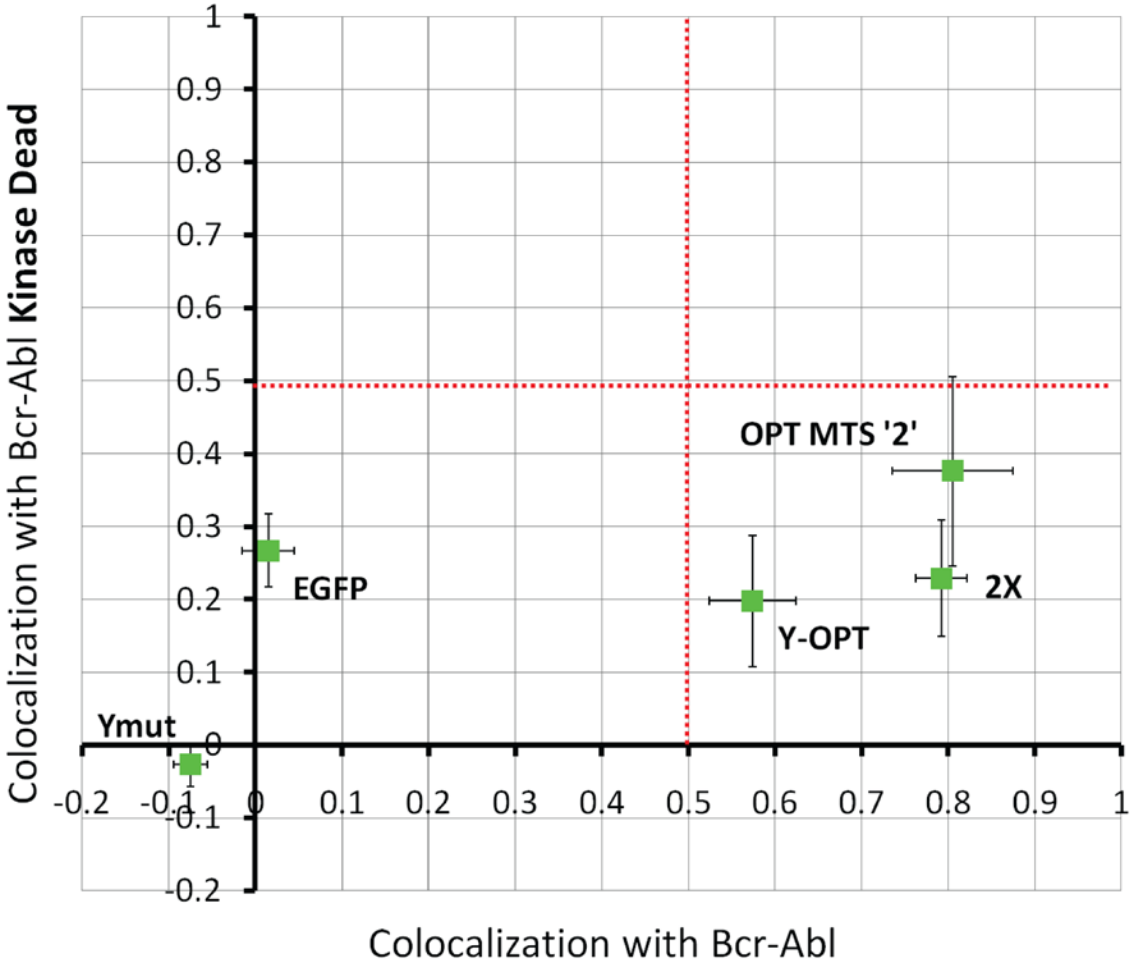
Colocalization with Bcr-Abl Kinase Dead
Colocalization with Bcr-Abl
1
0.9
0.8
0.7
0.6
0.5
0.4
0.3
0.2
0.1
0
-0.1
-0.2
-0.2
-0.1
0
0.1
0.2
0.3
0.4
0.5
0.6
0.7
0.8
0.9
1
OPT MTS '2'
EGFP
2X
Y-OPT
Ymut

Figure A.2. Wild-type PKA/PKC activated cMTS (50 C-terminal residues of GSTA4-4) and the Bcr-Abl activated cMTS.

A) The cytosolic versus mitochondrial pool of GSTA4-4 is modulated through an approximately 50 residue C-terminal cryptic mitochondrial targeting signal (MTS) domain that is responsive to the oxidative state of the cell (8). Mitochondrial targeting of GSTA4-4 is induced by phosphorylation by protein kinase A (PKA) at S189 or Protein kinase C (PKC) at T193. Phosphorylation of Ser-189 or Thr-193 increases affinity for cytoplasmic Hsp70 and subsequently leads to the translocation of GSTA4-4 to the mitochondrial matrix (8). The integration of an Abltide-like Bcr-Abl recognition sequence within the GSTA4-4 MTS created a Bcr-Abl inducible cryptic MTS.

B) Integrating an Abltide-like sequence within the 'activation' region, where S189 and T193 are located (shown in bold), should change the substrate specificity from PKA/PKC to Bcr-Abl. The full consensus sequence for c-Abl was arrayed with the tyrosine at position 189 ('Y-OPT') or 193 ('2X' cMTS). A sequence that meets the minimum consensus was made around position 189 ('Y-mut') and 193 ('OPT MTS 2'; not shown, *see Table 2*).,

C) Using fluorescent confocal microscopy and statistical colocalization analysis Y-OPT (Full consensus sequence at position 189) did (unexpectedly) colocalize with Bcr-Abl (mCherry tagged and coexpressed) in K562 cells and in Cos-7 cells (Cos-7 cell shown on left). Red dashed line is the threshold for meeting colocalization (11). The correlation of Y-OPT with the mitochondria was highly variable and not strong, unlike the wild-type cMTS. Cytosolic distribution profiles often looked similar to Bcr-Abl and this prompted the colocalization analysis with Bcr-Abl. In addition, when the Y189 was mutated to

alanine the association with Bcr-Abl was abolished. Likewise, the association between the Y-OPT and Bcr-Abl (or between Y-OPT and the mitochondria) ceased when imatinib was present (data not shown). Based on interaction studies with the RIN1 binding domain (N-terminal 295 residues of RAS interaction/interference 1 protein) we hypothesized that our Y-OPT was being retained in the cytoplasm through binding to Bcr-Abl. At least three independent experiments ($n \geq 3$) were completed and images were collected in ≥ 4 fields with ≥ 10 cells per z-plane. Error bars are S.E.M.,

D) Hypothesized mode of Bcr-Abl binding. The Y-OPT structure may facilitate a RIN1 type binding interaction with Bcr-Abl where it is thought binding is mediated first through tyrosine phosphorylation and SH2 binding followed by SH3 binding of a poly-proline sequence (12). There are two potential Bcr-Abl interaction regions in Y-OPT. First, an Abl SH2 binding motif (10) is present upon phosphorylation at Y189 and second, a poly-proline sequence (matching a class II SH3 recognition sequence (11)) is present immediately c-terminal to the Abltide-like sequence.

E) Example of the heterogeneity in the mitochondrial association results in K562 cells. Top row, Y-OPT is clearly colocalized with MitoTracker dye signal while, on the bottom row, Y-OPT is strongly associated with Bcr-Abl. It is unclear what conditions favor mitochondrial versus Bcr-Abl association of the Y-OPT.

F) Cytofluorogram (scatterplot) generated using JaCOP (ImageJ) comparing EGFP-Y-OPT (y-axis) to mCherry-Bcr-Abl (x-axis). The separate pixel populations (solid and dashed lines) may represent different stoichiometries between the fluors and thereby indicate interaction in different subcellular compartments. The PCC is insufficient and inappropriate for distinguishing subpopulation relationships between channels. The

variability in PCC values generated among the cMTS mutants can be explained by different populations of interacting fluors as revealed in the cytofluorograms.

A.

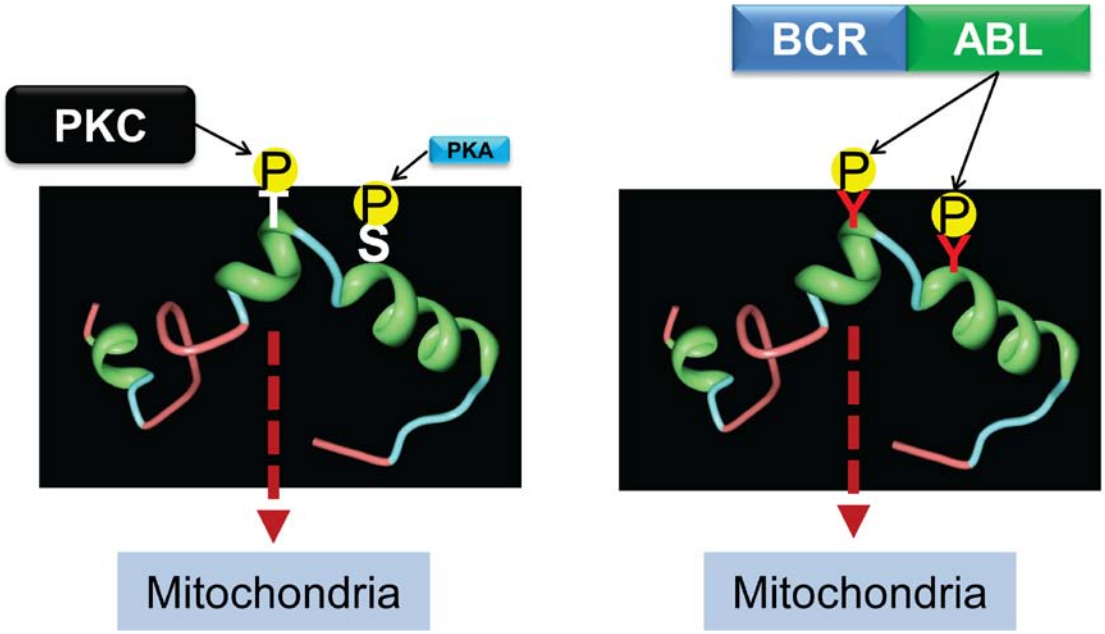
PKC
PKA
P
T
P
S
Mitochondria
BCR
ABL
P
Y
P
Y
Mitochondria

B.

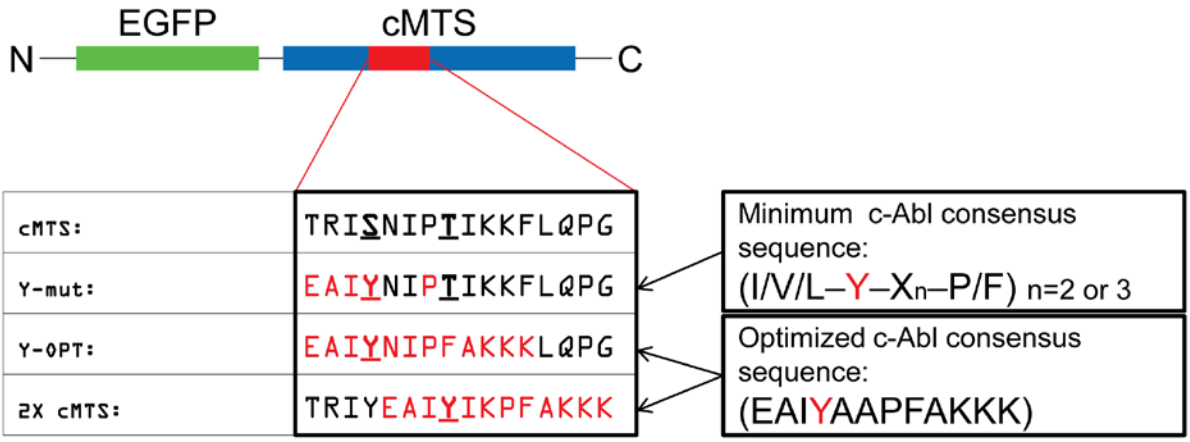
EGFP
cMTS
N
C
cMTS:
TRISNIPTIKKFLQPG
Y-mut:
EAIYNIPTIKKFLQPG
Y-OPT:
EAIYNIPFAKKKLQPG
2X cMTS:
TRIYEAIYIKPFAKKK
Minimum c-Abl consensus sequence:
(I/V/L–Y–Xn–P/F) n=2 or 3
Optimized c-Abl consensus sequence:
(EAIYAAPFAKKK)

C.

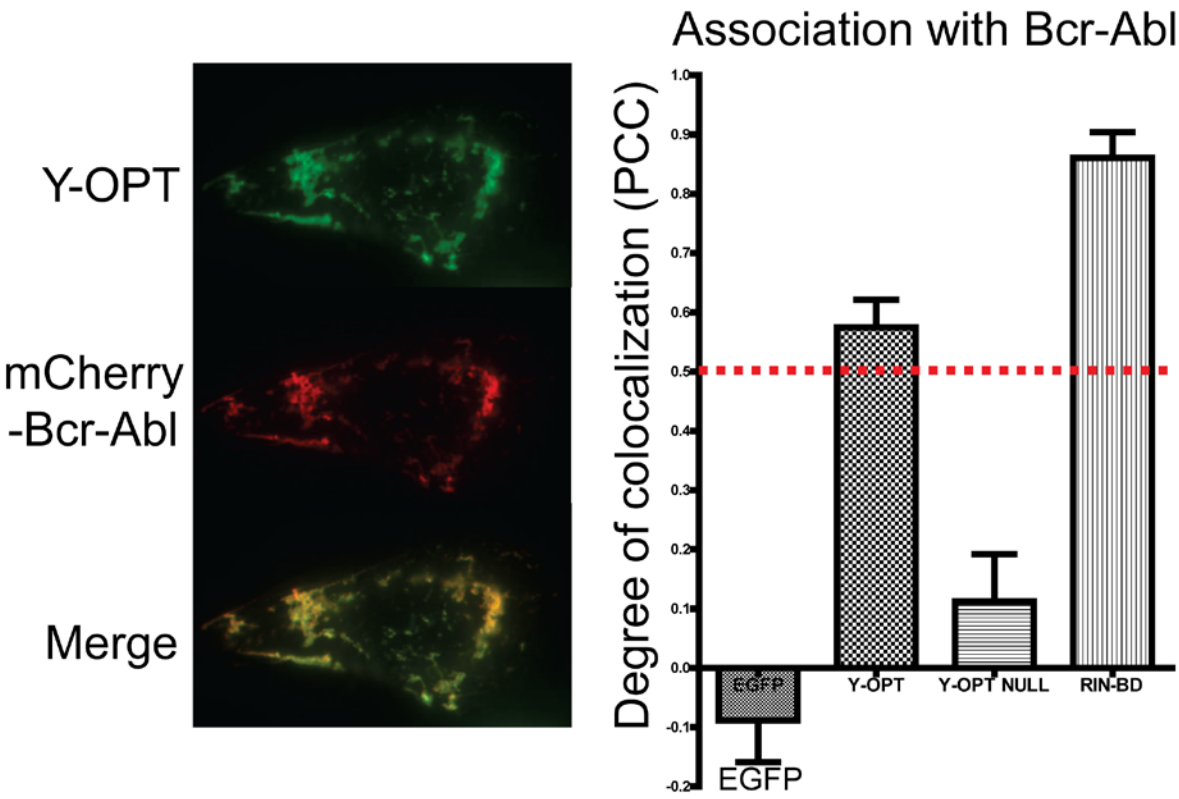
Y-OPT
mCherry
-Bcr-Abl
Merge
Association with Bcr-Abl
Degree of colocalization (PCC)
1.0
0.9
0.8
0.7
0.6
0.5
0.4
0.3
0.2
0.1
0.0
-0.1
-0.2
EGFP
Y-OPT
Y-OPT NULL
RIN-BD
EGFP

D.

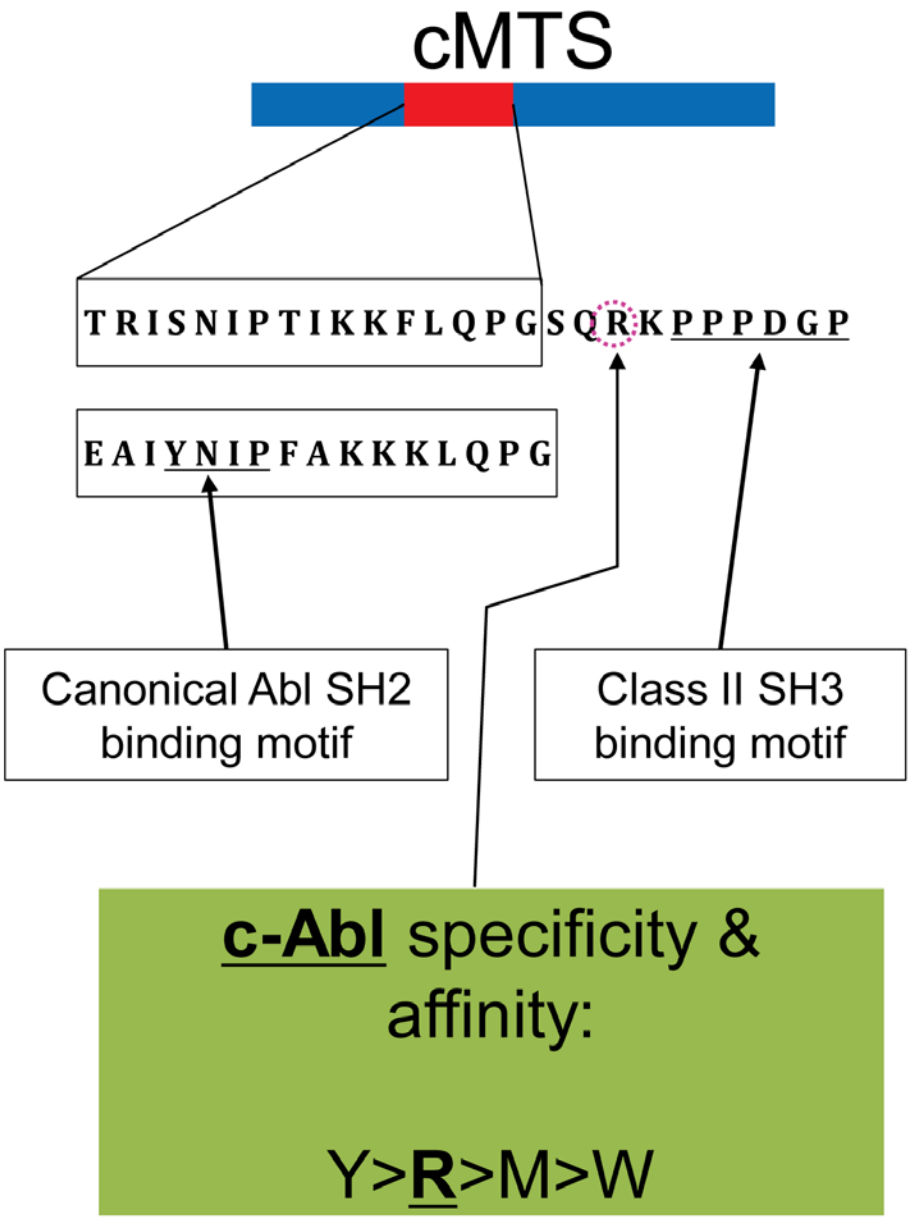
cMTS
TRISNIPTIKKFLQPGSQRKPPPDGP
EAIYNIPFAKKKLQPG
Canonical Abl SH2 binding motif
Class II SH3 binding motif
c-Abl specificity & affinity:
Y>R>M>W

E.

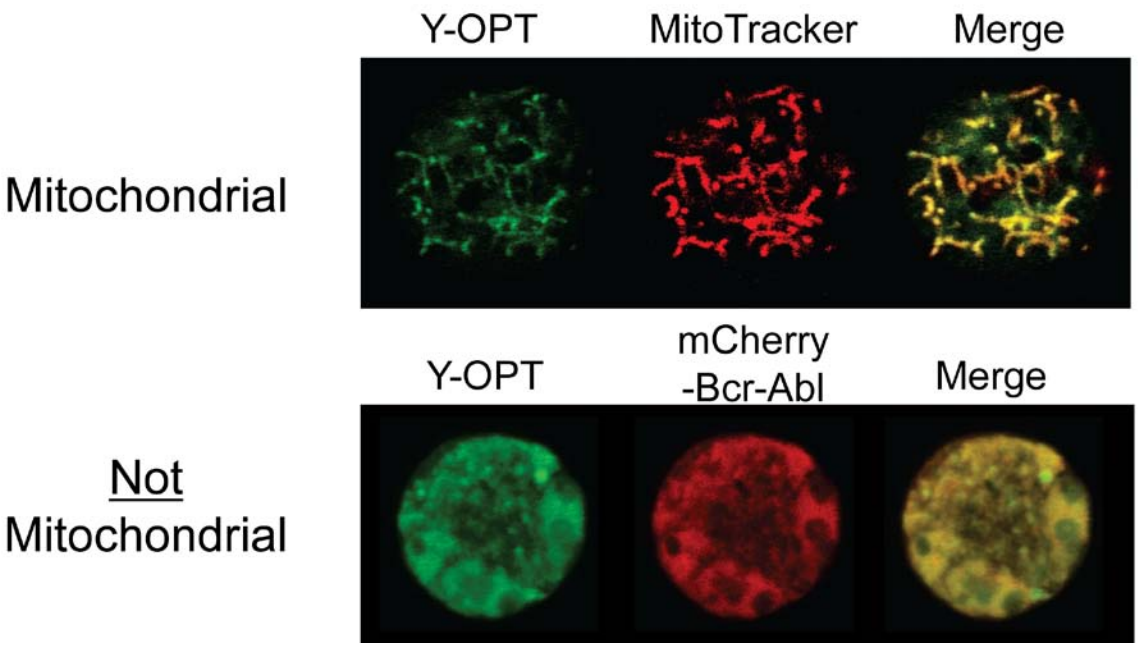
Y-OPT
MitoTracker
Merge
Mitochondrial
Y-OPT
mCherry
-Bcr-Abl
Merge
Not
Mitochondrial

F.

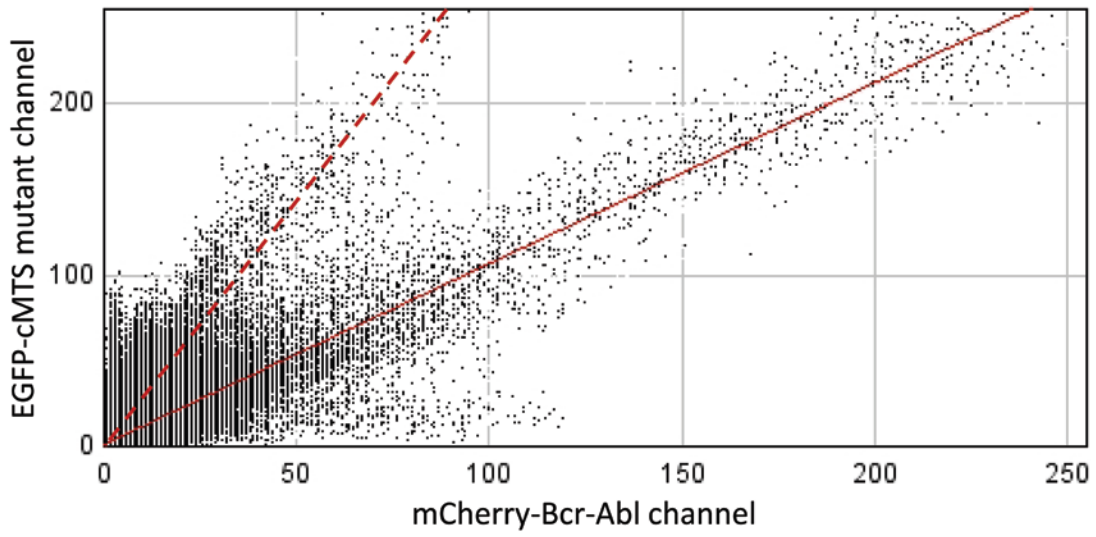
EGFP-cMTS mutant channel
0
100
200
0
50
100
150
200
250
mCherry-Bcr-Abl channel

A.

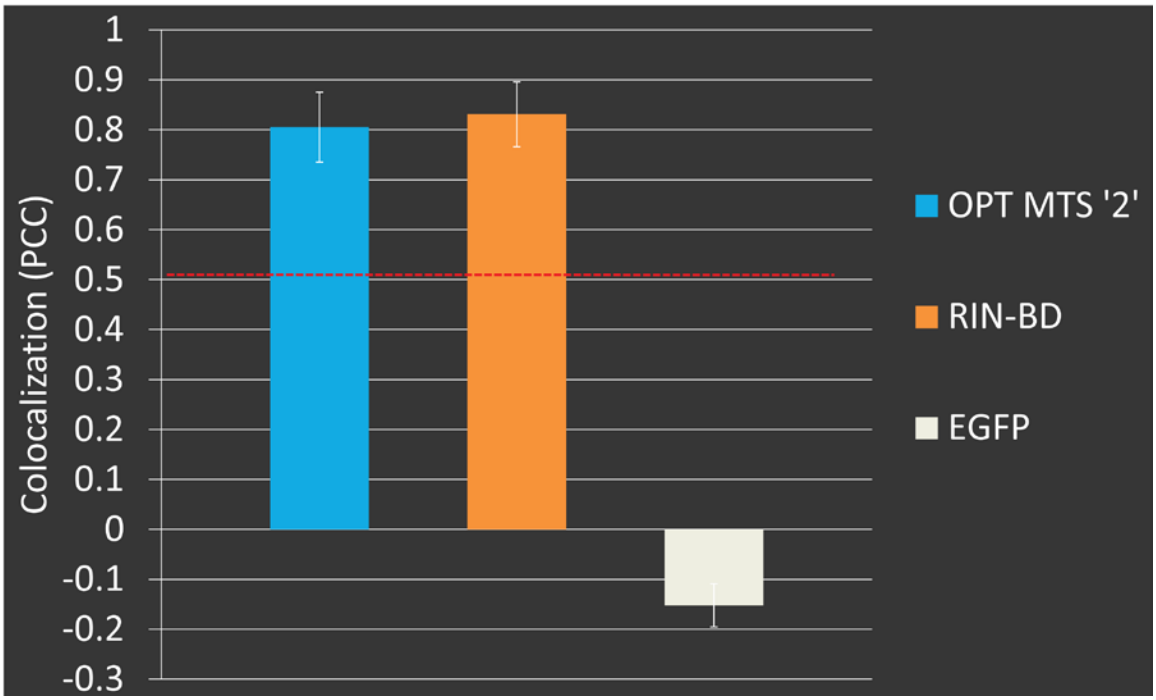

Figure A.3. OPT MTS 2 binds to Bcr-Abl like RIN-BD.

A) The minimum c-Abl consensus sequence at position 193 (OPT MTS 2; two residues different from wild-type, see Table 5.2) strongly associates with Bcr-Abl.,

B) Kinase dead mutant of Bcr-Abl abolishes association with the OPT MTS 2 but a SH3 domain mutant (P1013L) does not. Error bars are S.E.M and dashed red line indicates colocalization (A and B).,

C) Representative western blot image (false colored ‘fire’ in ImageJ) of Bcr-Abl activity in Cos-7 cells. Bcr-Abl (or a kinse dead mutant) was expressed in Cos-7 with or without RIN-BD or OPT MTS 2 present. RIN1 reportedly increases the activation of Bcr-Abl (by keeping Bcr-Abl in an ‘active’ conformation (9)) but the smaller RIN-BD and the OPT MTS 2 reduce the activity of Bcr-Abl. (N=3).

B.

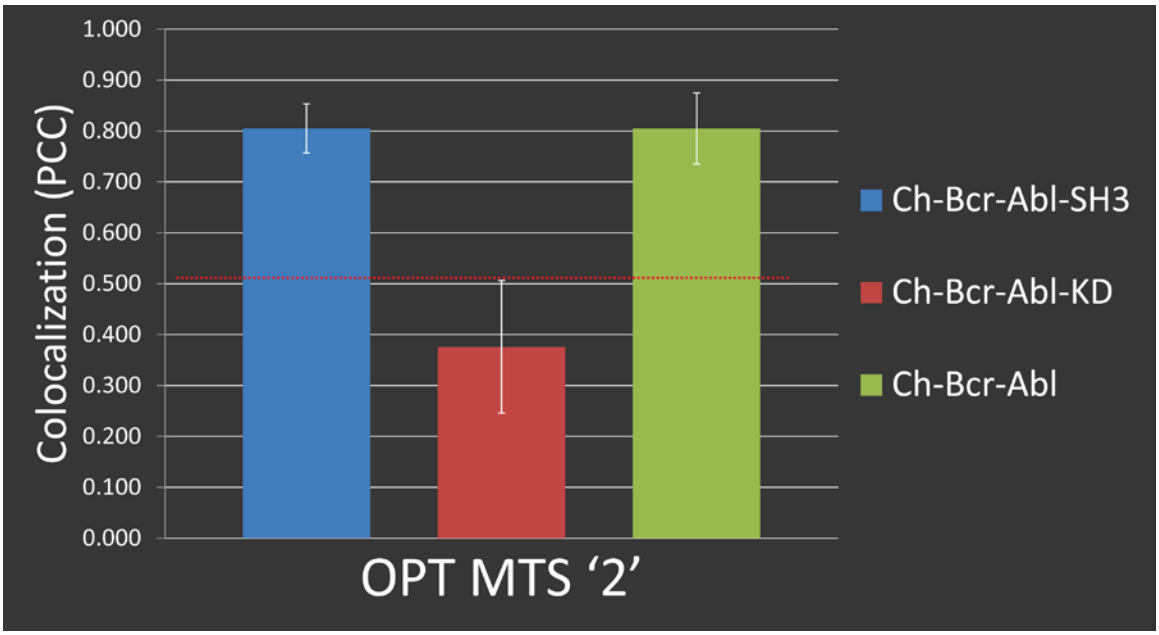

Figure A.3: Continued

C.

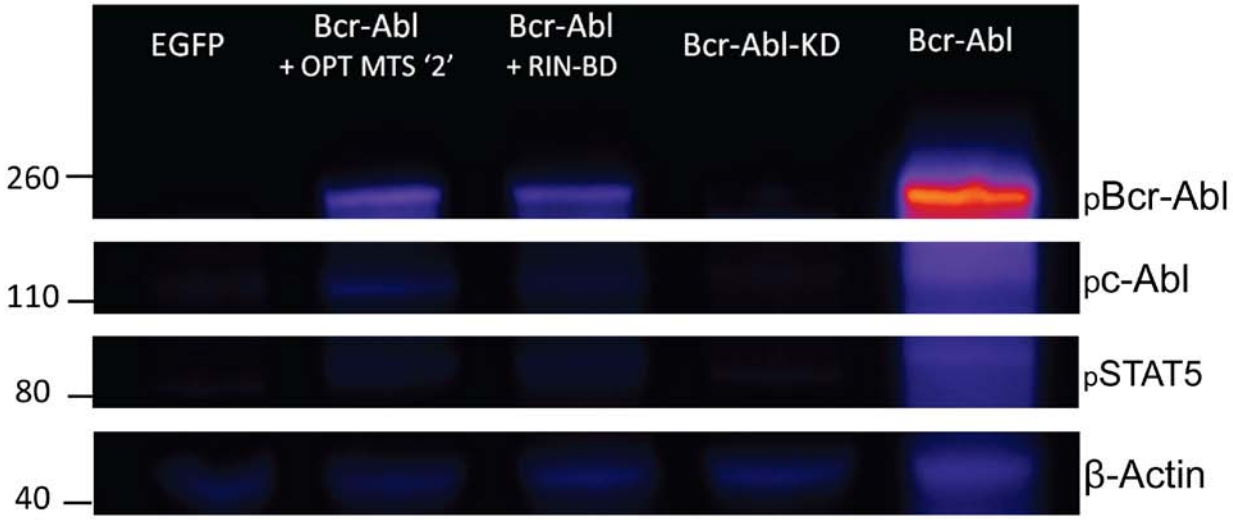

Figure A.3: Continued

Table A.2. cMTS mutant names and corresponding 'activation' region residue sequences.

NAME	Sequence of 'activation' region
cMTS:	TRISNIPTIKKFLQPG
Y-mut:	EAIYNIPTIKKFLQPG
Y-0PT "non-toxic":	EAIYNIPFIKKFLQPG
Y-0PT:	EAIYNIPFAKKKLQPG
Y-0PT null:	EAIANIPFAKKKLQPG
0PT cMTS 2:	TRISNIIYIKKFLQPG
Round 1 mut for 2x:	TRIYEAIYIKKFLQKK
2x cMTS:	TRIYEAIYIKPFAKKK

APPENDIX B

STATISTICAL COLOCALIZATION

PROTOCOL

Image processing protocol[1]:

Companion resources:

http://www.uhnresearch.ca/facilities/wcif/imagej/colour_analysis.htm

A practical guide to evaluating colocalization in biological microscopy (2011) Dunn et al.

Prior to the processing, images should be coded for blinded analysis.

ImageJ:

i) Open .tif z-stack file [FILE:OPEN]

ii) Convert to 8-bit [IMAGE:TYPE]

iii) Stack to images [IMAGE: STACK TO IMAGES]

(1) Make a list of parallel channel images (i.e., which images correspond each other)

(2) Minimize all images

(3) Expand two parallel images (i.e. GFP channel and MitoTracker channel)

(a) Subtract background (WCIF – Wright Cell Imaging Facility: ROI Background correction plugin)

(i) Subtract background from each image (and channel) throughout the stack individually – look for a region without cells. This can be verified even when a phase contrast is not available by using IMAGE:ADJUST:THRESHOLD. Use the histogram to determine all pixels present (displayed in red) and hit RESET prior to background subtraction or image analysis.

[1] Special thanks to Chris Rodesch, PhD. Director, University of Utah Cell Imaging Core Facility for scientific discussions.

1. Open ROI Manager [ANALYZE:TOOLS:ROI MANAGER] and save ROI that does not contain cells (This is the Background or BG ROI)
2. Select/highlight saved BG ROI within each channel image (and all images across stack – watch for moving cells (i.e., non-adherent lines))
3. Run Plugins/ROI/BG subtract from ROI – [subtracts mean of ROI form image plus an additional value equal to the sd of the ROI multiplied by a scaling factor [mean + (sd*scaling factor)]]
    a. Leave on default of 3 for scaling factor

(4) Expand parallel images (if multi-tiff)

(a) Select an ROI, import to the ROI manager [ROI MANAGER:ADD], copy ROI to parallel image [click on parallel image, double-click the ROI # in ROI MANAGER]

(b) 'Duplicate' each channel ROI [IMAGE:DUPLICATE:'OK']

(c) OPTIONAL: Remove pixels outside ROI [EDIT:CLEAR OUTSIDE] – do this for each duplicated image. ONLY use this if you are certain that 0:0 pairs are excluded – JACOP does NOT exclude 0:0 pairs.

(5) *Open JACOP [PLUGINS:JAR:JACOP]*

(a) Select each channel duplicate image [By convention (i.e., my way which is moving from blue through red in the spectrum) - Select GFP channel as A and Mitotracker as B] (always make note of which channel is which)

(b) In JACOP have these analysis checked: Pearson's correlation coefficient, M1 & M2, K1 & K2, Costes' automatic threshold, cytofluorogram, and Van Steensel's CCF. This is the output to the 'data log'. Evaluate cytofluorogram for 'lobeness' (more than one linear relationship amongst pixels suggests association in different ratios or compartments).

(6) *Open Colocalization Colormap [PLUGINS:COLOCALIZATION COLORMAP] – This is a modification of Li's ICA and is a representation of spatial co-variation ("cross view of biological compartments"). This is highly sensitive to background noise.*

(a) 'display nMDP statistics' should be checked.

(7) *Open Colocalization Finder [PLUGINS:COLOCALIZATION FINDER] An advantage to this feature is to select ROIs within the scatterplot. This can be used to identify 'compartments' in the generated overlap image where only ROI pixels show as white.*

(a) In order to visualize pixels in the interactive scatterplot you may need to open [IMAGE:ADJUST: BRIGHTNESS AND CONTRAST]: click on AUTO. Now the selected pixels in the scatterplot can be identified spatially in the image.

(i) If more than one lobe is present or a nonlinear association is evident select a ROI in the scatterplot and save in the ROI Manager for use in identifying that 'compartment'.

(b) OPTIONAL (in JACOP): Manually set the channel A and B thresholds to predetermined values for the given image stack. (however, you must specify how threshold was arrived at for reproducibility)

(8) Save: [FILE with original z-stack image should have: 1) data log, 2) the duplicated images of ROI in tiff format, 3) the cytofluorogram as JPEG, and 4) the Costes' mask as tiff. Each analyzed image ought to have five items in a folder].

(9) Compile all log data (by 'copy and paste' into a Word document)

(a) Save the complete document into the file that contains the individual 'CELL ROI' folders.

(10) Select the relevant statistic(s) and graph data

References

1. Z. Songyang, K.L. Carraway, 3rd, M.J. Eck, S.C. Harrison, R.A. Feldman, M. Mohammadi, J. Schlessinger, S.R. Hubbard, D.P. Smith, C. Eng, and et al. Catalytic specificity of protein-tyrosine kinases is critical for selective signalling. Nature. 373:536-539 (1995).

2. D. Wu, J.E. Sylvester, L.L. Parker, G. Zhou, and S.J. Kron. Peptide reporters of kinase activity in whole cell lysates. Biopolymers. 94:475-486.

3. D. Wu, M.R. Mand, D.R. Veach, L.L. Parker, B. Clarkson, and S.J. Kron. A solid-phase Bcr-Abl kinase assay in 96-well hydrogel plates. Anal Biochem. 375:18-26 (2008).

4. N. Kondo and S. Nishimura. MALDI-TOF mass-spectrometry-based versatile method for the characterization of protein kinases. Chemistry. 15:1413-1421 (2009).

5. M.R. Mand, D. Wu, D.R. Veach, and S.J. Kron. Cell treatment and lysis in 96-well filter-bottom plates for screening Bcr-Abl activity and inhibition in whole-cell extracts. J Biomol Screen. 15:434-440.

6. M.A. Robin, S.K. Prabu, H. Raza, H.K. Anandatheerthavarada, and N.G. Avadhani. Phosphorylation enhances mitochondrial targeting of GSTA4-4 through increased affinity for binding to cytoplasmic Hsp70. The Journal of Biological Chemistry. 278:18960-18970 (2003).

7. J.E. Constance, S.D. Despres, A. Nishida, and C.S. Lim. Selective targeting of c-Abl via a cryptic mitochondrial targeting signal activated by cellular redox status in leukemic and breast cancer cells. Pharmaceutical Research (2012).

8. A.S. Dixon, J.E. Constance, T. Tanaka, T.H. Rabbitts, and C.S. Lim. Changing the subcellular location of the oncoprotein Bcr-Abl using rationally designed capture motifs. Pharm Res. 29:1098-1109.

9. D.E. Afar, L. Han, J. McLaughlin, S. Wong, A. Dhaka, K. Parmar, N. Rosenberg, O.N. Witte, and J. Colicelli. Regulation of the oncogenic activity of BCR-ABL by a tightly bound substrate protein RIN1. Immunity. 6:773-782 (1997).

10. S. Rao, O. Schmidt, A.B. Harbauer, B. Schonfisch, B. Guiard, N. Pfanner, and C. Meisinger. Biogenesis of the preprotein translocase of the outer mitochondrial membrane: protein kinase A phosphorylates the precursor of Tom40 and impairs its import. Mol Biol Cell. 23:1618-1627 (2012).

11. S. Bolte and F.P. Cordelieres. A guided tour into subcellular colocalization analysis in light microscopy. J Microsc. 224:213-232 (2006).